A PULSED NMR RELAXATION AND DIFFUSION STUDY OF WATER IN TREATED AND UNTREATED WATERLOGGED WOOD

By

David A Bannister

Thesis submitted to the University of Nottingham

for the Degree of Doctor of Philosophy

January 1990

Proton N.M.R. Relaxation and Self Diffusion in Waterlogged Woods.

Contents.

ABSTRACT

Freezing curve, NMR relaxation data, and Steady field gradient and Pulsed field gradient experiments were conducted on samples of water-logged woods excavated from the Tudor warship, the Mary Rose, and on similar samples impregnated with Polyethylene-Glycol solutions; the polymer used as a bulking agent to prevent decay.

At least two distinguishable populations of water molecules are found in wood. Freezing curves indicate the presence of approximately 0.38 g/g of hydration water, close to that observed in fresh timbers. Relaxation measurements on pre-treated samples provides evidence of a very tightly bound fraction, present at water contents of below 0.14 g/g of hydration water, with a second population of hydration water being present upto 0.38 g/g. Above this value a third, 'free' population is observed.

The relaxation decays in longitudinal and transverse direction have been analysed in terms of a sum of exponentials. These indicate the presence of two populations of water which do not correspond to populations observed in freezing curve analysis.

Exchange mechanisms dominate the temperature dependency of the relaxation behaviour in pre-treated samples, which is similar to that observed in other fibrous materials such as meat. However, the different components do not appear to correspond to the physical characteristics of the wood, and the spin populations cannot be associated with a distribution between identifiable compartments within the system.

In PEG impregnated samples the contribution to the signal from the polymer is not resolvable on the equipment used. Samples treated with PEGs for which the degree of polymerisation is greater than 1540 show a dependency of relaxation characteristics on the water content of the sample. At low water contents PEGs of low molecular weight impart a mobility to the

ABSTRACT

Freezing curve, NMR relaxation data, and Steady field gradient and Pulsed field gradient experiments were conducted on samples of water-logged woods excavated from the Tudor warship, the Mary Rose, and on similar samples impregnated with Polyethylene-Glycol solutions: the polymer used as a bulking agent to prevent decay.

At least two distinguishable populations of water molecules are found in wood. Freezing curves indicate the presence of approximately 0.38 g/g of hydration water, close to that observed in fresh timbers. Relaxation measurements on pre-treated samples provides evidence of a very tightly bound fraction, present at water contents of below 0.14 g/g of hydration water, with a second population of hydration water being present upto 0.38 g/g. Above this value a third, 'free' population is observed.

The relaxation decays in longitudinal and transverse direction have been analysed in terms of a sum of exponentials. These indicate the presence of two populations of water which do not correspond to populations observed in freezing curve analysis.

Exchange mechanisms dominate the temperature dependency of the relaxation behaviour in pre-treated samples, which is similar to that observed in other fibrous materials such as meat. However, the different components do not appear to correspond to the physical characteristics of the wood, and the spin populations cannot be associated with a distribution between identifiable compartments within the system.

In PEG impregnated samples the contribution to the signal from the polymer is not resolvable on the equipment used. Samples treated with PEGs for which the degree of polymerisation is greater than 1540 show a dependency of relaxation characteristics on the water content of the sample. At low water contents PEGs of low molecular weight impart a mobility to the

"bound" water molecules which is not seen in untreated samples.

Their diffusion coefficients for water molecules in wood are anisotropic, and are reduced from those observed in distilled water. This reduction is brought about because water molecules are both held in a hydration layer, and bounded by the cellular structure of the wood.

In impregnated samples the diffusion rates are lowered by a factor of 10. though this is not reflected in the relaxation behaviour. The anisotropy is reduced, and proton exchange mechanisms are blocked.

ACKNOWLEDGEMENTS

I would like to express my appreciation to the following:

Prof. W. Derbyshire - for his supervision and the provision of laboratory facilities.

Dr. J. Harvey - for initiating the project and indentifying sample species.

Prof. E. Clough - for his patience.

Mr. S. Booth - for his incredible hard work in keeping the equipment operational.

The Mary Rose Trust - for providing samples, cash and helpful information.

The S.E.R.C. - for financing the case award.

The Phonon Bunch and Dr. F. Zelaya - for friendship, enthusiasm and assistance.

R. Underwood's kitchen table - for its support!

Mum and Dad.

CHAPTER 1 NMR AND THE STUDY OF WATER IN WATER-LOGGED WOOD.

There have been numerous reports on the study of water in heterogeneous systems using a variety of techniques [1-3]. Despite this, an understanding of the nature of water within these systems, and its interaction with these systems, has not been well established. One system which has received little attention in the literature is that of water-logged wood.

Current procedures used in the preservation and conservation of water-logged artefacts are, at best, pragmatic, and are certainly not well understood. Methods that have been developed over the past thirty years or so in many cases prove unsatisfactory, largely because it is not known how the preservatives interact with the materials which they are employed to preserve. In order to optimise the processes used at present, it is obviously important that the penetration properties be determined and, for this, it is considered that some knowledge of the dynamics of both the system and the preservative is necessary.

The dynamic properties of water in biological systems are modified from those of bulk water to varying degrees, depending upon the water content of the system and its environment. It has not yet been established that to explain the properties of water in these systems it is necessary to invoke a biological effect and/or that explanations based upon the systems being dispersed and heterogeneous do not prove sufficient. In general, the application of the standard investigative techniques to such systems is non-trivial, sometimes in terms of techniques, but more often in terms of interpretation of observation.

Some of the common experimental techniques capable of detecting different types of physical processes are shown in figure 1.1. The first class encompasses the thermodynamic techniques such as sorption isotherms and calorimetric and volumetric analysis, useful in the study of bulk phenomena such as phase changes, energy relationships and the determination of

fractions of unfreezable water. However, thermodynamic measurements do not enable us to assign water molecules to specific sites, nor do they offer information on the kinetics of molecules or mechanisms of binding processes.

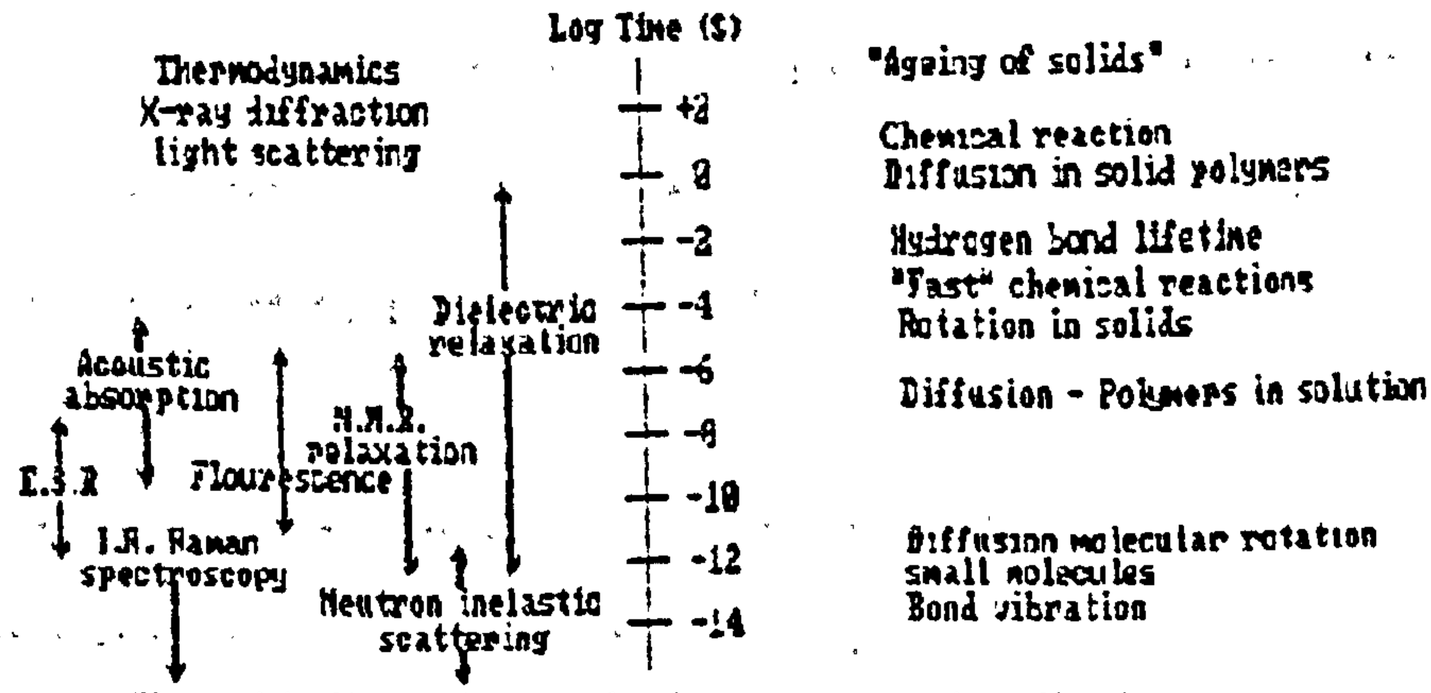

Figure 1.1 Time scales of molecular processes and application ranges of experimental techniques.

The second group of techniques examines the molecular structural parameters and perturbations thereof, together with the dynamic properties of water and molecular substrates. The group includes dielectric relaxation, infa-red reflectance, photo-acoustic effects, neutron elastic scattering, nuclear magnetic resonance and electron spin resonance. These techniques can be used to monitor rotational and translational diffusion of water molecules and can discriminate between water in the bulk and water which is undergoing restricted motion. Of this group, Nuclear Magnetic Resonance (NMR) is possibly the most powerful and useful in the study of water-logged woods and their preservation, as it has several important advantages over the other methods.

NMR offers high selectivity. As a result, the NMR spectroscopist can choose to study atomic nuclei of any element provided that they possess a magnetic moment. The proton, with a nuclear spin number I=1/2 is the most commonly exploited, due to its high natural abundance and large magnetogyric ratio (gamma = 2.673 x 10^8 CKg). Others in common use include deuterium oxygen-17 and carbon-13.

The magnetic field experienced by a nucleus (B) is the applied field (Bo), perturbed by small local magnetic effects. Some of these are induced by the external field and hence related to it, while others are due to magnetic elements in the system, including all other nuclei possessing magnetic moments. The local fields associated with these perturbations have both steady and fluctuating components. Consequently, the position and width of the spectral lines are extremely sensitive to the environments of the nuclei under examination, i.e. to the structure and dynamics of the molecules containing the nuclei in question.

Within different systems there are a variety of inter-molecular interactions, such as molecular reorientation, diffusion, and chemical exchange, which give rise to different properties of the NMR signals. These interactions may be resolved using the versatility of NMR. One can deduce different types and information about a system by changing either the type of NMR measurement, or the system itself.

One of the most important advantages in using NMR is that it is essentially a non-invasive and non-destructive probing technique. Samples may be subjected to a series of NMR experiments without structural or chemical damage.

There are two major disadvantages in the use of NMR. Firstly, the parameters of interest, such as chemical shifts and magnetisation decay rates, are phenomenon rather than system-based. In other words, the results of NMR measurements require extensive interpretation in order to relate these derived parameters to the properties of the system expressed in familiar units. Further complications occur because of the differential dependences of the different NMR techniques upon the different interactions. Whilst this has been relatively direct in the case of simple systems, it has proved very difficult in those of greater complexity. Secondly, whilst the selectivity of NMR is high, the sensitivity is low. Since the technique involves transitions between energy levels for populations which are distributed

amongst those levels according to Boltzmann statistics, and the available field strengths are low, i.e. the magnetic energy $2\mu.B$ is much less than the thermal energy KT, the signal strengths are inherently poor. NMR experiments require relatively large samples and are not suitable for trace analysis.

The low sensitivity does not present difficulties in the study of water-saturated timbers and NMR signals can readily be obtained. However, in a complex system such as that of water-logged wood, one is operating at the extreme limits, if not beyond the limits, of applicability of current NMR theories. In attempting to improve our understanding of the system, we are simultaneously testing the applicability of current NMR theories.

It should be stressed that in this work it is primarily the properties of the water in the system that are of importance to us, the emphasis being on the manner in which its interactions with the cellular material of the wood, and the preservatives used to stabilise the woods ,modify its dynamic behaviour from that of bulk water. It is considered that the detailed composition of wood on a molecular level is relatively unimportant from this point of view. What is of interest to us however,is the macroscopic structure of the wood and the method by which water preservatives may penetrate and reside in the wood. One would expect the compartmentation of the water to have profound effects on its NMR properties. A description of the macroscopic structure is therefore given in chapter 2.

Wood differs from other cellular systems in that the water contents normally encountered are low; usually in the order of 38% by weight, or below. Consequently, water in wood is normally found in close association with the wood cell wall, or in vapour form. In contrast, samples of wood from the Tudor battleship, the "Mary Rose", are highly saturated, having water contents which are similar in magnitude to those of other biological cellular systems. One would expect the dynamic behaviour of the water molecules in water-logged timbers, therefore, to be markedly different from that of water in fresh wood, and that this should be

reflected in its NMR properties. One does not necessarily expect to observe the behaviour which is shown in other cellular systems because the water in wood is not in equilibrium with its environment.

In this work measurements of T1 and T2 and the self diffusion coefficients of the water-logged wood have been measured as a function of water content, degree of degradation , and temperature of the samples in order to characterise its nature and contrast its behaviour with that observed for water in fresh wooden timbers. The NMR properties of water in samples treated with different grades of the stabilising agent Polyethylene-glycol have also been observed, and the modification of the dynamic properties of water in the treated samples is discussed.

References

1. Mathur-de-Vre R. "The studies of water in Biological systems." Prog. Biophys. Molec. Biol. Vol 35, pp 103-134. (1979)

2. Belton P.S., Ratcliffe R.G. "NMR and Compartmentation in Biological tissues." Prog. in NMR Spectroscopy. Vol 17, pp 241-279. (1985)

3. Lillford P.J., Clark A.H., Jones D.V. "Distribution of water in heterogeneous food and model systems." Water in Polymers, Chapter 10. Pub. American Chem. Soc. (1980)

4. Cooke R., Kuntz I.D. "Properties of water in Biological systems." Ann. Review Bioph. and Bioch. Vol 3, p 95. (1974)

5. Franks F. "Water - A comprehensive treatise." Pub. Plenum Press, New York. (1972)

CHAPTER 2 WATER-LOGGED WOOD AND ITS CONSERVATION

2.1 Introduction

In an archaeological context water-logged wood may be defined as that which has been completely filled with water instead of air and has been chemically broken down by the action of micro-organisms, causing considerable weakening of the structure of the wood.

The ability of different species of wood to absorb water is amazingly variable; alder, beech and maple, for example, take up water very rapidly and can become saturated within a few hours, while in other species such as oak the process can take weeks, or even years. In the case of porous woods the chemical breakdown occurs almost simultaneously throughout the sample, whereas in less hydroscopic species the breakdown is likely to occur from the outside, one cell layer at a time.

Despite the quite fresh appearance of most samples of water-logged wood, normal drying out procedures usually lead to the complete destruction of the samples within a matter of hours. The conservation of water-logged wooden artefacts is aimed at stabilising the size and shape of the samples, and at providing some durability, without destroying their aesthetic value.

The following chapter begins with a brief description of the structural and chemical compositions of wood and the ways that these are degraded as a result of water-logging. A short historical account is presented describing attempts which have been made to conserve saturated wooden artefacts, followed by an appraisal of the process of conservation by impregnation with polyethylene glycols, which is the most widely and successfully used method to date.

2.2 The Structure of Wood.

There is a great diversity in the appearance and physical properties of different types of wood[1-2], and yet the ultra-structure of the different species is basically the same. All woods are made up of cellular tissues composed of three main constituents. Each cell may be thought of as a lattice of crystalline cellulose encrusted by lignins and hemiceluloses.

Cellulose is a straight, fibrous and extremely long polysaccharide made up of several thousand, beta-glucose molecules that are C-1 C-4 linked. In wood, cellulose forms a rope-like structure. About forty polymer chains align parallel to each other to make up strands known as elementary fibrils. Several thousand of these fibrils threaded together form microfibrils, which themselves intertwine to form macrofibrils. The macrofibrils give form and strength to the cell wall by binding together in alignment. They are visible using electron microscopes, and appear as thin striations in the cell wall.

The elementary fibrils are surrounded by shorter chain molecules called hemicelluloses which have different monomeric units with degrees of polymerisation of around 100. The hemicelluloses are adapted to the cellulose crystalline system, and form the most hygroscopic fraction of the cell wall.

Lignin is deposited onto hemicellulose and is bonded to it. It does not bond with the cellulose itself. It is an amorphous substance derived from phenyl-propane building blocks and gives rigidity to the wood.

The cell walls are constructed of four layers; the primary wall, and the outer, middle and inner layers of the secondary wall. They are distinguished by the orientation of their macrofibrils (See figure 2.1). The thick secondary wall is deposited on the inner side of the primary wall and provides by far the majority of the cell wall substance.

Between the walls of adjacent cells is an amorphous region packed with lignins known as the middle lamella. The cell lumina are connected to each other via pores in the cell walls called pits. In fresh wood, pits act as valves and allow for the passage of water from one cell to another, but, in dead wood, most pits are closed.

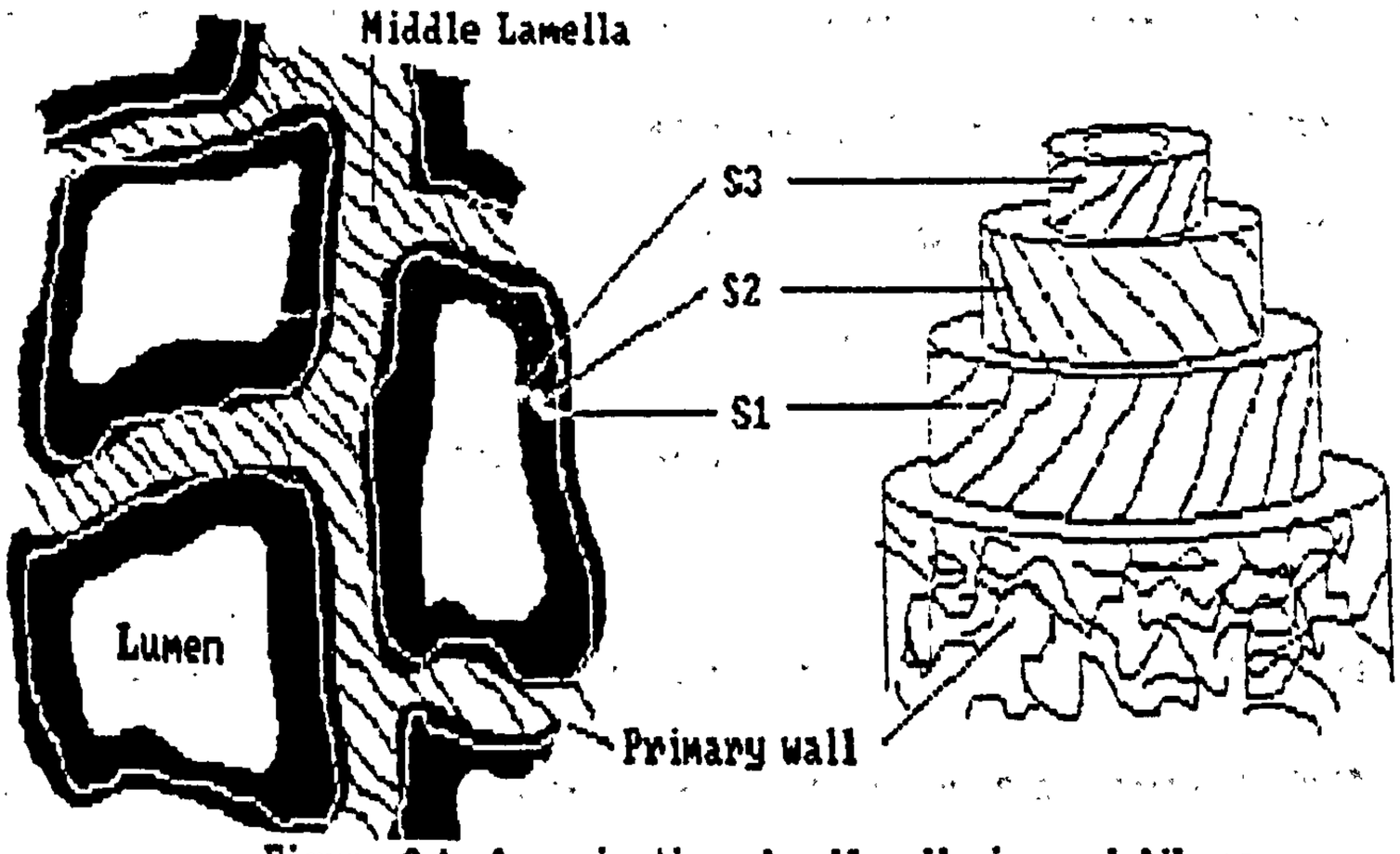

Figure 2.1 Organisation of cell walls in wood fibres.

The walls contain tanins, resins, fats and waxes, which occupy a proportion of the cavities and open capillaries existing between fibrils, microfibrils and elementary fibrils. The capillary system is extensive and makes up about 40% of the cell wall volume. For each cubic centimetre of cell wall, it is estimated that there is 100-200 square meters of surface area. A rough guide to the dimensions of pores in wood is given below:[3]

Fissures within elementary fibrils	1nm
Capillaries between elementary fibrils	10nm

Capillaries between fibrils	up to 80nm
Pores in pit membranes	up to 150nm
Diameter of a water molecule	0.2nm

There is a great diversity in size, shape and juxtaposition of cells from one species to another. The different species of wood may be broadly divided into two groups. These are angiosperms, known as hardwoods, and gymnosperms, known as softwoods. Both are constructed by two inter-penetrating systems of cells; one oriented radially and the other longitudinally, which are interspersed by intercellular spaces called resin canals.

The two groups can be distinguished by their different cellular compositions. The large pores, evident only in angiosperms, are called vessels. These are made up of smaller tubular units that are joined end to end to form passageways that can vary in length from a few centimetres to several meters. They are used in the transportation of water. Most are oval in shape, and their spatial arrangements are fixed, making them useful when identifying species.

The tissue between vessels is made up predominantly of two types of cells. These are thin walled trachieds, and thick walled fibres. These types of cells are common to both angiosperms and gymnosperms. In gymnosperms, as much as 90% of xylems made up of vertically stacked trachieds which are elongated cells that are arranged uniformly, and have lengths of between 3 and 7 millimetres. Fibres resemble trachieds but have thicker walls, fewer pits, and smaller lumens. Fibres form the bulk of the solid matter found in angiosperms.

There are a number of other types of cells found in wood such as the parenchyma, and the resin-producing epithelial cells. The majority of cells in wood are oriented in the longitudinal direction. The radial elements are called rays. These are composed of passageways which radiate outwards like the spokes of a wheel. They are usually 10 to 15 cells wide, and are often associated with horizontally oriented resin canals. (See figure 2.2)

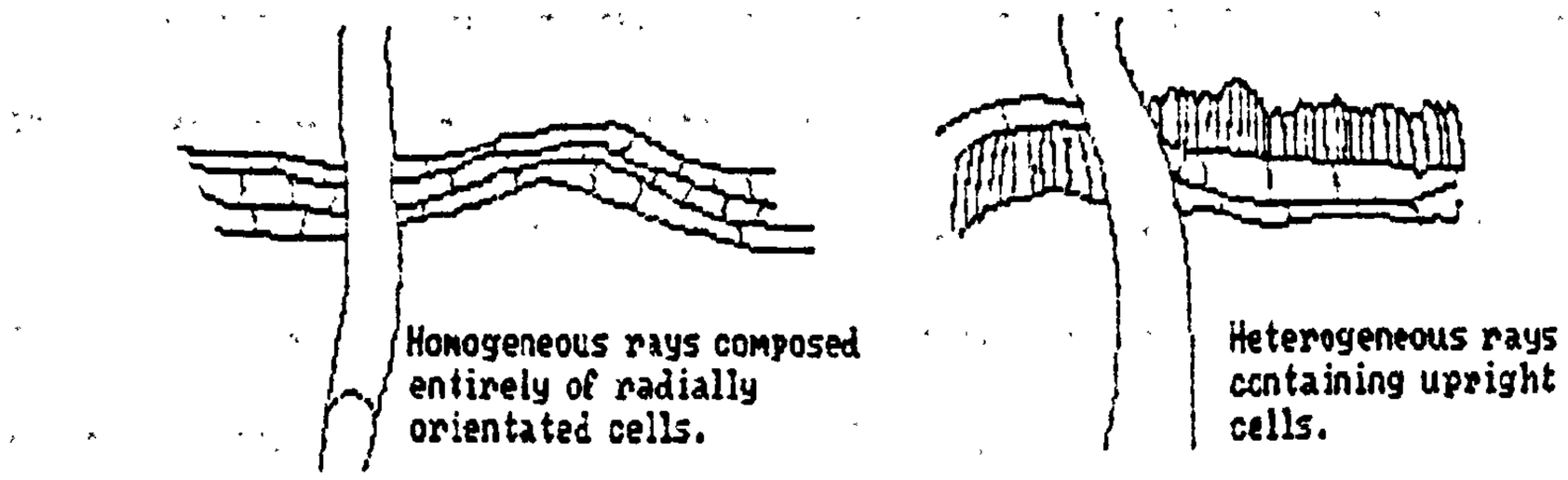

Figure 2.2 Ray patterns in wood

2.3 The Decomposition of Wood

There are three methods of attack causing the decomposition of wood[4]; a chemical attack caused by oxygen and water, a vegetable attack by fungi, micro-organisms and bacteria, and an animal attack caused by insects.

In the first process, the long cellulose molecules are broken down with the result that the mechanical strength of the cell walls is weakened and the wood becomes brittle. The cellulose undergoes a slow, natural, decomposition in the presence of oxygen, heat and light. Oxygen is the main deterioration agent, and the process is accelerated by the presence of U.V.light and high temperatures. Lignin decomposes in the same manner, but at a much slower rate.

Water causes the hydrolysis of certain compounds in xylem and can also be the basis for other decomposing factors, such as fungal growth. A number of fungi are able to live from wood, using it as a nutrient. This results in the physical decay and weakening of the wood, which gives rise to both horizontal and vertical cracks.

Attack from micro-organisms may occur aerobically and anaerobically. Anaerobic processes occur under water, or in the mud at the bottom of salt or fresh water. The micro-organisms attack the cellulose, breaking it down into ethyl alcohol, acetic acid and, finally, carbon dioxide and water. Methane fermentation processes may occur by means of anaerobic micro-organic attack, and the wood can lose up to 65-85% of its solid content. Lignin is not decomposed directly by methane fermentation, but xylem can be converted to humus if it stays in water long enough. Enzymic attack is least effective in acidic conditions.

Animal decomposition arises because many insects, or their larvae, digest xylem.

The process of deterioration of wood in wet anaerobic conditions is a combination of the above. Firstly, the readily soluble materials in the wood dissolve into the surrounding medium, followed by readily hydrolysed compounds such as pectins and pentosans. Microbiological degradation of the more stable cellulose and hemicellulose will then follow. Finally, lignin remains, though this too may be decomposed by micro-organisms in an anaerobic environment. Both fungi and bacteria cause the breakdown of xylem, and both use extra-cellular enzymes to hydrolyse the cellulose, hemicellulose and lignin. Degradation spreads through the capillary system of the wood as far as the extra-cellular enzymes can penetrate.

The degree of degradation can thus be expressed by the remaining cellulose, hemicellulose and lignin[4]. Scanning electron microscopy[4-8] reveals that degradation occurs initially in the secondary wall, starting in the lumen, and progressing into the cell wall. Structures in which degradation is extensive may contain only 30% of the original cell wall substance, with 90-95% of the carbohydrate material having disappeared. Even the middle lamella may be corroded and dissolved. As carbohydrates are removed from the fibrils of the cell wall, cavities are produced which fill with water. In these structures, water acts as a bulking

agent, which keeps the wood in shape as long as it is kept wet, by preventing the remaining cellulose molecules from combining with each other via hydrogen bonding of adjacent hydroxyl groups.

The result of the decay of cell material is a considerable loss of original strength. If the wood is extremely decomposed, the water content can be as much as 90-96%. Even in air at 98% relative humidity, such wood will start to collapse. When drying, old water-logged wood shows very strong shrinkage, warping and cracking, and even complete disintegration, as the strength of the capillary system is exceeded by the contracting capillary forces of the evaporating water.

In many timbers, the decay is non-uniform, and three regions of degradation can be identified. The decay is most advanced at the surface of these samples, which become extremely soft, and greyish-brown in colour. Below this lies a thin fibrous layer in which the breakdown of the cell walls is less advanced than the outer layers. The inner core of these samples has the appearance of fresh timbers, but is completely saturated with water. Collapse of the cells is much greater on the outside layer due to greater voids in the cell wall, caused by the removal of cellulose. Cells in this region contain little more than the middle lamella and some primary wall. In the two less degraded layers the secondary wall is still present, although frequently contracted and loosened from its position.

2.4 Methods of Conserving Water-logged Wood

When restoring water-logged artefacts, it is the aim of the conservationist to produce a finished product that is stable in the environment in which it is to be kept, while maintaining as many of the original aesthetic qualities of the artefacts as possible.[9]

In the case of water-logged wood artefacts, the problem is reduced to that of drying out the samples whilst preserving their overall shape and appearance. Once dried, the artefacts must be able to withstand changes in the surrounding temperature and relative humidity. Some protection against fungal and organic attack is also desirable.

The first successfully employed method of conservation of water-logged wood was the alum method, introduced by Jorgensen[91] in 1859. The samples were soaked in boiling potassium aluminium sulphate until the water in the samples had been replaced by the alum, and the samples were then left to cool. The alum solidified in the pores and capillaries of the wood, acting as a bulking agent and thereby preventing subsequent collapse.

The method had several disadvantages. It required that the surface of the samples be cleaned and treated with varnish, or some such protective outer layer. It was not reversible. It was found that the water was removed from the samples faster than the alum could impregnate the structure, leading to internal stresses and some collapse. Furthermore, the success of the method was unpredictable, and depended on the amount of alum absorbed by the wood, and the condition of the wood itself.

The degree of shrinkage in wood as it dries is proportional to the capillary forces of the evaporating liquid, and shrinkage is less pronounced when drying is fast. It is possible to reduce these forces by replacing the water with volatile, low surface tension liquids which, upon evaporation, exert far smaller forces on the cell wall. Ethyl ether and tertiary butanol were successfully used in early trials in a number of cases where the degradation was not severe.

An alternative way of reducing these forces is by freeze-drying the samples. The technique depends upon the sublimation of ice within the wood being such that the drying water phase is avoided.

In general, some consolidation will be required with both of these techniques. Freeze drying from water often gives rise to innumerable cracks, caused by stresses set up when the water freezes. These can be avoided if the samples are pre-treated with bulking agents, while a final treatment may be required when using the alcohol exchange method.

Consolidation of the saturated xylem cells has been carried out using a variety of bulking agents. Early attempts involved embedding the wood in a hard wax by impregnation at high temperatures. Substitution of the water in the wood for alcohols was necessary where the waxes used were insoluble in water. Objects that are totally impregnated in this way can be expected to remain in a fixed state over long periods of time, but the surfaces usually require extensive cleaning, which is normally difficult on anything but the simplest of surfaces. The process can be slow if the waxes do not readily penetrate the wood.

To speed up the rate of impregnation, several attempts have been made to impregnate the wood with monomers such as vinyl acetate, methylmethacrylate, and moncethylene glycol, and then to polymerise these inside the cell walls using catalysts. The toxicity of the monomers and fire risk are serious drawbacks to using this method, however, and it can be difficult to obtain a satisfactory surface. The technique is non-reversible, and can result in some shrinkage in the wood upon polymerisation.

2.5 Stabilisation of Water-logged Wood using Polyethylene Glycol.

The most effective method of conserving water-logged wood to date is by impregnation with polyethylene glycols (PEGs)[10]. These are water soluble polymers of ethylene oxide. PEGs are produced in different grades that are designated a number representing the average molecular weight of the grade. In general, PEGs with molecular weights of between 200 and

600 are clear, viscous liquids at room temperature, while those with weights of between 1000 and 20,000 are white, waxy, solids[11]. At higher molecular weights, there is a decrease in solubility, vapour pressure and hygroscopicity. The changes in the polymer properties with molecular weight are significant when deciding which grade to use in the preservation of water-logged timbers. Low hygroscopicity of the finished product is desirable but, at the same time, the conservationist must consider the ease with which the different grades can penetrate the water-logged artefacts, as well as the effectiveness of the different grades in stabilising the timbers.

The treatment of water-logged artefacts using polyethylene glycols was first introduced in the early 1950's by Centerwall and Moren[9]. They adopted a technique whereby the artefacts were immersed in PEG solutions at 65 degrees centigrade. The concentration of the solution was increased daily from 0% to 100% by increments of 15%.

In early experiments, samples treated using PEGs with molecular weights between 15,000 and 20,000 developed hollow cheeks after being allowed to dry for several days. Samples treated with molecular weights between 1,500 and 3,000 underwent little or no dimensional changes, but it was noticed that these samples became greasy and increased in weight when the humidity of the air rose.

PEGs having molecular weights in the intermediate range, i.e. from 4,000 to 10,000, provide good dimensional stability to the water-logged woods, which show no tendency to take up water at relative humidities of less than 83%. Treatments using PEG 4,000 were favoured, as the lower molecular weights could penetrate the wood faster than the larger molecules.

Today the conservationist is still dependent on the PEG-water system. It is relatively cheap and does not provide a health risk to those working with it[11]. In most cases, PEG 4,000 is still used or, for well preserved wood, PEG 1,500 may be chosen, as the smaller molecules will penetrate better into the wood. Treatment with PEG 400, followed by freeze-drying, has also proved useful.

The important factor in addressing the question of how PEGs prevent shrinkage is to determine the degree to which PEGs of different molecular weights occupy the cell wall spaces, and how much of the bound water is replaced, or how effectively PEG occupies cell lumina.

PEGs impregnate either the cell wall, the lumina, or both. The bulking effect then prevents the collapse of the cellular structure on drying. PEGs of molecular weights in the range 200 to 600 replace some of the bound water during soaking treatments, and it is assumed that they remain in the cell wall upon drying. These PEGs offer substantial dimensional stability to the wood even at concentrations well below the fibre saturation point of the wood.

PEGs in the molecular weight range 1000 to 3000 are also expected to infiltrate the ultrastructure of the wood but, at higher concentrations, are also expected to bulk the cell lumina as well. PEGs with molecular weights greater than 3000 are expected to resist shrinkage forces by bulking of the cell lumina only, as their solution sphere is too large to allow them to penetrate the cell wall.

The grade of PEG that is most suitable for the preservation of water-logged timbers depends heavily on the state of the wood itself. A detailed study of the preservation of water-logged wood, using PEGs, was carried out by Hoffman[10], in which he attempted to relate the degree of wood degradation and PEG molecular size to the amount of PEG taken up by the system, the stability achieved, and the resulting hygroscopicity.

Hoffmann used PEGs with different molecular weights from 200 to 4000 on woods with water content between 120% and 580%. The fluorescence tests developed by Young and Wainwright[10] were used to assess the extent of penetration of the PEGs. A yellow to green fluorescence is induced in wood by shortwave light of wavelength 450-490nm. The fluorescence originates from lignin. PEG stained with cobalt thiocyanate suppresses this natural fluorescence, which can be observed under a microscope.

The anti-shrink efficiency (ASE) of a treatment was defined as:

$$ASE = (BO - Bi)/BO \times 100\%$$

where BO is the shrinkage observed in untreated wood, and Bi is the shrinkage observed in treated samples. A good indication of the relationship between initial water content and the degree of shrinkage to be expected for the different treatments is given in figure 2.3.

The results showed that some PEG penetrated the wood, whichever grade was used, but that the penetration, using low molecular weights, was superior to that when using high molecular weights. The various degrees to which the fluorescence was suppressed was indicative of the ease with which PEGs penetrated different regions of the cell. The most accessible regions are the corners of the cells and the middle lamella. Next is the primary cell wall, and the most elusive region for the PEG molecules is the secondary wall.

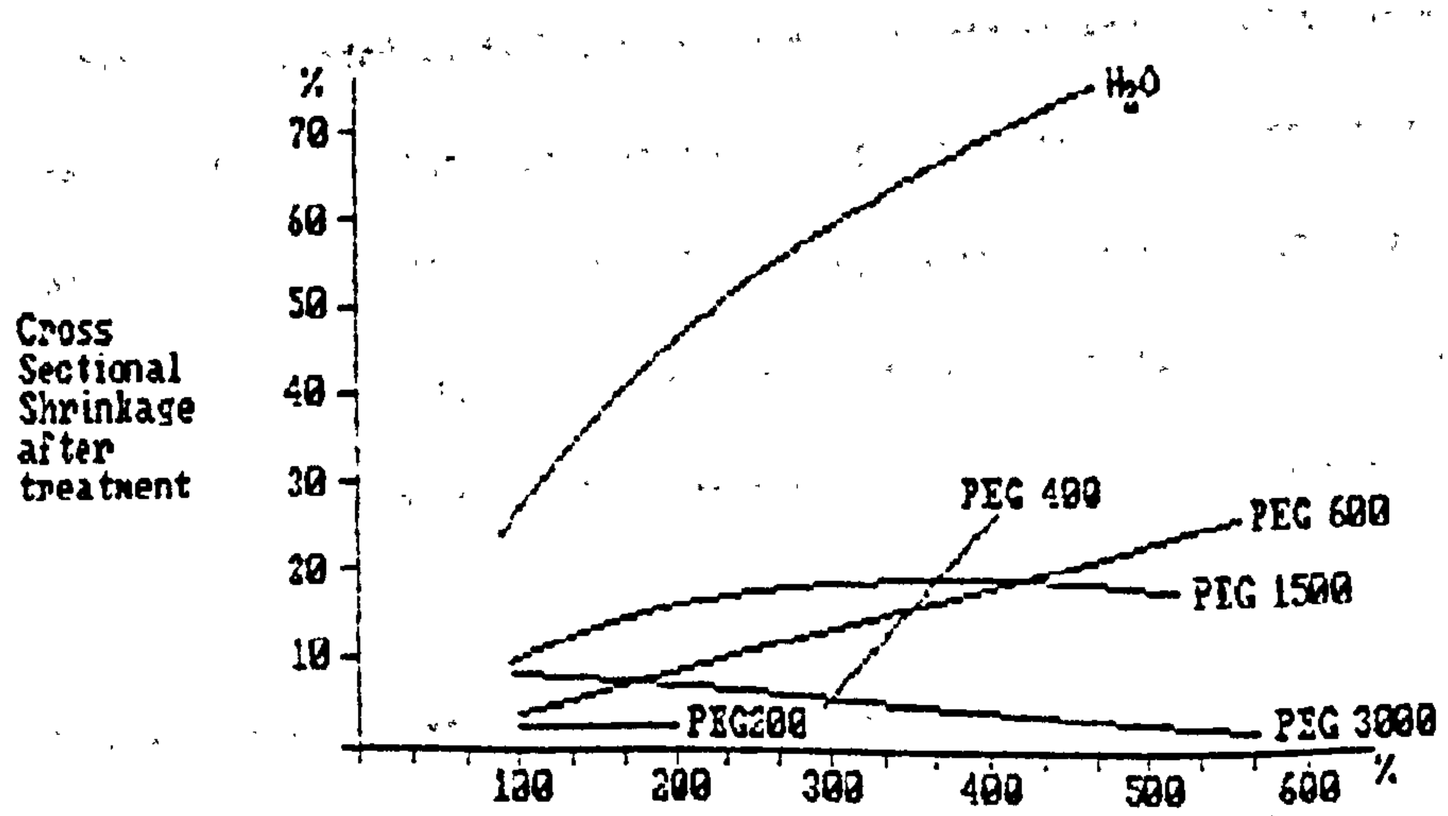

Figure 3.3 Stability acheived treating water-logged woods with different PEGs.

Hoffmann concluded with the following:

(i) PEG 1,500 was consistently poor at effecting the dimensional stability of water-logged wood for all water contents.

(ii) The hygroscopicity was greatest when low molecular weights were used but, even in these cases, relative humidities were 70%-80% before there was evidence of leaching.

(iii) In relatively fresh timbers, where degradation is not severe, stabilisation is brought about most effectively by low molecular weight PEGs, i.e. small molecules which enter into the large parts of the capillary system of the cell walls, middle lamella and cell corners. Here they replace the water and, on drying, keep the wood in a swollen state. Woods having water contents of up to 160% can be treated in this way.

(iv) In heavily degraded woods having moisture contents upwards of 400%, especially where the secondary wall has been destroyed, there is evidently not enough wood substance left to be kept swollen by small PEG molecules and, thereby, stabilise the whole corpus. In this case, stabilisation is more effective if the wood is bulked using higher molecular weights. Concentrations of around 70% are required in these cases.

(v) Between these two extremes there lies a region of wood containing both highly degraded and well preserved cells, each component of which requires a different grade of PEG. In this case, mixtures of different grades may be used, or consecutive applications of PEG may provide the solution.

References

1. Stamm A.J. "Wood and Cellular Science." Pub. Ronald Press, New York. (1964)

2. Morley P.R. "How Trees Grow." Pub. Edward Arnold Ltd. (1963)

3. Panshin A.J. and deZeeuw C. "Textbook of Wood Technonlogy." Chapters 4,5,11. Pub. McGraw-Hill, New York. (1980)

4. Borgin K. "The mechanism of breakdown of the structure of wood due to environmental factors." J. Inst. Wood Sci. Vol. 5, pp 26-30. (1971)

5. Jesperson K. "The decomposition of wood." Int. Symposium on conservation of large objects of water-logged wood. Amsterdam. (Sept 1977)

6. Borgin K. "The use of the electron scanning microscope for the study of weathered wood." J. of Microscopy. Vol 92, pp 47-55. (1970)

7. Findley G.W.D. and Levy J.F. "Scanning electron microscopy as an aid to the study of wood anatomy and decay." J. Inst. Wood Sci. Vol 4, pp 57-63. (1969)

8. Oddy W.A. (Ed) Maritime Monographs and reports. Vol 16, pp 45-49. (1975)

9. Christensen B.B. "The conservation of water-logged wood in the National Museum of Denmark." Studies in Museum Tech. Copenhagen. (1970)

10. Murray H. "Conservation of artifacts from the Mary Rose.", Jagels R. "A deterior-tion evaluation procedure for waterlogged wood.", Barbour R.J. "Condition and dimensional stabilisation of highly deteriorated samples.", Hoffman P. "Stabilisation of water-logged wood with PEG. - Molecular size v degree of degradation." Proceedings of the ICOM water-logged wood working group conference. Ottowa. (1981)

11. Union Carbide Material data safety sheet No. F-48039A-GB.

CHAPTER 3 The Theory of NMR Relaxation and Diffusion Measurements in Heterogeneous Systems.

3.1 Introduction.

The Nuclear Magnetic Resonance phenomena occurs when nuclei possessing magnetic moments interact with an applied magnetic field. The theory on which NMR is founded is well established and has been adequately described by a number of authors[1-3]. A considerable fraction of the theory can be explained using classical ideas and this simplifies its understanding. In this chapter a brief account of the resonance phenomena is given and the concepts of spin-lattice and spin-spin relaxation times are introduced by adopting where possible, this classical approach.

The interpretation of NMR relaxation times in terms of real, physical, molecular events is complicated, and there is no unique model that can account for all the types of behaviour that have been observed. An understanding of how molecular motions lead to an observed relaxation time was first proposed by Bloembergen, Pound and Purcell[4]. Their theory could predict the characteristic behaviour of relaxation times observed in bulk water, but could not account for those observed in less uniform samples, such as cellular systems and polymer solutions.

For water in these more complicated systems there are a number of effects[5], most notably multi-component relaxation, an increase in relaxation rates relative to bulk water, and a variety of temperature dependencies, which stem from the modified dynamic behaviour of the water molecules, and in some cases from the magnetisation of the substrate. These have necessarily led to a number of theories which extend the ideas put forward by Bloembergen et al. Some of these are described in this chapter. Although proton resonance in water is the main concern of this work, the description of the relaxation phenomena is kept as general as possible.

Self-diffusion coefficients for water in heterogeneous systems are conveniently measured using NMR techniques[4-8]. Two methods are used during the course of this work, namely the steady-field gradient technique and the pulsed field-gradient technique, and descriptions necessary for the interpretation of the results from both methods are presented in this chapter. The effects of anisotropy and compartmentation on the observed self-diffusion coefficients are also considered.

3.2.1 Fundamental Concepts.

A nucleus is a compound system which may have a non-zero angular momentum hI, and a magnetic moment μ. The two quantities are related by the equation

$$\mu = \text{gamma} \times hI \qquad 3.1$$

The constant of proportionality gamma is characteristic of the nuclear species. Nuclei other than those with even atomic and mass numbers possess a nuclear magnetic moment when in their ground state.

Quantum theory predicts that for a nucleus with spin quantum number I, the component of angular momentum resolved in any specific direction (e.g. the z direction),may have any one of 2I+1 observable values given by m(I), where m(I) can adopt integral values from m(I) = -I to m(I) = +I. When placed in a magnetic field of flux Bo the corresponding permissible energies μ.Bo are given by

$$Em = \text{gamma} \times hm(I).Bo \qquad 3.2$$

where the energy levels are separated by an energy

$$\delta E = Em(I) - Em(I \pm 1)$$

$$= \text{gamma} \times h \times Bo(m(I)-m(I \pm 1))$$

$$= \text{gamma} \times h \times Bo \qquad 3.3$$

The probability of spontaneous transitions between energy levels is proportional to the cube of the frequency of the energy associated with such an event. The frequencies encountered in NMR experiments are limited by the size of the magnetic fields available and are typically a factor of 10^8 down on those of optical spectroscopy, and thus the probability of spontaneous transitions are negligible. Transitions may be induced by the presence of electromagnetic radiation of angular frequency Wo, satisfying the resonance condition

$$h\text{Wo} = \delta E = \text{gamma} \times h \times Bo$$

i.e. $$\text{Wo} = \text{gamma} \times Bo \qquad 3.4$$

For a typical laboratory field the frequency is in the r.f. range.

A first order perturbation treatment yields a probability of transition proportional to the strength of the perturbing r.f. field together with the selection rule of $\delta m = \pm 1$.

In an ensemble of nuclei under the influence of a static homogeneous magnetic field Bo at temperature T, the 2I+1 energy levels are occupied at equilibrium according to the Boltzmann factor

$$\exp(-m(I).\text{gamma}.h.Bo)/KT$$

The relative populations Nm(I) of nuclei occupying the m(I)th energy level is then given by

$$Nm(I)/Nm(I \pm 1) = \exp (\text{gamma}.h.Bo)/KT \qquad 3.5$$

There is therefore a surplus of nuclei in the lower energy levels a consequently a net magnetisation Mo in the direction of the applied field. As the probability of excitation from a given state is proportional to the population of that state, and the lower energy levels are more highly populated there will be a net absorption of energy on radiation. (See figure 3.1)

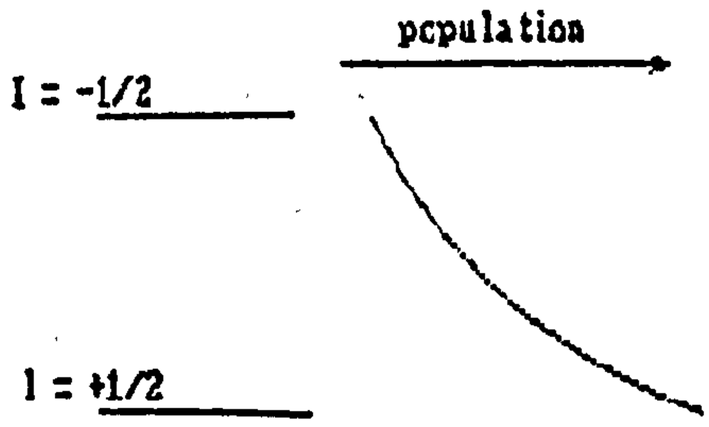

2 Possible energy levels with spins distributed amongst them according to Boltzmann's statistical theory.
(a)

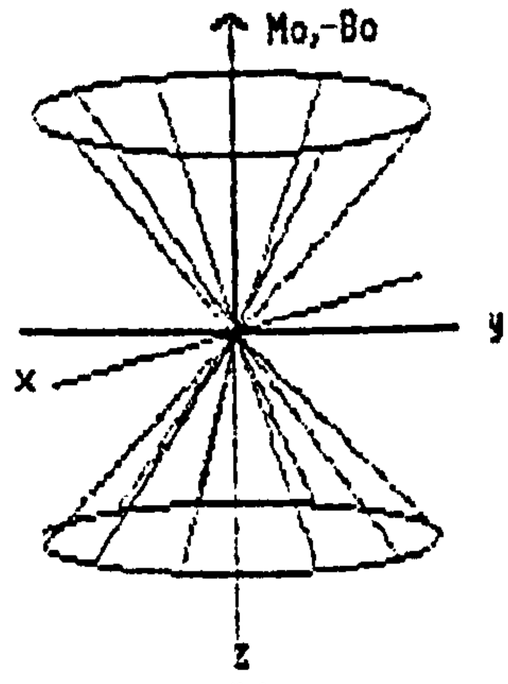

(b)

figure 3.1 The distribution of magnetic spins for a nucleus with I = 1/2.

3.2.2 The Bloch Equations.

The observable quantity measured in NMR spectroscopy is the vectorial sum of the individual nuclear magnetic moments M. The time dependence of the magnetisation vector in a magnetic field Bo is described classically by the famous Bloch'[9] equations. For a magnetic field in the z direction these can be summarised by a single vector equation,

$$dM(r,t)/dT = \text{gamma}.(M \hat{} Bo) - (Mx\,i + My\,j)/T2 - (Mz-Mo)k/T1 \qquad 3.6$$

The term gamma.M^Bo describes the effect of the torque experienced by the magnetic moment in the field. This torque causes the precession of the magnetisation vector about the z axis at the Larmor frequency Wo, which is identical to the angular frequency of the electromagnetic radiation required to match the resonance condition and induce transitions between energy levels.

The system has classical a classical analogue in a gyroscope. When a gyroscope rotating about its axis initially vertical is deflected frcm the vertical through an angle theta, the gyroscope, while continuing to rotate about its axis, precesses about the vertical. The rate of precession is depends on the mass distribution within the gyroscope and on the strength of the gravitational field.

In an analogous manner the individual nuclear magnetic moments and their resultant, the net magnetic moment Mo, when disturbed from equilibrium along the applied magnetic field will precess about the applied magnetic field Bo at a frequency proportional to that field, and dependent upon the 'mass' distribution within the nucleus, and therefore will be characteristic of it. In the event, the rate of precession is given by gamma.h.Bo where gamma has the same numerical value as in equation 3.1. Hence gamma is frequently termed the gyro-magnetic ratio.

It is this phenomena that allows the nuclear magnetic resonance to be observed. It is unnecessary to consider the nuclei individually; they can be represented by the net magnetic moment Mo. If this is disturbed from its equilibrium along the direction of the applied magnetic field Bo, Mo will precess about Bo. If a coil of wire is placed with its axis in the x-y plane perpendicular to the z axis, in the direction of the applied field direction, it will have a voltage induced in it as the flux passing through it changes as Mo precesses. This induced voltage signal which is proportional to the magnitude of Mo and the rate of precession, can be amplified and detected.

The second and third terms on the right of equation 3.6 were introduced by Bloch to account for the effects of spin-spin and spin-lattice relaxation respectively. They indicate that the component of magnetisation in the x-y plane decays in time to zero, whilst the component in the direction of the magnetic field relaxes to its equilibrium value Mo, as is determined by the Boltzmann distribution of nuclei amongst the available energy levels.

3.2.3 The Rotating Frame of Reference.

The application of an alternating magnetic field B1, perpendicular to the static field Bo and at the resonant frequency Wo = gamma.Bo, will induce transitions between the energy levels and cause a net absorption of energy from the radiation field. If the amount of energy absorbed by the spin systems is sufficient to equalise the populations, then the system is said to be saturated.

In addition to disturbing the equilibrium Boltzmann distribution of spins amongst the available energy levels, the perturbation caused by the field B1 also causes the individual spins to precess about the direction of the external field Bo in phase with each other to produce a net magnetisation in the x-y plane.

To understand the effects of the field B1, rotating at the Larmor frequency in the x-y plane it is convenient to consider the behaviour of the magnetisation vector M in a rotating frame of reference rather than the laboratory frame. Observed from a reference frame rotating at a frequency Wr about the z axis, a disturbed magnetisation would appear to precess at a frequency Wo ± Wr. Equation 3.6 is still valid provided that the magnetic field Bo is replaced by an effective field B_{eff}, such that

$$B_{eff} = Bo - Wr/gamma \qquad 3.7$$

Thus for a frame of reference (x',y',z'), rotating at the Larmor frequency Wo, the effective field B_{eff} is zero, and the magnetisation vector is stationary, existing as Mo in the z' direction at equilibrium.

The application of an oscillating magnetic field of strength 2.B1 and frequency Wo in the x-y plane of the laboratory frame of reference is equivalent to applying two counter-rotating fields each of strength B1 and rotating about the z axis with angular frequency +Wo and -Wo. One of these components rotates in the same direction as the nuclear spins and the other rotates in the opposite direction. The latter can be ignored as its interactions with the nuclei cancel to zero over each complete cycle. Viewed in the rotating frame of reference, however, the component rotating with the nuclei is stationary, and its interaction with Mo is not averaged to zero.

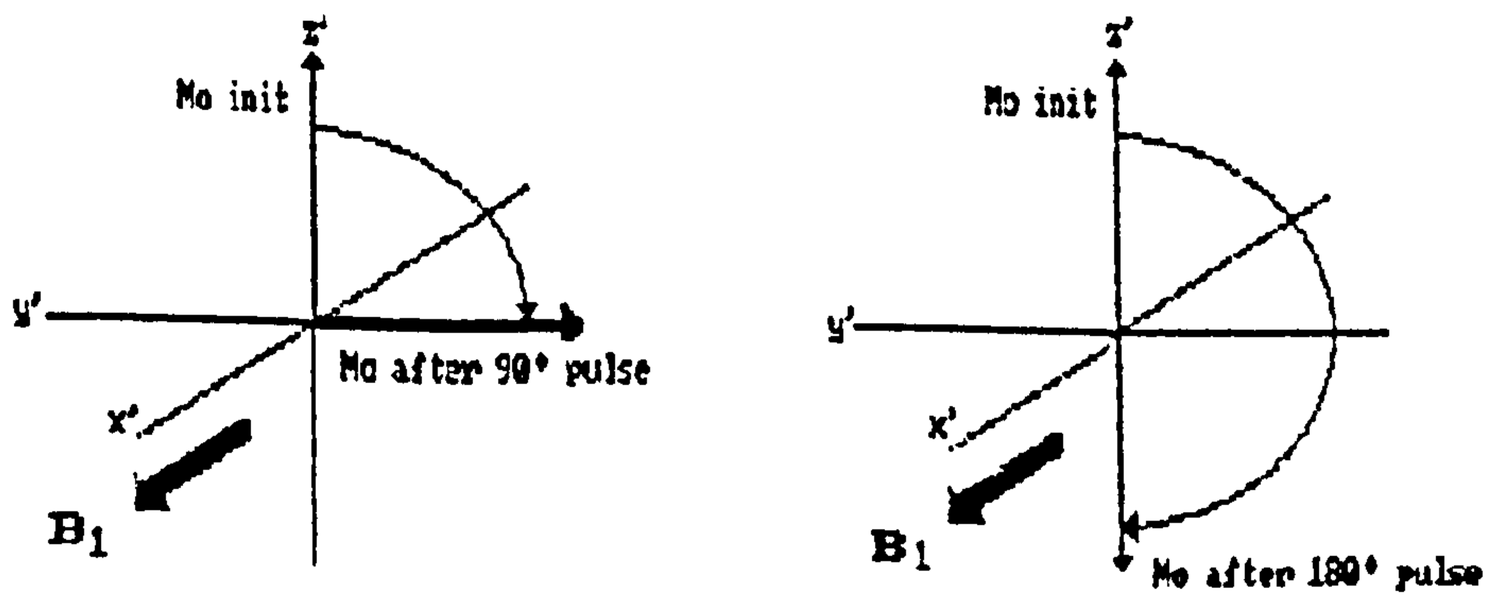

Figure 3.2 Effects on Mo of 90° and 180° pulsed magnetic field B1.

The laws of mechanics are independent of the frame of reference. Thus if B1 is applied along a specified direction (e.g. the x' axis) then the magnetisation precesses about the x' axis with an angular frequency of gamma.B1. In time t, the magnetisation vector precesses about B1 through an angle

$$\theta = \text{gamma.B1.t} \qquad 3.8$$

A pulse B1 of sufficient duration to tip the magnetisation vector into the x'-y' plane from the equilibrium along the z' axis is termed a 90 degree pulse. A 180 degree pulse rotates the magnetisation vector through 180 degrees about the direction of B1.(See figure 3.2)

3.2.4 Spin-Lattice (T1), and Spin-Spin (T2) Relaxation.

The return of an either completely or partially saturated system to equilibrium following the removal of a perturbing field B1, occurs via two simultaneous processes.

(i) Spin-Lattice Relaxation.

When attention is focused on a given spin system, all other nuclei and electrons in the sample are collectively referred to as the lattice. A transfer of energy to or from the lattice from the spin system, resulting from transitions of nuclei between upper and lower energy states, can be induced by the presence of fluctuating fields in the lattice, if there is a component at the appropriate frequency to induce transitions. This enables the return to a Boltzmann distribution of the nuclei about their energy levels at a rate which is characterised by the spin-lattice relaxation rate 1/T1.

(ii) Spin-Spin Relaxation.

The spins return to equilibrium with each other via spin-spin interactions between individual nuclei. This involves an exchange of energy between the nuclei of the same spin system so that a transition from an upper to a lower state is matched by a transition from a lower to an upper state. The simultaneous transitions cause a loss of phase coherence in the spin system without a change in the net energy of the system. Further loss of phase coherence arises from local field anomalies. Each nucleus in the spin system will interact

with non-zero magnetic fields produced by the lattice and other spins of the same system. As a result of these interactions there is a spread in the local fields, £B, experienced by different nuclei, which gives rise to a distribution of precessional frequencies.

The effect of spin flipping and local field anomalies on a system of nuclei precessing in phase following the application of an r.f. field B1, is a loss of phase at a rate gamma.£B. Hence the voltage induced in the detecting coil will decrease, representing a decrease in the component of the net magnetisation in the x-y plane. There will also be an additional loss of signal in the x-y plane as individual nuclear magnetic moments return to there equilibrium distribution with the lattice. The spin-spin relaxation rate 1/(T2*), is defined as the rate of loss of magnetisation in the x-y plane, which is therefore given by

$$1/T2^* = \text{gamma}.\pounds B + 1/T1 \qquad 3.9$$

3.2.5 Pulsed Nuclear Magnetic Resonance.

In pulsed NMR measurements B1 is applied to a spin system in a series of short duration, high powered pulses at the Larmor frequency. Usually these are in combinations of 90 degree and 180 degree pulses along the x' or y' axes of the rotating frame. The response of a nuclear spin system to a sequence of such pulses provides methods for measuring T1 and T2. Phase or diode detectors are employed to monitor the behaviour of the component of magnetisation in the x'-y' plane. Diode detection records the amplitude of the net voltage induced in the detecting coil and is in turn proportional to the net magnetisation in the x'-y' plane, whereas phase detection, using the r.f. source from which B1 is derived as a reference, detects the component of magnetisation along some particular direction in the x'-y' plane.

(i) The Free Induction Decay.

For a nucleus of spin 1/2 there are only two possible mj components, i.e. +1/2 and -1/2. These have different magnetic energies +μBo and -μBo. The ratios of the populations of these two states is given by

$$Nu/Nl = \exp(-2\mu Bo/KT) \qquad 3.10$$

In practice μBo << KT and the net magnetic moment is given by

$$\begin{aligned}(Nu-Nl) &= N/2 \times [(1+\mu Bo/KT)-(1-\mu Bo/KT-\ldots)] \\ &= N/2 \times 2\mu Bo.\mu/KT \\ &= (N\mu^2 Bo)/KT \qquad 3.11\end{aligned}$$

The amplitude of the signal immediately after a 90 degree pulse is therefore proportional to N, the number of resonant nuclei contained within the sample volume. In time the signal decays to zero as the nuclei return to equilibrium. The form of the decay is determined by T1, T2*, and experimental considerations such as the homogeneity of the applied magnetic field. This is the free induction decay (FID).

(ii) The Measurement of the Spin-Lattice Relaxation Time, T1.

Spin-lattice relaxation times in this work were measured using a 180-τ-90 pulse sequence. The application of a 180 degree r.f. pulse in the x'y' plane to a spin system in equilibrium inverts the magnetisation Mo, so that it lies in the -z' (-z) direction. Following this pulse spin-lattice relaxation begins and nuclei relax back to the +z' direction. After a time τ, the z' component of the magnetisation has a magnitude given by

$$Mz(\tau) = Mo \times [1 - 2\exp(-\tau/T1)] \qquad 3.12$$

To make the observation a 90 degree pulse is applied which enables an instantaneous measurement of Mz to be made by rotating it into the x'y' plane. Thus the initial height of the decay curve following the 90 degree r.f. pulse is proportional to Mz at time τ.

After a time of not less than 5 x T1 the spins have effectively returned to equilibrium and the sequence may be repeated using different values of τ. From the measurement of the initial signal amplitude, and using expression 3.12 a value of T1 may be determined.

(ii) The Measurement of the Spin-Spin Relaxation Time, T2.

An initial 90 degree r.f pulse applied along the x' axis to a spin system in equilibrium rotates the magnetisation Mo into the y' direction. The phase coherence is lost as a consequence of the combination of spin-lattice relaxation processes and the inhomogeneities in the static field at the site of the nuclear spins, some of which are due to other surrounding nuclear magnetic moments and some to the imperfections in the applied magnetic field. The observed FID does not therefore give a true measure of the spin-spin relaxation time T2, which should be independent of the applied field.

The loss of magnetisation in the x-y plane has been given by

$$1/T2^* = \text{gamma} \times \Sigma B + 1/T1 \qquad 3.13$$

Incorporating the two sources of the spread in the local fields at the sites of the individual nuclei, i.e. changes in the local field produced by other neighbouring nuclei and field inhomogeneities in the applied field, equation 3.13 may be expanded thus;

$$1/T2^* = \text{gamma} \times (\Sigma B\text{inhom.} + \Sigma Bs) + 1/T1 \qquad 3.14$$

The term $\delta B_{inhom.}$ is dependent upon the equipment whilst δB_s is determined by the sample. The spin-spin relaxation rate 1/T2 is defined as gamma.δB_s + 1/T1. To determine the spin-spin relaxation rate correctly some mechanism must be devised to eliminate the effects of applied field inhomogeneities, i.e. $\delta B_{inhom.}$ This can be achieved by the Hahn Spin-Echo experiment[10].

The sample is exposed to a 90 degree r.f, pulse causing the net magnetisation to rotate from the +z' direction to the y' direction. Nuclei will subsequently precess about the z' axis. Nuclei in the sample where the applied static field is higher than the mean will precess faster than those in weaker regions of the field. Viewed in the rotating frame of reference the spins dephase about the y' axis. An individual nucleus will precess through an angle θ relative to the mean.

$$\theta = \text{gamma} \times (\delta B_{inhom.} + \delta B_s) \times \tau \qquad 3.15$$

Incorporating the spin-lattice effects and resolving the magnetisation along the x' and y' axes

$$Mx'(\tau) = Mo \times [\sin(\text{gamma} \times (\delta B_{inhom} - \delta B_s) \times \tau)] \times \exp(-\tau/T1)$$

$$= Mo \times \sin(\theta) \times \exp(-\tau/T1) \qquad 3.16$$

and

$$My'(\tau) = Mo \times \cos(\theta) \times \exp(-\tau/T1). \qquad 3.17$$

If a 180 degree pulse is applied about the x' axis, Mx' remains unchanged but My' is reversed, becoming -My'. δB_{inhom} is unchanged, but as the 180 degree pulse has reversed the z' component of the fields due to all of the resonant nuclei, δB_s is also reversed.

The new precession rate is; gamma x (δB_{inhom} - δB_s)

After a further time τ,

$$My'(2\tau) = Mo \times [\cos(-\theta + \text{gamma} \times (\Delta B_{inhom} - \Delta B_s) \times \tau)] \times \exp(-2\tau/T1)$$

$$= Mo \times [\cos(\text{gamma} \times 2 \times \Delta B_s) \times \tau] \times \exp(-2\tau/T1) \qquad 3.18$$

The effects of ΔB_{inhom} have been eliminated, and summing over all resonant nuclei, 3.18 becomes;

$$My'(2\tau) = Mo \times \exp(-2\tau/T2^*) \qquad 3.19$$

The value of T2* could be derived by repeating the pulse sequence at different values of τ. Instead, spin-spin relaxation times in this work were measured using the method of Carr and Purcell[11], and incorporating the Meiboom and Gill[12] modification (CPMG).

An initial 90 degree pulse is applied to the spin system in equilibrium to rotate the magnetisation Mo into the y' direction. The effects of static field inhomogeneities on T2* can be removed if after a time τ a 180 degree r.f. pulse is applied along the x' axis. This rotates the spins about the x' axis so that the faster spins are now lagging in phase, while the slow spins are leading in phase. It requires a further time τ before the quickly precessing spins recover their phase loss and the slowly precessing spins lose their phase lead. At a time 2τ therefore, the spins will refocus along the y' axis and this will be seen as an echo in the magnitude of the magnetisation.

After the rephasing has occurred the spins once again begin to dephase. This process can be reversed by the same 180 r.f. pulse along the x' axis. A train of 180 degree pulses can be applied at intervals of 2τ, and echo signals observed in a one-shot experiment. This is the Carr-Purcell sequence.

This particular sequence is susceptible to a cumulative error. If the 180 degree pulse has been mis-set by an amount $\emptyset$, or is inhomogeneous, then an error of $\emptyset$ degrees will reduce the amplitude of the first echo by $\cos(\emptyset)$. After a second pulse the net error is $2\emptyset$ and the reduction in signal amplitude is $\cos(2\emptyset)$. After n pulses the cumulative reduction is $\cos(n\emptyset)$. Using the Meiboom-Gill modification of the Carr-Purcell sequence the phase of the 180 degree pulse is shifted so that the rotation induced by the refocussing pulse occurs about the y' instead of the x' axis. After the initial 90 degree pulse a nucleus precesses through angle of $+\frac{\pi}{2}$ relative to the y' axis. Following a rotation of 180 degrees the phase angle would be $-\frac{\pi}{2}$, and if the angle of rotation were to be less than 180 degrees by an angle $\varepsilon\emptyset$ then the magnetisation would be $\varepsilon\emptyset$ above the x'y' plane. After a time τ the dephasing has been cancelled out, but as the magnetisation is at an angle $\varepsilon\emptyset$ above the x'y' plane the signal is reduced by a factor $\cos(\varepsilon\emptyset)$. At a further time τ, the phase angle for the nucleus is again $+\frac{\pi}{2}$ relative to the y' axis, but $\varepsilon\emptyset$ above the x'y' plane. Rotation of an angle of $180-\varepsilon\emptyset$ about the y' axis using the same 180 degree r.f. pulse will take the magnetisation back into the x'y' plane and the effect of the mis-setting will have been reversed. (See Figure 3.3).

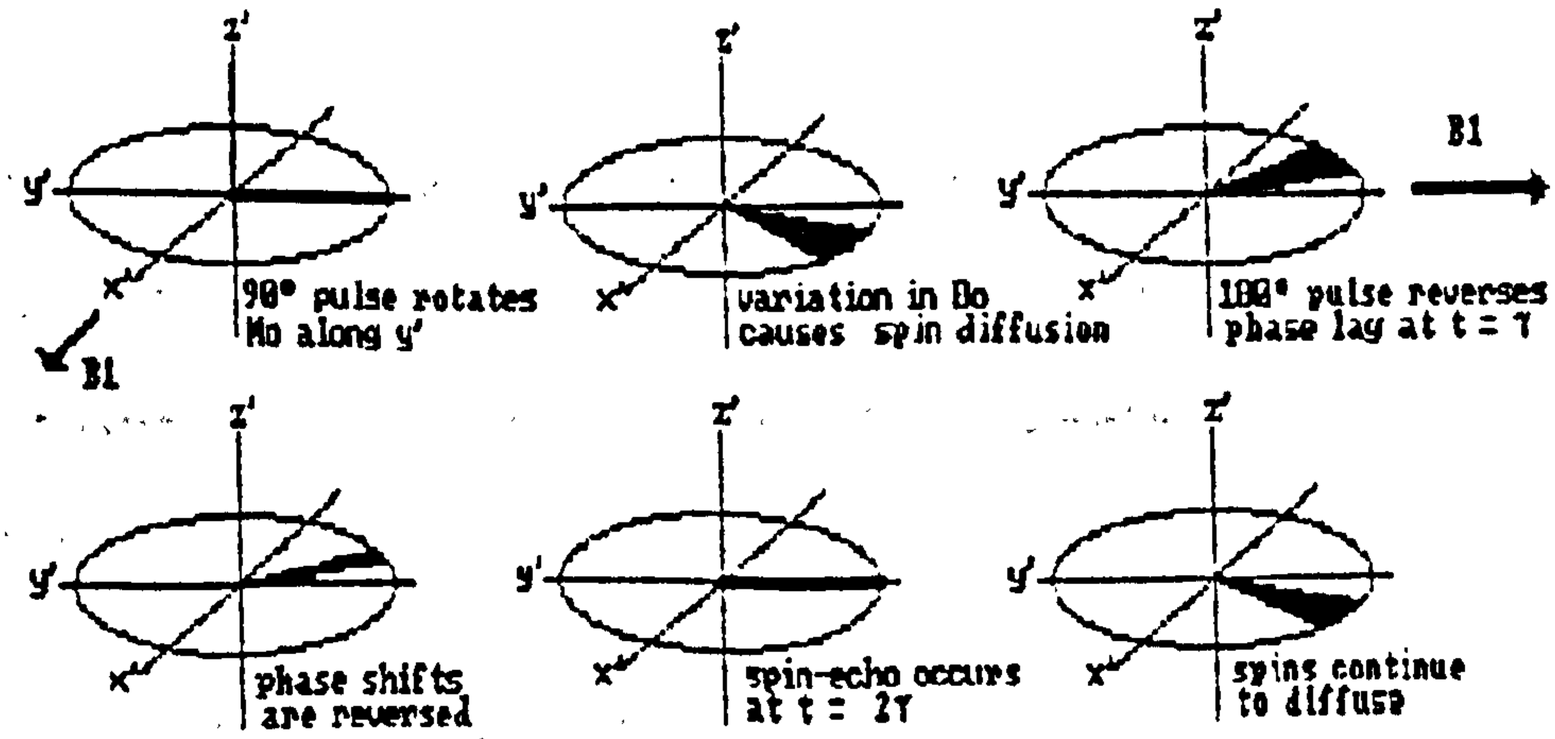

Figure 3.3a The formation of a spin echo using the CPMG pulse sequence for an ensemble of spins. External field Bo applied in -z' direction.

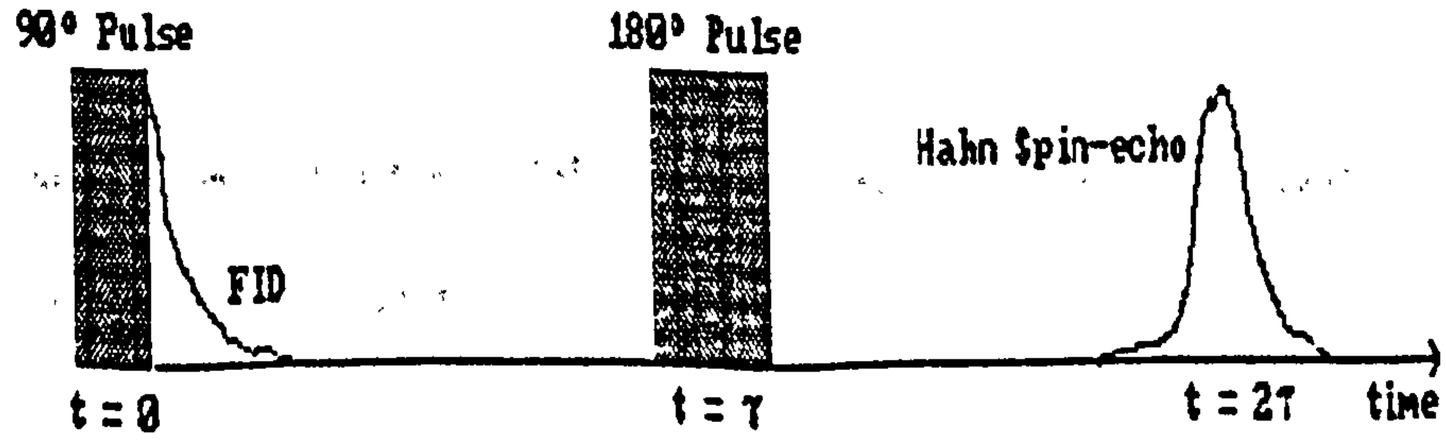

Figure 3.3b CPMG Pulse sequence. 180° pulse is phase shifted by 90°.

The spin-spin relaxation time may then be calculated via the relationship

$$M(t) = Mo \times \exp(-t/T2) \qquad 3.20$$

where M(t) is the height of the spine echo observed at time $t = 2n\tau$, $(n = 1,2,...)$.

3.3 The Interpretation of Relaxation times (T1 and T2) in terms of Molecular Events.

3.3.1 Mechanisms of Relaxation and the Bloembergen, Pound and Purcell[4] Theory.

Following the application of a sequence of pulses, a spin system will return to an equilibrium Boltzmann distribution. The principle mechanism of relaxation is through the interaction between nuclear magnetic moments and a magnetic field having a component of the correct frequency and polarisation to induce transitions between the energy levels of the spin system. In the case of dipolar spin-spin interactions these fields stem from the interaction of nuclear magnetic moment with the fields generated by its neighbouring nuclear magnetic moments.

In the presence of a large static magnetic field, the energy of a nucleus in the field due to its neighbours is represented as the sum of energies of that nuclear magnetic moment due to its magnetic interaction with each. The field at the nucleus i due to a neighbouring nuclei j is given by

$$\mu i.bj = (\mu i.\mu j / rij^3) \times (3\cos^2(\theta)-1)$$

$$\approx \frac{\text{gamma.h.li} \times \text{gamma.h.li}}{rij^3} \times (3\cos^2(\theta)-1) \qquad 3.20$$

rij is the separation of the two nuclei, and θ is the angle between the magnetic moment of the ith nuclei and the jth nuclei.

For nuclei of spin 1/2, mi can be +/- 1/2, leading to two quantum states which may be called αi and βi. For two neighbouring nuclei this leads to a total of four combinations of spin states; αiαj, αjβj, βiαj, βiβj.

Transitions can occur between all levels. The transition from αiαj to αiβj or βiαj, and transitions from αiβj or βiαj to βiβj represent changes in the state of a single nucleus that requires a change in the energy of state for the two nuclei of hWo.

The transition αiαj to βiβj involves the simultaneous transition of both nuclei and an energy 2hWo. The transitions from states αiβj to αiβj and from βiαj to βiαj involve the simultaneous transition of both nuclei, and no net transfer in energy between the system and the lattice is required.

The local internal field has several sources of origin. The magnetic moments of relaxing nuclei may be influenced by the fields produced by other magnetic particles such as other nuclei of similar or different spin systems, or unpaired electrons. The interactions between the moments may be direct dipolar couplings or indirect scalar couplings via electrons. Each nucleus in a sample will experience a field due to its neighbours which may add or subtract from the applied field. The dipole - dipole interactions predominate in the case of proton resonance spectroscopy.

The local field is determined by statistical considerations. At normal densities the width of the distribution is the order of 1 mT. In practice nuclei will move relative to each other and the field experienced by a given nuclei will change. One can define an auto-correlation function of the form

$$G(\tau) = \frac{B(\tau) \times B(t+\tau)}{B^2(t)} \qquad 3.21$$

where B(t) is the local field experienced by a given nucleus at time t. G(τ) describes the coherence of random molecular processes with time. The spectral density at a frequency W, representing the component of motion at a frequency W is the Fourier transform of G(τ);

$$J(w) = \int_{-\infty}^{+\infty} G(\tau)\exp(-iWt)\,dt \qquad 3.22$$

It is usual to assume that G(τ) is expanded in character so that

$$G(\tau) = G(0) \times \exp(-\tau/\tau c), \qquad 3.23$$

leading to;

$$J(w) = G(0) \times \frac{2\tau c}{1 + w^2\tau c^2} \qquad 3.24$$

τc is a function of the temperature of the sample, and figure 3.4 shows the form of J(w) for different values of τc. The component of the locally oscillating field at any frequency below the correlation frequency wc = τc^{-1} is constant. Above wc the spectral density function quickly falls to zero.

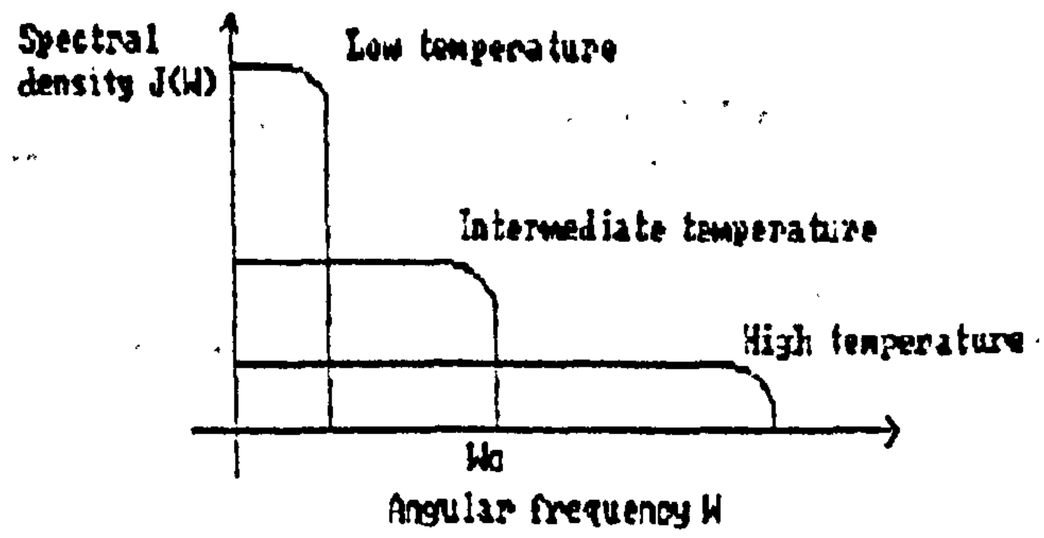

Figure 3.4 The spectral density function J(W) shown for high, low and intermediate temperatures.

Bloembergen, Pound and Purcell considered the magnetic relaxation for a system of similar spins with an angular spin quantum number I = 1/2, undergoing random isotropic motion. They assumed that the only contribution to the fluctuating lattice field was from the dipole-dipole interactions between the spins, which could be described by a single correlation time τ_c.

Using time-dependent perturbation[13] theory they showed that for such a system, components of the local field at frequencies ω_o and $2\omega_o$ could contribute to the spin-lattice relaxation such that

$$\frac{1}{T_1} = \frac{2}{3}\sigma^2.\left[\, J(\omega_o) + 4J(2\omega_o) \,\right] \qquad 3.25$$

$$= \frac{2}{3}\sigma^2.\left[\frac{\tau}{1+\omega_o^2\tau^2} + \frac{4\tau}{1+4\omega_o^2\tau^2}\right] \qquad 3.26$$

where $\sigma^2 = 9/20.\gamma^2.\Sigma\, r_{ij}^{-6}$, and r_{ij} is the distance between the ith and jth interacting spins. σ^2 is termed Van Vleck's rigid lattice second moment.

In addition to the component of the spectral density at ω_o and $2\omega_o$, there is a contribution to the spin-spin relaxation time from the low frequency component of J(0).

$$\frac{1}{T_2} = \sigma^2.\left[3\, J(0) + \frac{5}{3}J(\omega_o) + \frac{2}{3}J(2\omega_o)\right] \qquad 3.27$$

$$= \sigma^2.\left[\tau + \frac{5\tau}{3(1+\omega_o^2\tau^2)} + \frac{2\tau}{3(1+4\omega_o^2\tau^2)}\right] \qquad 3.28$$

The functions of equations 3.26 and 3.28 are described by the log-normal plot in figure 3.5. It has been assumed that the correlation time has an Arrhenius temperature dependence, i.e.

$$\tau = \tau \times \exp(E/RT) \qquad 3.29$$

where R is the universal gas constant. T is the absolute temperature. and E is an apparent activation energy for the motions described by the nuclei leading to the fluctuating local field.

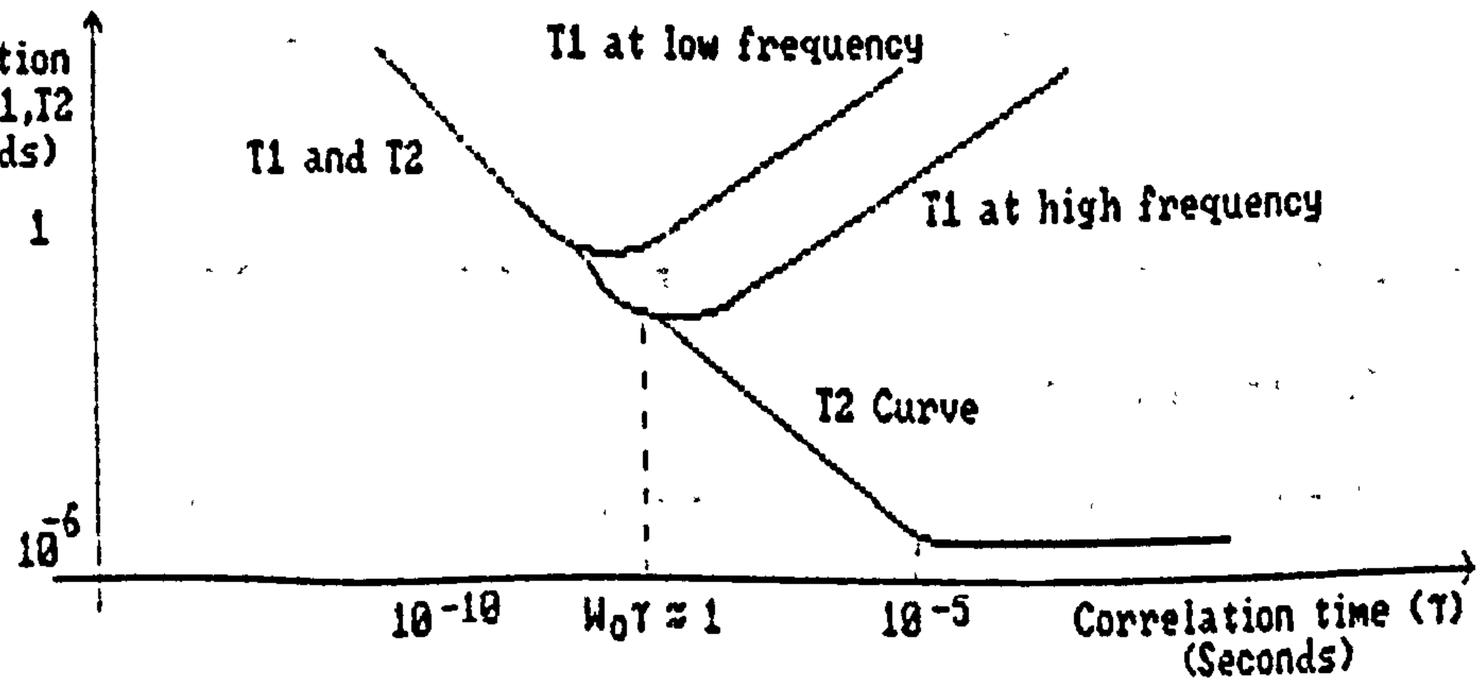

Figure 3.5 Behaviour of T1 and T2 with Correlation time (τ) - BBP Theory.

These curves have been used to predict the behaviour of T1 and T2 over a range of temperatures in liquids where a single correlation time may be used to describe the local field fluctuations. It can be seen that T1 passes through a minimum at the point where the rate of molecular motions are closest to the resonant frequency. i.e. when $\omega c\tau = 1$. At lower values of τ. T1 is equal to T2. This is a consequence of the extreme motional narrowing in this region. As τ increases, the J(0) term of equation 3.27 increasingly dominates the spin-spin relaxation. and causes T2 to decrease until the rigid lattice condition sets in.

The components of J(w) corresponding to rapid motions do not contribute to the dephasing process because they are averaged out. The time scale over which the dephasing occurs is T2. If dephasing were the sole factor determining relaxation. then because

$$\theta i = \int_0^{T_2} \text{gamma.Bi(t).dt} \qquad 3.30$$

is the dephasing angle of nucleus i at a time t, T2 would be defined such that

$$\langle \cos [\text{gamma}. \int_0^{T_2} Bi(t).dt] \rangle = 1/e \qquad 3.31$$

and only components of motion up to a frequency of 1/T2 would be effective in the dephasing process. 1/T2 is proportional to the integral of J(w) from 0 to 1/T2.

As the temperature is decreased a condition is reached where the correlation frequency is less than the static line width 1/T2, which is proportional to $\sqrt{\sigma}$, the square root of the rigid lattice second moment. Further reduction in the correlation frequency does not result in any change in the integral, and the spin-spin relaxation rate remains unchanged.

3.4 Heterogeneous Systems

The behaviour of T1 and T2 for bulk water is adequately described by the BPP theory of section 3.3.1. Hydration water in heterogeneous systems, however, exists in a variety of states of molecular motion arising from interactions with its environment. A single correlation time is no longer sufficient to characterise the kinetic properties of such complex systems, and a number of extended theories have been proposed to account for the T1 and T2 observations.

The characteristics are that the relaxation rates are considerably enhanced over bulk water values at all frequencies and temperatures, T1 values exceed T2 values at all temperatures including those above that at which the T1 value is a minimum, T1 exhibits a frequency dependence that is inconsistent with simple BPP theory. There is also a detectable unfrozen water component in many samples at temperatures below 0°C, which cannot be explained simply by assuming that the water molecules exhibit a restricted mobility, because the relaxation rates are considerable enhanced over bulk water values.

3.4.1 The discrete Multiphase model.

It has been proposed that water in heterogeneous systems exists in a number of discrete 'phases'[1][2]. Two such phases are normally envisaged; one containing 'free' water molecules with properties resembling those of water in the bulk, and the other containing water molecules which interact to some degree with the substrate material. The molecular motions of this interacting water may be restricted or modified in a number of ways. For this reason it has been termed 'bound water'.

Exchange of nuclei between the two phases proceeds at rates which determine the NMR relaxation characteristics of the system. In general an NMR measurement cannot resolve a population of nuclei into separate phases if the nuclei effectively experience all possible states during the period of magnetic relaxation. The two phases under these conditions are said to be in rapid exchange, and an observed relaxation rate 1/T' is given by the weighted average of the relaxation rates of the individual phases.

i.e.
$$\frac{1}{T'} = \frac{Pa}{Ta} + \frac{Pb}{Tb} \qquad 3.32$$

where Pa and Pb are the populations, and Ta and Tb are the relaxation times of the bound and free phases.

Water molecules in the bulk typically reorientate at a rate $Wc \approx 10^{12}$ Hz. 1/T2 is proportional to Wc and has a value of about 1 $sec._1$. In bulk ice the water molecule mobility is restricted and $Wc \approx 10^{4}$ Hz. The spin-spin relaxation rates are therefore in the order of 10^{4} sec^{-1}, giving T2 values of a few microseconds.

When adjacent to a surface of slow moving macromolecules the water molecules exhibit an intermediate reorientation rate characterised by Wc values in the order of 10^7 Hz, corresponding to intrinsic spin-spin relaxation times of milliseconds. Hence if a system exists where 1% of the water is bound and exchange is rapid between the bound and free phases then the relaxation will be dominated by the bound phase.

In the limit of slow exchange the lifetimes of the spins in each environment are long compared to the respective relaxation times, and each environment effectively relaxes independently. The two phases will be observed separately if the spectrometer conditions are appropriate. The observed magnetisation decay is a sum of two decays such that

$$M(t) = M(0) \times [\, Pa.\exp(-t/Ta) + Pb.\exp(-t/Tb) \,], \quad 3.34$$

where for longitudinal relaxation $M(t) = M(0)-Mz(t)$, and for transverse relaxation $M(t) = My'(t)$. In favourable conditions the two components of relaxation may be resolved and the true value of Pa, Pb, Ta and Tb found.

The extension of to three or more discrete phases is straight forward, and equation 3.32 becomes

$$\frac{1}{Tobs} = \sum_{i=1}^{n} \frac{Pi}{Ti} \quad 3.35$$

for the case of rapid exchange, and in the limit of slow exchange equation 3.34 becomes

$$M(t) = M(0) \times \sum_{i=1}^{n} Pi.\exp(-t/Ti). \quad 3.36$$

For intermediate rates of exchange where the lifetimes of the spins within each environment are comparable with the respective intrinsic relaxation times, the decay of magnetisation may still be described by equation 3.36 provided that the true values of Pi and Ti are replaced by apparent fractional populations Pi' and apparent relaxation times Ti'.

The case of intermediate exchange has been discussed by Zimmerman and Brittin. The expressions for the observed relaxation become simpler when Ta >> Tb, and Pa >> Pb, in which case

$$\frac{1}{T_{obs}} = \frac{P_b}{(\tau_b + T_b)} + \frac{P_a}{T_a} \qquad 3.33$$

where τ_b represents the lifetime of the spins in the bound phase.

In the two-phase case, expressions for Pa', Pb', Ta' and Tb' have been determined for a number of special cases[115-117]. The results are complex functions of the true parameters, the lifetimes of the spins in each phase, τ_a and τ_b, and the resonant frequency of each phase. A graphical description of the effects of nuclear exchange on these parameters, where it is assumed that the act of transfer is not itself a relaxation mechanism, is presented below.

In figure 3.6, the effects of nuclear exchange on the apparent fractional population of the slow relaxing component Pa' is shown in terms of a reduced nuclear transfer rate $R_{\tau b} = P_b.T_b/\tau_b$, for a system in which Pa = Pb, Ta = 100.Tb, and $W_{oa} = W_{ob}$. When $R_{\tau b}$ reaches approximately 3, Pa' tends to unity, and since Pa'+Pb' = 1, the apparent fractional population of the fast relaxing phase Pb' tends to zero. In other words the fast relaxing state appears to be emptying and in general if $R_{\tau b} > 2$ it is not possible to detect two separate relaxation times experimentally[117].

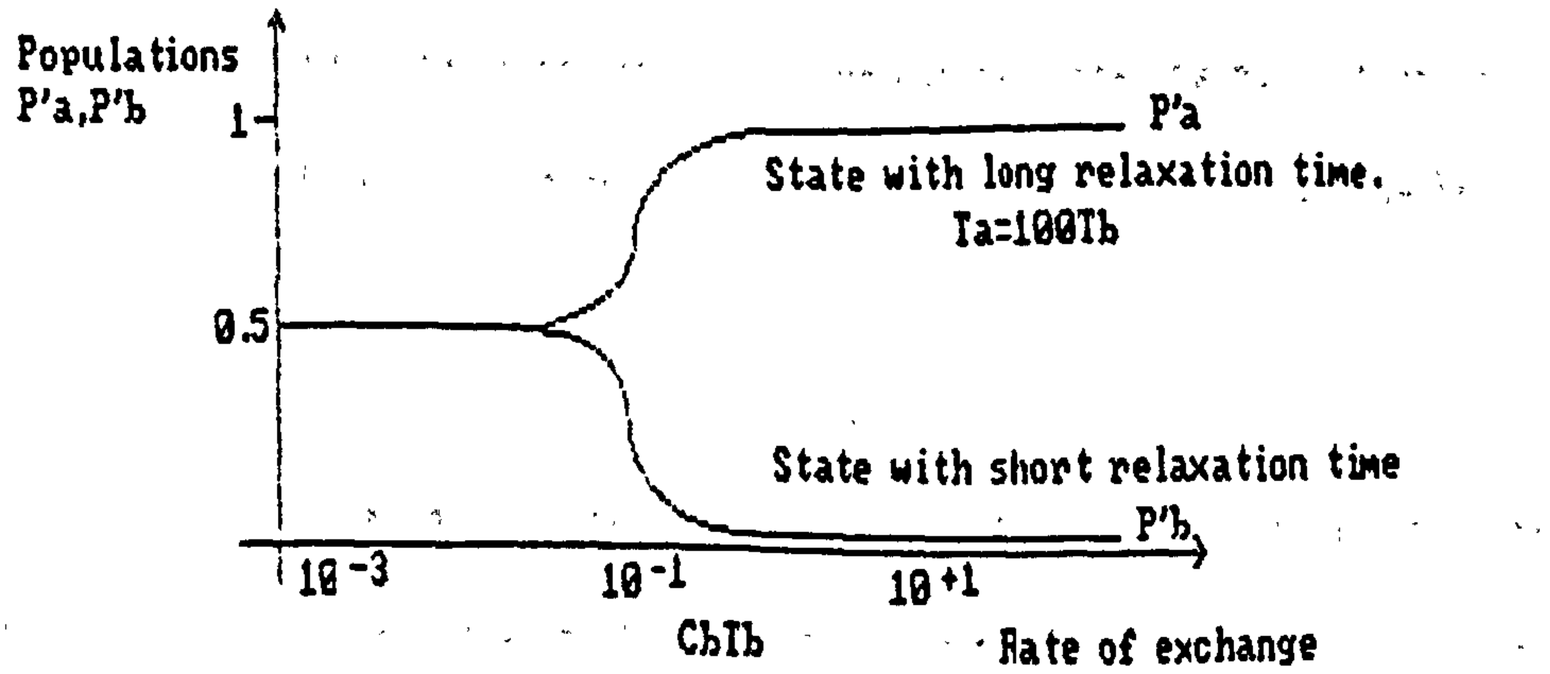

Figure 3.6 Apparent fractional populations as a function of exchange rate.

Figure 3.7 shows the effects of the reduced nuclear transfer rate R_{Tb}, on the ratio of the apparent spin-spin relaxation times to the true relaxation times. Similar curves are found for spin-lattice times. The most striking feature is that both apparent relaxation times decrease with increasing exchange rate, the effects on the long relaxation time being more pronounced at lower exchange rates than for the fast relaxing component. It is possible for Pa', Pb' and Tb' to be close to their true values while Ta' is several times smaller than Ta.

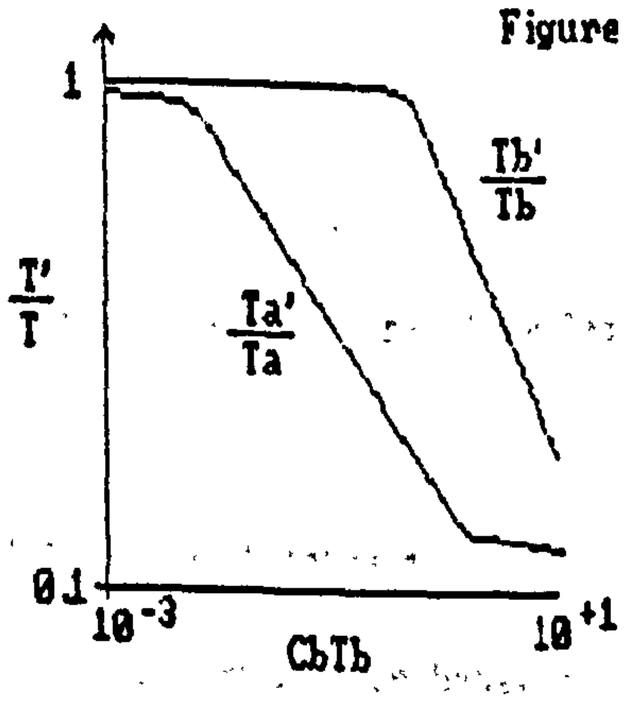

Figure 3.7 The effect of nuclear exchange on apparent relaxation times of a two state system, with Wa = Wb, Pa = Pb, and Ta = 100Tb.

Nuclei exchange bettween states a and b at a rate Ca, and vice-versa at a rate Cb.

The behaviour of Ta' and Tb' over a range of temperatures will be a function of the separate temperature dependences of the correlations times for phases a and b, modified by the effects of nuclear exchange described above. If nuclear exchange dominates then the relaxation times will decrease with increasing temperature in contradiction to the behaviour predicted by BPP theory.

Since T1 is usually greater than T2 for nuclei in absorbed systems it is possible that the exchange is rapid in comparison with T1, and yet slow compared with T2. In this case it is possible for two-phase behaviour to be observed for spin-spin relaxation but not for spin-lattice relaxation. since τb may satisfy both $Pb.T2b/\tau b << 1$ and $Pb.T1b/\tau b >> 1$ simultaneously.

In general, numerical solutions can be found for systems in which discrete phases exchange magnetisation via the transfer of nuclei. Bound water is often identified with non-freezing water. Typically relaxation times of non-freezable water ≈ 1 mS as used in our example. The T1 minimum for non-freezable water is typically between -10°C and -50°C and is frequency dependent. Room temperature is above the T1 minima, and exchange between the bound and free phases cannot explain why $T1 >> T2$, and why there is a frequency dependence of T1.

3.4.2 A Distribution of Correlation Times.

In the discrete multiphase model it is assumed that a quantity of highly immobilised water determines the relaxation behaviour of the bulk through exchange processes. A variation on BPP theory in contrast with this is one in which all the water molecules in heterogeneous systems are considered to be in continuous long-range interaction with the substrate. This

leads to a continuum of motional properties which may be described by a distribution of correlation times[18-20]. This distribution may be expressed as a density function $\mathcal{J}(\tau)$ such that;

$$\int_0^\infty \mathcal{J}(\tau).d\tau = 1 \qquad 3.37$$

The relaxation times T1 and T2 are then obtained by averaging the BPP expressions over the distribution to give;

$$\frac{1}{T1} = \frac{2}{3}\sigma^2.\left[\int_0^\infty \frac{\tau.\mathcal{J}(\tau).d\tau}{1+\omega_0^2\tau^2} + 4\int_0^\infty \frac{\tau.\mathcal{J}(\tau).d\tau}{1+4\omega_0^2\tau^2}\right] \qquad 3.38$$

and

$$\frac{1}{T2} = \sigma^2.\left[\int_0^\infty \tau.\mathcal{J}(\tau).d\tau + \frac{5}{3}\int_0^\infty \frac{\tau.\mathcal{J}(\tau)d\tau}{1+\omega_0^2\tau^2} + \frac{2}{3}\int_0^\infty \frac{\tau.\mathcal{J}(\tau)d\tau}{1+4\omega_0^2\tau^2}\right] \qquad 3.39$$

The density function which has been most frequently applied is that of a log-normal distribution. Here the binding energies of the water molecules are represented by a Gaussian distribution function. (See figure 3.8). The Gaussian distribution is specified in terms of a width parameter β, and a median correlation time τ^*

i.e. $$\mathcal{J}(\tau)d\tau = (\beta\pi)^{-\frac{1}{2}} \exp(-\beta^2Z^2) \qquad 3.40$$

where $$Z = \ln(-\tau/\tau^*) \qquad 3.41$$

Other types of distribution functions have been proposed to describe the variation in binding energies of the molecules in the system under investigation. All introduce variables that are analogous to τ^* and β.

Variations of τ^* with temperature are governed by thermal activation laws. Two such laws have been largely considered;

(a) the Eyring form given by $\tau^* = \frac{\tau^*_0 . \exp(E/RT)}{KT}$

(b) the Arrhenius form given by $\tau^* = \tau^*_0 . \exp(E/RT)$

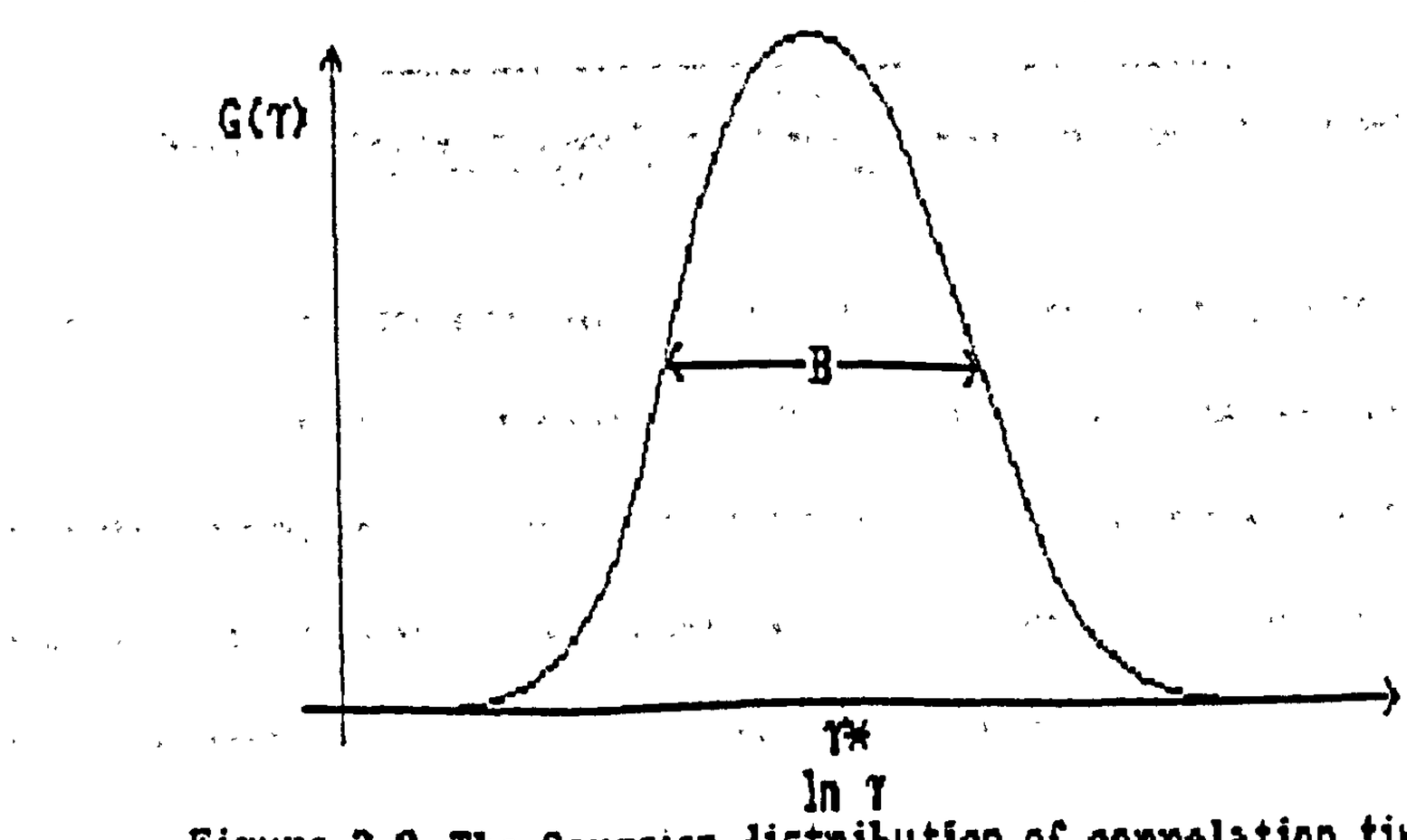

Figure 3.8 The Gaussion distribution of correlation times.

The effects of increasing heterogeneity in the system is reflected in an increasing width parameter β. An increase in the hydration level will decrease a without notably effecting τ^*.

Figure 3.9 shows the effect of changing the width parameter β on T1 and T2 as a function of reciprocal temperature, T, where the Eyring form of thermal activation law is assumed to describe the behaviour of τ^*.

As the heterogeneity increases the activation enthalpy as determined from the slope of T2 curve decreases. This is matched by an increase in the ratio T1:T2 at and above the temperature of the T1 minimum. The minimum itself becomes less pronounced as the curves become shallower with increasing β.

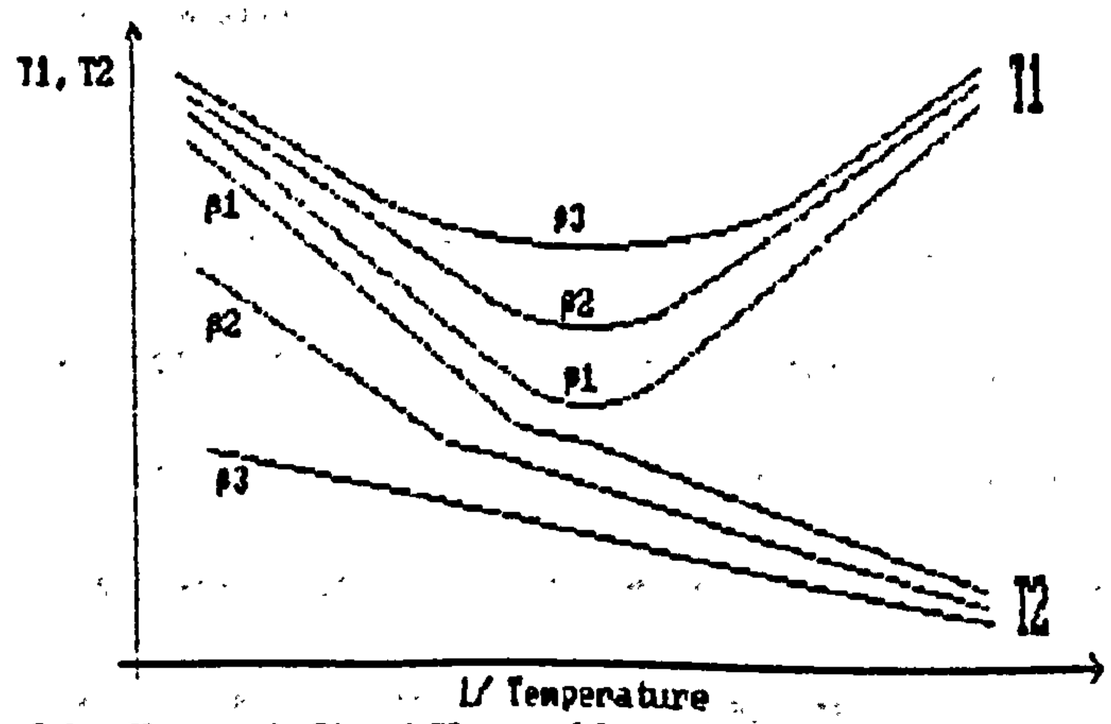

Figure 3.9 Changes in T1 and T2 caused by an increase in the range of distribution of correlation times, τ. $\beta 3 > \beta 2 > \beta 1$.

In some circumstances a may have a temperature dependence, and this causes the minimum in the T1 curve to be shifted from where $w\tau^* = 0.6158$. In addition T1 may vary asymmetrically about the minimum, and the temperature dependence on T2 will be increased as compared to the case when β is a constant. In models where a temperature dependent β has been required to match experimental data with theory, an inverse relationship has been used.

Resing[115] defined a cut-off value of the correlation time τ_R, above which rigid lattice behaviour is observed. On lowering the temperature of a system in which there is a continuous distribution of correlation times there is a gradual transition to the rigid lattice state, with those molecules having the longest correlation times reaching the rigid lattice cut-off point first. The result is a decrease in the observed population of the heterogeneous phase and has been consequently described as a phase transition. To incorporate this effect into the calculations for T1 and T2 the range of integration in equations 3.38 and 3.39 are changed to the cut off value τ_R. With this modification the model has been successful in predicting the behaviour of T1 and T2 in a number of systems.

In systems where a distribution of correlation times exist, values for Van Vleck's second moment, the distribution width parameter β, and the activation energy of relaxation mechanisms can be theoretically determined.

3.4.3 - Cross-Relaxation Effects.

In addition to the transfer of magnetisation via the exchange of nuclei between phases, it has been acknowledged that a transfer of magnetisation can result from magnetic interactions between nuclei at the interface[21-25]. Coupling by spin interactions across the interface results in cross-relaxation effects including magnetisation transfer between the phases. The mechanisms of magnetisation transfer at the interface, and diffusion of magnetisation within the bulk phases enable the population with the greater relaxation rate to act as a magnetic sink for the rest of the population. The driving force for this process of magnetisation transfer is the difference in 'spin temperatures' created by the different intrinsic relaxation rates of the two phases. If the intrinsic relaxation rates of the two populations are similar, then there is no detectable effect unless the populations are selectively excited to different magnetisations.

When the populations are each kept isothermal by rapid diffusion of spin magnetisation, which in liquids takes place via molecular or nuclear diffusion and exchange, and in solids where there is sufficiently strong spin-spin interaction, via spin diffusion, the contribution from the cross-relaxation effects may be incorporated into the relaxation equations for the two populations I and S to give;

$$\frac{d(I-Io)}{dt} = -(R_I - R_T).(I-Io) + \left[\frac{R_T}{F}\right].(S-So) \qquad 3.42$$

$$\frac{d(S-So)}{dt} = -\left[R_s + \frac{R_T}{F}\right] x\ (S-So) + R_T(I-Io) \qquad 3.43$$

Where Io and So are the magnetisation of the two phases at equilibrium, R_I and R_S are the relaxation rates appropriate to isolated I and S spins, R_r is the rate of transfer of magnetisation between I and S spin systems, and F is the ratio of the spin populations.

At equilibrium Io = So/F

The solution of these coupled equations is a two-component spin-lattice decay for the I and S components.

In most cases where data has been analysed by incorporating the cross-relaxation effect, the exchange of magnetisation and a resulting modification to the spin-lattice relaxation time have generally been considered to be the only consequences of the cross relaxation. It has been demonstrated experimentally, however, that direct spin-spin relaxation is also a consequence.

3.4.4 Anisotropic Motion.

The couplings which govern NMR relaxation mechanisms have been discussed in section 3.2.1. They are vector quantities. In liquids the constant tumbling motions of the spins causes an average value for their couplings to be observed. For example the local field experienced by one nucleus as a result of the dipole moment of a second depends upon the angle θ between the inter-nuclear vector and the external field. It may have one of two values depending on the relative orientation of the two spins, given by

$$\delta B = +/- K_\theta.(3\cos^2(\theta)-1) \qquad 3.44$$

where K_s is the dipolar coupling constant. An isolated water molecule would therefore yield a doublet resonance spectrum. In liquid water the local field effects are dynamically averaged to zero, and a single resonance is observed. The random orientations of the molecules produce no preferred orientations of the inter-proton vector and so there is no angular dependence or splitting of the spectrum.

When water molecules interact with molecular systems some motional anisotropy may be imposed on the water. If there is macroscopic anisotropy of the substrate such as occurs in fibrous and laminar materials, the anisotropy will extend throughout the sample and can be observed as a dependence of the magnetic resonance properties on the orientation of the specimen in the magnetic field[26-28].

In the case of dipolar couplings the local fields given by equation 3.44 may have a non-zero time average value. Since the rate of T2 relaxation is determined by these dephasing fields 1/T2 exhibits the same dependence on the angle θ.

Anisotropic effects are more noticeable in T2 than T1, since it is the low-frequency components of the local fields which have an angular dependence. If there exists macroscopic anisotropy but no long-range order in the sample powder type spectra will be obtained. If the scale of the anisotropy is such that the water molecules experience many domains in the time scale of the NMR experiment an isotropic averaging will occur, and there will be no observable angular dependence of the magnetic resonance properties.

3.5 Diffusion.

Diffusion may be described as the general transportation of matter from one part of a system to another, such that molecules or ions mix, through normal thermal agitation. In wood there exists two fundamental types of diffusion. the first being 'dynamic' or 'driven' diffusion caused by initial concentration gradients of the diffusing species. The second type of diffusion is 'static' or 'self' diffusion, whereby molecules diffuse with respect to one another without any changes in the local concentrations, and is a consequence of random motion.

In this work it is the latter which has been investigated. The self-diffusion coefficient $\underline{D}$ is defined by Fick's law; in a single or multi-component system where there exists uniform macroscopic concentrations, the one-dimensional form of Fick's[29] second law states that;

$$\frac{\underline{d}\,P(x,t)}{dt} = Dx\,\frac{\underline{d^2}P(x,t)}{dx^2} \qquad 3.45$$

where $P(x,t)$ is the probability that the position of one particular molecule of the species under consideration is at a position x at a time t.

In an isotropic medium this equation may be extended to a three dimensional form;

$$\frac{\underline{d}\,P(\underline{r},t)}{dt} = D\,\underline{del^2}P(\underline{r},t) \qquad 3.46$$

In an anisotropic medium the value of $\underline{D}$ is often orientationly dependent

and the equation 3.46 needs modification. Choosing a rectangular system of co-ordinates (x_1, x_2, x_3) for example, with D_1, D_2, and D_3 as the principle diffusion coefficients, equation 3.46 becomes;

$$\frac{d\,P(\underline{r},t)}{dt} = D_1\frac{d^2P}{dx_1^2} + D_2\frac{d^2P}{dx_2^2} + D_3\frac{d^2P}{dx_3^2} \qquad 3.47$$

3.5.1 Solutions to the Diffusion Equation.

Solutions to equation 3.46 describing diffusion in an isotropic medium may be found for a variety of initial and boundary conditions[30]. The method of separation of variables is used whereby the probability density function $P(\underline{r},t)$ is expressed as the product of a spatial and a temporal function. For an unbounded isotropic medium the solutions in one, two, and three dimensions are given below;

(a) One dimensional case, $P(x_0:x,t) = (4\pi Dt)^{-\frac{1}{2}}\exp[-(x-x_0)^2/4Dt]$ 3.48

where $P(x_0:x,t)$ is the probability that a molecule initially at x_0 will diffuse to position x in time t.

(b) Two dimensional case, $P(\underline{r}_0:\underline{r},t) = (4\pi Dt)^{-1}\exp[-(\underline{r}-\underline{r}_0)^2/4Dt]$ 3.49

where $\underline{r} = (x,y)$

(c) Three dimensional case, $P(\underline{r}_0:\underline{r},t) = (4\pi Dt)^{-3/2}\exp[-(\underline{r}-\underline{r}_0)^2/4Dt]$ 3.50

where $\underline{r} = (x,y,z)$

The one dimensional solution describes diffusion in a one dimensional medium, and also diffusion in any specified direction within an isotropic plane (i.e. two dimensions), or within a three dimensional isotropic medium. Figure 3.10 describes the shape of the probability density function for any specified direction at three successive values of time t.

The mean-square displacement $\overline{r^2}$ of molecules diffusing in an isotropic media is calculated from the density functions

$$\overline{r^2} = \int_{-\infty}^{+\infty} r^2 . P(\underline{P_0} : \underline{r}, t)\, d\underline{r} \qquad 3.51$$

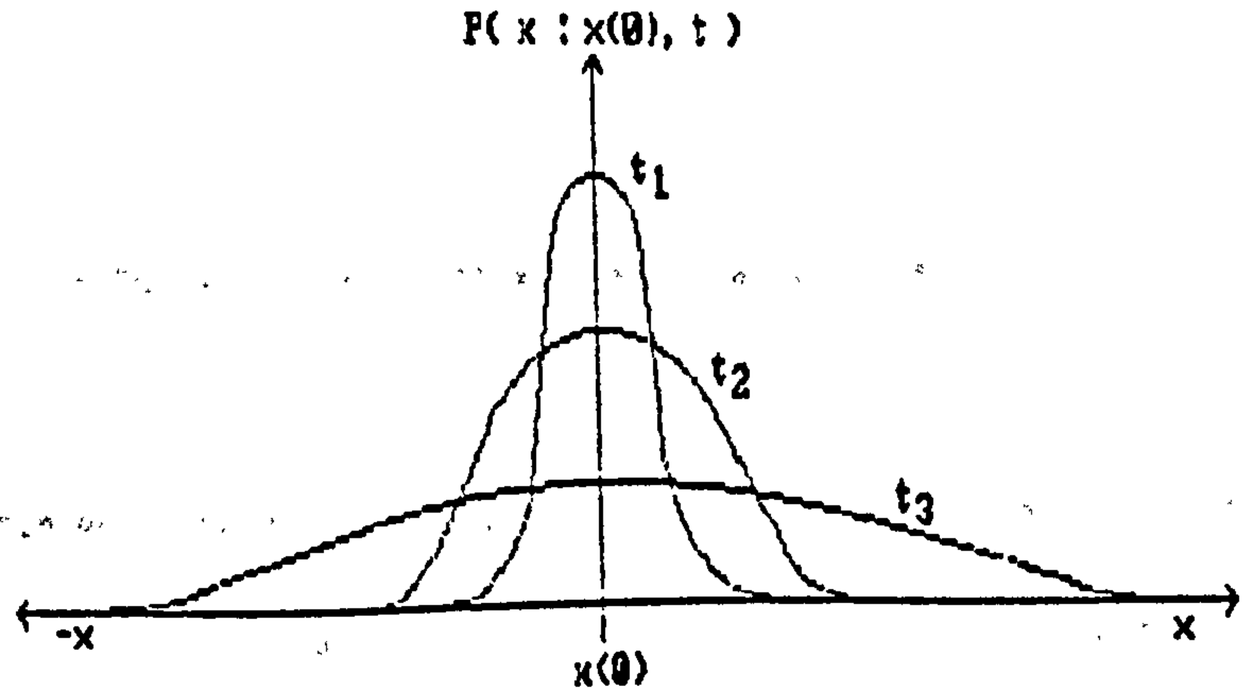

Figure 3.10 The shape of the probability density function P(x : x(0), t) for a molecule initially at x(0) for three successive times t_1, t_2, t_3.

For the one dimensional case this yields $\overline{x^2} = 2Dt$.

In a plane; $\overline{r^2} = 4Dt$, $\left(\overline{r^2} = \overline{x^2 + y^2} \right)$ 3.52

and in three dimensions $\overline{r^2} = 6Dt$, $\left(\overline{r^2} = \overline{x^2 + y^2 + z^2} \right)$. 3.53

Solutions to Fick's second law for anisotropic media described by equation 3.47 may be obtained in a similar manner to that employed in the isotropic case. For unrestricted diffusion in a direction parallel to one of the principle axes x_1, x_2, or x_3, the probability density function takes the form;

$$P(x_{o,i}:x_i,t) = (4\pi D_i t)^{-\frac{1}{2}}\exp[-(x_i-x_{o,i})^2/4Dt], \quad i=1,2,3 \quad 3.54$$

which is equivalent to equation 3.48. For the more general three-dimensional case;

$$P(\underline{r}_o:\underline{r},t) = (4\pi D_1 D_2 D_3 t^3)^{-\frac{1}{2}}\exp\left[-\frac{(x_1-x_{1o})^2}{4D_1 t} - \frac{(x_2-x_{2o})^2}{4D_2 t} - \frac{(x_3-x_{3o})^2}{4D_3 t}\right] \quad 3.55$$

The mean square displacements are then found using equation 3.51, and for diffusion along one of the main axes this yields $x^2_i = 2D_i t$, where i = 1,2,3.

3.5.3 The theory of Spin-Echo Self-Diffusion Measurements[4-8].

In the Hahn spin-echo experiment field gradients attenuate the amplitude of the echo when the resonant nuclei are susceptible to translational diffusion. Consequently pulsed NMR lends itself to the measurement of translational self-diffusion coefficients. Two methods were employed during the course of this work.

(i) The Steady Field Gradient (SFG) technique.

Between the 90° and 180° r.f. pulses in the spin-echo experiment, the spins dephase as a result of differences in the local magnetic fields experienced by the individual nuclei. These differences are caused by inhomogeneities in the applied magnetic field, and by fields produced by resonant and non-resonant nuclei in the vicinity. Inverting the population of resonant spins by application of the 180° r.f. pulse causes the dephasing angle of spins due to variations in the field experienced by the nuclei to be reversed time 2τ these effects are

cancelled and the height of the spin echo is theoretically therefore a function of the spin-spin relaxation rate due to interactions with other resonant nuclei, the local field due to the other resonant nuclei also having been reversed by the 180° pulse.

If however the molecules diffuse during the time 2τ, then the average fields experienced between the dephasing and rephasing periods will no longer cancel, resulting in an attenuation of the spin echo height given by;

$$My'(2\tau) = Mo\ \overline{\cos[\Phi(2\tau)]} \qquad 3.56$$

where $\Phi(2\tau)$ is the phase shift in radians experienced by individual spins due to their diffusion in time 2τ, and $My'(2\tau) = Mo$ in the absence of diffusion. The line above the $\cos[\Phi(2\tau)]$ term signifies an ensemble average of $\cos\Phi$ over all the nuclei in the sample. This may be re-written as;

$$My'(2\tau) = Mo \int_{-\infty}^{\infty} p(\Phi)\cos(\Phi)\, d\Phi \qquad 3.57$$

where $p(\Phi)$ is the probability density function described by the phase shifts due to diffusion.

In a linear field gradient, spins undergoing unbounded diffusion experience phase shifts for which the probability density function is Gaussian. i.e.

$$p(\Phi) = \left[2\pi(\Phi^2)_{av} \right]^{-1/2} \exp\left[- \frac{\Phi^2}{2(\Phi^2)_{av}} \right] \qquad 3.58$$

where $(\Phi^2)_{av}$ is the mean average square phase shift. Substituting this into equation 3.57,

$$My'(2\tau) = Mo \exp\left[\frac{(\Phi^2)_{av}}{2} \right] \qquad 3.59$$

The application of a known field gradient G allows the reduction in height to be related to differences in the magnetic fields experienced by the nuclei and therefore to the self diffusion coefficient D in the direction of the gradient.

The phase shift for a spin at time 2τ in a continuous field gradient applied in the z direction is:

$$\Phi(2\tau) = \text{gamma } G \left[\int_0^{\tau} z(t)\, dt - \int_{\tau}^{2\tau} z(t)\, dt \right] \qquad 3.60$$

where z(t) is the displacement of the spins in the z direction in time t, and the negative sign between the two integrals is due to the phase shift following the 180° pulse. For unbounded diffusion, z(t) is Gaussian. Evaluation of $(\Phi^2)_{av}$ from equation 3.60, and its subsequent substitution into equation 3.59 leads to[31]

$$\text{Ln} \left[\frac{A(G)}{A(G=0)} \right] = -\frac{2}{3} \text{gamma}^2 G^2 D \tau^3 \qquad 3.61$$

where A(G) is the amplitude of the echo in field gradient G.

Variation of either the spacing between pulses, τ, or the magnitude of the gradient, G, allows the diffusion coefficient to be determined via this relationship.

There are two main limitations in using this technique. It requires the application of short duration, high power 90° and 180° r.f. pulses to ensure that each nucleus is rotated an equal amount in the presence of a constant field gradient. Furthermore, because of the wide range of precessional frequencies induced by the field gradient, the spin echo is itself of short duration, and to detect it a wide receiver bandwidth is required, causing a reduction in the signal to noise ratio.

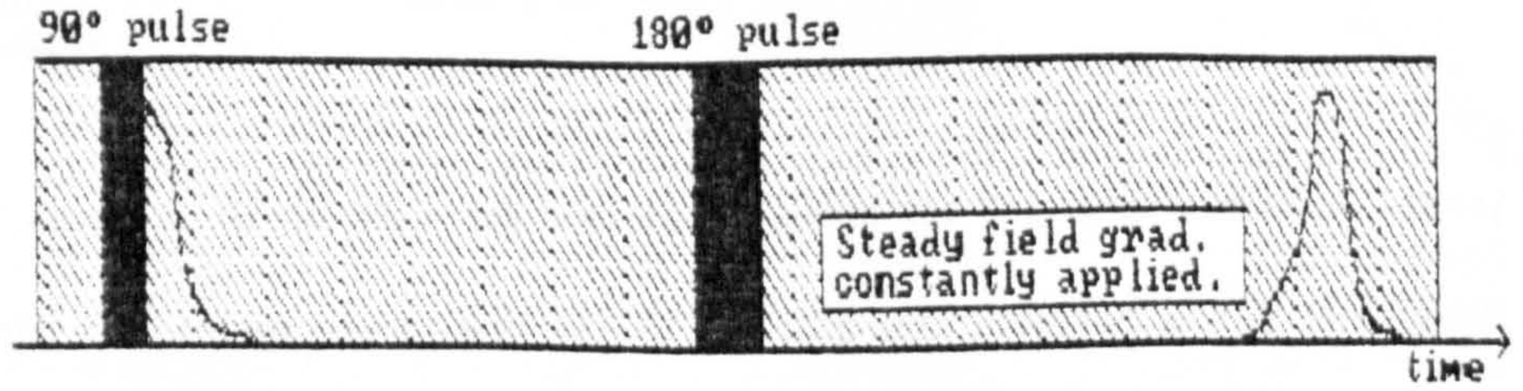

Figure 3.11 The SFG and PFG spin-echo diffusion experiments.

(ii) The pulsed Field Gradient (PFG) technique.

The difficulties encountered in the SFG experiment can be largely overcome if two pulses of field gradient are used as opposed to a continuous field gradient. The first pulse is applied between the 90° and 180° r.f. pulses. (See figure 3.11). It induces a phase shift for the resonant nucleus which is determined by its position in the field. The second pulse of equal intensity and duration to the first is applied following the 180° pulse, before the formation of the spin echo, and at a time DELTA after the first field gradient pulse. The phase shifts produced by the first pulse are reversed for all non-diffusing nuclei.

In the case of the PFG experiment, equation 3.60 becomes

$$\Phi(2\tau) = \text{gamma } G \left[\int_{t_1}^{t_1+\delta} z(t)\,dt - \int_{t_1+DELTA}^{t_1+DELTA+\delta} z(t)\,dt \right] \qquad 3.62$$

which, upon solving for $(\Phi^2)_{av}$ leads to[31]

$$\mathrm{Ln}\left[\frac{A(G)}{A(G=0)}\right] = -\,\mathrm{gamma}^2 G^2 D \delta^2 (\mathrm{DELTA}-\delta/3) \qquad 3.63$$

Variation of either G, δ, or DELTA can therefore lead to the determination of D. Using this technique the r.f. pulses may be applied and the spin echo observed in the absence of large field inhomogeneities.

3.5.4 Restricted and Anisotropic Diffusion.

The expressions quoted previously for the spin-echo attenuation in SFG and PFG experiments are only applicable if the diffusion in the direction of the field gradient is physically unbounded. In many biological systems the translational motion of molecules is restricted by the presence of barriers to diffusion.

A suitable criterion for unrestricted diffusion is that the r.m.s. distances travelled by the molecules during the time over which diffusion is observed should be substantially less than the separation of the barriers confining them. If this condition is not met then the amplitude of the spin-echo will depend upon the dimensions of the confinement.

In PFG experiments the time during which the effects of diffusion contribute to the attenuation of the spin-echo is conveniently described by the interval (Delta + δ). If Delta $\gg$ δ, then the condition for unbounded diffusion may be expressed as

$$\mathrm{Delta} \ll a^2/D$$

where a is the separation of the barriers.

In the case of restricted diffusion the application of equation 3.63, no longer yields the true self-diffusion coefficient, but may be used to define an effective diffusion coefficient D'. The dependence of D'on the experimentally adjustable parameter Delta often enables intrinsic diffusion coefficients to be measured ,and the nature of barriers to be investigated[32,33].

Tanner[34] has considered the effects on the spin-echo attenuation of molecules diffusing between two infinite, parallel and impermeable barriers, separated by a distance a;

$$\frac{A(G)}{A(G=0)} = \exp(-\gamma^2\delta^2G^2D\sin^2(\theta)).\frac{2}{\pi^2c'^2}\left[1-\cos\pi c'+2.\sum_{n=1}^{\infty}\exp[-n^2\pi^2D/a^2].\frac{[1-(-1)^n\cos(\pi c')]}{[1-(n/c')^2]^2}\right] \qquad 3.64$$

where $c' = \frac{\gamma.aG\delta\cos(\theta)}{\pi}$, and θ is the angle between the field gradient and the normal to the barrier.

This expression is valid provided that Delta >> δ, but gives an approximate representation even when this condition does not hold. The equation reduces to the usual form for the PFG experiment when $\theta = \pi/2$, i.e. the diffusion is parallel to the barriers.

Figure 3.12 shows the form of the measured apparent diffusion coefficient D', as the interval of observation Delta, is increased, and when the spin-echo attenuation is governed by equation 3.50, using $\theta = 0$. In contrast, the behaviour of D' is also shown for the case when the barriers are permeable to some degree. The diagrams illustrates that for large values of delta, D' is reduced to zero when the barriers are impermeable, but approaches an asymptotic value D'., when the barriers may be crossed.

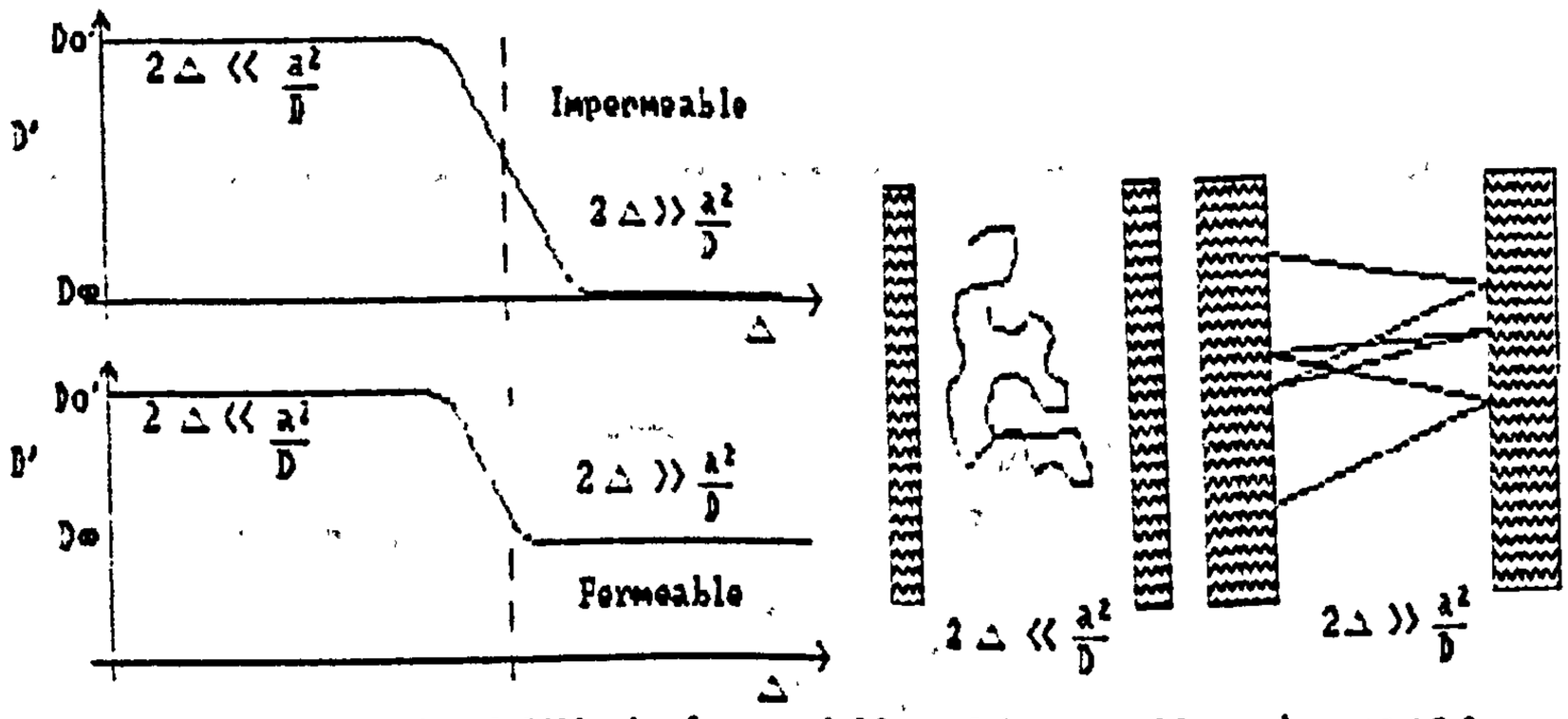

Figure 3.12 Restricted diffusion by permiable and impermeable membranes as a function of delta.

A value for the characteristic barrier separation a', can be derived from these plots by using the diffusion time Delta' at the point where

$$D' = (D'_o + D'_\infty)/2 \qquad 3.65$$

The characteristic length proposed by Tanner is given by:

$$a' = [2(D'_o - D'_\infty).Delta']^{\frac{1}{2}} \qquad 3.66$$

NMR measurements relate to the translational motional properties in the direction of the spatial field gradient G. By changing the orientation of G, the apparent self-diffusion coefficient D' may be tested for anisotropy.

It was found for example that for water in keratin fibres[135] there existed a ratio of 2:1 between the diffusivities parallel and perpendicular to the fibrillar axis. The angular dependence of the observed apparent diffusion coefficient can be written as;

$$D' = [\, D_{\parallel}\sin^2(\theta) + D_{\perp}\cos^2(\theta)\,] \qquad 3.67$$

where θ is the angle between the field gradient and the normal to the fibrillar axis of the

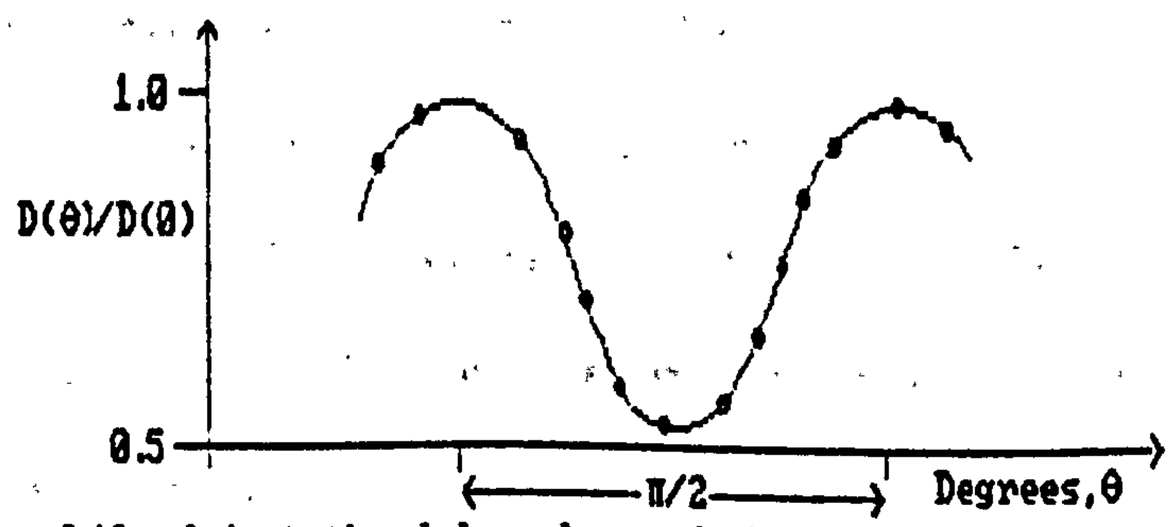

Figure 3.13 Orientational dependence of the diffusion coefficient of water in keratin fibres. $D(\theta) = \cos^2\theta D_{\parallel} + \cos^2(90-\theta)D_{\perp}$

keratin. and $D_{\parallel}$ and $D_{\perp}$ are the diffusion coefficients parallel and perpendicular to the fibrillar axis. (Figure 3.13)

The physical significance of an observed value for the diffusion coefficient D' for the molecules moving in heterogeneous systems requires careful interpretation, since it may be that D' is the intrinsic value of the coefficient, or that D' reflects the geometry of, and interactions with, the biological system in which the molecules reside.

References

1. Abragam A. "The Principles of Nuclear Magnetism." Clarendon Press, Oxford. (1961)

2. Slichter C.P. "Principles of Magnetic Resonance." Harper and Row, New York. (1963)

3. Farrar T.C., Becker E.D. "Pulse and Fourier Transform NMR. Introduction to theory and methods." Academic Press, New York (1971)

4. Bloembergen N., Purcell E.M., Pound R.V. Phys. Rev. Vol 73, p679. (1948)

5. Belton P.S., Ratcliffe R.G. "NMR and Comparmentation in Biological tissues." Prog. in NMR Spectroscopy. Vol 17, pp 241-279. (1985)

6. Stejskal, E.O., Tanner J.E. J. Chem. Phys. Vol 42, p 288. (1965)

7. Tanner J.E. Rev. Sci. Instrum. Vol 36, p 1086. (1965)

8. Stejskal, E.O., Tanner J.E. J. Chem. Phys. Vol 49, p 1768. (1969)

9. Bloch F. Phys. Rev. Vol 70, p 460. (1946)

10. Hahn E.L. Phys. Rev. Vol 80, p 580. (1950)

11. Carr H.Y., Purcell E.M. Phys. Rev. Vol 94, p 630. (1954)

12. Meiboom S., Gill D. Rev. Sci. Instrum. Vol 29, p 688. (1958)

13. Kubo and Tomita J. Physic. Soc. Japan. Vol 73. p 888. (1954)

14. Zimmerman J.R., Britten W.E. J. Phys. Chem. Vol 61, p 1328. (1957)

15. Resing H.A. J. Chem. Phys. Vol 43, p 669. (1965)

16. Resing H.A. J. Chem. Phys. Vol 80. p 186. (1976)

17. Woessner D.E. J. Chem. Phys. Vol 35, p1. (1961)

18. Odajima A. Progr. Theoret. Phys. (Kyoto) Suppl. Vol 10, p 142. (1959)

19. Miyake, J. Polym. Science. Vol 28, p 477. (1958)

20. McCall, Douglass and Anderson, J. Chem. Physics. Vol 30, p 1272. (1959)

21. Solomon I. Phys. Rev. Vol 99, p 559. (1955)

22. Campbell I.D., Freeman R. J. Magn. Reson. Vol 11, p 143. (1973)

23. Kalk A., Berendson H.J.C. J. Magn. Reson. Vol 24, p 343. (1976)

24. Brooks A.A. et al. J. Chem. Phys. Vol 49, p 1571. (1968)

25. Edzes H.T., Samulski E.T., Nature (London) Vol 265, p 521. (1977)

26. Woessner D.E. Mol. Phys. Vol 34, p 899. (1977)

27. Ahmed S.B., Packer K.J., Ramsden J.M. Mol. Phys. Vol 33, p 857. (1977)

28. Fung B.M. Science. Vol 190, p 800. (1975)

29. Fick A. Pogg. Ann. Vol 94, p 59. (1855)

30. Crank J. "The mathematics of diffusion." Clarendon Press, Oxford. (1956)

31. McCall D.W., Douglass D.C., Anderson E.W. Ber. Bunsenges. Physik. Chem. Vol 67, p

336. (1963)

32. Robertson B. Phys. Rev. Vol 151. p 264. (1966)

33. Neuman C.H. J. Chem. Phys. Vol 60, p 4508. (1974)

34. Tanner J.E., Stejskal E.O. J.Chem. Phys. Vol 49, p 1768. (1968)

35. Lynch L.J., Webster D.S. J. Polym. Sci. Symp. Vol 49, p 43. (1975)

CHAPTER 4. THE NMR OF WATER IN BIOLOGICAL SYSTEMS

4.1 Introduction.

Biological Tissues are complicated cellular systems in which there is a high degree of compartmentation and heterogeneity. The distribution of water and other metabolites in these systems amongst different environments leads to a number of populations with different NMR properties and characteristics. At an elementary level it may be possible to distinguish between intracellular and extra-cellular metabolites, or even between one intracellular component and another, since the intracellular component may itself be partitioned between several populations or intracellular environments. In leaf tissue for example a distinction might be drawn between populations existing in extra-cellular space, the cytosol, the vacuole and the chloroplast, where the only physical partitioning in this system is between the internal and external components[1]. Internal partitioning does not necessarily correspond to the membrane-bound subcellular compartmentation that is observable by microscopy.

The ability to distinguish one population from another is determined by the resolving power of the technique, which is subject to experimental and instrumental considerations. In spin mapping (imaging) experiments for example where the heterogeneity is on a cellular level, spatial resolution is important in order to distinguish one type of cell from another.

In most biological systems the temporal resolution is also an important concern as different populations are often in exchange with one another. A distinction between two populations can only be made if on the time scale of the experiment the exchange rate is slow, or if the dimensions of the compartments are such that the different populations are established without interference by diffusion.

The NMR approach to water in heterogeneous systems on an intracellular level is based upon the usual resonance properties of signal intensity, frequency, and relaxation behaviour, which reflect the dynamic properties of the water molecules. The state of water in biological tissues and in the vicinity of biological macromolecules is significantly different to the state of water in solutions of simple molecules and in pure water. NMR spectroscopy is a powerful technique for studying in detail the structure, mobility, and extent of ordering of water molecules in various biological systems. If these properties vary from one population of water to another then it should in principle be possible to distinguish between them.

This chapter begins with a description of the characteristics of hydration water, followed by a general review covering NMR studies of water in cellular systems. The application of NMR to the study of water molecules interacting with cellulose and wood cell walls is then reviewed in detail.

4.2 Hydration Water.

Water and biological macromolecules interact with one another via electrostatic forces. These interactions have two main sources;

(i) The high dipole moment of the water molecule.

(ii) Extensive hydrogen bonding arising from the large number of potentially available proton donor and proton acceptor sites potentially available on the macromolecule.

These weak macromolecular-water interactions restrict the rotational and translational motions of the water molecules, and give rise to a hydration layer in which the mobility and extent of ordering of the water molecules are distinctly different from the fast and random motions of water molecules in the bulk. These effects come into play when biological macromolecules interact with water in both solutions and biological systems.

In the bulk phase a water molecule will diffuse, rotate and exchange protons with characteristic rates τ_d, τ_r and τ_e respectively. Moreover, the lifetime of a water molecule in any one phase can be characterised by a time τ_l[2], since molecules of different phases exchange with one another.

The degree of restricted motion of water molecules throughout the hydration layer is non-uniform and anisotropic, and the dynamic modes of these molecules can no longer be described completely by a single correlation time but require a distribution of correlation times. Diffusion in these layers is also anisotropic, and the hydrogen bonding interactions between water molecules and several proton donor and acceptor groups of macromolecules give rise to a continuous hydrogen bonded path in the hydration layer, which promotes proton transfer along the macromolecular chain. There is evidence that diffusion processes in the hydration layer involve the breaking of one hydrogen bond, while the exchange of protons involves the breaking of two[3,4], and it should therefore be possible to determine which, if either of these two processes dominates the NMR characteristics of a system.

At temperatures well below the freezing point of bulk water the hydration water molecules remain unfrozen and mobile. Evidence for this comes from the NMR signals of water in biological samples at temperatures between -5°C and -60°C, which arise from only a fraction of the total water content. This fraction is proportional to the macromolecular concentration, which indicates

that the water NMR signals in frozen samples arise from water associated with macromolecules, i.e. the hydration layer.

Two types of water molecules contribute to the hydration layer. The interactions between water and specific binding sites on macromolecular chains result in a specific hydration or 'irrotationally bound' layer[3]. Between this and the bulk phase there exists an intermediate layer of 'rotationally bound' water molecules arising from the spatial and orientational mismatch between the two regions. This non-specific hydration layer contributes to the non-freezing freezing fraction and water molecules residing in this layer have rates of molecular motions which are lower than for molecules in the bulk, but greater than for the specifically bound layer. (Figure 4.1)

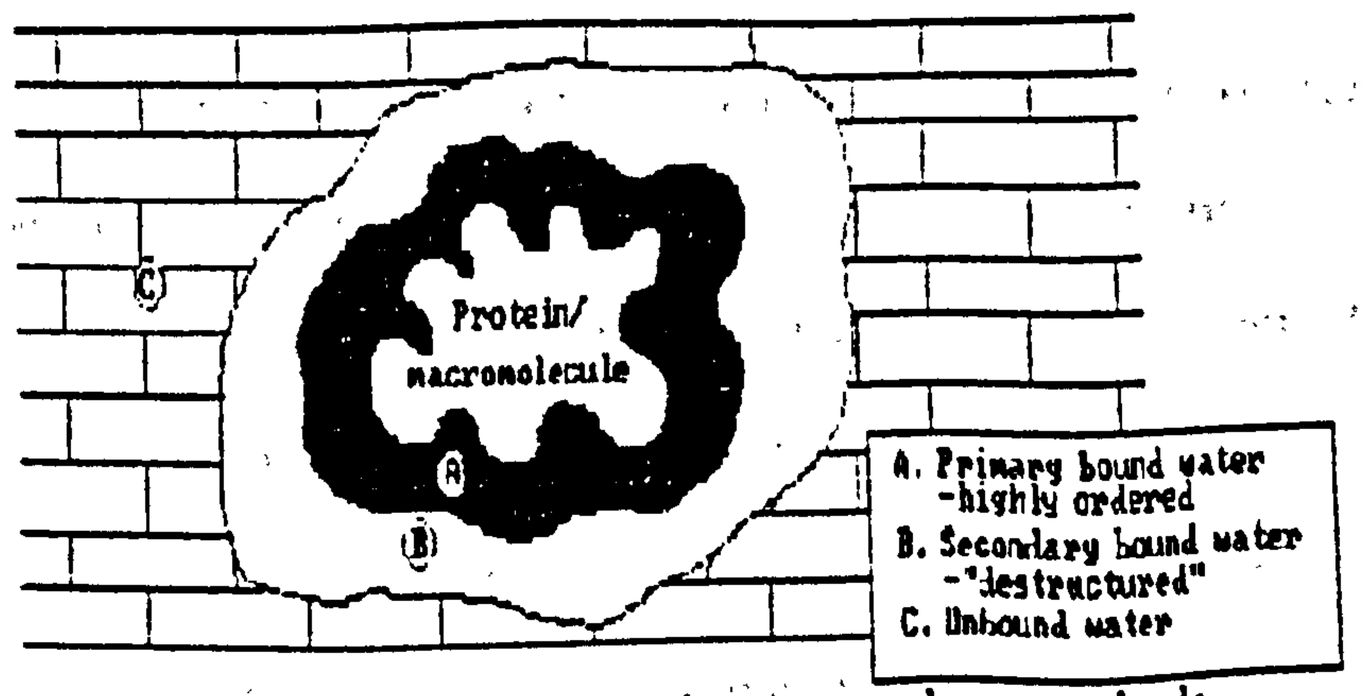

Figure 4.1 The three levels of structure in water around a macromolecule.

Under the condition of rapid exchange between the hydration and bulk water in liquid solutions of macromolecules, the observed relaxation rate is given by

$$(1/T)obs = Xf(1/Tf) + Xh(1/Th) \qquad 4.1$$

Although the fraction of free water Xf is much greater than the fraction of hydration water Xh, the term Xh(1/Th) makes an important contribution to (1/T)obs. since (1/Th) >> (1/Tf) because of the considerably restricted motion of water molecules in the hydration layer.

There have been a number of studies carried out to investigate the phenomena occurring when hydrated systems are cycled above and below 273K, in order to asses the quantity of 'bound' water based on the definition that its properties are so modified as to render it non-freezable. Most assessments of the amount of non-freezable water by NMR methods have chosen the intensity of the mobile water signal at a specific temperature below 273K as being proportional to the amount of bound water. One can use either the integrated intensity of the absorption signal, or the initial intensity of the transverse relaxation of the mobile water component as a measurement parameter[8-9].

In most cases the quantity of mobile water below any freezing point has been found to be temperature dependent[10-12]. It is questionable that the non-freezable quantity and hydration water are the same. Conflicting evidence comes from the comparison between NMR and calorimetric studies carried out on the denaturation of collagen[13], where NMR studies indicate a decrease in the quantity of bound water while calorimetric studies indicate an increase. Resing[14] asserted that non-freezable water in muscle is not necessarily related to an identifiable phase at room temperature since the act of freezing alters the structure of the muscle.

In some systems there does seem to be a close correlation between the identifiable hydration layer and the non-freezable component[11,15,16]. For a study of this relationship systems that can tolerate a wide range in their level of hydration are useful, e.g. wool-keratin fibres[11]. On this system three independent measurements were made to determine the quantity of hydration water within the system;

(i) The observation or signal intensity change across the freezing event.

(ii) The resolution of the mobile water signal above the freezing event into two components and the measurement of the intensity of the non-interacting component.

(iii) The measurement T2 below the freezing event as a function of water content.

In the latter the spin-spin relaxation time increases with water content until a plateau is reached at the fibre saturation point. Results of these studies were generally consistent with calorimetric and quantitative techniques[17,18]. There has been good correlation using other NMR techniques such as measuring the height of the C.W absorption peak as a function of water content using high power r.f. fields, where a maximum in the peak represents the maximum hydration point because the further addition of non-interacting water leads to enhanced r.f. saturation due to its long T2[19]. In collagen the ^2H coupling constant has been used to assess the quantity of non-freezable water.

In general there are four phenomena observable in temperature scanning experiments[12,20-22]:

(i) A Sharp transition in the intensity of the signal and in relaxation times during cooling for samples with higher water contents, occurring as a result of the stepwise changes in the amount and nature of mobile water in the system.

(ii) Super-cooling. The water in the sample is often seen to freeze at temperatures below that of pure water.

(iii) A decrease in the mobile water signal at temperatures below the freezing event.

(iv) Thermal hysteresis in the amount and nature of the mobile fraction as the temperature is cycled above and below the freezing event.

(i) and (ii) are consistent with the presence of non-interacting water. The temperature dependence of the NMR signals arising from the mobile water content have been explained using the following effects:

1. An 'apparent phase transition' effect, whereby molecules progressively transfer from the motional narrowing state to the rigid lattice state as a result of thermal deactivation[11,12,23].

2. Capillary effects. Water contained in pores having a range of different sizes will progressively freeze according to the Helium equation[24,25];

$$\text{Freezing point} \propto 1/\text{Pore Diameter}.$$

3. A non-specific effect where the freezing point of water is lowered depending on the degree of perturbation to the water structure caused by the interaction with the substrate material.

To explain the NMR behaviour, all of the above are dependent upon a distribution of states for the interacting water leading to a distribution of correlation times. A schematic representation is given in figure 4.2. The apparent phase change proposed by Resing[23] corresponds to a transfer of the most strongly perturbed or least mobile molecules from the mobile regions to the lattice state. The capillary and non-specific effects correspond to the least modified water molecules passing through a change of phase[26].

Calorimetric studies show a diffuse endotherm extending over temperature intervals below 273K for samples with low water concentrations[27]. As the water content is increased the endotherms concentrate close to 273K. The endotherms correspond to a gradual fusing of some water that is modified by interactions with the substrate to the extent that the freezing point is depressed but not prevented. In terms of a distribution of correlation times this

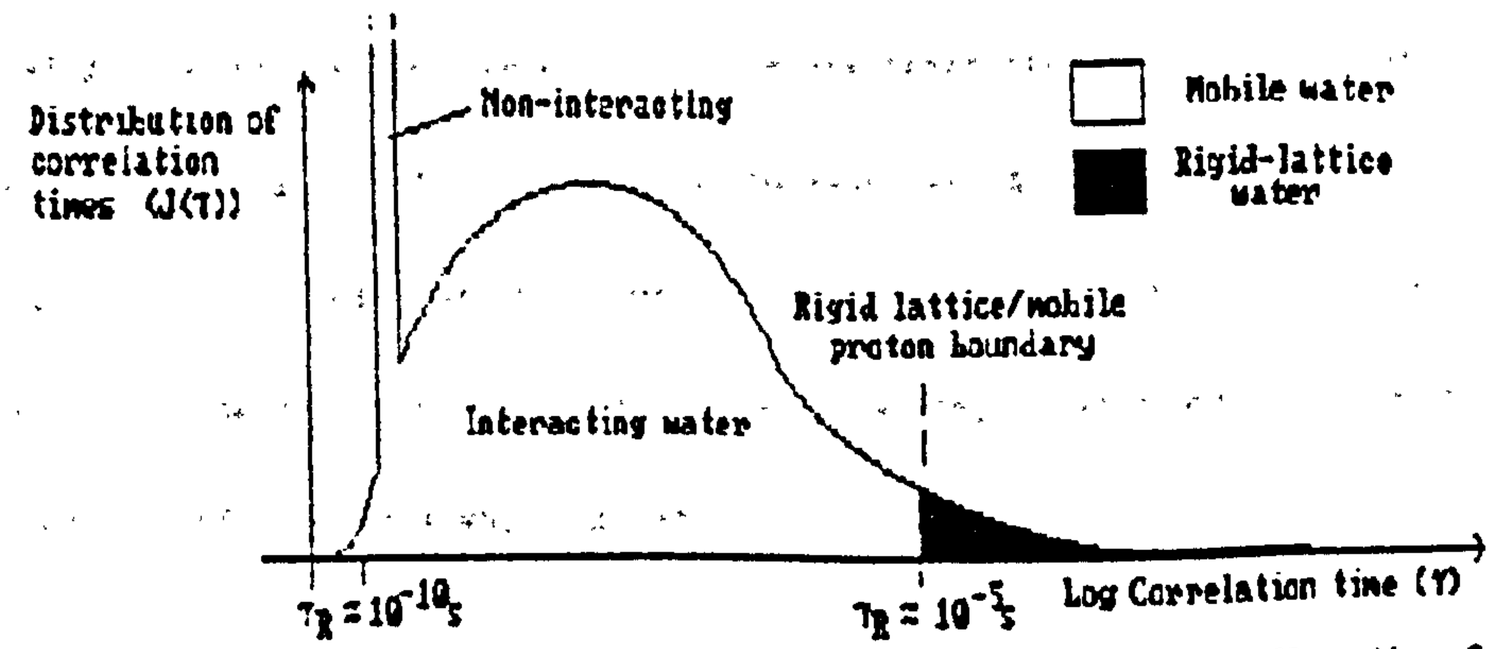

4.2(a) Temperature above 273K. Non-interacting water is unfrozen. A small portion of the interacting water falls into rigid-lattice state.

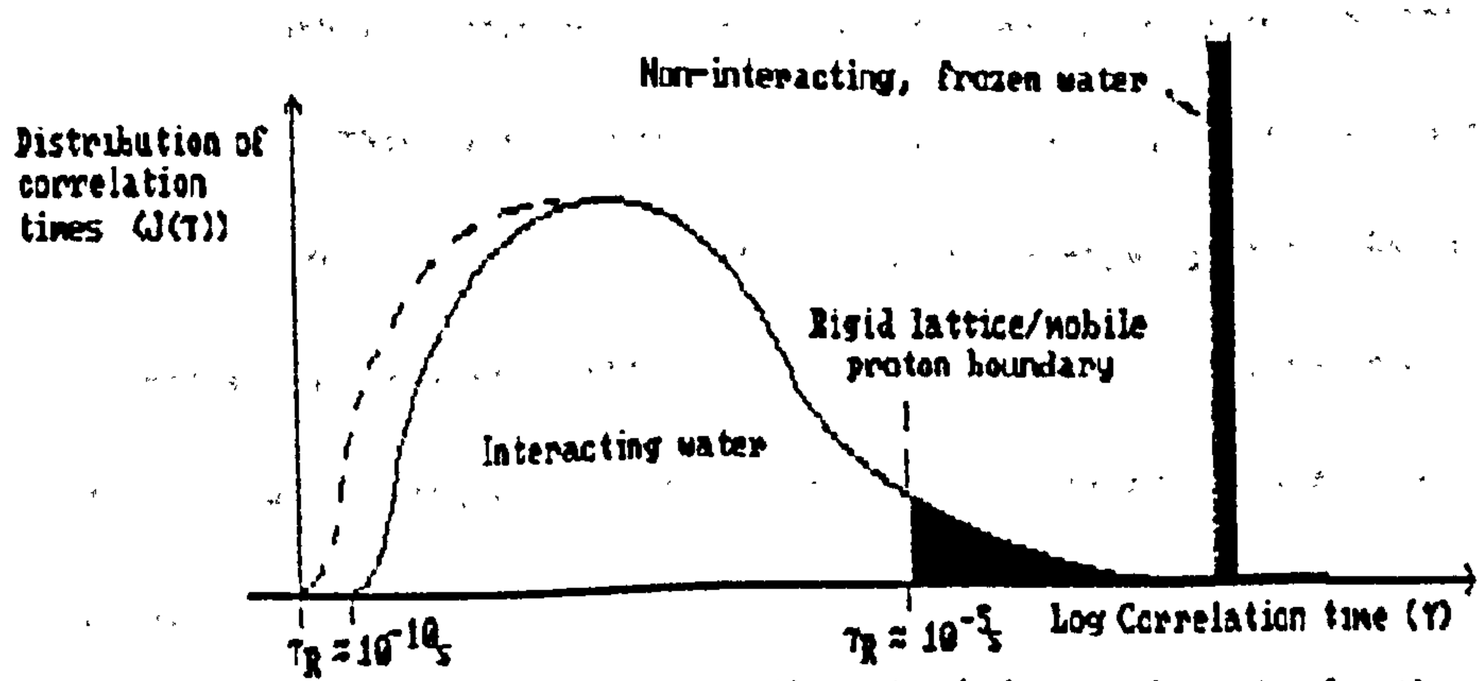

4.2 (b) Temperature below 273K. Non-interacting water is frozen. A greater fraction of interacting water falls into rigid-lattice state.

relates to a shift in the distribution to lower temperatures so that there is a gradual transition of molecules between the populations of the mobile and rigid lattice states. The narrowing of the temperature range over which the endotherm is observed results from a destructuring of the substrate leading to a more open structure and a narrower distribution of correlation times.

Studies on wool above 273K indicate that the mobile water population increases above the freezing event with temperature and this is also attributed to the apparent apparent phase transition effect[17,27,28], as water molecules progressively attain sufficient mobility to exceed the rigid lattice limit and therefore to contribute to the population weighted average relaxation process instead of the solid.

Ramirez[29] interpreted the gradual disappearance of the mobile water on cooling in terms of a classical binary solution model. Lowering the temperature below the initial freezing event causes the formation of ice, allowing the resultant more concentrated solution to remain liquid. As the temperature is further reduced the quantity of ice increases and the concentration of the remaining solution becomes more concentrated until the eutectic temperature is reached and the whole solution freezes.

Hysteresis effects have been explained in a number of ways. Morariu and Mills[30] observed hysteresis in both spin-spin relaxation behaviour and in the amount of mobile water adsorbed on silica gel. They explained this in terms of a physical shift in the phase boundary relating to the gradual transition between frozen and unfrozen states. Pearson and Derbyshire[31] explained hysteresis effects in terms of an overlap of super-cooling and super-heating for water structurally ordered within pores. Barnes[32] suggested that the act of water freezing disturbs the sorption equilibrium, and therefore that unfrozen water moves away from the pores to the surface of the substrate where it freezes as a result of experiencing a lower pressure. On re-heating the specimen the water would then become liquid at a higher temperature. In addition to these effects one should also consider the possibility of structural changes in the substrate itself as a result of freezing.

4.3 NMR Relaxation Studies of Water in Protons and Biological Systems.

4.3.1 Possible origins of non-exponential relaxation behaviour.

The NMR properties of water in biological systems have been studied extensively in time domain experiments because of the ease with which such experiments can be carried out and the sometimes dramatic differences in NMR properties observed. Such measurements provide information about the dynamics of water molecules within the system.. Changes in chemical shifts are proportionally and are often masked by the increased peak width in the NMR signal.

The most useful NMR parameters in the study of water are the relaxation times T1, T2 and Tp from which one can derive correlation times and diffusion coefficients. Water relaxation has been studied using ^{1}H, ^{2}H and ^{17}O nuclei. The use of ^{3}H nuclei has been limited because of their radioactive nature. ^{1}H nuclei are popular because of their high natural abundance. Proton signals are complicated by signals from other components however, as well as by chemical exchange between the protons of water and labile protons of proteins, etc., and by cross-relaxation effects.

Deuterium undergoes exchange but does not suffer from cross-relaxation effects or masking by signals from other components. ^{17}O suffers from none of these difficulties but has intrinsically a multi-exponential decay because of its nuclear spin quantum number I = 5/2. Spin-spin decay curves using ^{17}O are single component to a high degree if a single nuclear environment exists, but T2 is multi-exponential, especially in cases where $J(0) \gg J(\omega_0)$, which is generally the case in cellular systems. Both ^{17}O and ^{2}H often require some enrichment due to their low natural abundance.

The nature and significance of water relaxation behaviour have been reviewed by a number of authors[1,4,24,33-35] and the general features of the behaviour which are described in chapter 3, may be summarised as:

(i) The spin-lattice relaxation time is greater than the spin-spin relaxation time, i.e. $T1 > T2$.

(ii) Relaxation rates of water in biological systems are faster than in the bulk.

(iii) Lowering of the temperature leaves a residual signal, even at temperatures below the freezing point of the bulk.

(iv) The magnetisation decay curves are often multi-exponential.

A common feature observed in proton and ^{2}H relaxation is single component spin-lattice relaxation, but multi-component spin-spin relaxation processes. ^{17}O exhibits multi-exponential behaviour in both spin-lattice and spin-spin relaxation. These features are usually explained using models based on exchange processes between phases or compartments of water, the exchange being rapid on the time scale of T1, but slow on the time scale of T2 for protons and deuterons. In the case of ^{17}O nuclei however, where relaxation proceeds at much faster rates for both T1 and T2, the exchange rate is relatively slow.

This mechanism is not universally accepted, and two alternatives have been put forward:

(i) Based on diffusion-dominated properties.

(ii) Based on residual static effects.

Both again depend upon sites of varying relaxation characteristics, but the origin of these sites and the nature of their effect on the bulk relaxation characteristics differ.

In the first case it is assumed that proteins and substrate materials within biological systems act as potent magnetic sinks for the relaxation of water molecules. If a water molecule is sufficiently close to the surface of the substrate so that within the lifetime of its own intrinsic relaxation it can sample the sink, then its relaxation will be strongly effected, otherwise it will relax at its own intrinsic rate. Using this model, a variety of relaxation times are to be expected for water in cellular systems which depend upon the size and shape of the cells.

The mathematical approach to such a model has been developed by Brownstein and Tarr[36,37], who assumed that proton relaxation of water in heterogeneous systems is due to magnetic sinks contained within active volumes or surfaces to which molecules must diffuse in order to relax. The general solution to this problem has the form:

$$M(t) = \sum_{n=0}^{\infty} I(n) \cdot \exp(-t/Tjn) \qquad 4.2$$

i.e. the observed magnetisation M(t) at time t is the sum of an infinite number of components. I(n) is the intensity of the nth component with relaxation time Tjn, (j=1,2,p). Calculations based on models containing only active surfaces showed that the intensities and relaxation times are functions of the geometry of the system, the dimensions of the system (a), the strength of the magnetic sinks (M), and the diffusion coefficients of the resonant nuclei, (D). Brownstein and Tarr identified three regions characterised by the parameter Ma/D;

(i) $Ma/D < 1$. This is the region of fast diffusion, where all the nuclei sample the sink. It is equivalent to the region of fast exchange in the discrete multi-phase model. In this region only the first term of equation 4.1 has any significant intensity, i.e. $I(n > 0) \simeq 0$, and single exponential relaxation is predicted. The corresponding decay time for the lowest mode is given by $To = V/Ms$, where V is the sample volume and s is the active surface area.

(ii) $1 < Ma/D < 10$. In this region a larger proportion of the resonant nuclei sample the magnetic sinks due to their intermediate diffusion rates. The lowest mode still dominates but n = 1,2 modes now contribute a few percent to the total relative intensity. The decay time of the lowest mode is greater than was predicted for the region of fast diffusion, and is about one or two orders of magnitude greater than the decay times of the first two higher modes.

(iii) $10 < Ma/D$. In this region few nuclei sample the magnetic sink as a result of their slow diffusion rates. The majority of the relative intensity is still in the lowest mode; 60%-80%, depending upon the geometry of the system, and the intensities for terms with $n > 2$ are still negligible. The relaxation times of the $n = 0,1,2$ components are greater than in the intermediate region, with the decay times of the first two higher modes now being only about one order of magnitude less than that of the lowest mode.

It was suggested that multi-exponential relaxation may be observed for water in heterogeneous systems when the water molecules are in the range of 1 to 30μm away from a magnetic sink[39]. To diffuse this distance a water molecule would require between 10^{-3} and 1 second.

The success of this model in predicting relaxation characteristics of real biological systems is mixed. In their case study, Brownstein and Tarr showed that the model could account well for the transverse relaxation behaviour observed in rat gastrocnemius muscle if the diameter of the cells was assumed to be about 88μm. Since this value was in the expected range the model was thought to hold. However, if the sinks are due biopolymers then this model no longer holds because the distance between the fibrils of muscle is nearer 2-3μm, and the distance between the fibres is around 10-30nm. Moreover, the space between the fibrils is filled with sarcoplasmic reticulum and mitochondria. To determine whether only the membrane plays a relaxing role in these systems, tests were carried out on giant squid axon[38]. The cells of giant squid axon are around 500μm in diameter and contain very little internal structure. Measurements carried out on extruded axon containing virtually no membrane show that the relaxation times of the internal medium are independent of the boundary, which suggested that the multi-exponential relaxation observed is caused by protein-water interactions, and not membrane-water interactions. For such systems the description of relaxation characteristics in terms of the diffusion model appears untenable.

Systems to which it may be applicable are those in which compartments are of the order of micrometers across, with little or no internal structure, i.e. only localised relaxation sinks such as cell walls such as the vacuoles of plants. Even in systems where the Brownstein and Tarr model is not expected to work, there is support for the role of diffusion in ordered systems[39].

As a second alternative to the discrete multi-phase model, Fung and Puon [40] suggested a very different origin of multi-exponential transverse relaxation, based on the fact that protons and deuterons are in constant chemical exchange with species such as NH_2, OH and SH on the protein surface. They point out that it is customary to analyse the decay in terms of sums of exponentials and then assign each fraction to a type of proton. Four groups can be identified from their characteristic relaxation times:

(i) T2 ≈ 24μs. This signal originates from protons in proteins and other macromolecules.

(ii) T2 ≈ 0.4ms, made up from irrotationally bound water and highly mobile protons in large molecules.

(iii) T2 ≈ 40-60ms. Typically this is assigned to the intracellular water.

(iv) T2 ≈ 150-400ms. Extra-cellular water.

In their work, Fung and Puon studied T2 decays in skeletal muscle and found that after a period of longer than 10ms the decay curve could be described by a two component model for both proton and deuteron spin-echo decays, which they identified with components (iii) and (iv) above. However, the assignment of (iii) to intracellular and (iv) to extra-cellular water was questioned on the grounds that:

(a) In deuterated samples, the slowly decaying part constituted a larger fraction than for the proton decay, whereas if the long component were due to extra-cellular water it should have accounted for the same fraction as in the non-deuterated samples.

(b) In glycerinated muscles, where all the membranes were disrupted, the proton spin-ecnoes were similar to those from intact muscles.

(c) Non-exponentiality increased as rigor mortis set in.

(d) The lifetime of intracellular water in exchange would not account for the characteristics of the two resolvable components observed.

Based on these observations, Fung and Puon rejected the idea that the slowly relaxing component was due to Extra-cellular water, and proposed that the unusually short T2's and the non exponential character are due to hydrogen exchange with functional groups in protein filaments. The extremely slow motions of SH, NH_2 and OH groups are the cause of a dipolar splitting or a quadroupolar splitting in the case of deuterium, and if the minor fraction in exchange with protons has a shift δW due to chemical shift, spin-spin dipolar or quadrupolar interaction, then non-exponential behaviour is observed if

$$\delta W/10 \leq 1/(T2b + \tau b) \leq 10\delta W. \qquad 4.3$$

Where τb is the lifetime of the protons on the proteins, and T2b is the spin-spin relaxation time of protons attached to the macromolecules. The dipole interaction between two protons separated by distance r, and at angle Ψ, is given by

$$\delta W = 3\text{gamma}^2.h^2.(1-3\cos\Psi/2r^2) \qquad 4.4$$

but this value is reduced by the rotation of the functional groups. The authors estimated that, for the NH_2 groups, $\delta W \approx 10^4 - 10^5$ and $T2b \approx 10^{-4}$s, and from studies on the protonation of methylamine τb is given by

$$\tau b = 2.7 \times 10^3.[H+] \qquad 4.5$$

where [H+] is the hydrogen ion concentration in mol/dm³. This model predicts therefore that non-exponential behaviour should be observed for pH < 10. Glycerinated rabbit muscle shows multi-exponential relaxation when the pH = 9, whereas the curve is linear for pH = 7 and pH = 5, until 95% or 98% of the magnetisation has decayed away. The model can also account for anisotropic relaxation, which can be explained by the angular dependence of $\delta\omega$.

This model is contested by several authors. Oakes[41] observed single exponential relaxation in bovine serum albumin/water mixtures with up to 70% protein content. Also, in samples from frozen muscle, the transverse decay of the unfrozen component is single exponential whereas above the freezing point multi-exponential relaxation is observed. Since this unfrozen water is intimately assiciated with the proteins, and the exchange rate between water and protein groups is not expected to have changed very much, one would expect to see multi-exponential behaviour at below the freezing point using this model.

In the case of protons, the model depends upon the static dipolar interaction arising from proton pairs, and exchange with other protons will modify this interaction. When the modulation rate is of the same order of the splitting $\delta\omega$, the condition of motional narrowing will apply, since the splitting will be turned on and off at a rate comparable to the interaction strength. This will occur when the rate is 10^{-4} - 10^{-5} s^{-1}, corresponding to a pH in the range 7.4 - 8.4, which is close to that in muscle. The quadroupolar interaction will not be destroyed by exchange and thus, while the model is tenable for deuterated muscle, it does not appear to apply in the case of protonated muscle.

The origin of non-exponential relation then, has many possible sources. In addition to the compartmentation of water molecules, there is good evidence that protein-water interactions are important. The exchange of whole water molecules, or just protons between dif-

ferent water populations, or between water and other species. complicates the relaxation behaviour observed in compartmented and heterogeneous systems. These processes may be active jointly or separately in any one system, and careful interpretation of data is required.

4.3.2 Applications to unicellular systems.

In simple unicellular systems such as suspensions of human erythrocytes, relaxation data has been interpreted satisfactorily in terms of two components[42], i.e. intracellular water and extra-cellular water. Usually both components have the same observed relaxation time indicating rapid exchange between the two fractions, but doping with paramagnetic impurities for which the cell membrane is impermeable. e.g. Mn^{2+} in concentrations >100μmole. enhances the relaxation rate of the external water so that the two components become resolvable. Higher concentrations enhance the relaxation rate to such an extent that the signal from the external water is no longer observable, and leads to a change in the value for internal water which may be used to determine the lifetime of molecules inside the cells from the relationship

$$\frac{1}{\tau a} = \frac{1}{Tb} - \frac{1}{Ti} \qquad 4.6$$

where Tb is the relaxation time for the intracellular water in the doped system, Ti is its intrinsic relaxation time, and τa is the lifetime of water molecules in the cell. The backflux of the magnetically labelled water into the cell must also be considered in cases where the doping of extra-cellular water does not reduce the relaxation time sufficiently.

Both spin-spin and spin-lattice relaxation times have been used[43,44]. A complication arising from the use of spin-lattice times is that there is an additional signal present from the mitochondria (T1 ≈ 100μs) which must be subtracted from the water signal, whilst with spin-spin relaxation there is a possibility that one might not be measuring the true rate of

transverse relaxation due to chemical shift effects, which arise when large amounts of doping are used. Insufficient doping leads to problems with the backflux term however. Further complications with T1 measurements arise from spin diffusion through the membrane unaccompanied by material transport.

An alternative approach to the study of water transport in erythrocytes has been to use ^{17}O which has intrinsically low relaxation times and gives double-exponential decays in spin-lattice relaxation studies[48], which again can be attributed to the internal and external cellular water. Here it is seen that extra-cellular water has a relaxation time which is reduced as a result of exchange with the fast relaxing internal component. Once again a comparison of its intrinsic relaxation rate with that observed leads to a measure of the lifetime of water molecules in the cell. A value of τ_a = 9.3ms at 37°C was found using this method, which is in good agreement with other methods.

In more complex cells, e.g. Lettree cells, proton relaxation is double exponential even with concentrations of doping agent as low as 20 μmoles[49]. The relaxation time of extracellular water is reduced when in contact with cells compared to when it is not. Moreover, the relaxation rates of the intracellular component in doped samples is greater than the rates of the extra-cellular component, in contrast with the results found in studying erythrocyte suspensions. The explanation formulated to explain these observations is that the manganese resides as three different forms within the system, i.e. in solution, loosely bound to the cell wall, and tightly bound to the cell wall. Water in the vicinity of the cell walls therefore relax faster and intracellular relaxation is then fast because of interactions with the more tightly bound Mn^{2+}.

Treatment of Lettree cells with Sendai virus increases the permeability of cells to Mn^{2+} ions and this leads to tri-exponential behaviour, i.e. two types of intracellular water of equal populations become apparent. Microscopy does not show two compartments of equal volume, however, and it is thought that one component originates from the nucleus, mitochondria, and endoplasmic reticulum, which bind manganese differently to other components.

In between the simple erythrocytes and complex lettree cell systems are the lymphocytes. In viable cells ^{17}O relaxation is bi-exponential, but in non-viable cells is single exponential[47]. The results are ascribed to the intracellular compartmentation as the nucleoplasm and cytoplasm have volume ratios of 2:1, which is the same as the relative populations observed by NMR.

The examples given above demonstrate the origins of multi-exponential behaviour in cellular systems, i.e. physical partitioning between environments with different relaxation characteristics, and interactions between water molecules and intracellular components. With respect to the values of the relaxation times observed in these systems, two factors have been considered, namely the conformation of the substrate material and the total water content of the system, both of which play a role in the dynamic behaviour of water in the system. Beall et al[48] correlated the T1 of water protons with the total water content of Hela cells during their life cycle. It was found that the relaxation time increased with the amount of water in the cells, and was also determined by conformational changes in the macromolecules of the cells during growth and division. In cancerous cells it has been demonstrated that T1, T2 and the diffusion constant are greater than in normal tissues[49]. It is thought that at temperatures above the freezing point the observed relaxation rates are the weighted average of free and hydration water as given by equation 4.1, and indeed studies on the non-freezable component in cancer cells indicate a reduction in the amount of water occupying the hydration layer.

4.3.3 Applications to Muscle and other Tissues.

In the case of muscle and similar tissues data has usually been interpreted in terms of compartmentation between extra-cellular components, intracellular water in myofibrils and sarcoplasmic reticulum, and water associated with proteins and phospholipids[150-152]. In general both the relaxation times and the diffusion constant of water in these systems are found to be reduced from the values observed for pure water. For spin-spin relaxation the exact shape of the decay curves observed using the Carr-Purcell-Meiboom-Gill pulse sequence are found to depend on the pulse spacing τ[136], and the average relaxation rate passes through a maximum in the temperature range -5 to 25°C. These results indicate the presence of some kind of exchange process, and therefore that the observed populations of the components cannot be taken as accurately reflecting the number of spins in each environment.

The motions of water molecules in muscle cannot be described satisfactorily by a single relaxation time, and the observed decay curves are usually resolved into a number of discrete components. The slowest relaxing component has been assigned to the extra-cellular water on the grounds that it is likely to be the most remote from proteins and other interfaces, and also because its relative population is close to that expected from studies of extra-cellular spacing.

Neville and White[153] measured the extra-cellular space in various frog leg muscles by an ion efflux method and found good correlation with the magnitude of the slow component in resonance studies. Moreover in single cells of the giant barnacle which does not contain extra-cellular space in the normal sense but does contain clefts on the outer surface which contain about 6% of the total water volume, Foster[154] observed a slow relaxing component with a relative intensity of around 3%. Similar results were obtained by Packer and Belton[155] who showed that by adding hypertonic ringer solution which could open or shrink

the cletts, the signal intensity of the slow relaxing component could be increased or decreased. It therefore seems likely that the slow relaxing component is due to extra-cellular water.

Diegai and Pintar[31] observed that when water in muscle was exchanged with D_2O Ringer solution there was still a slow relaxing ^1H component and suggested therefore that the origin of this resonance was highly mobile organic species. However, Fung and Puon[40] demonstrated that in the proton NMR spectrum of deuterated samples there was a peak at the appropriate chemical shift for water but not any other, and so suggested that the origin for the slow relaxing component was from an incomplete exchange of protons.

The fast relaxing component can be fitted equally well by the use of either one or two time constants. It seems likely from the results of deuterium studies which demonstrate a non-exchangeable fraction with a relaxation time of the order of milliseconds. that some part of the signal of the fast relaxing component arises from non-water species. It is suggested therefore that the fast resolving component is a composite of protons from water and proteins. Hazelwood[32] decomposed the spin-echo curves observed in skeletal muscle at 24°C into two fast decaying components and one slow decaying component with the following ratios;

(i) Water associated with macromolecules having T2 < 5msecs; 8%

(ii) Intracellular water associated with the myoplasm with T2 ≈ 45msecs; 82%

(iii) Extra-cellular water, T2 ≈ 196msecs; 10%

Hazelwood believed that water in these three fractions did not exchange rapidly, and considered the possibility that each fraction may be composed of fast exchanging sub-fractions. Belton found similar results with T2's of 9, 40 and 250 msecs. Both Foster[34] and Fung[34] have suggested that the 8% fraction with the fastest relaxation arises from non-rigid protons of macromolecules rather than bound water.

Not all muscle and such tissue exhibit multi-exponential relaxation behaviour. In post-mortem studies on mouse muscle it was observed that the slow relaxing component was not present immediately post-mortem, but developed after 15-60 minutes[56]. Similar results have been found in experiments with frog muscle[53], where the slow relaxing component was increased by immersion in Ringer solution which was matched with an increase in extra-cellular space as measured by the ion efflux method. In porcine muscle T1 is single exponential, while T2 is initially single component but becomes two component after several hours[57].

This bi-exponential behaviour can be induced using freeze-thaw cycles. To explain this behaviour it was postulated that two compartments exist in slow exchange with each other, both consisting of bulk water and water interacting with proteins[57]. The population of interacting water remains fixed but there is a shift in the population of bulk water from one region to the other inducing changes in the relaxation times in accordance with equation 4.1.

Experiments performed at different frequencies and temperatures indicate a distribution of correlation times and a dispersion of relaxation times for water in fibrous materials[58-60].

Finch and Homer[61] reported T1, T2, and Tp values for frog muscle water protons at different temperatures above 0°C and over a wide range of frequencies. This revealed a distribution of correlation times ranging from 10^{-8} to 10^{-11} seconds. Results were interpreted in terms of an exchange of water molecules between two fractions; one with a distribution of different degrees of motional freedom, and the other with unrestricted motion like ordinary water, having a relative population of 97%.

NMR experiments on frozen samples of rat gastrocnemius muscle over the frequency range 4.5 - 60MHz and temperature range -70 - +27°C indicate that the relaxation times of the unfrozen fraction are frequency dependent. In samples at subfreezing temperatures the unfrozen

fraction exhibits a distribution of correlation times while above -8°C a single T1 was observed which was short enough to render it frequency independent. Based on these results Fung and McGaughy[42] supported a two phase model consisting of an unfrozen phase with a distribution of correlation times and a phase with a single relaxation time.

Several authors have shown that the water content of a system exerts a determining role on the relaxation behaviour of water nuclei. Cook and Wein[43] studied T1 and T2 of various partially hydrated muscle proteins, and found that the relaxation times decreased as the ratio of water to protein decreased. 1/T was found to be directly proportional to the protein concentration.

Fung[44] measured the T1 of water protons for dehydrated mouse muscle at three different frequencies; 5, 30, and 100 MHz, down to very low water contents, and at all three frequencies T1 decreased as the water content fell until it reached a value of less than 7% when it began to show an increase. This phenomenon may have occurred because of a change in the structure of the hydration layer at low water contents.

Belton and Packer[45] correlated the stepwise dehydration of muscle with a decrease in the relaxation times. Dehydration followed by rehydration was also investigated, and it was shown that the amount of unfrozen (hydration) water in the rehydrated samples was the same as in normal muscle, but the relaxation behaviour at low temperatures was quite different. This suggested that the amount of hydration water in a system depends upon the concentration of macromolecules in the system, whereas differences in relaxation times arise because of a change in the structure and distribution of the water amongst different fractions, which is determined by the structure of the macromolecular system.

Further evidence of the importance of the macromolecular structure on the relaxation behaviour comes from studies on infected, dead and dying tissues, and in studies on contracted muscles[64,66,67]. Healthy tissues generally have shorter relaxation times than unhealthy or post-rigor tissues, in which the amount of ordering of water is considered to have decreased, leading to an increase in its molecular mobility. In contracted muscles where there is no change in water content from the relaxed state also suggests that the observed reduction in the spin-lattice relaxation time is brought on by a change in water structure and mobility, as a result of changes in the structure of the macromolecular substrate.

4.3.4 Application to plant cells and tissues.

A variety of characteristic relaxation behaviours have been found for water in plant cells and tissues, ranging from the single relaxation time observed in thylakoids[68] to multi-exponential behaviour seen in more complicated systems such as leaves, ivy bark and wheat cell crowns[69]. In leaf tissues the different spin-lattice relaxation times, assigned to water molecules residing in different compartments, were found to be anisotropic[70]. This orientational dependence, it was suggested, resulted from highly ordered thylakoid membranes containing manganese.

The structure and size of plant cells makes interpretation of NMR relaxation data very difficult. Cells within a single piece of tissue may have a large range of sizes; from 1 to 300μm for example in zea maize root tips[71]. Plant cells contain vacuoles which may be 90% of the cell volume but which contain very little in the way of proteinacous structure. This diversity of size and absence of internal structure makes plant material fit closely to the conditions described by Lillford et al[39], and in cases where external relaxation reagents have been added, the conditions fit almost exactly the assumptions of the Brownstein-Tarr[36-37] model, with the added complication of a distribution of cell dimensions.

In light of the above, it may well be incorrect to analyse multi-component relaxation in plant tissues in terms of discrete populations, even in cases where discrete components do exist.

4.3.5 Applications to Porous Media

A good deal of attention has of late been centred on the application of NMR to a study of geometrical properties of porous rocks, where the assumptions of the Brownstein-Tarr model appear to hold[72]. Paramagnetic impurities at the surface of pores within the rocks act as magnetic sinks, and this results in relaxation behaviour, which is determined by the diffusion of magnetisation within the pores and the structure and dimensions of the pores, (i.e. by the factor Ma/D).

Cohen and Mendelson[73] asserted that, when diffusion between adjacent pores is sufficiently fast, the nuclear magnetisation throughout the sample is uniform and decays exponentially, and the relaxation rate is linearly related to the surface to volume ratios of the entire pore space of the sample. As the diffusion between pores is reduced, the magnetisation may differ from pore to pore, resulting in non-exponential decay. Where the pores are weakly coupled, the relaxation function for the nuclear magnetisation is the Laplace transform of the probability distribution of relaxation rates, which are linearly related to the surface to volume ratios of the individual pores.

In other studies, Banavar et al[74-75] noted a good correlation between the Darcy permeability K, and the function $(Q^4T1^2)^{1.13}$ for a large number of sandstones and carbonates. (Q=porosity). They analysed the main lattice decay in terms of a stretched exponential which they suggested as a consequence of the random nature of the system:

$$M(t) = M(0)\exp(-t/T1)^{\alpha} \qquad 4.7$$

Fitting their data in this way compared favourably in 60% of the cases to analysing in terms of a number of discrete components, and produced a single value for the spin lattice relaxation time of the system. This was then related to the dimensions of the rocks, using a similar line of thought to that introduced by Brownstein and Tarr. Since both porosity and permeability are also determined by the geometry of the rocks, they were able to establish the relationship above.

In an attempt to quantify the parameter which characterises the surface magnetisation relaxation effects, M, Lipsicas et al[174] performed pulsed field gradient diffusion measurements on dolomite samples. They noted that, in the limit DELTA >> δ and DELTA >> a^2/D, the diffusion is bounced and the dephasing of spins becomes independent of DELTA.

$$M(t) \approx M(0).\exp(-\text{gamma}^2G^2\delta^2a^2/5 - t/T2_s) \qquad 4.8$$

where $T2_s$ is the spin lattice relaxatin time of the bulk.

Under these conditions the dephasing of spins is determined by two independent mechanisms. In large pores the dominant mechanism is expected to be caused by the field gradients, and the dependence of the spin echo on $G\delta$ in this regime is given as:

$$-\ln \frac{M(t)}{M(0)} \approx \frac{1}{T2_s} + \left(\frac{27}{20}M^2t^2\text{gamma}^2G^2\delta^2\right)^{1/3} \qquad 4.9$$

M is the strength of the paramagnetic sinks on the pore surface.

in smaller pores, more molecules sample the paramagnetic sinks on the surface. The relaxation is predominantly via this interaction and the dependence of the signal on Gδ is given by:

$$-\ln \frac{M(t)}{M(0)} \approx \frac{1}{T2_b} + \left(\frac{4}{5} \text{gamma}^2 G^2 \delta^2 D t \right)^{1/2} \qquad 4.10$$

The power dependence of the Gδ term for the two regimes was noted and, in their experiments, Lipsicas et al found a 2/3 dependence of M(t) on Gδ, suggesting that, for the dolomite samples, at least, the system was in the fast diffusion region. From the results, they deduced a value of 6.7×10^{-5} cm/s for M. It was suggested that the same technique could be applied to a variety of porous or cellular systems.

4.4 Nuclear Magnetic Resonance of Water in Cellulose and Wood.

4.4.1 Studies of water absorbed on cellulose.

Cellulose is an important constituent of many common systems, including wood. The properties of cellulose are determined to a certain extent by the degree of hydration of the system, and a number of NMR studies have been conducted to establish the nature of the interactions between the polymer and water molecules.

A model for water sorption by cellulose was proposed by Child[77], who studies spin-lattice and spin-spin relaxation in samples derived from a variety of sources for water contents up to 25%. The temperature dependence of the proton NMR signal at the low moisture contents indicated a strong interaction between cellulose and water, together with the presence of a distribution of binding energies for the water molecules. The molecular action of the water molecules was found to depend on the degree of crystallinity of the cellulose.

The T1/T2 ratio, which should be near to unity according to BPP theory, was found to be three orders of magnitude greater than expected which Child suggested was caused by a distribution of correlation times for the tightly bound water. There was evidence of proton exchange in the water-cellulose system from the behaviour of the spin-spin relaxation time with variations in temperature.

An anomaly in the absorption behaviour was observed in the T1 data as a function of moisture contentat moisture contents of between 5 and 10%, where a minimum is noted . A mechanism of water uptake by cellulose was put forward whereby the initial sorption occurs at hydroxyl groups. This causes a breakdown in the weak inter-chain hydrogen bonds in favour of stronger chain-water-chain bonds. This is reflected in a reduction in macromolecular mobility. As further hydration takes place the length of the bridges between the chains increases until they eventually break, and the molecular motion increases.

Froix and Nelson[178] studied the spin lattice and spin-spin relaxation times in cellulose as a function of moisture content and identified two types of bound water which they termed 'primary' and 'secondary'. The primary bound water was observed below water contents of 9% and corresponds to the bridging water in Child's proposed hydration mechanism. As the water content increased above 15%, three sources of proton NMR signal became apparent and could be associated with the cellulose itself, the tightly bound water phase, and the mobile fraction corresponding to free layers of capillary water. A limit to the amount of bound water of 15 g/g can therefore be inferred, which is in agreement with that reported by Carles and Scallan[179].

Sasaki[180] et al studied the spin-spin and spin-lattice relaxation times for water absorbed on cellulose as a function of water content and temperature, in order to establish whether the correlation time of Brownian motion measured by NMR is consistent with that measured by dielectric relaxation. Using samples with water contents between 12 and 148%,

they found that the spin-lattice relaxation was non-exponential and two time constants were required to describe the decay of the magnetisation, whereas the spin-spin relaxation was adequately described by a single time constant. The benaviour of the two T1's as a function or water content is described by figure 4.3.

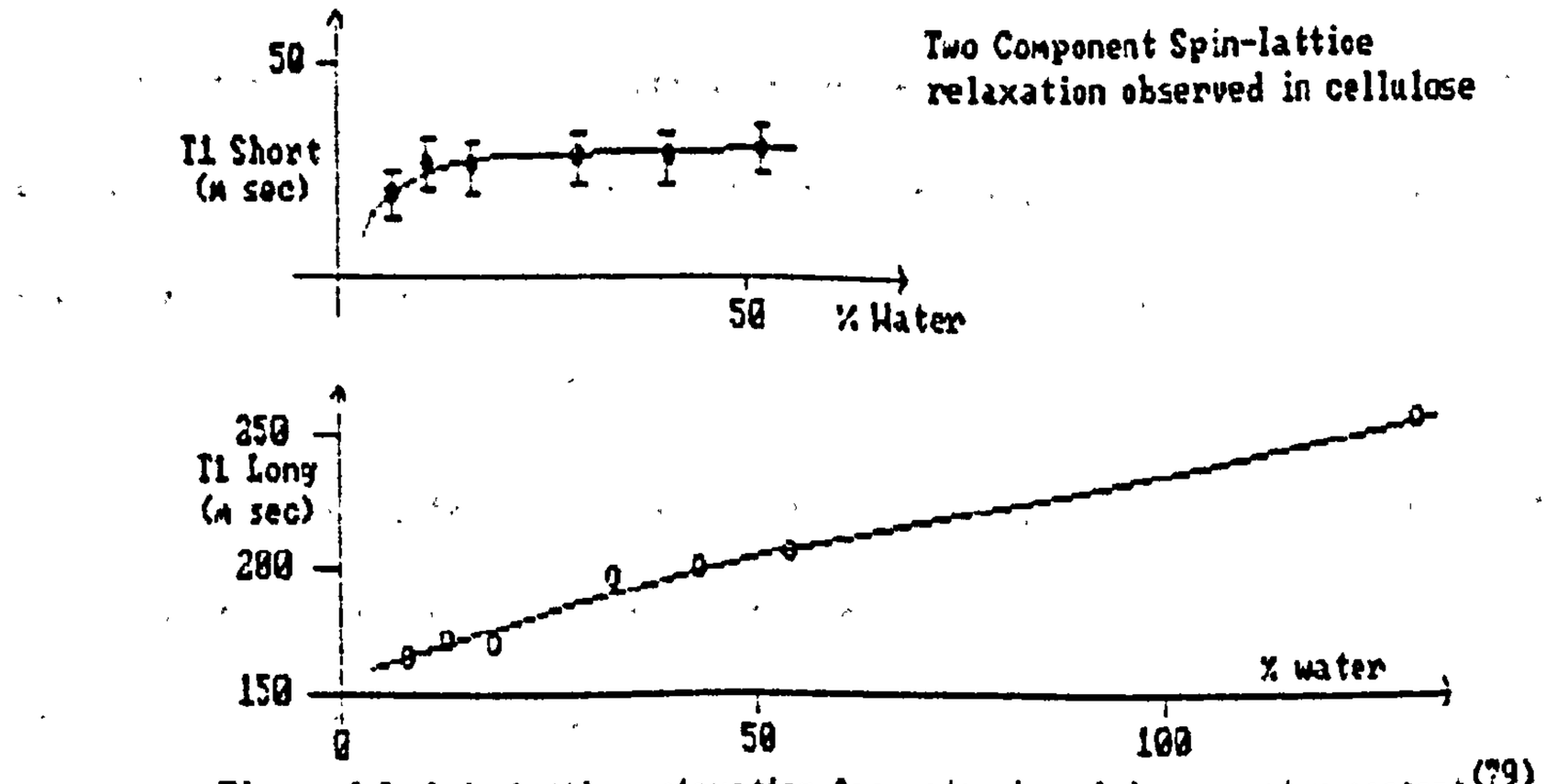

Figure 4.3 Spin-lattice relaxation for water in celulose v water content.[79]

The multi-component nature of the spin-lattice relaxation led them to postulate the co-existence of two water phases, with the rapidly relaxing phase being associated with tightly bound molecules, which are probably bonded to free OH groups on the cellulose, and the phase with the longer T1 originating from a more mobile unbound fraction. The contribution to the total signal amplitude of the fast relaxing component was found to have a temperature dependence, suggesting protons exchange between the two populations. By assuming slow exchange between the bound and unbound phases, they found the correlation times for the two phases from Kubo and Tomita's revises BPP theory to be 10^{-10} and 10^{-11} seconds for the fast and slow relaxing components respectively, and these are consistent with times observed in dielectric relaxation. in contradiction to Odajima's[81] earlier findings.

Hsi et al[82] found similar relaxation characteristics in their study on the behaviour of T1 and T2 in frozen suspensions of cellulose as a function of temperature. It was found that there existed a significant amount of water in the systems which does not freeze at low temperatures. Once again, two constants were required to describe the spin-lattice relaxation while the spin-spin relaxation was described by a single exponential function. 70% of the signal was attributed to the component with the longest relaxation time, and this proportion was found to be independent of temperature below the freezing event, indicating that the rate of exchange between the two populations had been reduced beyond detection.

The larger T1 exhibited a minimum of 230K. There was a considerable difference between the values of T2 and the T1's at the minimum which, according to Resing, is indicative of a distribution of correlation times. The data could be fitted, using a gaussian distribution of $\ln(\tau)$, but this idea was refuted by the author, who chose to explain the results in terms of cross-relaxation effects.

Freezing minimises the possibility of chemical exchange, and all the unfrozen water must be associated with the surface in some way. To explain the multiple behaviour of the spin-lattice relaxation alongside exponential relaxation in the transverse plane, both Sasaki and Hsi considered the possibility of a cross relaxation interaction between protons on the solid and on the liquid. These effects are expected to contribute solely to the spin-lattice relaxation. Using samples saturated with Deuterated water, a clear doublet was evident below the freezing event that was not observed above. This is consistent with the inducement of a prererential orientation by the cellulose surface.

It is difficult to say whether the two populations observed by Hsi and those observed by Sasaki are the same, as the two experiments were conducted on opposite sides of the freezing event.

4.4.2 NMR of water in wood.

Nuclear Magnetic Resonance provides a non-destructive method for studying water in wood. The most simple application has been to measure the water contents of wood by observing the amplitude of the decay following a single 30-degree pulse[83]. Provided that the applied r.f. field does not overload the receiver for more than a few microseconds, the transient response will consist of a signal due to the solid content of the wood superimposed upon the signal from water protons. The amplitude of each component to the total signal is proportional to the number of protons contributing to it and so, by resolving the two fractions and making some assumptions about the proton density in each, it becomes a simple matter to derive the moisture content of samples.

A rather more sophisticated method was used by Carles and Scallon[79] to estimate the amount of bound water resident in wood and cellulose gels. They measured the line width in steady state measurements on samples with moisture contents as high as 300% and, from these measurements, they derived a value for the T2 of the water. A two-state model for water in the system was evoked with water molecules residing in a bound layer and in an equilibrium mixture of structured and unstructured water. Rapid exchange between these two fractions leads to an observed relaxation time which is the weighted average of the relaxation times of the separate relaxation times. This is represented mathematically as:

$$\frac{1}{T} = \frac{B}{Tb} + \frac{F}{Tf} \qquad 4.8$$

where B and F are the probabilities but, at a given time, a proton is in the bound or free state.

The three orders of magnitude that separate Tb and Tf leads to the simplified equation:

$$Tobs = Tb \times [H2O]t/[H2O]b \qquad 4.3$$

where [H2O]t and [H2O]b are the total population, and the population of water molecules in the bound phase respectively. From this it can be seen that, provided the bound water fraction remains fixed, the observed relaxation time depends upon the relaxation time of the bound fraction, and on [H2O]b.

Carles and Scallan found a linear dependence of Tobs on [H2O]t for moisture contents of above 0.38g/g. From the linear portion of the graph they estimated the value Tb/[H2O]b, and from the intercept on the Tobs axis they obtained an upper limit to the value of Tb, thus giving a maximum estimate from the value of [H2O]b. The point at which the curve deviates from linearity was taken as a measure of the fibre saturation point within the samples. The amount of bound water within the samples appeared to correspond to a monolayer upon all the accessible surface area.

Transverse NMR relaxation times of water in wood were the focus of a study by Riggin et al[84], using spruce sapwoods with moisture contents as high as 176%. A value of several microseconds was found for the T2 of protons in wood, and this increased slightly with increasing moisture content.

Below 30% moisture content the FID attributed to the water was exponential, and increased from approximately 80 microseconds at 5% moisture content, to a value of about 0.9 milliseconds at 30% moisture content. At higher water contents the relaxation of the magnetisation due to the water content is the sum of two exponentials. The behaviour of the two time constants is shown in figure 4.4 as a function of the moisture content. Three phases of hydrogen nuclei were used to explain the nature of these curves, which corresponded to the protons residing in wood for which Nanassy[85] claimed that 38% were exchangeable with protons in the water, and two water phases that corresponded to the bound and non-bound water

components. The exchange between protons in wood and water is expected to be relatively slow to enable the two signals to be resolved. The exchange is restricted to the bound fraction of water. The bound and mobile fractions are also expected to be in exchange with each other on a time scale which is slow compared to the observed relaxation times of each component.

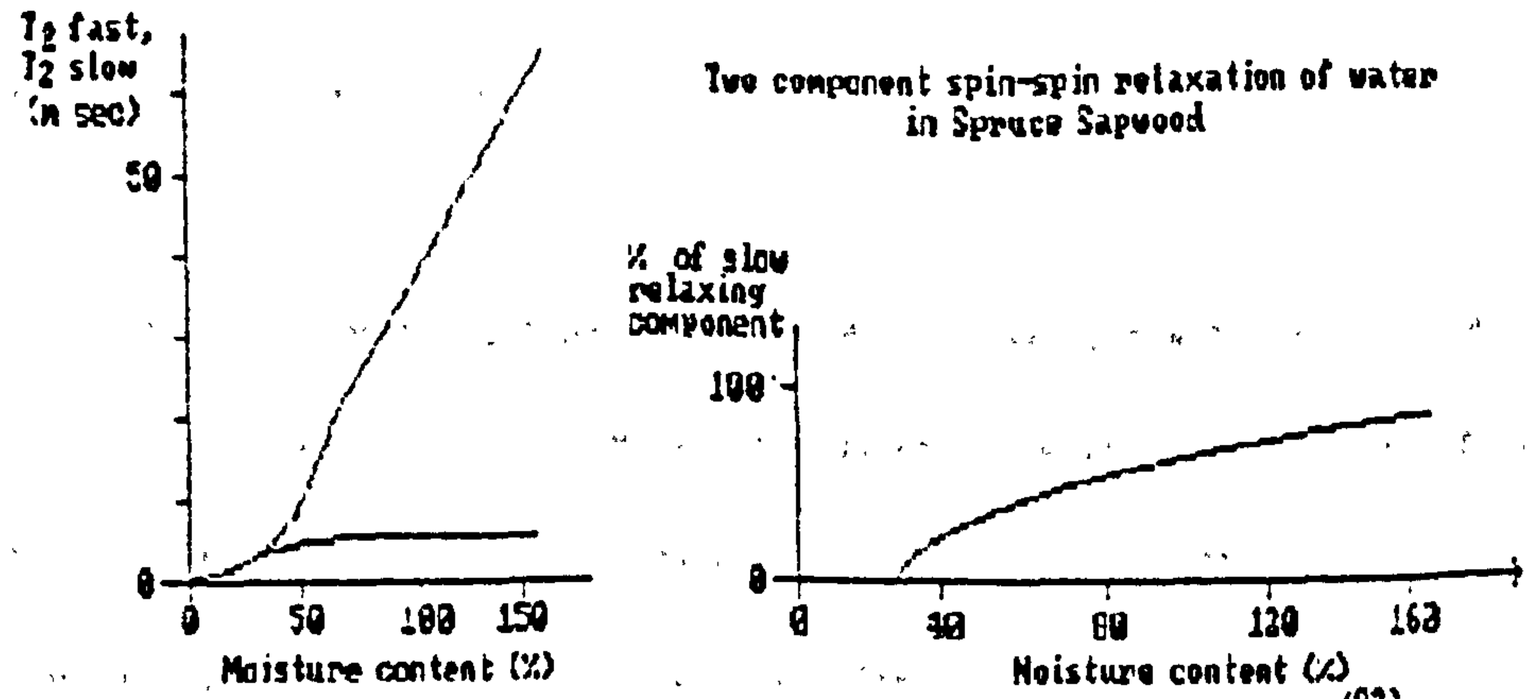

Figure 4.4 Spin-Spin relaxation in Spruce sapwood v. moisture content.[83]

Using this model, Riggin et al could account well for the data. They pointed out that the observed values of the populations and relaxation times for the three families of protons were not the true values because of the exchange between fractions. It was also noted that in steady state experiments the width of the NMR lines were greater than predicted by the theory of chemical exchange, leading the authors to suggest that the relaxation times reported actually represented complicated ensemble averages over many different phases of the system.

Hsi, Hossfeld and Bryant[84] undertook a similar study to that performed by Riggin and found that in general, both T1 and T2 were double-exponential for moisture contents greater than 30%. Below this value the transverse relaxation was characterised by a single parameter, but the longitudinal relaxation still required two time constants. Two types of behaviour were observed for the signal intensity as a function of temperature: below 0.38 g of water per gram of wood no freezing event was evident, whereas a clear freezing event was

observed in samples of higher moisture content. A slight decrease in the FID amplitude with decreasing temperature could be seen below the freezing event. Below the freezing event, and for samples containing moisture contents of above and below the 30% identified as the fibre saturation point, the transverse relaxation was exponential, while the longitudinal relaxation required two time constants. In both cases the rapidly relaxing fraction contributed 30% to the total signal amplitude.

The appearance of a second component of transverse relaxation was adequately explained by assuming that below 30% moisture content all the water is associated with the surface and, above 30%, the additional water is not absorbed by the cell wall matter. It was postulated that the non-exponential longitudinal behaviour arises from coupling between the solid wood protons having a long T1 but short T2 and water protons with a shorter T1.

Evidence of a distribution of correlation times was found from the ratio of the transverse to longitudinal relaxation times. The depression of T2 may also have been caused by chemical exchange between solid protons and those in the liquid state.

The data of Hsi et al was used by Brownstein[87] to support his theory that, as the moisture content is varied, the behaviour of the two transverse relaxation times could be explained using a model based on the diffusion equation. The model assumed that water could reside in a layer within or bound to the wood where the diffusivity of the molecules is severely reduced, or in a non-absorbed layer where the diffusivity is close to that observed for water in the bulk. The relaxation of the proton spin magnetisation of the water molecules was considered to be due to a combination of diffusion and magnetic sinks on the surface of the cell wall.

The solution to the Brownstein and Tarr equations in section 4.3, subject to the boundary conditions that evolve from the Brownstein model, is a sum of exponentials for which the relaxation times Tn are given by:

$$(b/a - 1)\,\xi_n \tan \xi_n = 1 \qquad 4.10$$

where ξ is defined by $T_n = a^2/(D\,\xi_n^2)$ 4.11

a is a measure of quantity of unbound water, D is the diffusivity of water in the absorbed layer, and b represenrs the thickness of the non-absorbed layer.

Using n = 0,1 the model adequately predicted the values of the two transverse relaxation decay times observed by Hsi et al as a function of moisture content.

Wood is a highly structured and fibrous material, and anisotropy of the proton NMR spectrum and T1 relaxation times was found by Vriesenga[88] et al who made measurements as a function of the angle between the wood fibre and the magnetic field. Their steady state experiments implied that three types of water existed in the samples at 100% relative humidity and the resonant frequency of each was a function of the orientation of the samples. From the nature of this orientation dependence, the authors concluded that the vast majority of sorbed water exists in the inter-fibril region of the cell wall and that the three types of water-filled regions exist, each possessing a different symmetry relative to the fibre axis. This symmetry must persist throughout the sample in order for its effect to be observed.

In de-lignified samples, the positions of the resonance peaks as a function of the sample orientation were markedly different from those observed in the fresh timbers. The authors suggested that the orientational dependence was not a result of direct alignment of water molecules with the celluloses in the cell walls because the resonances did not appear as

doublets. Instead they believed that the symmetry was caused by a magnetically anisotropic environment within the inter-fibrillar regions that originated from ordered magnetic components of the lignin such as phenolic rings. The ordering in the lignin could be caused by its interaction with the cellulose via the hemicelluloses.

The effective self diffusion coefficients of water in wood were measured by MacGregor et al[99] using the pulsed field gradient technique. The values obtained were reduced from the value for the self diffusion coefficient of distilled water and depended upon the orientation of the fibres to the field gradient. In general, diffusion was the greatest in the longitudinal direction, i.e. along the direction of the fibres.

The depression of the diffusion coefficient in the wood was explained by assuming that the water molecules were bounded by the cell walls. This leads to restricted diffusion, and the dimensions of the boundaries could be estimated from the magnitude of the diffusion coefficients. For diffusion perpendicular to the direction of the fibres, the dimensions agreed reasonably well with the known width of the cells. In the longitudinal direction, however, the distance between boundaries is too great to influence the diffusion coefficient. To explain the reduced value, it was necessary to treat the observed diffusion coefficient as the weighted average of coefficients for water residing in the cell lumen that is not bounded, and water residing in the pits in cell walls and bounded by the spiral thickenings that protrude into the lumen, which lower the measured rate of diffusion. If exchange between these regions is slow, then two component diffusion decay would have been observed. Non was reported however.

The major conclusions to be derived from such studies are that the NMR properties of water in wood are complex and need careful interpretation. Nevertheless, they provide useful and probably unique insights into the molecular dynamics of water within the system[100].

References:

1. Belton P.S., Ratcliffe R.G. "NMR and Compartmentation in Biological tissues." Prog. NMR Spectroscopy. Vol17, pp241-279. (1985)

2. Packer K.J. "The dynamics of water in heterogeneous systems." Phil. Trans. R. Soc. B. Vol 278, pp 59-87. (1977)

3. Michelson C., Berendsen H.J.C. "Proton exchange and molecular orientation of water in hydrated collagen fibres." J. Chem. Phys. Vol 59, pp 296-305. (1973)

4. Mathur-De Vre R., Bertinchamps A.J., Berendsen H.J.C. "The effect of gamma-radiation on the hydration of DNA and polynucleotides. I. An NMR study of frozen H_2O and D_2O solutions." Radiat. Res. Vol 68, pp197-214. (1976)

5. Franks F. "Solvation interactions of proteins in solution." Phil. Trans. R. Soc. B. Vol 278, pp 89-96. (1977)

6. Katayama S., Fijiwara S. J. Phys. Chem. Vol 84, p 2320. (1980)

7. Katayama S., Fijiwara S. J. Am. Chem. Soc. Vol 101, p 4485. (1979)

8. Carles J.E., Scallan A.M. J. App. Polymer Sci. Vol 17, p 1855. (1973)

9. Hsi E., Bryant R.G. J. Am. Chem. Soc. Vol 97, p 3220. (1975)

10. Derbyshire W., Parsons J.L. J. Mag. Resonance, Vol 6, p 244. (1972)

11. Lynch L.J., Webster D.S. J. Coll. Interface Sci. Vol 69, p 238. (1979)

12. Lynch L.J., Webster D.S. Fuel Vol 58, p 429. (1979)

13. Mrevlishvili G.M., Sharimanov Y.G. Biophysics Vol 23, p 242. (1978)

14. Resing H.A., Foster K.R., Garroway A.N. Science Vol 198, p 1181. (1977)

15. Golton I.C., Gellatly B.J., Finney J.L. Studia Biophysica Vol 84, p 5. (1981)

16. Leung H.K., Steinberg M.P. J. Food Sci. Vol 44, p 1212. (1979)

17. Haly A.R., Snaith J.W. Biopolymers. Vol 7, p 459. (1969)

18. Ashpole D.K. Proc. Royal Soc. London. Vol A212, p 112. (1952)

19. Mousseri J., Steinberg M.P., Nelson A.I., Wei. L.S. J. Food Sci. Vol 39. p 114. (1974)

20. Woodhouse D.R., Derbyshire W., Lillford P.J. J. Magn. Res. Vol 19, p 267.

21. Narebska A., Streich W. Coll. Polym. Sci, Vol 258, p 379. (1980)

22. Fung B.M., Durham D.L., Wassil D.A. Biochim. Biophys. Acta. Vol 399, p 191. (1975)

23. Resing H.A. J. Chem. Phys. Vol 43, p 669. (1965)

24. Morariu V.V., Chiricuta I.C. Oncologia Vol 16, p 291. (1977)

25. Oakes J. J. Chem. Soc. Farad. Soc. Trans. I. Vol 72, p 216. (1976)

26. Lynch L.J. "Water relaxation in heterogeneous and biological systems." Magnetic Res. (2) Chapter 5. (1983)

27. Haly A.R., Snaith J.W. Biopolymers. Vol 10, p 1681. (1971)

28. Dehl R.E. Science. Vol 170, p 738. (1970)

29. Ramirez J.E., Cavanaugh J.R., Purcell J.M. J. Phys. Chem. Vol 78, p 807. (1974)

30. Morariu V.V., Mills R. J. Coll. Interface Sci. Vol 39. p 406. (1972)

31. Pearson R.T., Derbyshire W. J. Coll. Interface Sci. Vol 46, p 232. (1974)

32. Barnes G.J. Z. Angew Math. Phys. Vol 13. p 533. (1962)

33. Packer K.J. "Nuclear spin relaxation studies of molecues adsorbed on surfaces." Prog. in NMR Spectroscopy. Vol 3, pp 87-128. (1967)

34. Cooke R., Kuntz I.D. "The peoperties of water in biological systems." Ann. R. Biophys. (3) article 9035, pp 95-126. (1974)

35. Packer K.J. Phil. Trans. R. Soc. London Vol 278, p 59. (1977)

36. Brownstein K.R., Tarr C.E. "Spin-lattice relaxation in a system governed by diffusion." J. Mag. Reson. Vol 26, pp 17-24 (1977)

37. Brownstein K.R., Tarr C.E. "Importance of classical diffusion in NMR studies of water in biological cells." Phys. Rev. A. Vol 19(6), p 2446. (1979)

38. Chang D.C., Hazlewood C.F. Biochim. Biophys. Acta. Vol 630, p 131. (1980)

39. Lillford P.J., Clark A.M., Jones D.V. A.C.S. Symp. Ser. \vol 127, p177 (1980)

40. Fung B.M., Puon P.S. Biophys J. Vol 33, p 27 (1981)

41. Oakes J. J. Chem. Soc. Faraday Trans. Vol 31, p 207 (1976)

42. Conlon T., Outhred R. Biochim. Biophys. Acta. Vol 288. p 354. (1972)

43. Fabry M.E., Eisenstadt M. Biophys. J. Vol 15, p 1101. (1975)

44. Pirkle J.L., Ashley D.L., Goldstein J.H. Biophys. J. Vol 25, p 389. (1979)

45. Shporer M., Civan M.M. Biochim. Biophys. Acta. Vol 773, p 219. (1984)

46. Getz D., Gibson J.F., Sheppard R.N., Michelin K.J., Pasternale C.A. J. Membr. Biol. Vol 50, p 311. (1979)

47. Shporer M. Haas M., Civan M.M. Biophys. J. Vol 16, p 601. (1976)

48. Beall P.T., Hazlewood C.F., Roa P.N. Science NY. Vol 192. pp 904-907. (1976)

49. Damadian C. Science NY. Vol 171, pp 1151-3. (1971)

50. Belton P.S., Jackson R.R., Packer K.J. Biophim Biophys. Acta. Vol 286, p 16. (1972)

51. Diegel J.G., Pinter M.M. Biophys. J. Vol 15, p 855. (1975)

52. Hazlewood C.E., Chang D.C., Nichols B.L., Woessner D.E. Biophys. J. Vol 14, p 583. (1974)

53. Neville M.C., White S. J. Physiol. Vol 288. p 71. (1979)

54. Foster K.R., Resing H.A., Garroway A.N. Science. Vol 194, p 324. (1976)

55. Belton P.S., Packer K.J. Biochim. Biophys. Acta. Vol 354, p 305. (1974)

56. B.M. Fung Biophys. J. Vol 18, p 315. (1977)

57. Pearson R.T., Duff I.D., Derbyshire W., Blanshard J.M.V. Biocim. Biophys. Acta. Vol 362, p 188. (1974)

58. Outhred R.K., George E.P. Biophys. J. Vol 13, pp 83-96. (1973)

59. Outhred R.K., George E.P. Biophys. J. Vol 13, pp 97-103. (1973)

60. Knispel R.R., Thompson R.T., Pintar M.M. J. Mag. Res. Vol 14, pp 44-51. (1974)

61. Finch E.D., Homer L.D. Biophys. J. Vol 14, pp 907-921. (1975)

62. Fung B.M., McGaughy T.W. Biochim. Biophys. Acta. Vol 343, pp 663-673. (1974)

63. Cooke R., Wein R. Biophys. J. Vol 11, pp 1002-1017. (1971)

64. Fung B.M. Biochim. Biopnys. Acta. Vol 497, pp 317-322. (1977)

65. Belton P.S.. Packer K.J. Biochim. Biophys. Acta. Vol 354. pp 305-314. (1974)

66. Chang D.C.. Hazlewood C.F., Woessner D.E. Biochim. Biophys. Acta. Vol 437. pp253-258. (1976)

67. Hazlewood C.F.. Nichols B.L.. Chang D.C., Brown B. Johns Hopkin's Med. J. Vol 128. pp117-131. (1971)

68. Menke W. "Biochemistry of Chloroplasts. Vol 1." Ed T.W. Goodwin. p3 Academic Press. London. (1966)

69. Stout D.G.. Steponkus P.C.. Cotts R.M. Plant Physiol. Vol 62. pp 636-641. (1978)

70. McCain D.C., Selig T.C., Govidjee, Markley J.L. Proc. Natl. Acad. Sci. USA. Vol 81. p 748. (1984)

71. Clowes F.A.L., Juniper B.E. "Plant Cells." Chapter 2. Blackwell, Oxford (1968)

72. Banavar J.R.. Koplik J.. Winkler K.W. "Physics and Chemistry of Porous media. II." AIP Conference proceedings 154. Am. Inst. Phys. NY 1987.

73. Cohen M.H., Mendelson K.S.,"Nuclear Magnetic Relaxation and the internal geometry of sedimentary rocks." J.Appl.Phys. 53(2), February 1982

74. Banavar J.R.. Schwartz L.M. "Magnetic Resonance as a probe of permeability in porous media." Phys.Rev.Lett. 58(14) April 1987.

75. Schmidt E.J., Valesco K.K., and Amos M. "Quantifying solid fluid interfacial phenomena in porous rocks with proton nuclear resonance." Nmr.J.Appl.Phys 59(8), 15 April 1986.

76. Lipsicas M., Banavar J.R, Willemsen J. "Surface relaxation and pore sizes in rocks - a nuclear magnetic resonance analysis." App.Phys.Lett.48(22) June 1986.

77. Child T.F. "Pulsed NMR study of molecular motion and environment of sorbed water on cellulose." Polymer Vol 13 June 1972

78. Froix M.F., Nelson R. "The interaction of water with cellulose from NMR relaxation times." Macromolecules 8(6) Nov-Dec 1975.

79. Carles J.E., Scallan A.M. J. App. Polym. Sci. Vol 17, pp 1855-1865. (1973)

80. Sasaki M., Kawai T., Hirai A., Odajima A. "A study of sorbed water on cellulose by pulsed NMR technique." J. Phys. Soc. Japan 15(9) Sept 1960.

81. Odajima A. "Nuclear Magnetic Resonance studies of water sorbed on fibrous materials." J. Phys. Soc. Japan 14(3) March 1959.

82. Hsi E., Vogt G.J., Bryant R.G. "NMR study of water absorbed on cellulose." J. Coll. and Interface Sci. 70(2) June 1979.

83. Sharp A.R., Riggin M.T., Kaiser R., Schneider M.H. Wood and Fibre. 10(2) 1978.

84. Riggin M.T., Sharp A.R., Kaiser R. "Transverse NMR relaxation of water in wood." J. Appl. Polym. Sci. Vol 23, pp 3147-3154. (1972)

85. Nanassy A.J. Wood Sci. Vol 5, p 187. (1972)

86. Hsi E., Hossfield R., Bryant R.G. J. Coll. Interface Sci. Vol 62. p 389. (1977)

87. Brownstein K.R. "Diffusion as an explanation of observed NMR behaviour of water absorbed on wood." J. Mag. Res. Vol 40, pp 505-510. (1980)

88. Vriesenga J.R., Chandrasekaran S., Luner P. "Proton NMR of adsorbed water in wood." J.App. Polym. Sci. : App. Polym. Symposium 37. pp 911-921. (1983)

89. MacGregor R.F., Peemoeler H., Schneider M.H., Sharp A.R. "Anisotropic diffusion of water in wood." J. App. Polym. Sci. : App. Polym. Symposium 37. pp 901-909. (1983)

90. Mendelson K.S. J. Electrochem. Soc. Vol 133. p 631. (1986)

Chapter 5. Experimental Detail and Sample Preparation.

5.1 Introduction.

Two experimental systems were used during the course of this work, and a description of each is given here. A number of changes were made to both systems. The changes included modifications to the hardware, and a revision of the data handling techniques. For convenience the two systems were called the B225 system and the A140 system. Ancillary equipment common to both systems is described in section 5.4.

In section 5.7 a description is given of the methods used in preparing samples of both polymer solutions, and the xylem itself.

5.2 The B225 Spectrometer.

5.2.1 The Magnet.

An A.E.I. M12 water-cooled electromagnet provided the static field Bo. The magnet has nine inch pole pieces and using a pole gap of up to 5 cm was capable of producing a field of 1.4 Tesla. The original A.E.I. power supply was changed to a solid state supply which lead to a long term stability in the magnetic field of better than 1 part in 10^4, although the short term stability was significantly less than this.

5.2.2 The Spectrometer.

The basis of the spectrometer was a second hand Bruker B-KR-302 machine designed to operate at 14MHz and 60MHz. It incorporated a home made pulse programmer from which logic level pulses were amplified and fed into the r.f. gates of the Bruker transmitter. The power amplifier could deliver approximately 400 volts peak to peak into an impedance of 50 Ohms. (See figure 5.1).

Figure 5.1 The B225 Spectrometer. MKI.

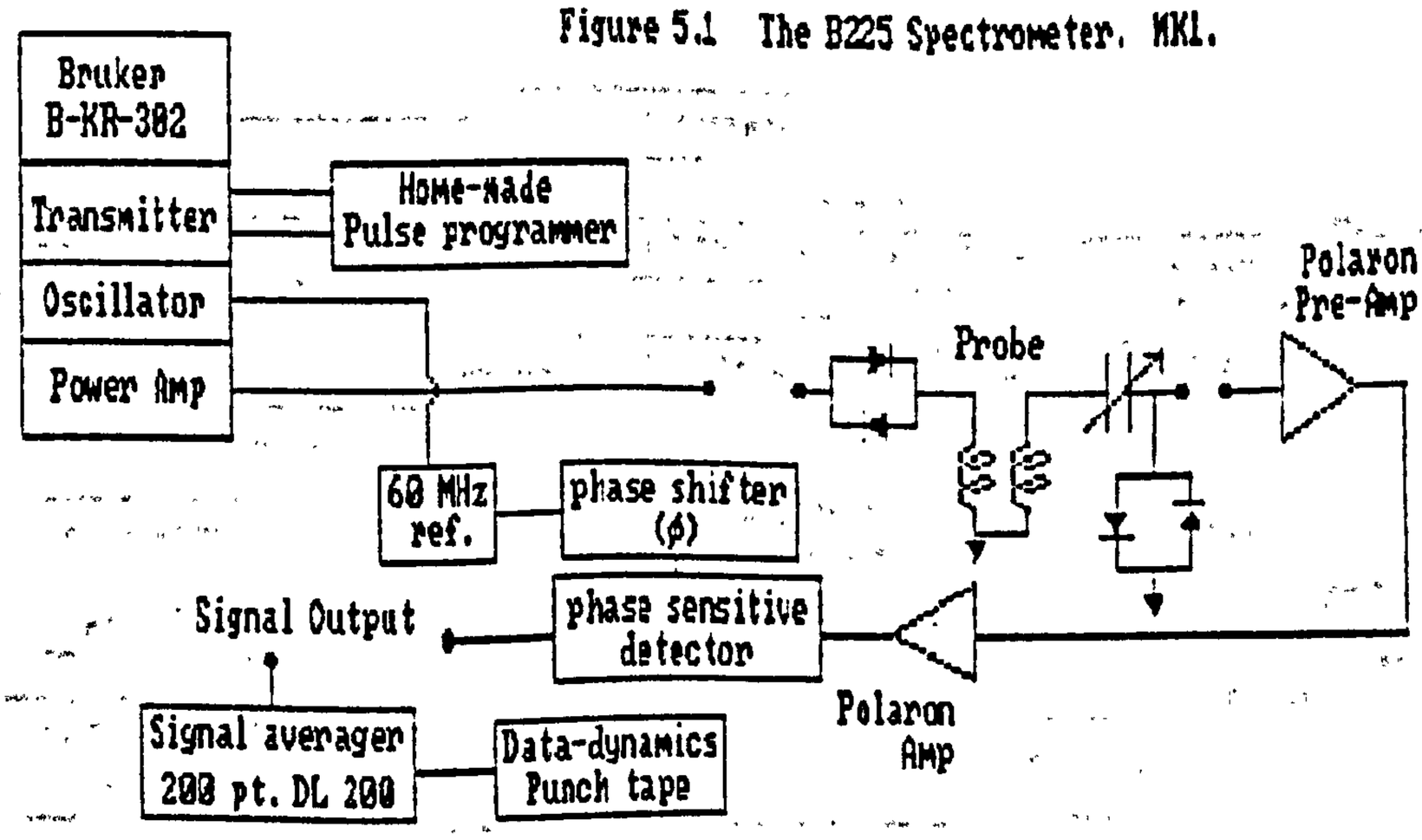

The reliability of this system was poor, and the B-KR-302 was replaced by a home built spectrometer, for which the r.f. source was a Schlumberger frequency synthesiser with a frequency range of between 2 and 40 MHz. The output from this was split into three channels, two of which formed the r.f. signal channels, and the third was used as a reference channel. The r.f. channels were phase shifted and gated. The output from the gates were then combined and the signal frequency was doubled before being fed into a Bruker high power r.f. amplifier requiring an input of just 1 volt peak to peak.(See figure 5.2)

The r.f. pulse lengths set using the pulse programmer were continuously variable up to 10 ms. and 90° or 180° r.f. pulses were easily obtainable by the observation of the nuclear signal upon adjustment of the pulse length to give a maximum or minimum in the signal. The phases of the first and subsequent pulses could be shifted independently so that the shifts required by the CPMG sequences were simple to produce.

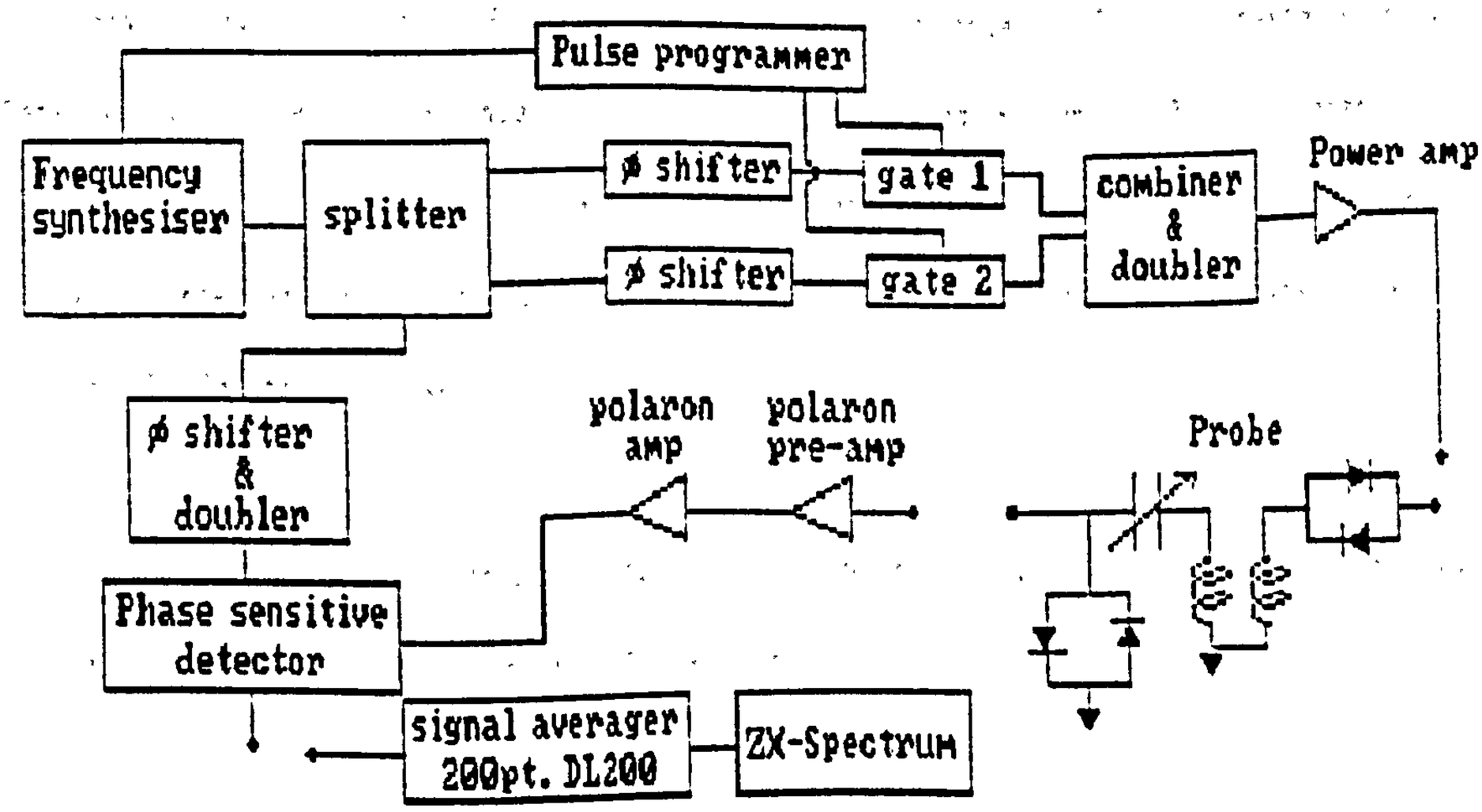

Figure 5.2 The B225 Spectrometer. MK2.

Measurements made on this system were at 60 MHz, where the pulse length for a 90° r.f. pulse was approximately 3 μs.

The probe assembly is described in section 5.4. The nuclear signal was amplified using a commercial Polaron receiving system consisting of pre-amplifier and amplifier units. The output from this was fed into a home built phase-sensitive detector, for which the reference signal was derived from the oscillator in the spectrometer that was fed into a 60 MHz tuned amplifier and then phase shifted. The overall dead time of the receiver mechanism was quoted as 40 μs.

A diode detection system provided an alternative to the phase sensitive detector, but because of the non-linearities in response at low signal strengths phase detection was preferred.

5.2.3 Data Handling.

Signal averaging on the B225 system was achieved in the case of T2 measurements using a Data Lab DL200 linked to the paper-tape punch of a Data Dynamics type 1133 teleprinter. For signal averaging of transients such as those in T1 measurements, P.F.G. diffusion measurements and freezing curve experiments, a Biomation 600 transient recorder interfaced to a Sinclair ZX Spectrum was used.

Data processing was carried out on either the departmental Data General Corporation Nova 1220 minicomputer, or directly on the ZX Spectrum.

5.3 The A140 Spectrometer.

5.3.1 The Magnet.

An A.E.I water-cooled magnet similar to that used in the B225 system was employed here. The power supply was found to be far more reliable however, and a stability of better than 1 part in 10^4 as easily maintained over a period of several hours.

5.3.2 The Spectrometer.

The spectrometer was a home built broad-band system, operating over a frequency range of 4 to 30 MHz. It was designed to be controlled using either a modified hard-wire pulse programmer, or by the use of a software controlled pulse programmer.

The output of a Fluka 6160 A/DX frequency synthesiser was split into four and each was presented at the inputs of a wide band phase shifter. (See figure 5.3). Two fixed phase shifters produced shifts of either 0°, 90°, 180°, or 270° and two were available as manually variable channels. The outputs of selected phase shifters were fed into a signal and a reference multiplexer, and the output of these was determined by either the software of a programmable Hazeltine unit, or via the manual operation of hard-wired pulse programmer.

The output from the signal channel multiplexer was split into two. These channels were passed through a stage of r.f. amplification and the r.f. gates, following which they were combined and entered two further stages of amplification. The first stage was accomplished using a Polaron wide-band RF 460-BA2 amplifier, and the second stage was carried out by a home built Mullard design amplifier which supplied a 500 volt peak to peak signal into a 50 Ohm impedance.

The reference channel from the multiplexer was fed into a variable phase shifter and then to the detector.

The pre-amplifier of the receiving system was attached to the same mounting as the probe assembly and was designed around a Plessey SL 610 r.f. amplifier with automatic gain control. The input stage was a conventionally tuned F.E.T. amplifier. The overall gain of the pre-amp was 40dB. The output of the pre-amp was fed into a Hewlett Packard wide band amplifier with switched 20dB or 40dB gain, and the output from this went directly into the signal channel of the detector.

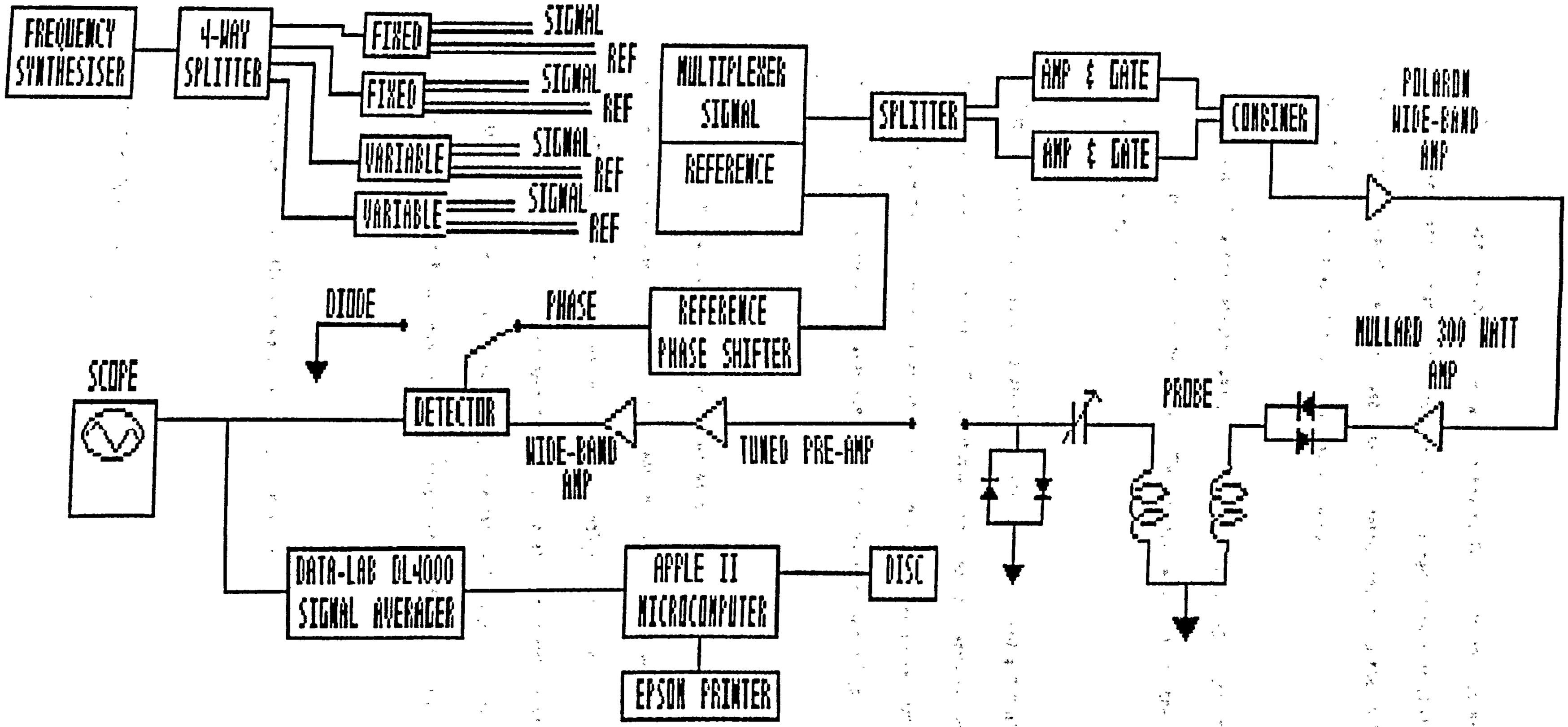

Fig 5.3 The A140 Spectrometer.

The detector was designed around a Minicircuits SRA-1 passive double-balanced modulator. The local oscillator input to the modulator was arranged to be connected to the output of the reference phase shifter for phase sensitive detection, or to the earth for diode detection. This switching was done using a coaxial relay.

The output from the detector was amplified and a simple L-C filter on the output of this provided a time constant for the signal. The overall dead time for the system was approximately 25 μs.

The software controlled pulse programmer was designed around a Z80 microprocessor and a second hand Hazeltine terminal. The programmer operated on a menu system whereby one of a number of pre-defined pulse sequences could be selected. Variables such as the number of repetitions and the delays between specific sequences were entered on request via the Hazeltine keyboard.

For the hardware system the pulse sequences and parameters were set manually using pole switches, and was found to be more convenient when carrying out experiments where a single parameter in a sequence was constantly changed, such as the value of τ in a 180°-τ-90° r.f pulse sequence used in T1 measurements. The system also incorporated an nth point sampling facility so that τ could be maintained at a constant value during T2 measurements, thereby eliminating the effects of varying τ in systems where diffusion of the resonant nuclei takes place.

Measurements on this system were made at 16MHz - 18MHz.

5.3.3 Data Handling.

Signal averaging on the A140 system was achieved using a Data Lab DL4000 signal averager, interfaced with an Apple II microcomputer with two disc drives for data storage. A hard copy of results could be made using an Epsom MX-80 printer.

5.4 Ancillary Equipment.

5.4.1 The Probe Assembly.

The probe assembly was a conventional two coil design with transmitter and receiver coils wound coaxially on a 10 mm glass former. This then fitted inside an evacuated jacket enabling a gas-flow temperature system to be used. The inner diameter of the former was sufficiently large to accommodate a 7 mm sample tube. Separate probe inserts that could be tuned to set frequencies were employed on the 60 MHz spectrometer and the 16MHz system. Fine tuning was made possible in the receiver coil by means of a home made series capacitor system.

5.4.2 The Temperature Controller.

Temperature control of the sample was achieved using an Oxford Instruments EA 2349 temperature control unit in conjunction with a gas flow mechanism. For temperatures of 25°C and above, air was used from the laboratory supply, and for temperatures below this nitrogen was used as the cryogenic, being boiled off from a dewer vessel.

Control of the gas temperature was achieved by means of a heater placed in the gas line in front of the probe. A copper-constantan thermocouple sensor, situated just below the r.f. coil, fed the signal back to the temperature controller and regulated the heater current.

The controller was calibrated against a glass thermometer with its bulb immersed in a sample tube containing glucose solution. The system was accurate to within 0.7 degrees over the temperature range 210K to 370K.

5.4.3 The Bruker Minispec.

On loan to the Mary Rose Trust was a Bruker CP-2 Minispec. This is a device which operates at a frequency of 10 MHz, using a pole temperature of 40°C. It has the ability to measure solid:liquid ratios, and single component T1 and T2s.

The solid:liquid ratios were measured by the delivery of a single 90° pulse to the sample. The resulting FID is then sampled at two points, chosen at 11μs and 70μs for the purposes of this work. The FID can be monitored using a CRO attached to the minispec, for which there is a choice of diode or phase detection.

5.5 The Diffusion Equipment

5.5.1 The Pulsed Field Gradient Coils.

Standard Bruker field gradient coils were used throughout this work. These were a Helmholtz arrangement where the coils were electrically in series, but magnetically opposed. The coils each consisted of four pancake layers of copper wire coils embedded in a resin block, fixed to low eddy current plates. They were mounted on the side plates of the probe head so that the sample lay in the region of the most linear field gradient, and so that the gradient was in the direction of Bo.

The largest region of uniform magnetic field gradient in such an arrangement is found to be when the radii of the coils are 3·⁴ times their separation, and although this condition was not met by the Bruker coils the field was expected to by approximately linear over the small volume of the sample.

To ensure that the diffusion coefficients determined using this configuration were reliable the coils were calibrated. This is done using one of two methods. The first makes use of the fact that the shape of a spin echo for a sample in a field gradient G is determined by both the geometry of the sample, and the magnitude of the field gradient. For a cylinder of radius r, the height of the echo at time t is dominated by the first order Bessel function given by[11];

$$\frac{J_1(\text{gamma}.G(2\tau-t)r)}{\text{gamma}.G(2\tau-t)r}$$

If the time between the first two zeros on either side of the echo centre is denoted by δt, then the field gradient when observing protons is given by;

$$G = \frac{2.865 \times 10^{-4}}{r.\delta t} \text{ gauss cm}^{-1}$$

The shape of the spin echo was observed for a cylindrical water sample as the steady current through the field gradient coils was increased. The values of the field gradient were then estimated from the separation of the null points and using the expression given above. The results are shown in figure 5.4. The gradient was found to be independent of the diameter of the sample within experimental error, indicating that at the site of the sample the region of linearity was sufficiently large.

The coils could also be calibrated by assuming a value of $2.3 \times 10^{-5} cm^2 s^{-1}$ for the self diffusion coefficient of distilled water at 25°C. Steady field gradient and pulsed field

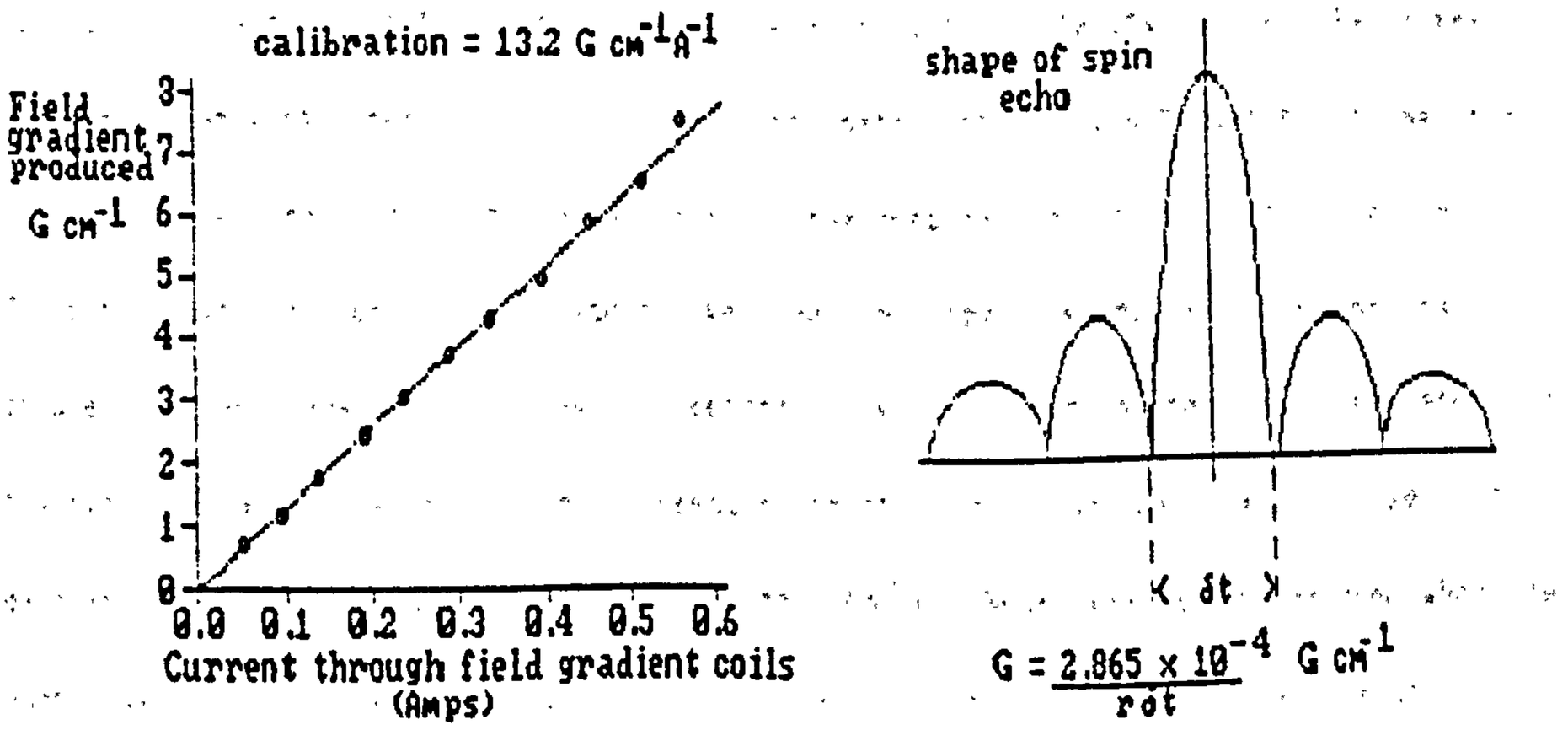

Figure 5.4 Calibration of the field gradient coils.

gradient measurements for water at 25°C were made from which the strength of the field gradients could be inferred. In the steady field gradient experiment the current through the coils was measured directly using a digital ammeter, while for the PFG experiment the current through the gradient coils was determined from the voltage of the pulses viewed across a 0.2 Ohm monitor resistor. A comparison of these results is shown in table 5.1, and are consistent to within 10%.

Source	Field gradient. G cm⁻¹
Echo width	13.2 ± .7
PFG experiment	13.5 ± .5
SFG experiment	12.4 ± .8

Table 5.1 Calibration of the Field gradient coils.

Having established that the apparatus was functioning adequately, the daily calibration of the apparatus was performed by measuring the self diffusion coefficient of distilled water at 25°C using either the PFG or SFG techniques, and diffusion coefficients were measured relative to this value.

Tests were carried out previously[2] to ensure that the field gradient coils did not produce any field gradients in the direction perpendicular to the static field Bo as this would cause motions other than those along Bo to contribute to the attenuation of the spin-echo amplitude, and lead to an over-estimate of the component of diffusion parallel to Bo. The method employed consisted of placing two fine capillary tubes containing water inside a sample tube, and separated by a few millimetres. Any difference in the field experienced in the two tubes would then result in different resonant frequencies, which would cause a beat pattern to appear superimposed on the spin-echo. No such beat pattern was observed when the common axis of the tubes was perpendicular to the static field in the SFG experiment.

5.5.2. The Pulsed Field Gradient Unit.

The unit was designed in the laboratory to produce two identical field gradient pulses of variable separation delta, and duration δ. The first of the two pulses was triggered with reference to the initial 90° pulse in the 90°-τ-180° pulse sequence produced by the spectrometer. The second field gradient pulse could be triggered using either the 90° pulse, the 180° pulse, or the first field gradient pulse as a reference. The delays of the leading edges of the field gradient pulses were set relative to their respective triggers.

The width and delay of each pulse were digitally controlled and could be varied over the range 10μs to 8 seconds. The width of the second pulse could be finely adjusted to match that of the first. In general the 4x12 volt rechargeable batteries which provided the source of the DC field gradient pulses did not have sufficient time to recover between pulses in order to deliver a second pulse of the same amplitude as the first, especially when the time interval between pulses was small. In order to compensate for this the length of the second field gradient pulse was extended by means of the fine adjustment facility, to ensure that the 'area', Gδ (See figure 3.11), for each pulse was identical, and that the height of the

resulting spin echo was maximised. Failure to match the pulses in this way leads to an incomplete refocussing of the spins and therefore to an over-estimate of the diffusion coefficient.

5.6 Data Analysis.

The decay of the magnetisation following a series of r.f. pulses in both the longitudinal direction and in the transverse plane, are in general complex functions that may be expressed in terms of a summation of exponential decays. In the CPMG sequence the height of the magnetisation's spin-echo envelope at a time t may be expressed as;

$$M(t) = \sum_{I=1}^{n} Mo_I \times \exp(-t/T_{2,I})$$

where $T_{2,I}$ and Mo_I are the apparent spin-spin relaxation times and initial magnetisations for the ith component, and n represents the total number of components that contribute to the signal. According to the theory of Brownstein and Tarr[3], although n should take an infinite value, in practice only the first few terms make a significant contribution to the decay curve and orders of n greater than 3 or 4 may be ignored. If one assumes that the decay is not determined via the mechanics put forward by Brownstein and Tarr, but rather that each component represents a different population of spins, then n should equal the total number of different populations. However, trying to resolve a decay into more than 3 or 4 components generally leads to ambiguous results. Consequently in this work, a maximum of n = 4 has been assumed.

Using a Newton-Raphson least squares fitting routine, the transverse decays for n = 1,2,3 and 4 were resolved using as many as 4000 data points for each decay envelope. The ability of the programme to resolve the decay into these components is determined in part by the mag-

nitudes of the M_{0i}s, and by the differences in the relaxation rates of the separate components. As a measure of the reliability of the fit each the standard deviation to noise ratio was calculated following each iteration of the fit, which should be close to unity for an ideal fit.

In the case of T1 measurements using a 180°-τ-90° pulse sequence the magnetisation decay is expressed as:

$$M(t) = \sum_{i=1}^{n} M_{0i} \times (1 - 2.\exp(-t/T_{1i}))$$

Since each point describing the decay has to be derived from a complete pulse sequence, which should be repeated several times in order to improve on the signal to noise ratio, fewer measurements are made. The decay is usually defined by between thirty and fifty of these points, and this makes fitting using the computer method rather inaccurate. The separate decays in T1 measurements were therefore determined using grapnical methods, whereby the longer relaxation times are successively peeled away from the curve. Once again the method relies on sufficiently large values of M_{0i}, and a significant difference in successive T_{1i} values.

Results of single component fits for both T1 and T2 measurements are generally thought to be accurate to around ± 5%. Systematic errors may increase this value in cases where non-exponential decays are treated as single component to around ± 10%. Due to the degree of difficulty in separating the different components in multi-exponential fits by graphical methods the inaccuracies for the independent relaxation times may vary. It is usually simple to derive a value for the longest relaxing component to within ±5%, since the figure can be resolved from the part of the dacay following the disappearance of the fast relaxing component. The fast relaxing component is then derived with a knowledge of the slow relaxation rate, and is therefore subject to cumulative errors of around ±10%. In the case where the

fit is by computer, the errors in the fit are indicated by the r.m.s : noise ratio. For a good fit, this value is close to unity, and errors in the relaxation times are about ±5%. Where the fit is not so good, the r.m.s. : noise ratio may increase to 3-4, and errors in relaxation times are then accurate to ±10-15%.

The basis for the measurement of self diffusion rates using the SFG and PFG methods has been discussed in chapter 3 and may be summarised by the two equations;

$$\text{for SFG,} \qquad \ln\left[\frac{A(G)}{A(G=0)}\right] = -\frac{2}{3}\,\text{gamma}^2 G^2 D \tau^3$$

$$\text{for PFG,} \qquad \ln\left[\frac{A(G)}{A(G=0)}\right] = -\,\text{gamma}^2 G^2 \delta^2 D(\text{Delta}-\delta/3)$$

To derive D experimentally using either of these equations one can vary either G or τ in the SFG case, and either G, Delta or δ in the PFG case. Under favourable conditions the SFG experiment lends itself to the derivation of the different self diffusion coefficients within multi-component systems.

Attempts to resolve the different values of D_{PEG} and D_{water} for PEG/Water mixtures proved unsuccessful, however, due to the difficulties in resolving the two signals in the presence of the field gradient. The measurement of the self diffusion coefficient for the polymer in solution was made possible by using heavy water as a solvent.

Errors incurred while measuring the diffusion rates are relatively high at about ±15% due the the need to closely match the size of the pulses in the case of the PFG experiment, and due to the low signal:noise ratio in the case of the SFG experiment.

5.7 Sample Preparation.

5.7.1 Polyethylene Glycol Solutions.

Polyethylene Glycols were obtained from the British Petroleum Company under the trade name Breox. The different grades supplied varied in size from PEG300 to PEG6000. They were stored in air-tight containers and were used without any other treatments.

Solutions were made up on a weight to weight basis with either distilled water or D_2O. The solutions were gently agitated and kept in air-tight containers for two to three days to homogenise[4,5].

5.7.2 Xylem

Samples of water-logged wood were kindly provided for use in this work by the Mary Rose Trust. The Mary Rose sank in action in 1545, and rested in the silts at the bottom of the solent until the restoration and reclamation work began in the late 1970s. During this time underwater the wood has naturally become severely water-logged, and degradation of the wood has taken place to varying degrees throughout the wreck depending on the type of wood, and its exposure to the elements.[6]

Divers who excavated the wreck have retrieved samples that were made from a variety of woods that were common in Europe during the fifteenth and sixteenth century, such as oak, ash, poplar, birch and so on. These samples were stored, prior to treatment, in a large cascade system of baths, where fresh tap water could flow around the samples, flushing away the salt water and silts from the wood. Following this they were stored in large tanks of water, to which a small amount of fungicide was added to reduce bacterial growth.

Small blocks of wood were cut from planks and beams that had been treated in this manner, and were sealed in plastic to maintain their moisture contents before being sent to the laboratory. The size of the blocks was typically about 8cc, and the species of wood were identified from the different cellular patterns, which were clearly visible on most of the samples. On arrival at the laboratory, the woods were placed into fresh water tank still in their plastic jackets.

Small cores of wood, 5mm in diameter and 7 mm in length, were carefully taken from these blocks so that the grain was as near parallel as possible to the long axis of the cylinder. The samples were checked for obvious defects in the regular cell patterns, and were then thoroughly washed with distilled water to remove any residual soluble material, before each was placed into a separate container of distilled water for periods of upto four days; the distilled water being changed daily[7].

Following the soaking period, excess surface water was removed by carefully dabbing the wood with absorbent tissue paper. The cylinders were weighed and then gently inserted into the base of a sample tube with a 7mm outside diameter, and a glass insert sealed with teflon tape was used to plug the tube near to the snugly fitting sample, thereby reducing the space around the sample to a minimum and preventing water from seaping from the wood. This was particularly important in cases where the temperature of the sample was raised above room temperature, at which water was prone to evaporate from the wood. The sample tube could be further sealed either hermetically, or by means of a stopper and more teflon tape. After each measurement had been taken, the sample was re-weighed to test for loss of moisture.

Between measurements the samples were allowed to dry. With fully water-logged samples this is a natural process once the wood is exposed to air, but in drier samples the evacuation of water could be accelerated by the gentle application of heat using a 60 Watt light-bulb. After a period of a time the samples were reweighed and re-sealed. They were then allowed to equilibrate for a period of twenty-four hours before further measurements were made.

Tests were carried out on the samples to establish the effects on the relaxation properties of wood caused by para- and ferromagnetic impurities. In many cases the wood brought up from the remains of sea-faring vessels have been contaminated with iron compounds that have leached from the iron work on the boats, such as cannons etc. These compounds can be extracted to a large degree by treatment with EDTA (Ethylenediamine Tetra-acetate) solution, which forms various complexes with the iron that can be removed by further washing. There appeared to be no measurable differences between the NMR decays for samples treated with EDTA, and those that were not.

Impregnation of samples using the various grades of PEG was accomplished by submerging the samples for periods of upto 18 months in concentrated solutions that were periodically refreshed. The uptake of PEG was indicated to a degree by the slight increase in weight that the samples underwent during this time.[8,9]

The absolute moisture contents of the samples were determined at the end of each experiment by completely drying the samples in an oven at 105°C for six to twelve hours, or until the mass of the sample had become constant.

References:

1. McCall D.W., Douglass D.C., Anderson E.W. Ber. Bunsenges. Physik. Chem. Vol 67. p 336. (1963)

2. Wassall S.R. PhD. Thesis. Nottingham (1981).

3. Brownstein K.R, Tarr C.E. Physical Rev. A. Vol 19(6) p 2446. (1979)

4. Union Carbide Corporation. Tech. Bulletin F-42933. "Polyox water soluble resins." (1972).

5. Union Carbide Corporation. Carbowax catalogues.

6. Murray H. "Conservation of artifacts from the Mary Rose." Proc. ICOM water-logged wood working group conference. Ottowa. (1981)

7. Panshin A.J., DeZeeuw C. "Textbook of Wood Technology." McGraw-Hill. NY. 1980.

8. Stamm A.J. For. Prod. J. Vol 9 p 27. (1957).

9. Stamm A.J. For. Prod. J. Vol 10, p 524. (1960)

CHAPTER 6. A Pulsed NMR Study of Water in Water-logged Wood.

6.1 Introduction.

The NMR properties of water in wood have been reviewed in chapter 4. In previous studies the moisture contents of wood has been monitored under equilibrium conditions at relative humidities of 100% and below. This chapter presents the results of NMR measurements made on samples of water-logged wood having moisture contents far in excess of those normally encountered, and in which the cell wall structures have been broken down by long degradation processes.

In general the NMR properties of water in wood are complicated by the degree of heterogeneity within the samples. The nature of interactions between the water molecules and the tissues of the wood cell walls are determined in part by the structure and degree of degradation of the wood. This is reflected in the behaviour of measurable NMR parameters as a function of moisture contents and temperature, such as the signal amplitudes, the relaxation of the magnetisation in transverse and longitudinal directions, and the self diffusion coefficients. These have been used in order to characterise the molecular dynamics of the water in water-logged wood.

The samples are fragile and unstable, and unless they are maintained in a saturated condition strong capillary forces come into play which cause the woody tissues to collapse. The shrinkage can be arrested by the action of water-soluble polymers impregnating the system, which not only consolidate fragile cellular components, but also stem the flow of water from the wood as a result of their hygroscopic nature. The molecular dynamic of the water and polymer within the wood are modified in different ways depending upon the molecular weight of the polymer used. Different grades penetrate different parts of the xylem cells, and the effects on the water in the samples may be monitored by NMR techniques.

Broadly speaking this work has addressed the following questions:

(i) How does water in water-logged wood differ from that in the bulk, or from water found in normal xylem tissues, and are the NMR properties of the water in water-logged wood indicative of the degree of degradation of the samples?

(ii) Does water in water-logged wood exhibit similar multi-exponential behaviour to that found in other systems, and if so can these be related to the macroscopic structural properties of the wood such as cellular composition and pore sizes? Are perhaps the NMR properties of the system consistent with the existence of 'bound' and 'free' phases. and is there any evidence of exchange between the two?

(iii) What are the effects of the impregnation of polymers on the nature of water within the wood, and how do these effects vary with grade and concentration of polymer used?

(iv) What factors effect the self-diffusion of water within the system, and how does the impregnation of polymers modify this behaviour?

(v) Can NMR be effectively used in assessing the treatment parameters required for the successful preservation of water-logged wooden artefacts.?

In an attempt to answer these questions, three types of NMR experiments were performed: 1) Freezing curve analysis. 2) NMR relaxation of water in samples of treated and untreated water-logged wood. 3) Pulsed Field Gradient measurements of self-diffusion coefficients.

6.2 Freezing Curves.

Previous studies have shown that water in proximity to a macromolecular system exists in a number of fractions that can be classified as 'bound' and 'free'[1,1]. In fresh everyday samples of wood 'free' water is only in evidence above the fibre saturation point of about 0.38 grams of water per gram of solid[1,2]. The 'bound' phase is the water of hydration of the

system which is intimately related to the constituents of the wood cell wall. Tests were carried out to establish the presence of bound water in water-logged wood, and to see how it relates to the hydration water found in fresh timbers. In other systems it has been found that the quantity of hydration water is related to the amount of substrate material that is accessible to water[3]. The effect of drying the sample could cause the number of accessible binding sites to diminish as the pores in the sample collapse and the effective surface area within the sample is reduced. If there is no change in the number of available surface sites, and the bound water bound water should remain fixed during the drying process until all of the 'free' phase has been removed. The ratio of the quantities of bound to free water can be found with the aid of freezing curves, whereby the amplitude of the F.I.D. following a 90 degree pulse is measured as a function of the temperature of the sample.

The immediate amplitude of the F.I.D. is proportional to the number of resonant nuclei within the sample that are capable of making a contribution to the signal. For protons in the solid state the relaxation time in the transverse direction takes place on a time scale of several microseconds, which is close to the dead time of the receiver mechanism for many spectrometers. If the first observation of the F.I.D. is made at times in the order of tens of microseconds, then the signal from the solid component will have decayed away and will not be included in the signal, the only contribution to the amplitude being from protons residing in mobile molecules with longer relaxation times.

Freezing curves are therefore capable of monitoring the transition from the liquid to solid states and vice-versa across freezing events. Figures 6.1a - 6.1d show the freezing curves for water in water-logged poplar as the water content of the sample is reduced. The temperature was cycled between 230K and 300K, and the amplitude of the signal was sampled at 70 microseconds. Corrections to allow for the change in the Boltzmann factor with temperature, and for the increase in sensitivity of the receiver unit at lower temperatures have been applied to the curves.

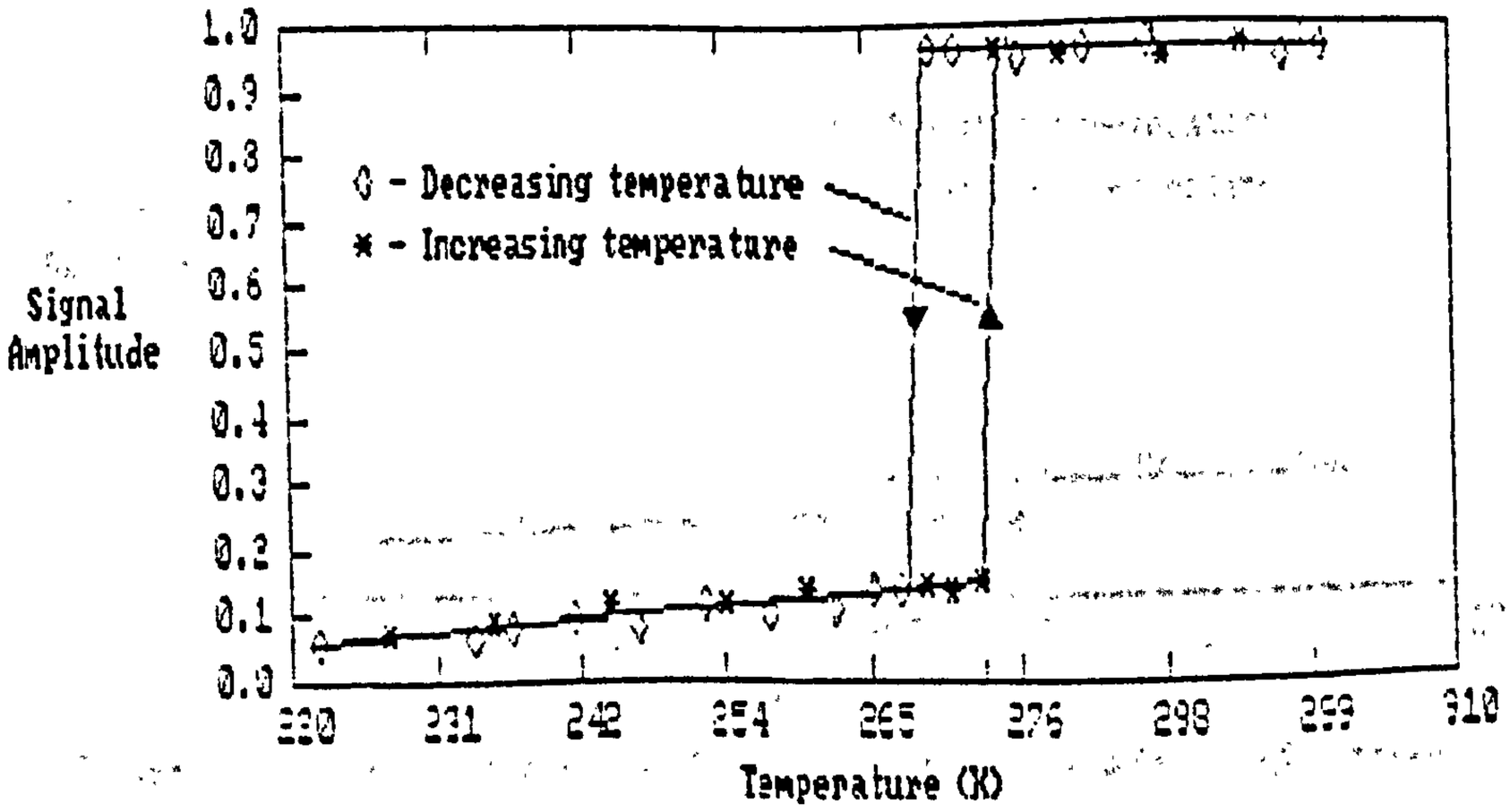

Figure 6.1 (a) Freezing curve for poplar. Sample weight = 0.191 grams

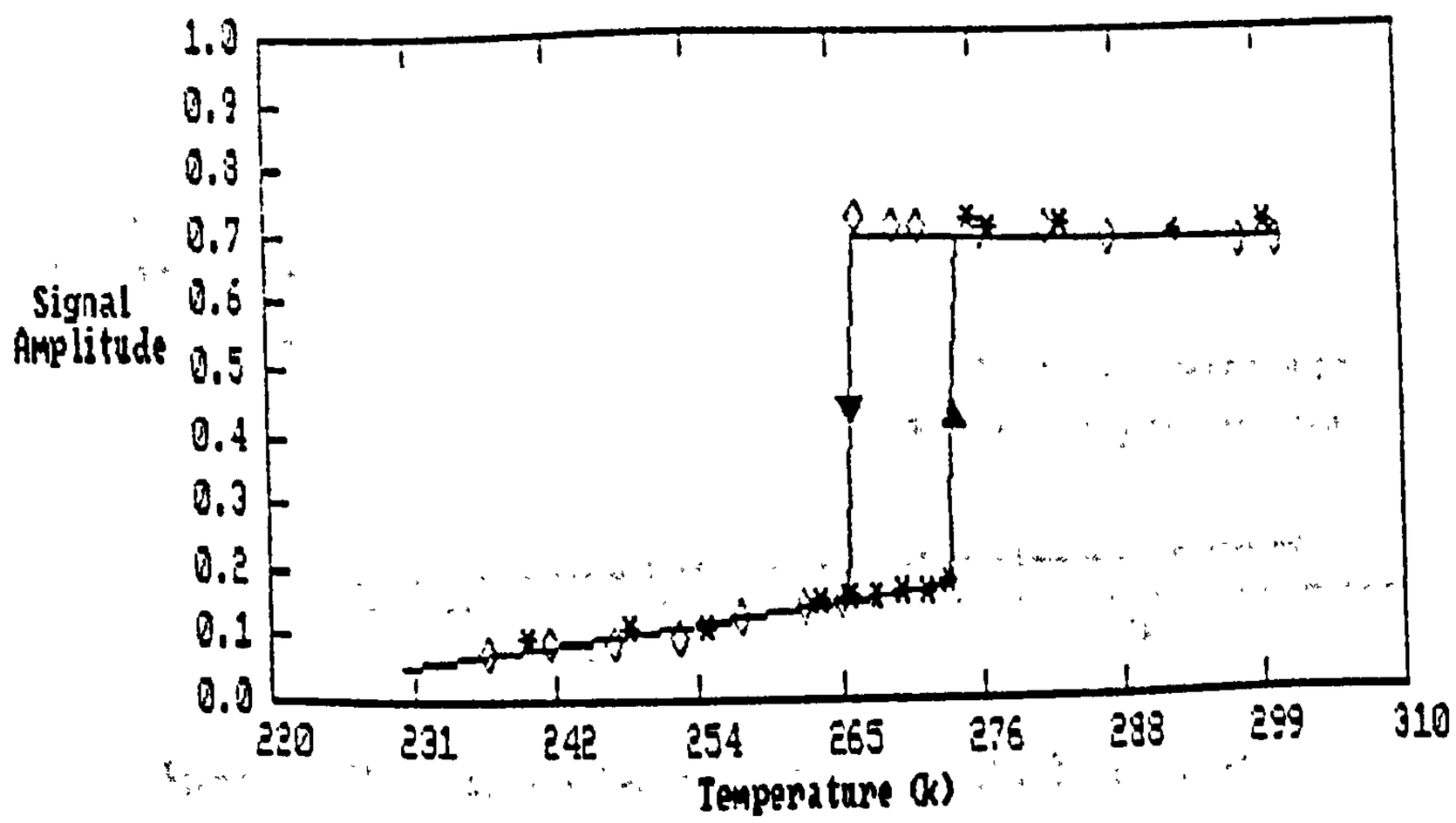

Figure 6.1 (b) Partially dried sample. Weight = 0.155 grams.

On the downward cycle a clear freezing event was observed at about 266K for samples containing high moisture contents. This indicates that the bulk of water within the sample behaves in a similar way to ordinary water. The depression in the temperature from the freezing point of distilled water is caused by supercooling of water within the sample. Below the

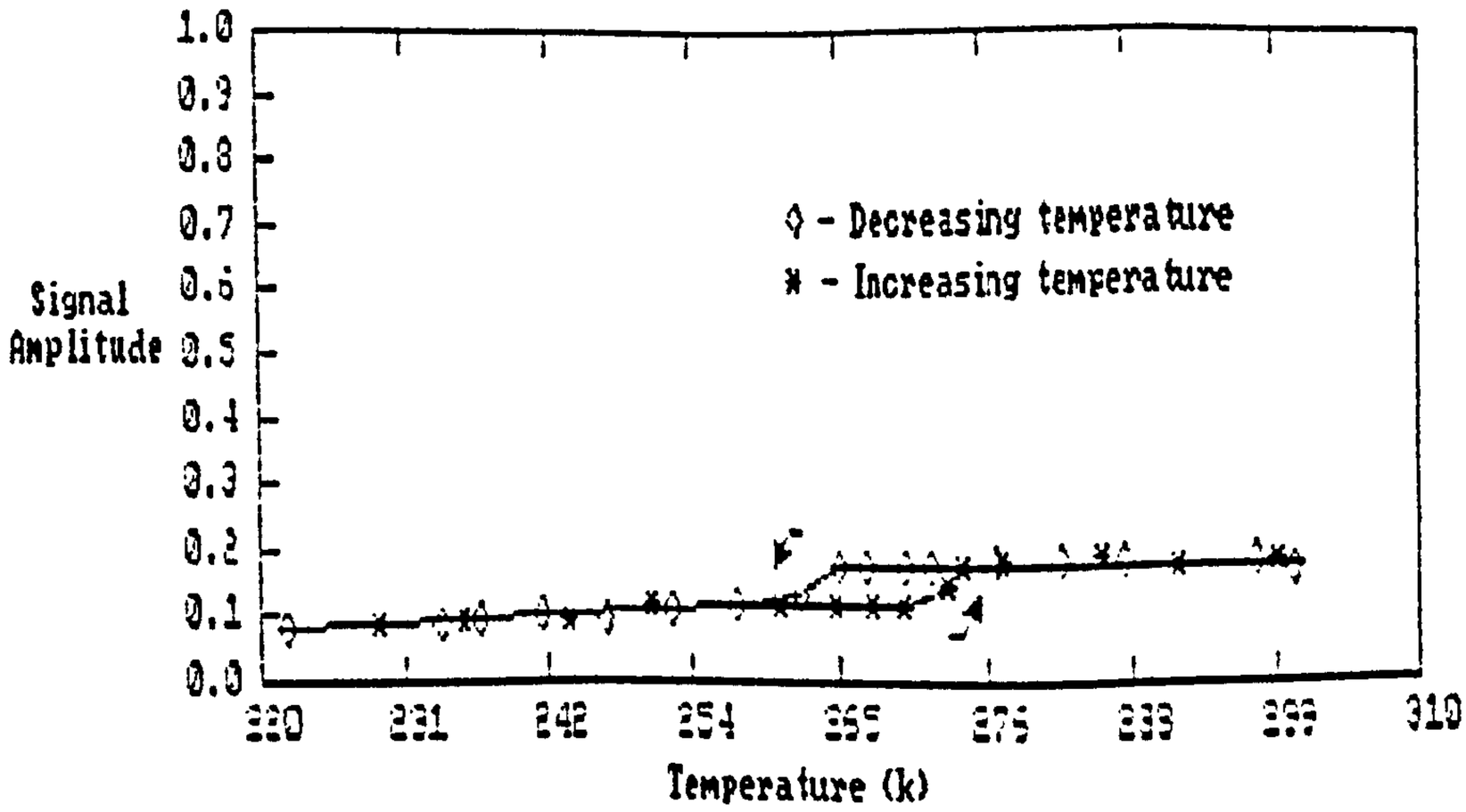

Figure 6.1 (c). Freezing curve after further drying. Sample weight = 0.083 gramms

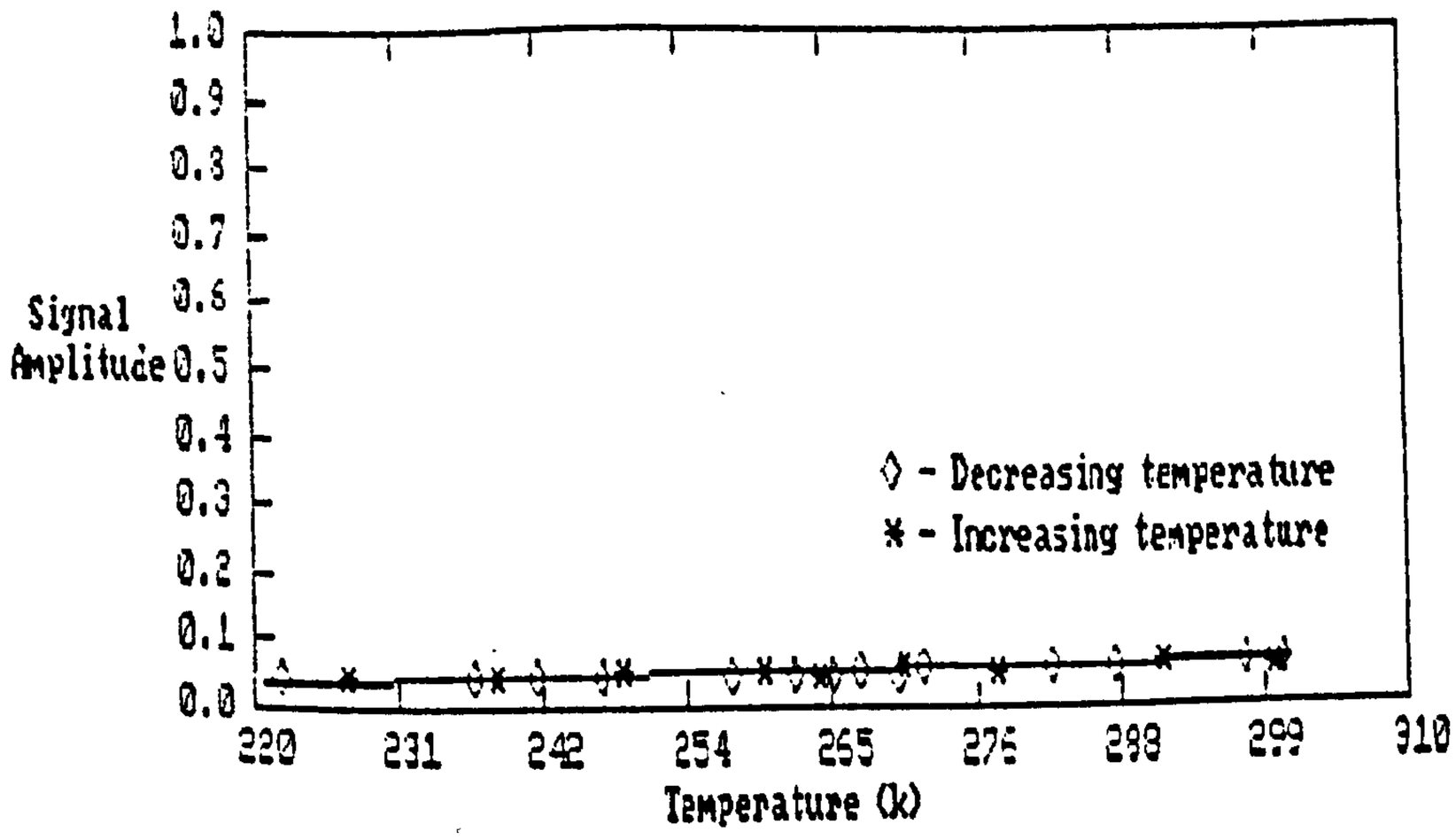

Figure 6.1 (d) Final freezing curve. Sample weight = 0.256 gramms

freezing event there exists a significant quantity of water which is left unfrozen. This is the bound water that remains in a mobile state through interactions with the substrate. The amplitude of this signal decreases steadily with temperature, suggesting that a smooth distribution of interaction strengths exists, so that there is a gradual freezing of the bound component. On the upward cycle the frozen water thaws at approximately 273K as expected.

As the sample dries and the total number of water molecules within the sample is reduced, the signal amplitude at temperatures above freezing is diminished. The height of the signal below the freezing event shows very little attenuation. It is therefore the free water that is primarily removed from the wood on drying. In figure 6.2 the total signal amplitude is plotted against the weight of the sample. The contribution to the total signal from the bound and free components are also shown. It would appear that nearly all of the free water is removed from the sample before any of the the bound water is lost. Mo indicates the oven dried weight of the sample. The intercept of the broken line in figure 6.2 indicates the point at which all the free water in the sample has been removed and the remaining water is that in the bound phase. It therefore gives a measure of the fibre saturation point of the water-logged wood which is approximately 0.4 g/g, and within experimental error is equivalent to the value found in fresh wood[41].

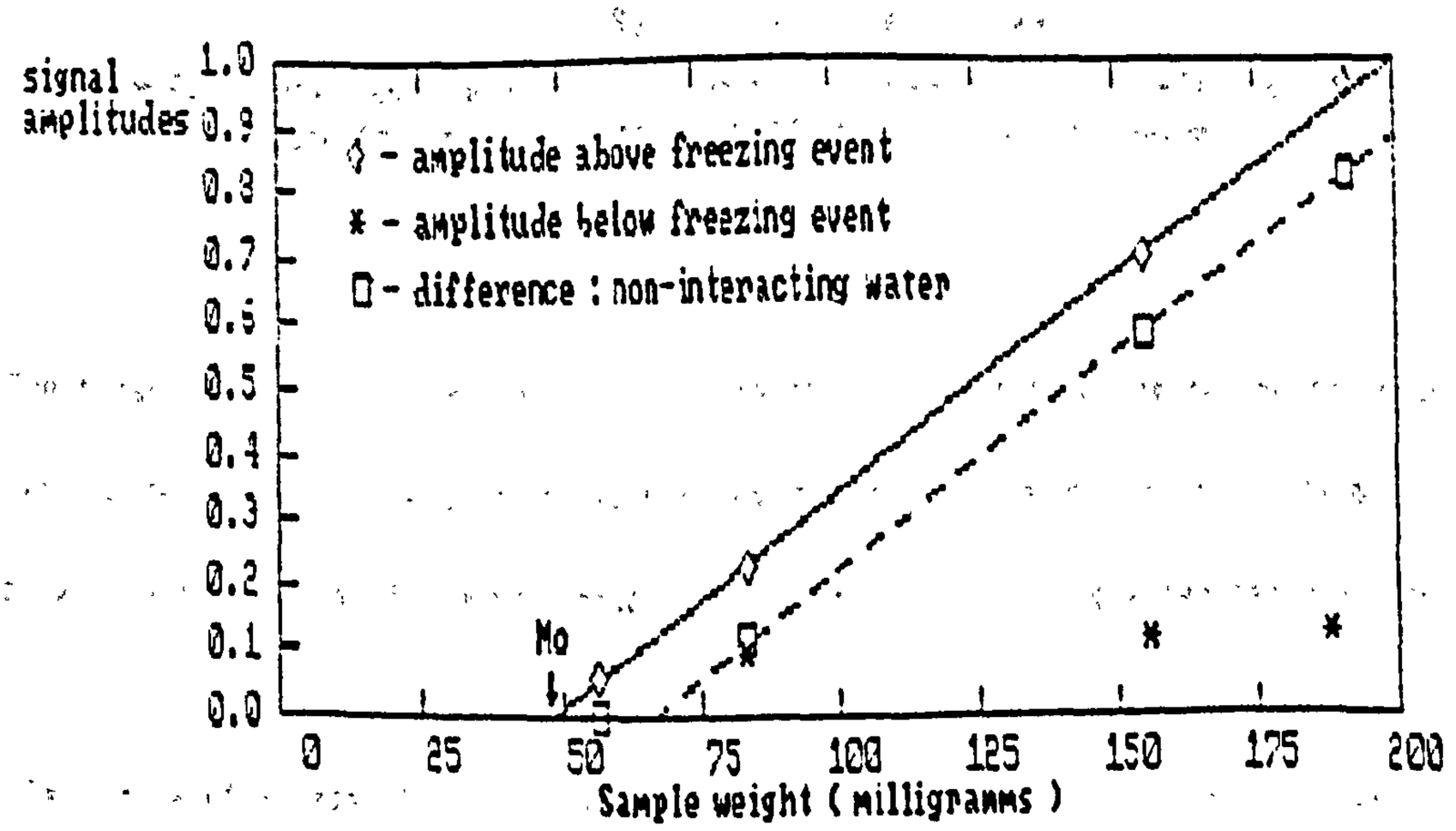

Figure 6.2 Signal amplitudes of interacting and non-interacting components in water-logged wood as a function of sample weight.

The observed signal has been related to the total water content of the wood. However it is conceivable that the signal is enhanced by a contribution from the more mobile protons residing in the solid content of the wood, or reduced because water molecules that are tightly bound to the substrate relax at such a rate that they no longer produce an observable

contribution. Figure 6.3 shows how the signal amplitude grows for a sample of oven-dried poplar as it is re-hydrated. For comparison it is plotted alongside the signal amplitude observed from different quantities of distilled water. Within experimental error the two curves are the same, but displaced by 37 mailgrams along the X axis. This displacement corresponds to the oven-dried weight of the sample, and one may conclude that the observed signal arises from the water alone, with no contribution from the protons in the wood.

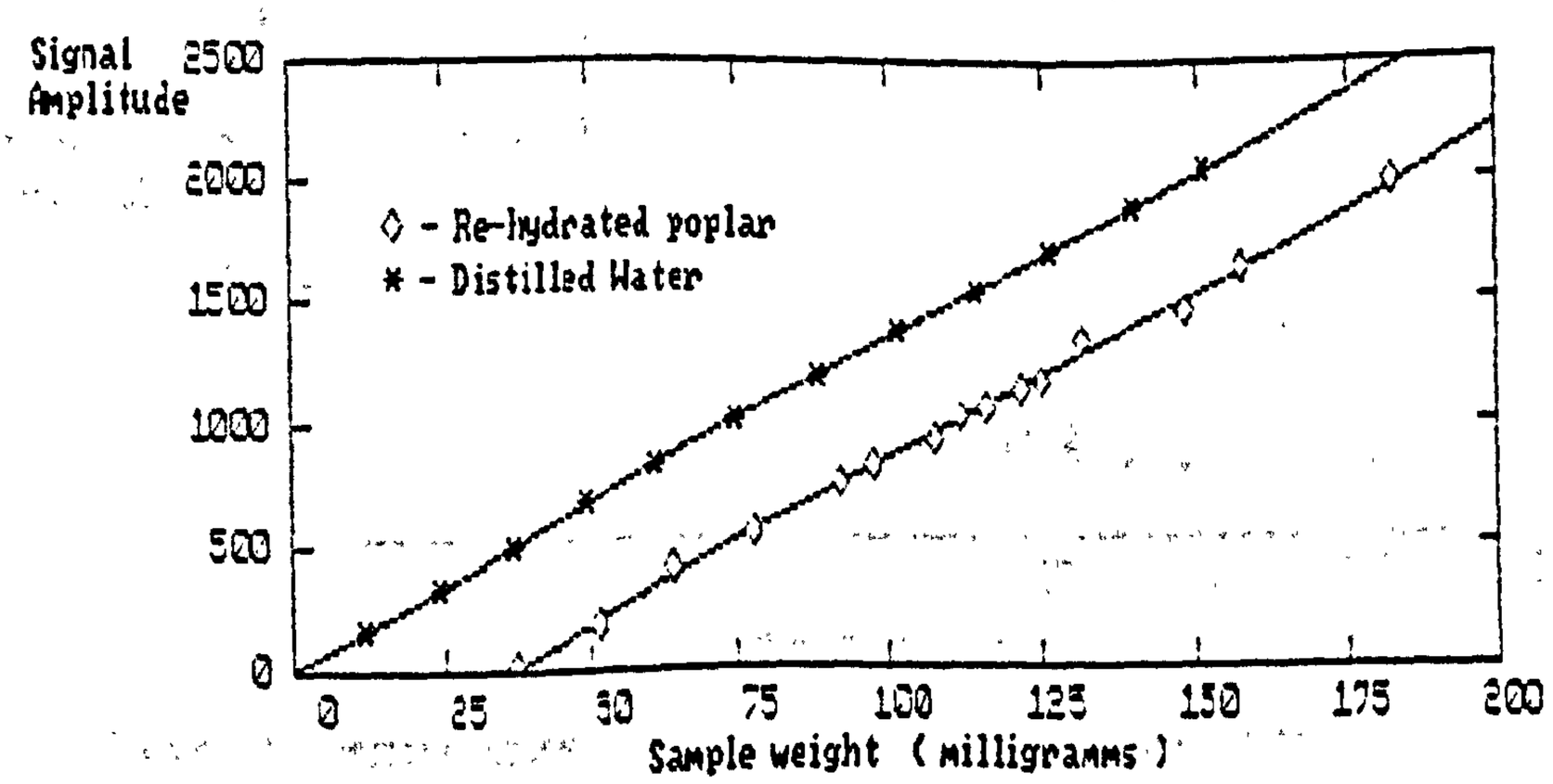

Figure 6.3 Signal amplitude as a function of sample weight for re-hydrated poplar. Results are compared to those obtained for distilled water.

The fixed quantity of bound water within the sample over the drying period suggests that the shrinkage of the sample does not significantly effected the number of accessible binding sites within the matrix of the substrate material until most of the water has been removed.

The degree of accessibility of the binding sites to water is a mark of the open structure of the system. To test for exchange between the free and bound phases, and between protons attached to the xylem and in the water experiments were carried out on deuterated samples. Figure 6.4 represent the freezing curve derived from a sample of poplar that was soaked for eighteen months in D_2O. During this time one would expect the D_2O molecules to establish an equilibrium with the system, so that deuterium resides in the bulk, and on all sites that are accessible to water molecules. The proton NMR signal amplitude observed in fully water-logged

samples was reduced, but the residual signal is consistent with fully protonated samples. with a ratio of bound to free protons of 8:1, suggesting that the deuterium nad penetrated both free and bound phases to the same degree. As the samples dry the free water molecules are preferentially removed from the wood, leaving the the majority of bound water in situ until it is the only water remaining.

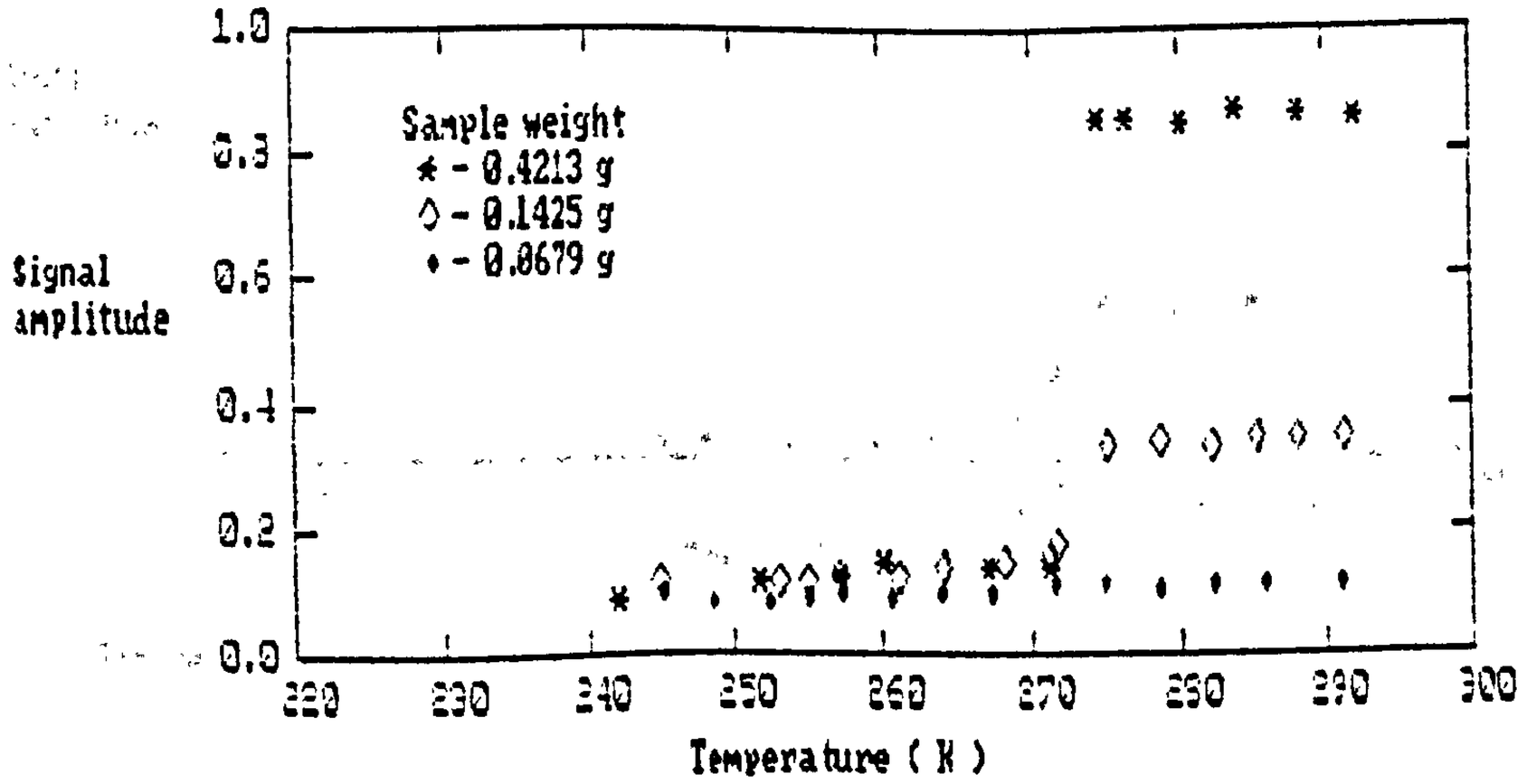

Figure 6.4 Freezing curves observed during dehydration of deuterated poplar

The sample was dried out until no NMR signal could be detected, and then soaked in a vial of deuterated water for a period of 10 days. The resulting freezing curve is shown in figure 6.5. The proton signal amplitudes indicate that the 8:1 ratio of protons in the free and bound phases has been re-established. The amplitude of the signal detected in the re-swollen sample significantly increased from that observed in samples at low moisture contents before the sample was fully dried. This increase in amplitude is explained by assuming that prior to drying the exchange between protons in the xylem and the deuterium had reached an equilibrium. The concentration of protons in the water of the wood remained fixed throughout the drying process, so that at low moisture contents the number of water protons approaches zero. When further D_2O is added to the system protons attached to the xylem once again exchange with the deuterons, so that there is an increase in the number of protons in the liquid phase, and hence in the proton signal amplitude. The mass attained by the re-deuterated samples was less than the mass of the original sample despite the length of the re-

deuteration period. This indicated that the ability of the sample to hold water had been reduced by the extensive drying, probably due to some collapse of the ultrastructure of the cell walls.

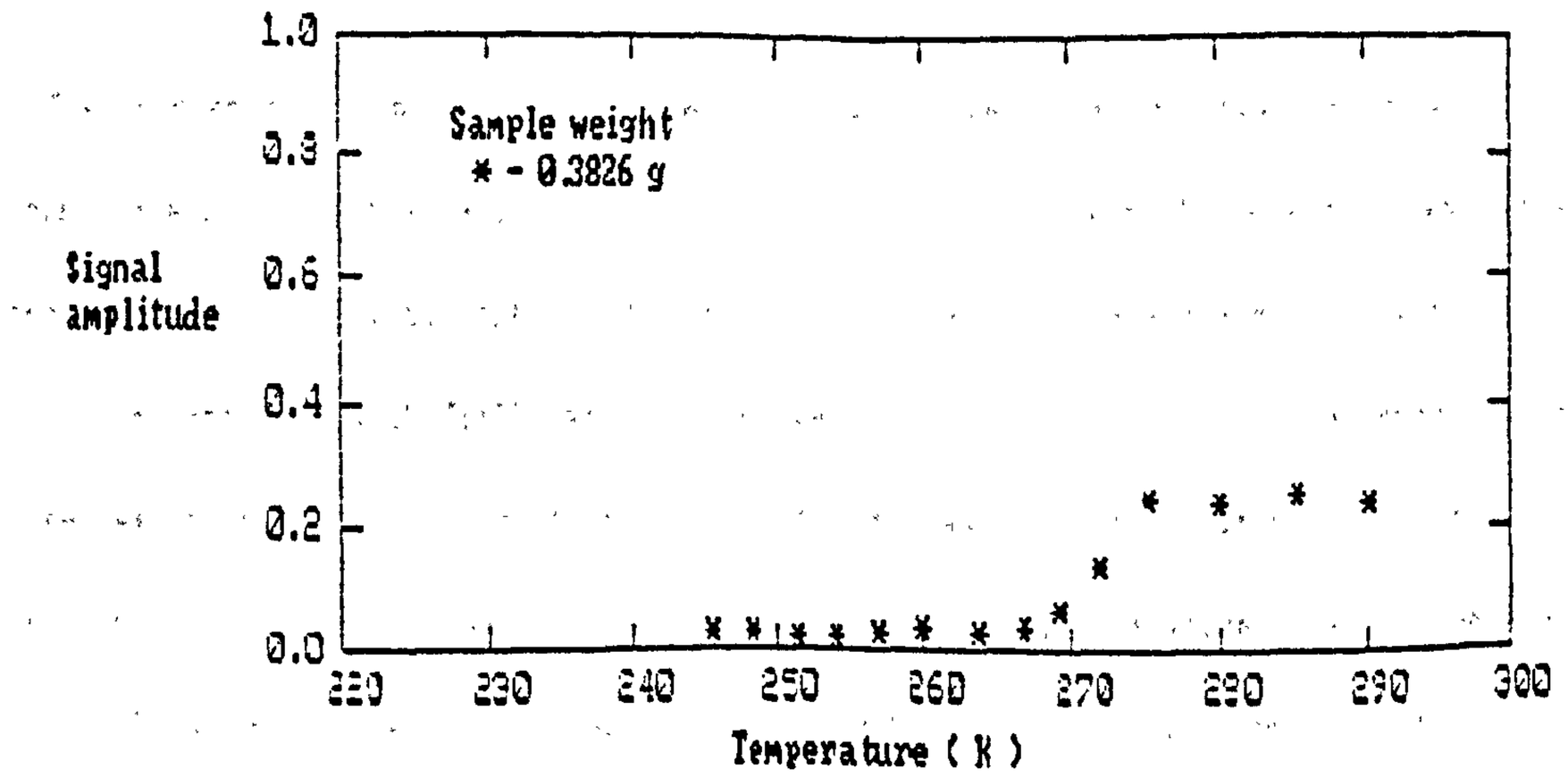

Figure 6.5 Freezing curves for re-deuterated sample. Proton signal.

From the results performed above one can conclude that water in water-logged wood exists in at least two states, one of which remains unfrozen at low temperatures. This fraction is identified with the water of hydration observed in fresh timbers, and is less readily removed from the sample upon drying. The structure of water-logged wood is a very open one in which there are no observable inaccessible regions. The two fractions undergo exchange with each other, and there is some chemical exchange evident between protons attached to the xylem and those within the water. Irreversible denaturation of the cell walls does not take place until all of the non-interacting, and much of the interacting water has been removed from the wood.

6.2 Nuclear Magnetic Resonance Relaxation of Water in Water-logged Woods.

6.2.1 Single-Component Measurements of T1 and T2.

The spin-spin and spin-lattice relaxation times of water in wood are sensitive to the temperature at which they are measured, and on the water content of the wood. They differ from the relaxation times observed for water in the bulk, being reduced by typically a factor of ten or more, and with T1:T2 ratios of between 2 and 5. In the case where bound and free phases exist in rapid exchange a single relaxation time is observed which is determined by the quantity of water in the bound phase, and the intrinsic relaxation times of the two fractions. These quantities are themselves determined by the macroscopic and microscopic details of the cellular system, which provoke different motional responses in the water molecules. Is it possible then to derive any information from the values of T1 and T2 about the wood/water interaction, and in turn about the cellular composition of the wood in relation to the degree of degradation?

Measurements were made using a Bruker PC-2 Minispec on samples of wood which were water-logged and degraded to different degrees, to establish whether a two phase model is viable and if so to see what additional information could subsequently be inferred. This device which operates at a constant probe temperature of 40 degrees centigrade can be used to make simplified measurements of solid:liquid ratios, single component spin-lattice relaxation times, and single component spin-spin relaxation times.

Cylindrical samples of water-logged wood from a variety of species were cut from blocks found on the Mary Rose. The samples were placed into the Minispec and allowed to reach a thermal equilibrium with the probe. The spin-lattice, spin-spin, and solid:liquid ratios were

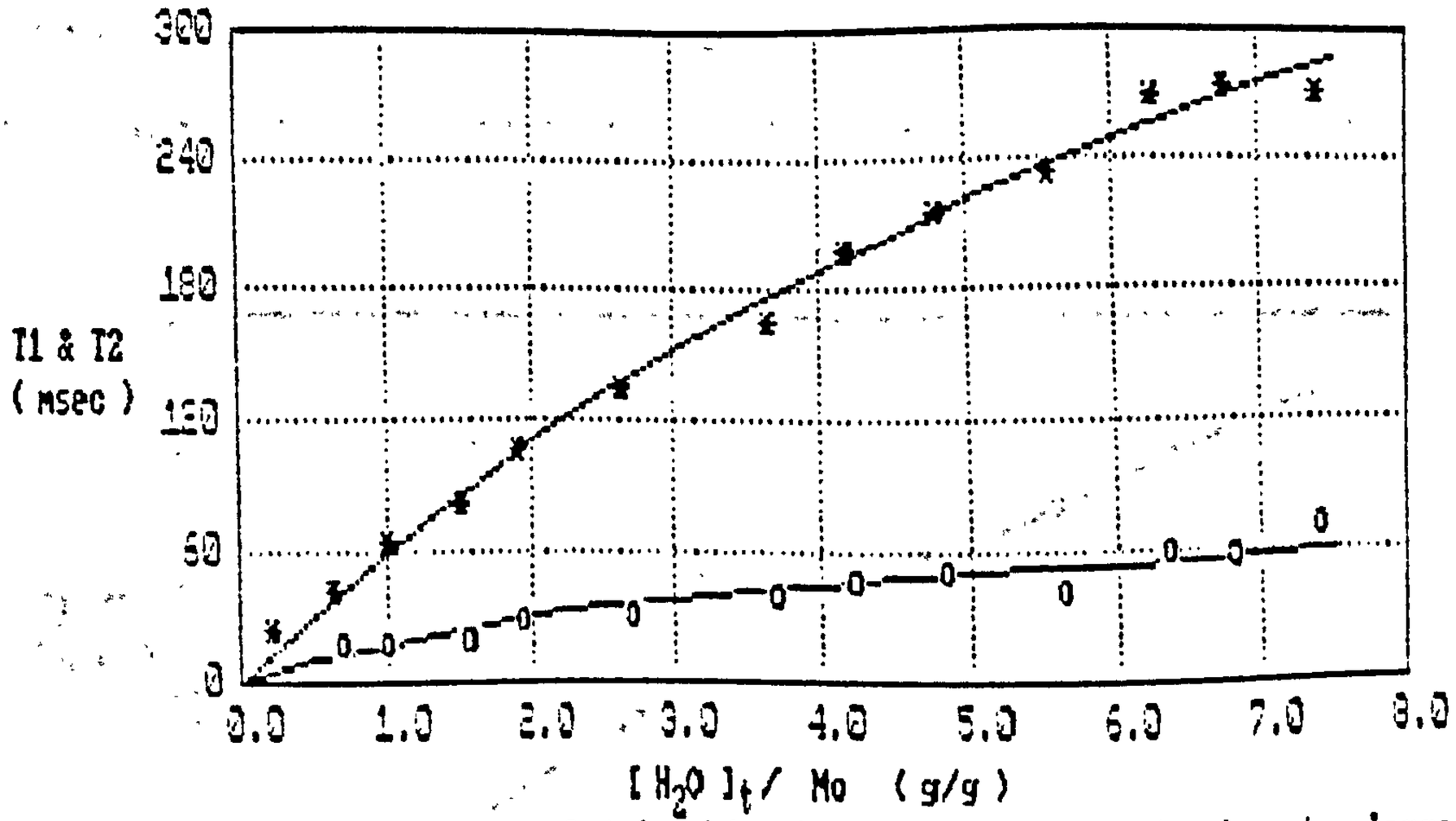

Figure 6.6 Spin-Spin (o) and Spin-Lattice (*) relaxation times for water in water-logged Wicker. Initial water content = 7.65 g/g.

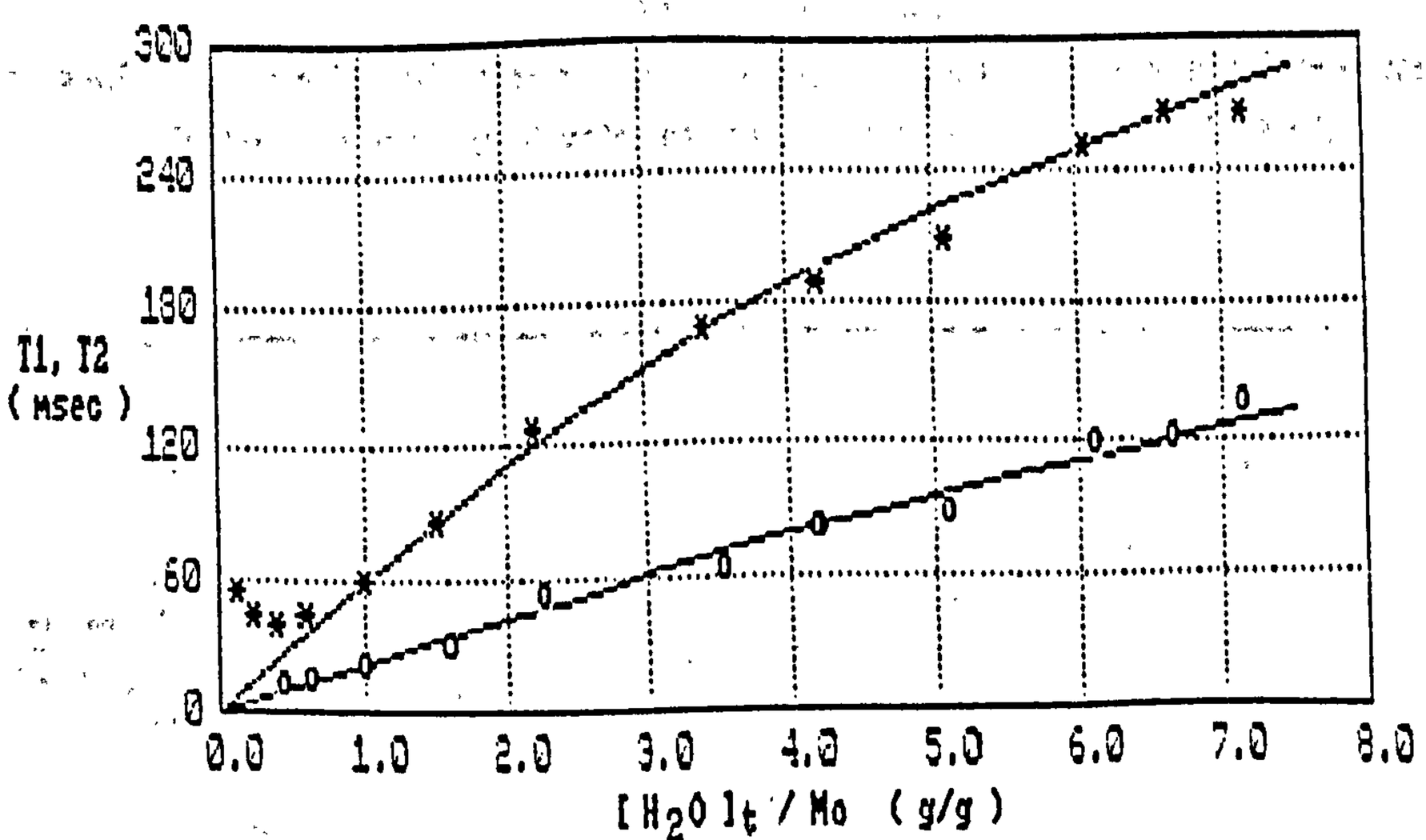

Figure 6.7 Spin-Spin (o) and Spin-Lattice (*) relaxation times for water in water-logged Ash as a function of water content. Initial water content = 7.37 g/g

measured as a function of the weight loss of the samples as they dried out. The sample weight was measured immediately after each set of measurements had been taken, and the oven-dried weight was determined at the end of the experiment.

The results of relaxation measurements made in this way are shown in figures 6.8 - 6.9. The timbers chosen included three highly degraded samples of poplar, ash, and wicker, and a piece of water-logged birch heartwood, for which the degree of degradation was less severe.

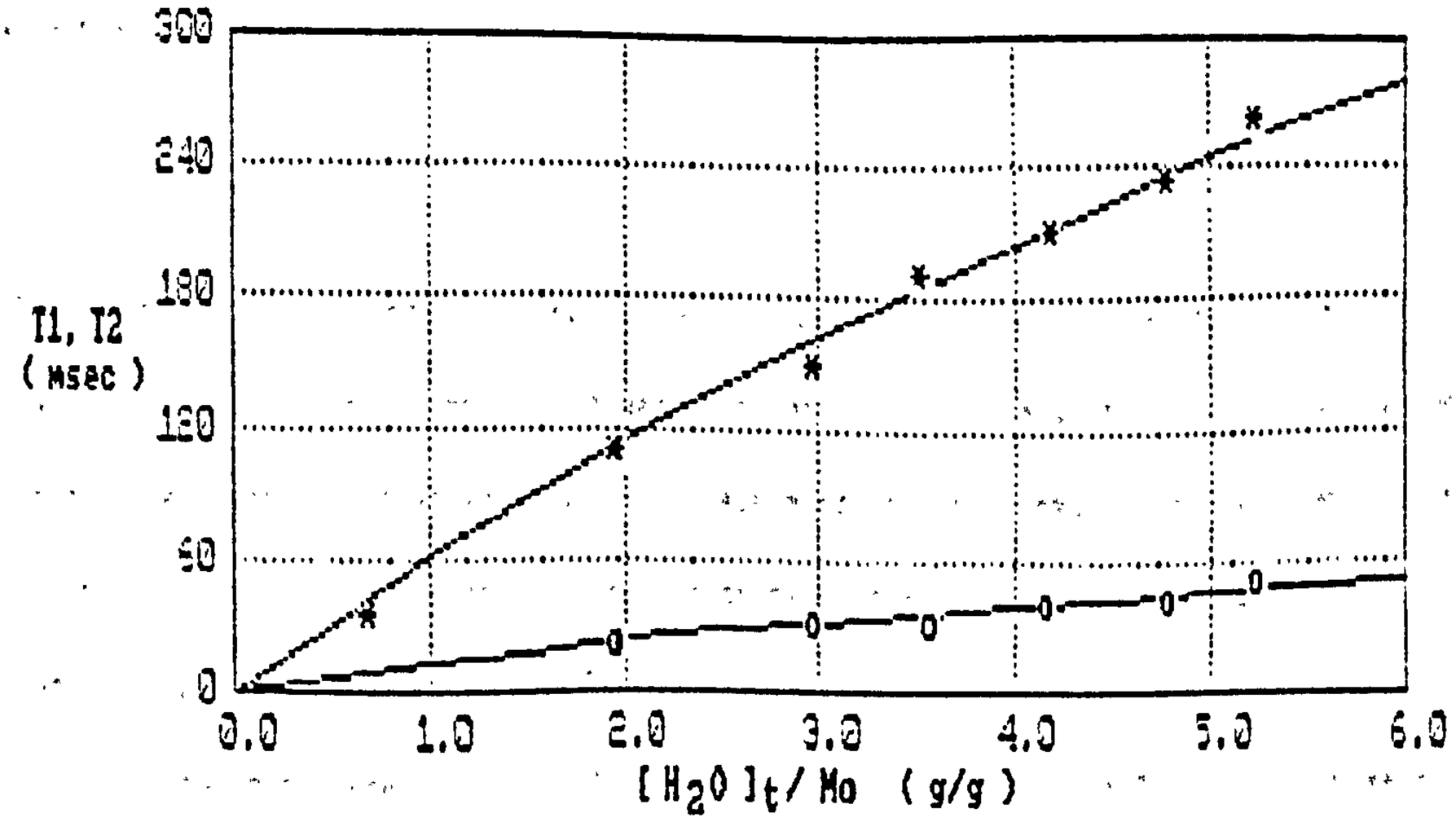

Figure 6.8 Spin-Spin (o) and Spin-Lattice (*) relaxation times for water in water-logged Poplar as a function of water content. Initial water content = 5.40 g/g.

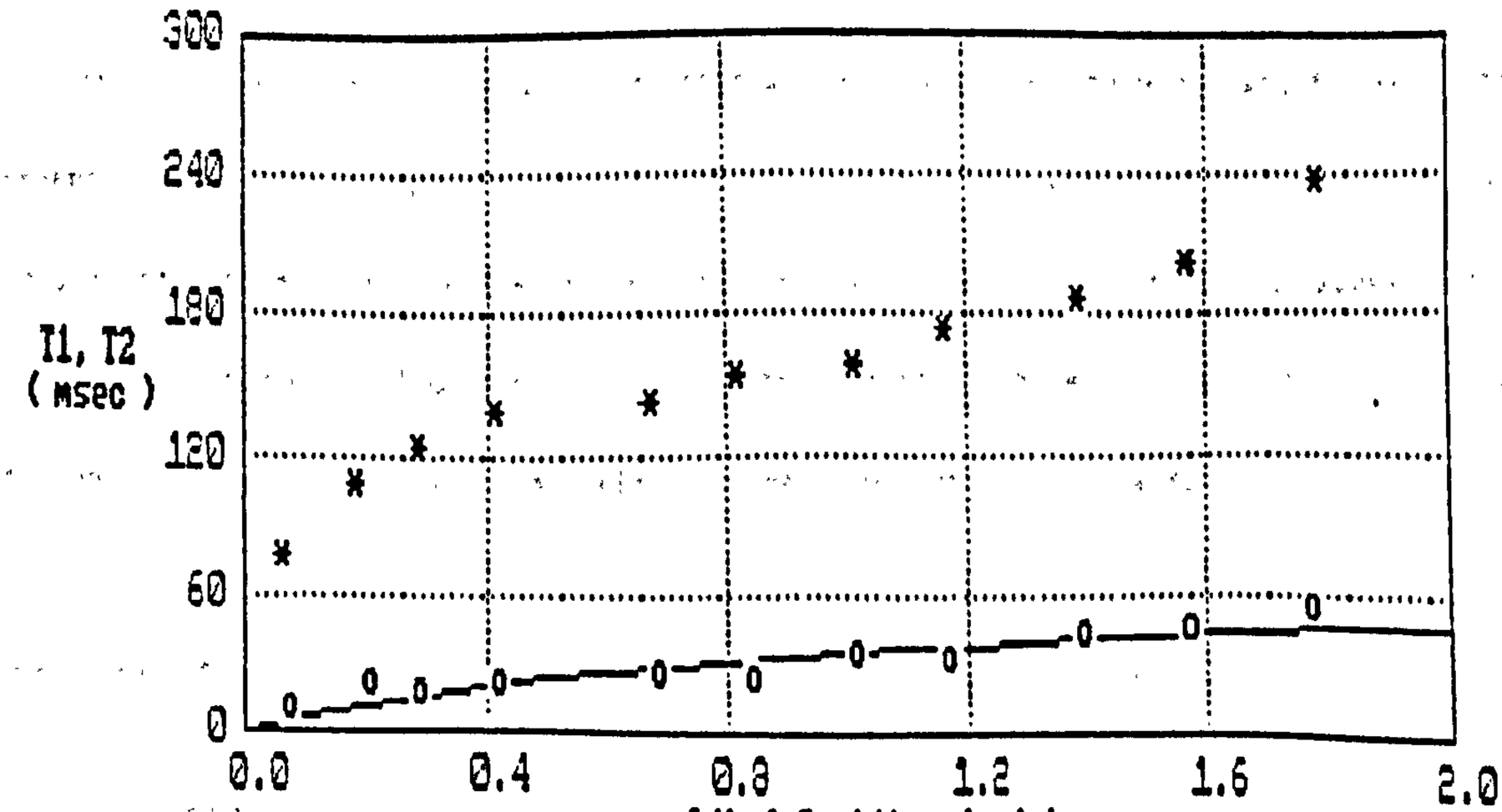

Figure 6.9 Spin-Spin (o), & Spin-Lattice (*) relaxation times for water in water-logged Birch Heartwood as a function of water content. Initial water content = 1.79 g/g.

An indication of the extent to which degradation has taken place is given by the ratio of the initial weight of the sample to the oven-dried weight. In all cases where the moisture content is greater than 0.14g of water per gram of wood both the spin-spin and spin-lattice relaxation times decrease monotonicly with water content. There is a considerable difference between the values of T1 and T2 for all of the samples, with T1:T2 ratios varying from about 2 to 5.

For the three heavily degraded samples the relationship between the water content and the relaxation times is a linear one at high water contents. This linearity is predicted by the two phase model used by Carles and Scallan[5]: Assuming that one fraction of water exists in a bound phase, and a second exists as a free component in exchange with the bound fraction, then using equation 4.9 of section 4.4.2, the gradient should give a measure of the value $Tb/[H_2O]b$, where Tb represents either T1 or T2 of the bound fraction, and $[H_2O]b$ represents the quantity of bound water present, which is assumed to be constant until all of the free water has been removed.

If the conditions exist under which equation 4.9 are satisfied, then one would expect the intercept of the graph to be at the origin. As can be seen from table 6.1, however, there is a broad distribution of values for the intercept times, and while this condition appears to hold good for the sample of poplar, it does not for the other three. In the other samples the points on the graph bend towards the origin as the water content is lowered.

Equation 4.9 is a special case of equation 4.8, which can be re-written as

$$\frac{[H_2O]t}{Tobs} = \frac{[H_2O]b}{T_{bound}} + \frac{([H_2O]t-[H_2O]b)}{T_{free}} \qquad 6.1$$

where $[H_2O]t$ and $[H_2O]b$ are the total and bound water contents in the wood. Tobs. T_{bound}, and T_{free} are the observed relaxation time, and the relaxation times of the bound and free water phases respectively. The equation equation holds for both spin-spin and spin-relaxation times.

Sample	Intercept of T1 curve	Intercept of T2 curve
Poplar	3 ± 5 msec	1 ± 5 msec
Ash	23 ± 5 msec	4 ± 4 msec
Wicker	33 ± 7 msec	9 ± 5 msec
Birch	85 ± 20 msec	12 ± 10 msec

Table 6.1 Intercept times for single component fits to T1 and T2 data as samples are dried.

Equation 6.1 may be simplified to give.

$$Tobs = \frac{[H_2O]t \times T_{bound} \times T_{free}}{[H_2O]b \times (T_{free} - T_{bound}) + [H_2O]t \times T_{bound}} \qquad [H_2O]t > [H_2O]b \qquad 6.2$$

Provided that T_{bound} is sufficiently small then the above equation reduces to that used by Carles and Scallan[9].

The solid lines drawn in figures 6.6-6.9 are plots of Tobs as a function of $[H_2O]t$ using equation 6.2. The form of the lines are sensitive to the three variables T_{bound}, T_{free} and $[H_2O]b$. In each case the quantity of bound water was found to be close to 0.14g of water per gram of wood. This compares favourably with the quantities of bound water found by Ogiwara[6] in wood pulps (0.2g/g), and suggested by Boesen[7] for cellulose in cotton (0.12g/g), but is inconsistent with the value found for samples of fresh timbers[8].

Table 6.2 presents the fitting parameters used for the curves. For the spin-lattice relaxation times these are relatively consistent. with $T1_{...}$ in the order of 0.7 seconds. and $T1_{.....}$ = 9 milliseconds. In ash the value of $T2_{...}$ appears to be close to the value of $T1_{...}$, suggesting that it has properties like those of bulk water. where as in Wicker and in popiar there the T1f:T2f ratio is approximately 8:1. Within experimental error the two-phase model accounts well for the data in degraded samples at high water contents.

Sample	$(M_{t=\infty} - M_0)/M_0$	$T1_{...}$	$T1_{.....}$	$T2_{...}$	$T2_{.....}$
Wicker	7.65	700	9	90	3
Ash	7.37	700	9	600	3.2
Poplar	5.04	1000	9	120	2
Birch	1.79	varaible	variable	70	9

Table 6.2 Fitting parameters for solid lines in figures 6.6-6.9 using equation 6.2. $[H_2O]b$ = 0.14g/g.

At low moisture contents the signal to noise ratio does not permit accurate measurement of the spin-spin relaxation times using the Minispec. Values of T1 were obtained for ash with moisture contents that are lower than 0.14g/g, where the signal is believed to originate from water that is bound to the wood. As the moisture content is reduced T1 passes through a minimum at 0.3 - 0.2g/g. A similar minima has been reported by a number of authors for samples of cellulose derived from a variety of sources, including wood pulp. Child[9] made a detailed study of this phenomena. As the moisture content is reduced the mobility of the water in the samples is decreased because of an increase in the interaction rate with the macromolecules. Above the minimum free water exists between the macromolecules, bulking the system, and imparting a degree of mobility to the macromolecules. As the amount of free water is reduced the bound water molecules are no longer separated, and are expected to form bridges between the macromolecules via hydrogen bonding with hydroxyl groups. This causes a reduction in the mobility of the macromolecules, This is reflected in the lower values of T1. As the water

content is further reduced. the number of bound water molecules that are able to form bridges between macromolecules is diminished. The number of brioges falls, and there is therefore an increase in the mobility of the macromolecules. and hence of the bound water, causing the T1 to increase.

An alternative interpretation of the minima in the T1 data may be to invoke spin-exchange. In the absence of spin-exchange the 'bound' water molecules would have a mobility placing them somewhere in the region of their T1 minima. In contrast the cellulose protons have a mobility putting them under rigid lattice conditions, i.e. T1 > T1 minimum, and T2 ≈ 10 - 20 μsec. Spin-exchange occurs in 10 - 30 μsecs, and is very efficient. Thus the spin-lattice relaxation time observed is dominated by the value for the bound water. As the total amount of water in the system is reduced the amount of bound water varies the proportions alter, and the solid protons exert a greater influence, increasing the observed T1.

In birch heartwood where the wood is less degraded the two-phase theory appears to break down, certainly in the case of T1, and probably in the case of T2 also. There is initially a sharp rise in the relaxation times as the water contents increase. This increase is arrested at moisture contents of around 0.4g of water per gram of wood, at which point there is a plateau. At higher moisture contents the relaxation times once more begin to increase.

The point at which the behaviour of the relaxation times appears to change, i.e. 0.4 g/g, coincides with the measurement of the fibre saturation point by Hsi et al[10] in Northern white-cedar chips. In figure 6.10 the spin-lattice relaxation times measured as a function of water content have been replotted. The solid line has been calculated using equation 6.2 by assuming that the values of the spin-lattice relaxation times for the free and bound phases, and the quantity of bound water, are functions of the moisture content. The nature of this curve is relatively insensitive to the value of $T1_{free}$, provided that it is large enough. It is more sensitive to the values of $[H_2O]t$ and $T1_{bound}$. The values used to calculate the curve

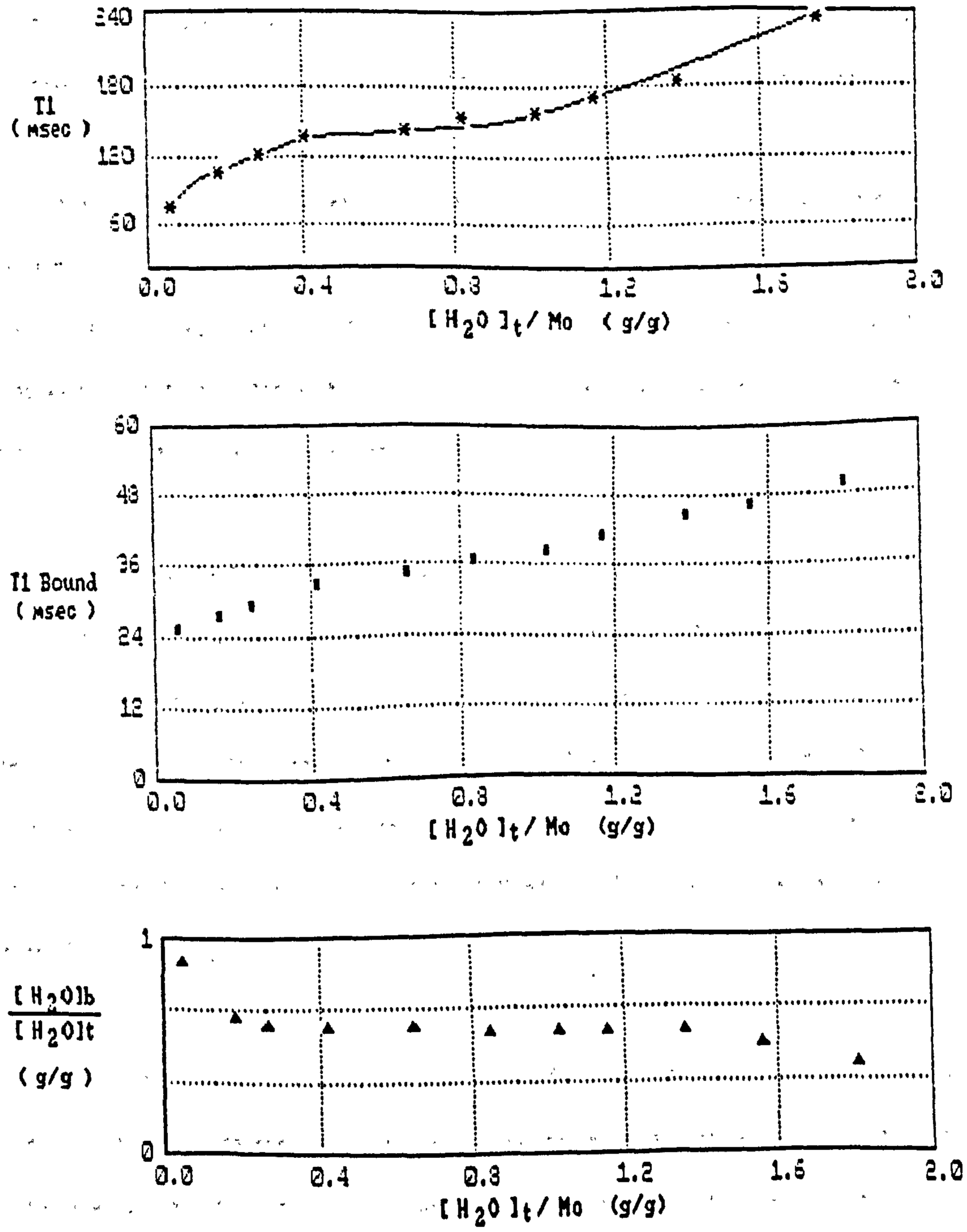

Figure 6.10 Theoretical changes in T1 bound (▪) and [H₂O]b/[H₂O]t (▲) for birch heartwood, used to predict nature of T1 observed (*).

are shown in the figure. The value of $T1_{bound}$ increases almost linearly with the water content, probably as a result of the increase in mobility of the bound phase as the structure of the wood becomes more open. The proportion of the total water content that constitutes the

bound phase is initially nigh. but drops dramatically as the water content of the wood tends towards 0.14g/g. Between 0.14 g/g and 1.4 g/g, the proportion of total water held in the bound phase is relatively constant at around 50%. beyond which it steadily declines.

Both trends were obtained theoretically via equation 6.2. The same trends were observed experimentally by Hsi et al[10], although the magnitude of $T1_{bound}$ and $T1_{free}$ that were observed by Hsi are lower than the theoretical values. This is to be expected as the water-logged wood constitutes a far more open and less rigid structure, and is therefore likely to contain far more mobile water molecules.

The behaviour of $[H_2O]b/[H_2O]t$ lends support the model of moisture distribution based on the existence of four stages of water uptake proposed by Froix and Nelson[11]. In the dry state the system exists as a network of macromolecular chains held together by intermolecular hydrogen bonding. Upon the initial addition of water, strong hydrogen bonding occurs between water molecules and active surface sites on the cellular structure, which may be hydroxyl groups. During this stage the majority of water within the wood exists in a 'Primary' bound phase.

Above 0.14 g/g the surface sites are wholly occupied, but the addition of further water causes the network of macromolecules to swell, opening up the structure and revealing further active sites which are occupied by 'Secondary' bound water. During this region the proportion of the water bound water in the wood is relatively stable, suggesting that the degree of swelling is proportional to the water content.

At around 1.4 g/g the swelling of the structure is slowed down, and fewer active sites are revealed by the addition of more water. At this point the proportion of water in the bound phase begins its decline, causing the free water in the wood to dominate the behaviour of the spin-lattice relaxation time. It would appear that the secondary bound phase does not

exist in severely water-logged wood, suggesting that the severely water-logged wood does not experience a swelling phase. The quantity of bound water per gram of wood at the point of saturation for the secondary bound water is 0.35 g/g. This is consistent with the fibre saturation point for fresh timbers. The deterioration in the structure of the cell walls of degraded timber lowers the fibre saturation point in the water-logged samples.

Carles and Scallan[53] suggested that the bound phase exists as a monolayer of destructured water on the surface of macromolecules, and the quantity of bound water is therefore a measure of the accessible area of the wood. The area covered by a single water molecule was calculated as $(\Gamma 18/N)^{(2/3)}$, where 18 is the molecular weight of the water molecule, N is Avagadro's number, and Γ is the specific volume of the destructured water which is taken as 0.9 cc/g. Each gram of bound water therefore covers a surface area of 3000 m^2. In highly degraded timbers the accessible surface are is approximately 440 m^2/g, and in the heartwood timbers the accessible surface area, following this line of thought is approximately 1050 m^2/g, but it is possible that the water in these samples resides in multiple layers that are supported by the capillary system that may still exist in well preserved wood.

6.2.2 Multi-component Relaxation of Water in Water-logged Wood.

The results of section 6.2.1 are analysed in terms of a two-component system, for which the observable T1s and T2s are treated as the weighted averages of these components. The values of T1 and T2 were found to be functions of the degree of degradation and the total water content of the sample. However, to analyse relaxation in water-logged wood in this way is to adopt a simplistic approach as in general the behaviour of the magnetisation following a sequence of r.f. pulses is complicated and cannot be adequately described in terms of single component exponential decays.

The results of multi-exponential analysis are presented in this section. In studies of water in fresh timbers, two components of relaxation have been observed, and related to the molecules in the bound and free phases. Here we question whether the two component fit is sufficient to describe the relaxation curves, and if so whether this assignment is valid. In other water-logged cellular systems where multi-exponential behaviour has been observed the data has often been interpreted in terms of populations of water that are resident in different compartments within the sample. In water-logged wood there are numerous different environments that could lead to different populations of water that could be seen in relaxation experiments. Perhaps the different values of T1 and T2 are related to the pore size distribution within the wood? Perhaps the multi-component decays are not a consequence of compartmentation or to the existence of bound and free phases? It may also be possible that multi-component interpretation is itself incorrect.?

Measurements on a number of samples of water-logged wood were made using a resonant frequency of 17MHz as the temperature, water content and degree of degradation of the wood were varied. The magnetisation curves were resolved into two or more components. In general it was found that the fit using two components is satisfactory. Some improvement in the fit takes place with three or more components, but this is slight, and is likely to be a consequence of the greater number of parameters used in the fit.

The measurements of spin-lattice relaxation times were made using the 180°-τ-90° pulse sequence and the spin-spin decays were observed using the Carr-Purcell-Meiboom-Gill pulse sequence. The resolution of the longitudinal magnetisation into two or more components is less reliable than in the case of the transverse relaxation experiment, as accurate accumulation of data is time consuming and depends heavily on the reliability of the apparatus over that period of time. Since the magnetic field and amplifier gains are prone to change over a period of hours, results are often ambiguous.

The components of spin-spin relaxation can be extracted with more confidence, as upto 4000 sampling points can be observed during the decay following a single pulse sequence, giving a vast improvement in the data quality and reliability. Transverse decay times have thererore been the prime focal point of this work.

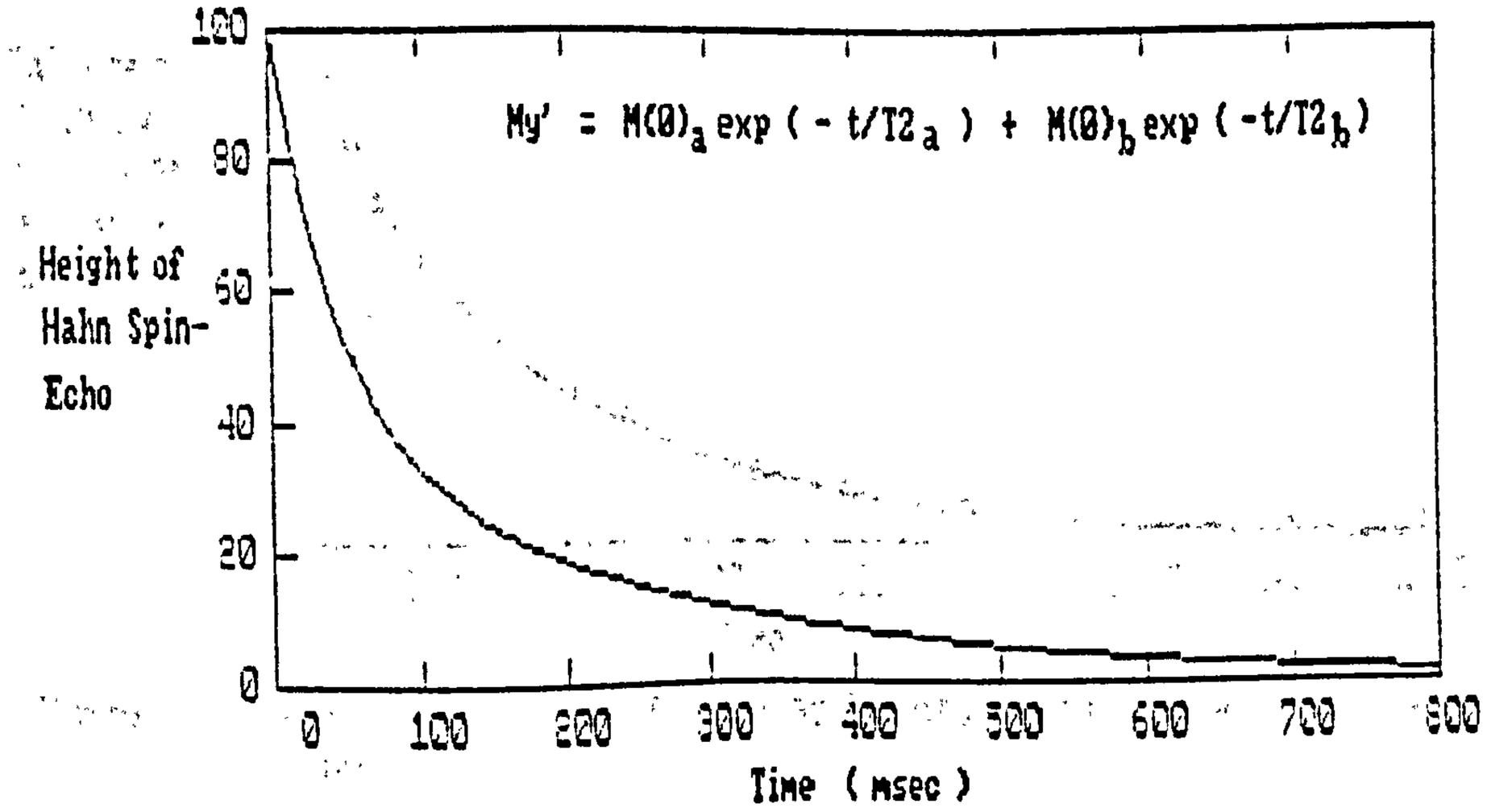

Figure 6.11 Non-exponential spin-spin decay observed in transverse relaxation of water in water-logged ash.

The magnetisation decay curves in the transverse and longitudinal directions for water in water-logged wood are shown in figures 6.11 and 6.12. The log-normal plots of the observed magnetisation against time are non-linear, indicating their multi-exponential nature. The magnetisation decay is expressed by the function;

$$M(t) = \sum_{i=1}^{n} Mi(0).\exp(-t/Ti) \qquad 6.3$$

where n = 1,2 or 3. A measure of the goodness of fit is given by the r.m.s. deviation to noise ration. For an ideal fit this value should equal unity. In water-logged wood there is a distinct improvement in the fit for n=2 over n=1, but the further improvement in the fit

where n=3 is marginal. The spin-spin and spin lattice relaxation times have therefore been analysed in terms of two and sometimes three components. The value of Mi(0) is a measure of the number of nuclei within the 'phase' relaxing at the rate 1/Ti.

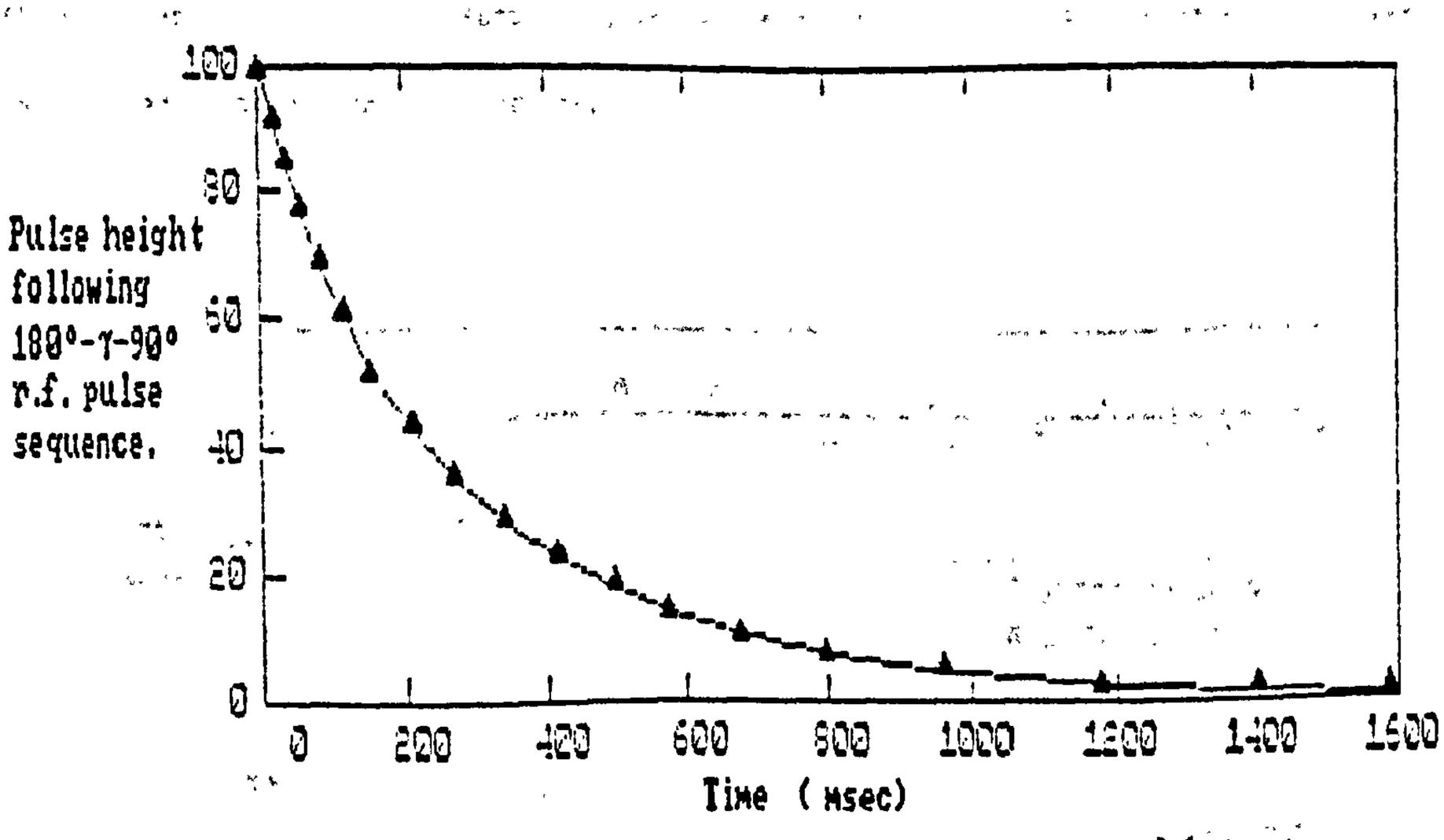

Figure 6.12 Non-exponential Spin-lattice decay for longitudinal relaxation in water-logged ash.

6.2.3 NMR Relaxation Times of Water in Water-logged Wood as a function of Moisture Content and Temperature.

Figure 13a shows the behaviour of the spin-spin relaxation times at a temperature of 300K for water in poplar, as the amount of water within the sample is steadily reduced. The initial water content of the poplar is given by

$$(M_{initial}-M_{oven\ dry})/M_{oven\ dry} \approx 3.$$

The sample is relatively well preserved in terms of the amount of solid matter still residing within the wood. The data has been resolved into two components. The shorter relaxation time is usually attributed to nuclei within molecules that are motionally restricted by strong interactions with the substrate, while the component having a slow rate of relaxation is assigned to a more mobile fraction.

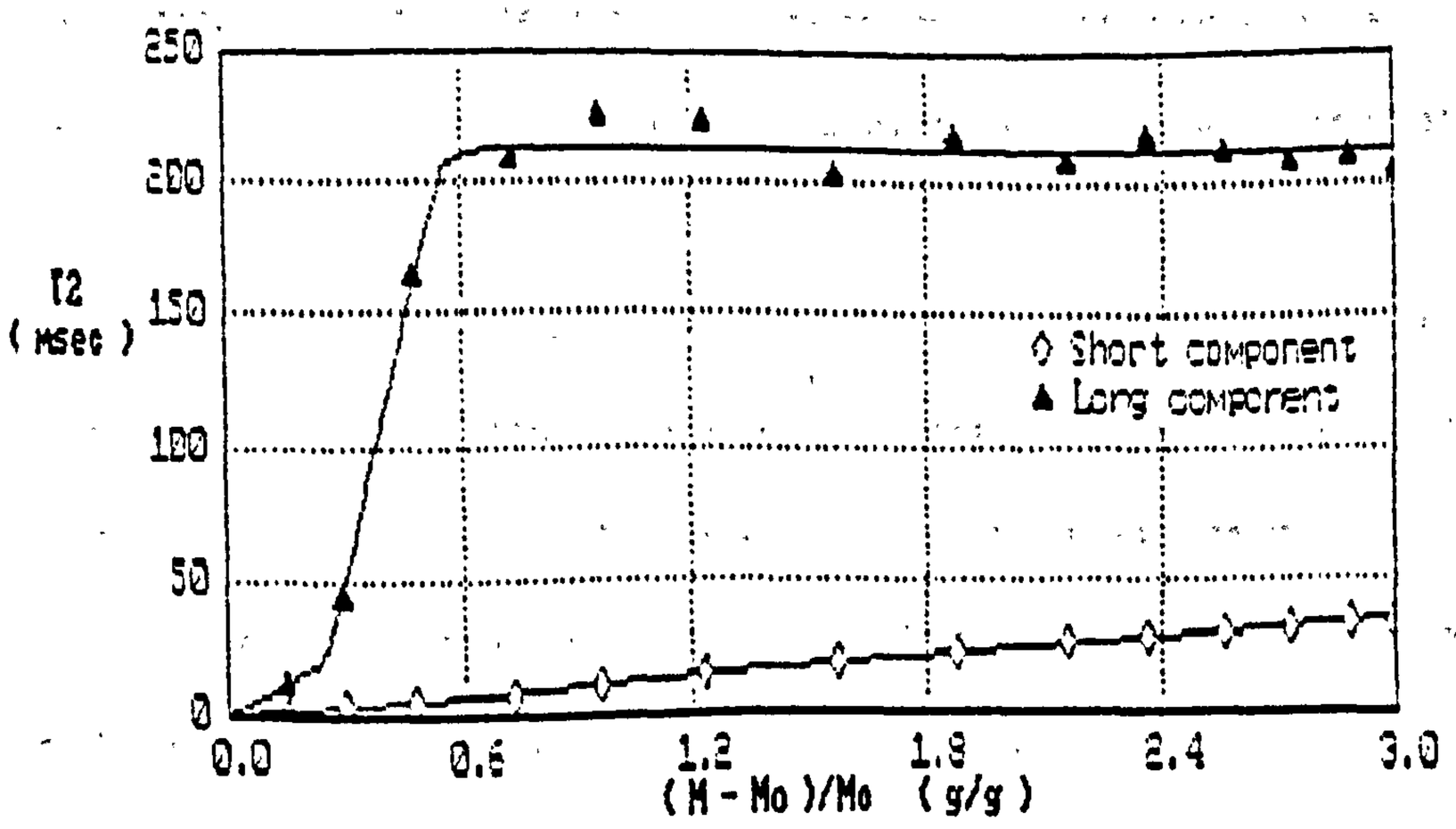

Figure 13a. Spin-spin relaxation times in poplar as a function of moisture content. Two component fit. Initial water content = 3.8 g/g.

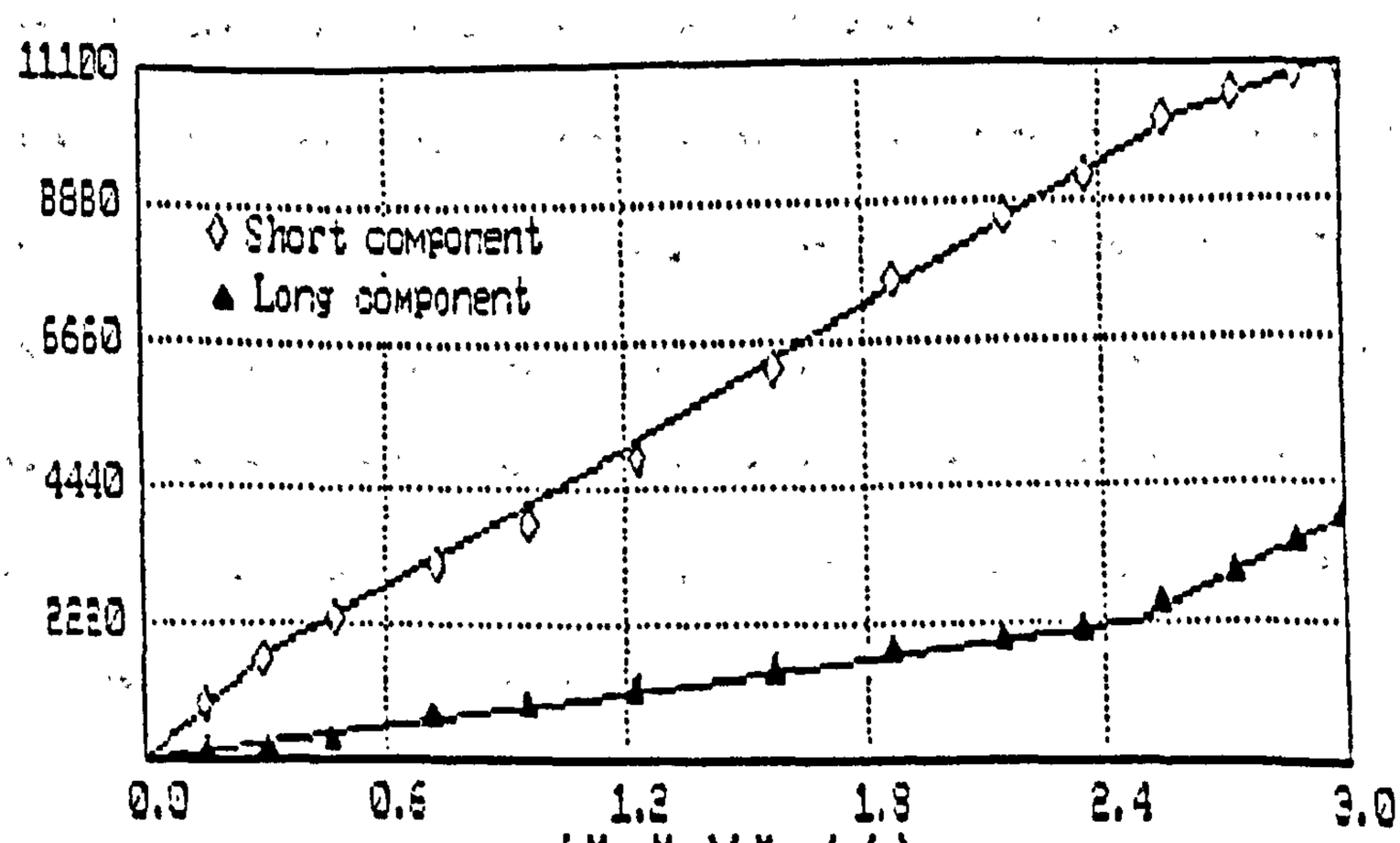

Figure 6.13b Relative amplitudes for two component Spin-spin relaxation in poplar having an initial water content of 3 g/g.

The figure also shows the amplitudes in arbitrary units of the two populations (figure 13b). The most striking feature of this graph is that the population of the rapidly relaxing component is much greater than that of the slowly relaxing component. From the analysis of the freezing curve data one would have expected the tightly bound fraction to contribute approximately 15% of the total signal. The two fractions observed in the T2 measurements do not therefore correspond to the 'bound and 'free' fractions that were observed in the freezing curve experiments. In addition the relaxation time of the long componentis reduced from that of free water. Hence it is considered that both components contain bound and free water.

Above a water content 2.5 g/g the most readily removed water is that which resides in the 'mobile' fraction. At 2.5 g/g, however, there is an increase in the rate at which water is removed from the 'immobile' fraction. and the water in the mobile fraction becomes harder to extract from the wood. This is matched by a transition in the spin-spin relaxation time of the immobile fraction which falls at an increased rate with water content below this point.

The relaxation time of the mobile fraction maintains a constant value of around 215 milliseconds until the water content reaches a value of between 0.35 g/g and 0.6 g/g. The low number of data points on the graph does not allow the transition point to be defined more accurately. Once again the transition coincides with a change in the manner that the two amplitudes behave as a function of sample dehydration, and the rate at which the mobile fraction of water is removed is again reduced in favour of the removal of water from the less mobile fraction. At the transition point the value of T2 for the mobile fraction falls rapidly as the sample is further dehydrated.

At water contents of 2.5 g/g and above, a third component is resolvable from the decay, which has an intermediate relaxation rate. The low number of data points does not allow this fraction to be well characterised, and tests were carried out on samples on wood with increased initial water content in order to study this component.

Figures 6.14a-6.15c show the spin-spin relaxation times and amplitudes for water in poplar having an initial water content of 4.2 g/g. The decay has been resolved into two components at all water contents, and could be resolved into three components at water contents greater than 2.6 g/g. Below this value the computer could not resolve a third component using the Newton-Raphson method.

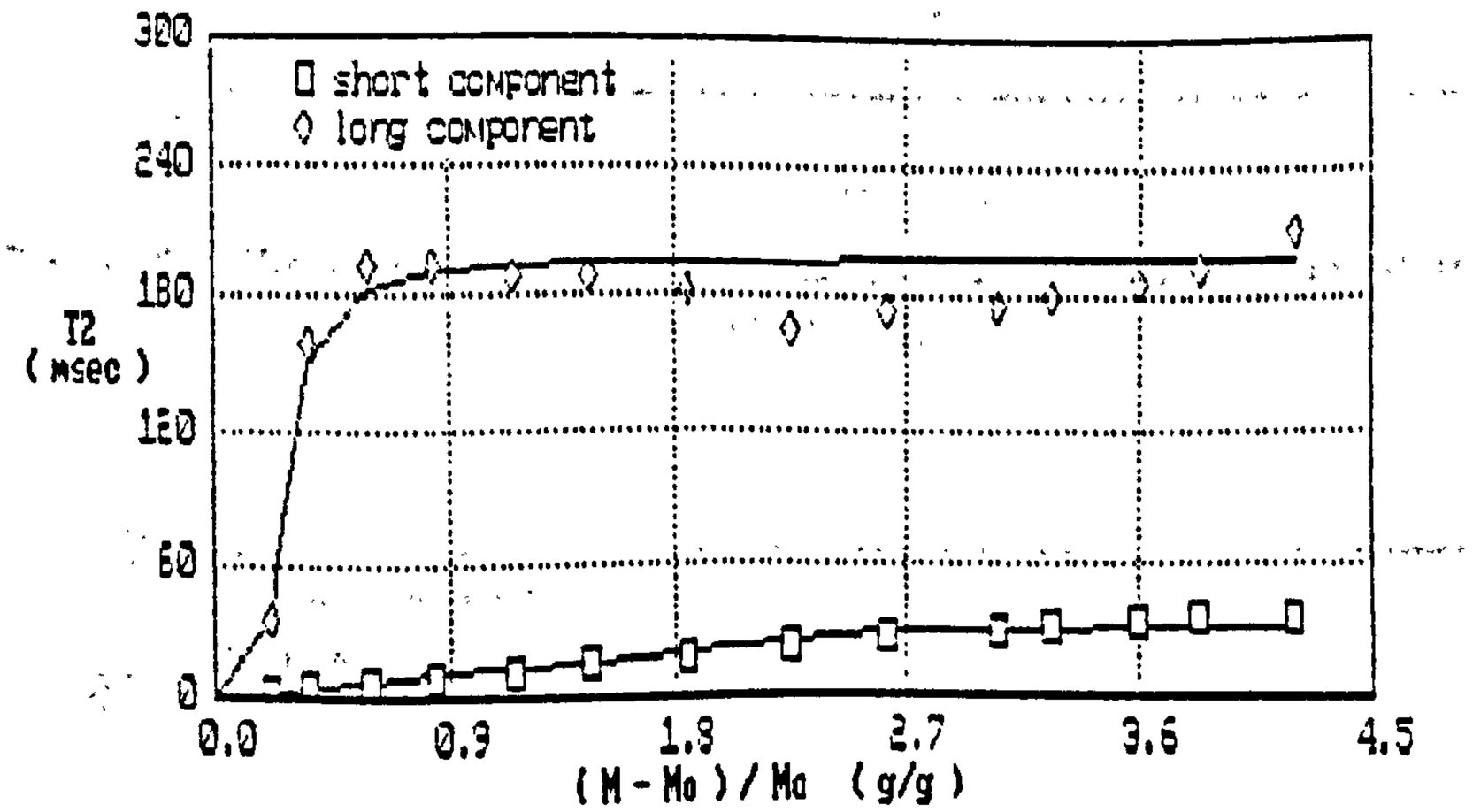

Figure 6.14a Variation in two component relaxation times for poplar, initial moisture content 4.2 g/g, as a function of weight during drying.

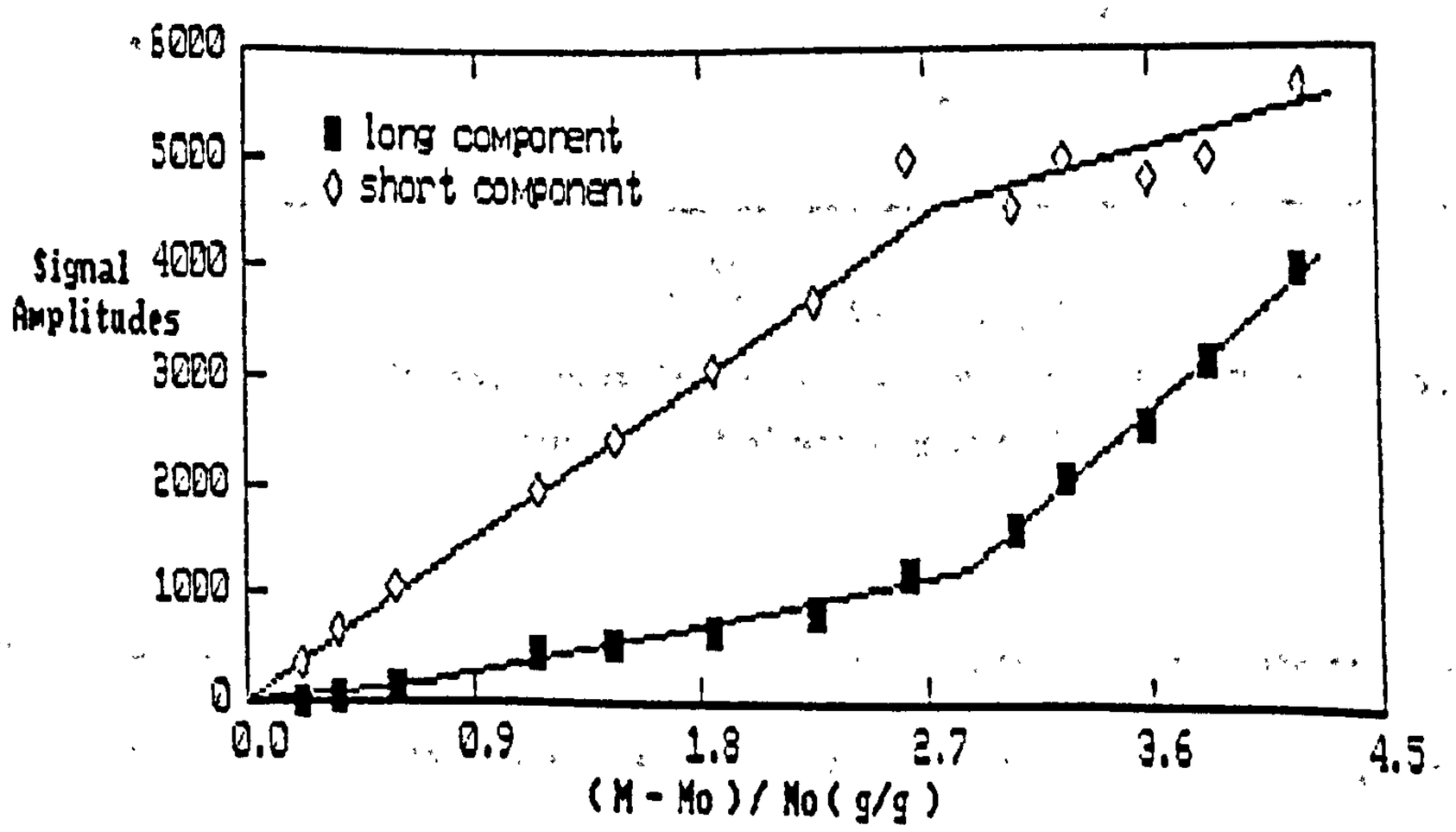

Figure 6.14b Signal amlitudes of two-component relaxation in water-logged poplar. Initial water content = 4.2 g/g.

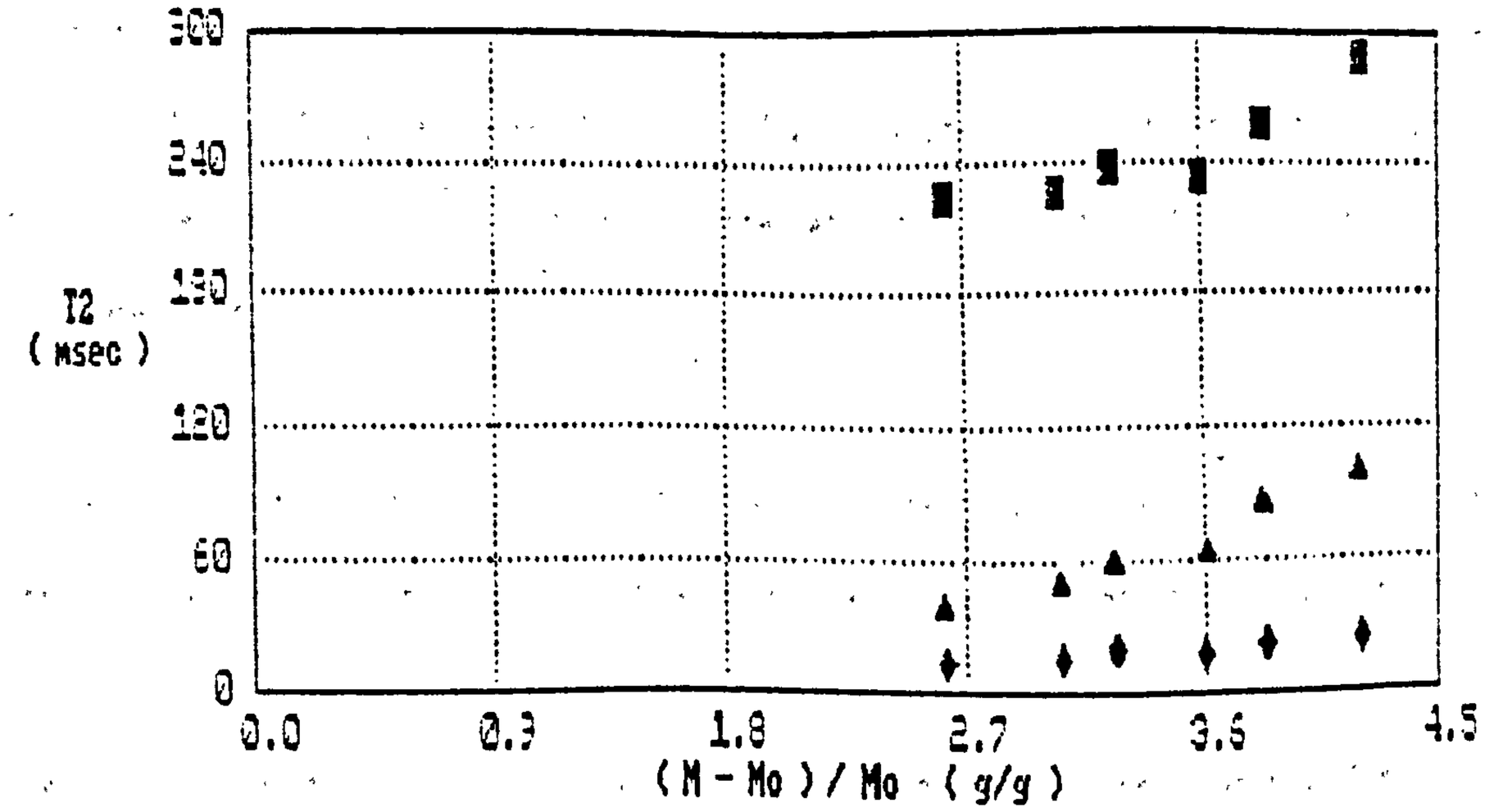

Figure 15a. Three component spin-spin relaxation in water-logged poplar having initial water content of 4.2 g/g.

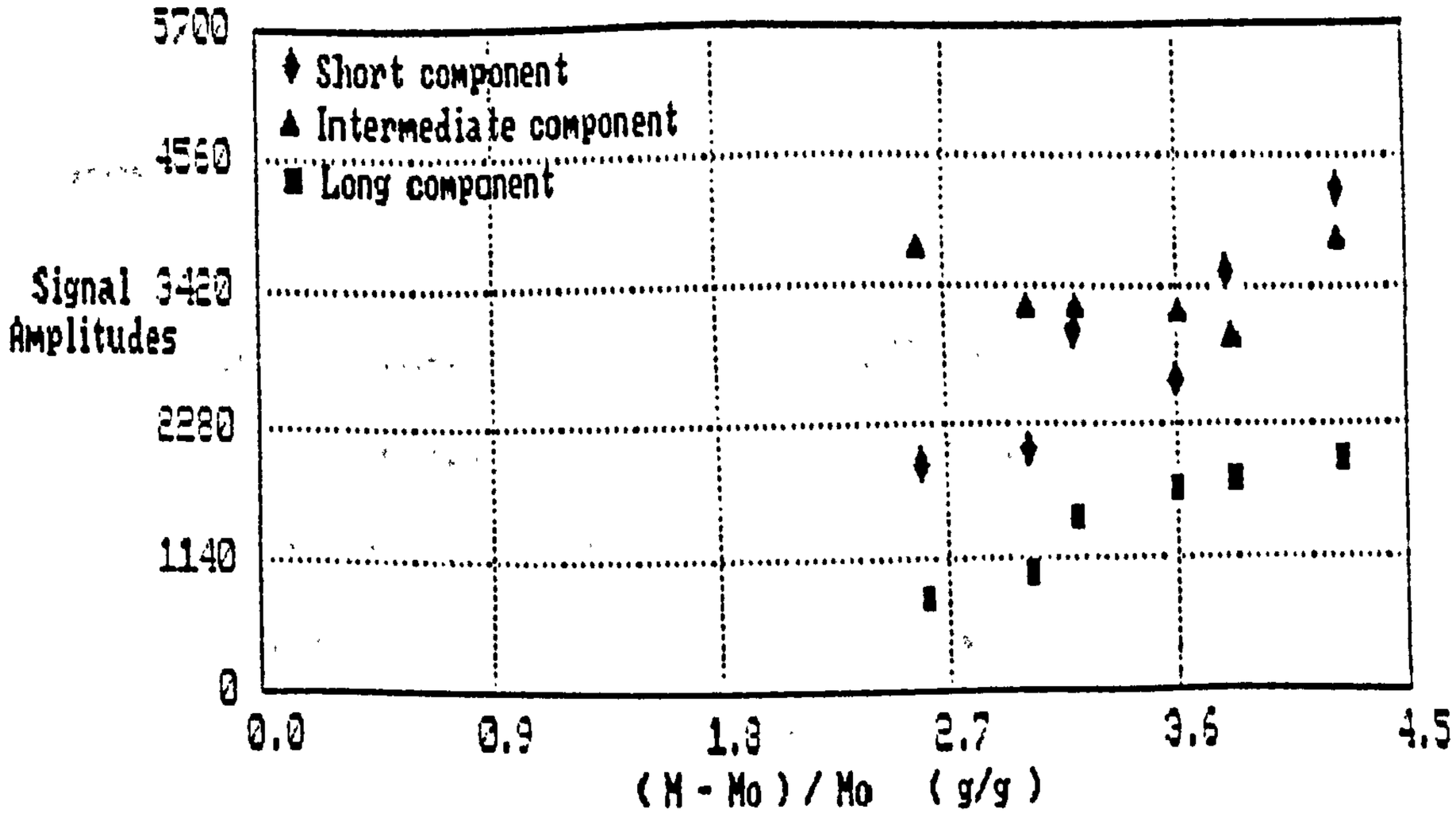

Figure 6.15b Signal amplitudes for three-component relaxation in water-logged poplar. Initial water content 4.2 g/g.

The initial water content of the wood indicates that degradation is more advanced in this sample, although it still contains a considerable amount of solid content. The characteristics of the two-component fit are similar to those observed in the previous sample, and two transition points can be identified at water contents of 2.7 g/g and 0.4 - 0.8 g/g. The

reduced scatter in the data points marking the long T2 values allows for a trend to be observed: as the water content is reduced from its initial value of 4.2 g/g to the transition point at 2.7 g/g, $T2_{long}$ decreases. At 2.7 g/g $T2_{long}$ reaches a local minimum of around 170 msecs. It then shows a steady increase until the water content reaches the second transition point, when it falls rapidly.

Ideally one would like to assign the different components of relaxation to known populations of water residing in the wood, and yet the relative populations for the two components are not consistent with water residing in a hydration layer, and water external to this layer. Looking closer at the macroscopic structure of the samples one notes that Poplar, like many of the timbers found on the Mary Rose is a angiosperm, and as such is composed of two main types of cells, namely the vessels and fibres. Typical dimensions for these are given in below[12],

Parameters observed in fresh poplar

Length of vessels	2-200 cm
Diameter of vessels	100-300 μm
Percentage of Woody tissue in vessels	20-23 %
Length of fibres	900-1100 μm
Diameter of fibres	23-26 μm
Percentage of woody tissue in fibres	56-79 %
Thickness of cell walls	2.8-4.3 μm
Total solid content of wood	28-40 %

(by volume).

In water-logged timbers a good deal of the solid content of the wood will have been replaced by water molecules, and it can be estimated from freezing curves that 14-20% of the water within the wood resides in close proximity to substrate materials, and will constitute a 'bound' phase.

For fresh water at ambient temperature, the distance diffused during the spin relaxation time is give by equation 3.53, and using $D \approx 2x10^{-5}$ $cm^2 sec^{-1}$, and T2 ≈ 2 seconds, this distance is of the order of 10^{-4} meters. It is therefore likely that the vast majority of water within the wood will diffuse to regions where 'bound' water exists. Once there it will undergo exchange with that fraction, and an average relaxation rate will be observed.

An obvious divide which provides the correct initial populations observed in poplar in the two component case is to associate the fast relaxing component with water held within the fibres, and the component with the long relaxation time with the water in vessels. This tentative assignment can explain the relaxation data for the two component fits, and the validity of this model is discussed below.

Vessels are the main conducting elements of the wood. They form the primary route of access for water molecules moving between the exterior and the interior. The initial drying can therefore be related to a reduction in the population of water within these ducts which is seen as the fall in the population of the slowly relaxing component. As the water content of the wood falls, the water molecules within the fibres leave the cells, and their passage from the wood is directed primarily via the vessels. Water therefore passes from the fibres into the vessels, producing an increase in the rate at which water leaves the quickly relaxing

component. The rate at which the population of the slowly relaxing component population falls is reduced by the influx of molecules from the quickly relaxing component, corresponding to the first transition noted in figure 6.13a and 6.14a.

Water in both vessels and fibres is expected to consist of 'bound' and 'free' phases. In this model the 'bound. phase is thought to reside on the surface of the cell walls, and in the voids created by the removal of hydrolysed cell wall materials. The solid lines in figures 13 and 14 are fitted using equation 6.2 which predicts the relaxation time observed when two populations are in rapid exchange with each other. The parameters used in making the fits are listed below:

Parameter	Short Component	Long Component
$T_{2,obs}$	200 msecs	200 msecs
$T_{2,bound}$	10 msecs	50 msecs
[H2O]b	0.7 g/g	0.002 g/g

[H2O]b represents the amount of water within the sample that is motionally restricted by the wood cell walls for each phase expressed in grams of bound water per gram of the total solid content within the sample. The sum of [H2O]b for the slow component and fast component is the total amount of bound water within the sample. Initially 19% of all the water in the wood resides in the bound phase . which is in agreement with the findings from freezing curve experiments. One might therefore question whether the values of [H2O]b can be justified by assuming that the two components relate to water in fibres and vessels.

Given that the sample of poplar before degradation had dimensions similar to those listed above, one can calculate the fraction of the total volume of the sample that was taken up by the cell walls of the fibres and vessels in the fresh state. The volume of each fibre is divided fairly evenly between the cell wall substance and the lumen. In vessels the cell wall

only contributes between 4.6 and 5.9% of the volume. If one assumes that in water-logged wood the solid content of the cell wall has been replaced by water, and that this water acts as a bulking agent for the remaining skeleton of xylem, then the motional properties of this fraction will be modified and it will constitute the bound phase. If bulking is extensive then the volume of the cell wall prior to degradation can be equated to the volume of the bound phase in the water-logged wood.

If all of the volume previously associated with the cell walls is occupied by bound water then this would lead to values of [H2O]b ≈ 2.0 g/g for the fibres, and 0.08 g/g for the vessels. It is not likely that all of the cell wall material has been replaced by water and it is plausible that the remaining solid content in the fibre cell walls reduces [H2O]b to around the 0.3 g/g observed. A similar amendment to the value of [H2O]b for vessels, however leads to 0.02 g/g, which is one order of magnitude greater than observed. One would expect, provided degradation is not too severe, that preservation of the cell walls is more efficient in the fibres than in the vessels. If this is so, then the case may arise whereby the cell walls of the vessels are weakened by the loss of cellulose and hemicellulose to such an extent that they can no longer sustain a full population of bound water leading to a fall in the value of [H2O]b. The network of hydrogen bonds giving rise to the bound phase loses its integrity, and the remaining molecules within this phase become more mobile, leading to the higher mean transverse relaxation time.

In fitting the data by this method it was assumed that the parameters Tb, Tf, and [H2O]b do not change during the drying process. This assumption is likely to be false at low water contents, when the gradual shrinkage of the wood produces changes in cellular structures which cause a redistribution of water molecules throughout the system, and a modification of their motional properties. The sudden fall in the value of $T2_{1...}$ may therefore be a conse-

quence of both the two-component nature of the water within vessels, and of this change in structure. To achieve the fit of the curve at a water content of about 0.2 g/g the calculation has been made using $T_{2_{short}} \approx 10$ msecs.

The notions put forward above may be sufficient to account for the behaviour of the spin-spin relaxation times in water-logged wood for which the degradation is not advanced. The appearance of a third component at higher moisture contents however, leads to speculation about the validity of this model.

Above a water content of 2.7 g/g the two component fit is not as effective as the three component fit, for which there is a two-fold improvement in the standard deviation : noise ratio. The third component appears as a population with an intermediate relaxation rate, and has a constant amplitude over the range of water contents for which it can be resolved.

More information about the third component has been obtained from studies on highly degraded timbers for which the initial water content is approximately 7.3 g/g (See figures 16a-17b). The third component could be resolved from the magnetisation decay even when the water content withinthe sample had been reduced to values as low as 1.6 g/g. The amplitudes for the two component fit exhibit characteristics that are similar to those observed in less degraded timbers. The transition at low moisture contents has not been observed as the data points do not extend to low enough water contents. This is because the signal to noise ratios were unfavourable at these values, and this has led to the scatter in values of $T2_{short}$ that can be seen in figure 6.17. It is possible that the second transition would not be visible in any event, as the behaviour of $T2_{short}$ is different in this sample, and decreases from the offset. The sudden drop in the values of $T2_{short}$ at low water contents does not occur, and so the transition may not exist.

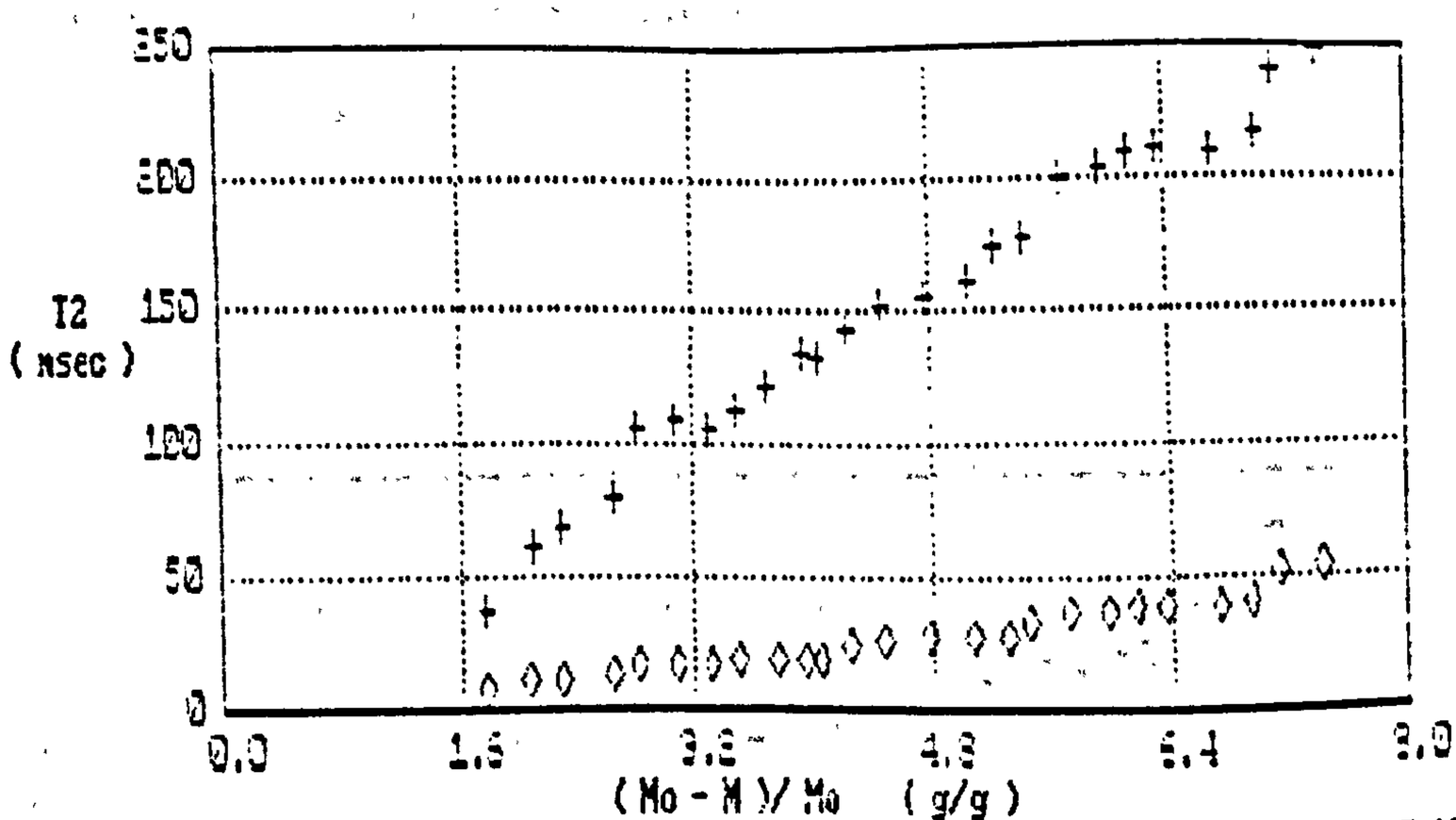

Figure 6_16a Two component relaxation in poplar with initial water content = 7.43 g/g as a function of weight loss during drying.

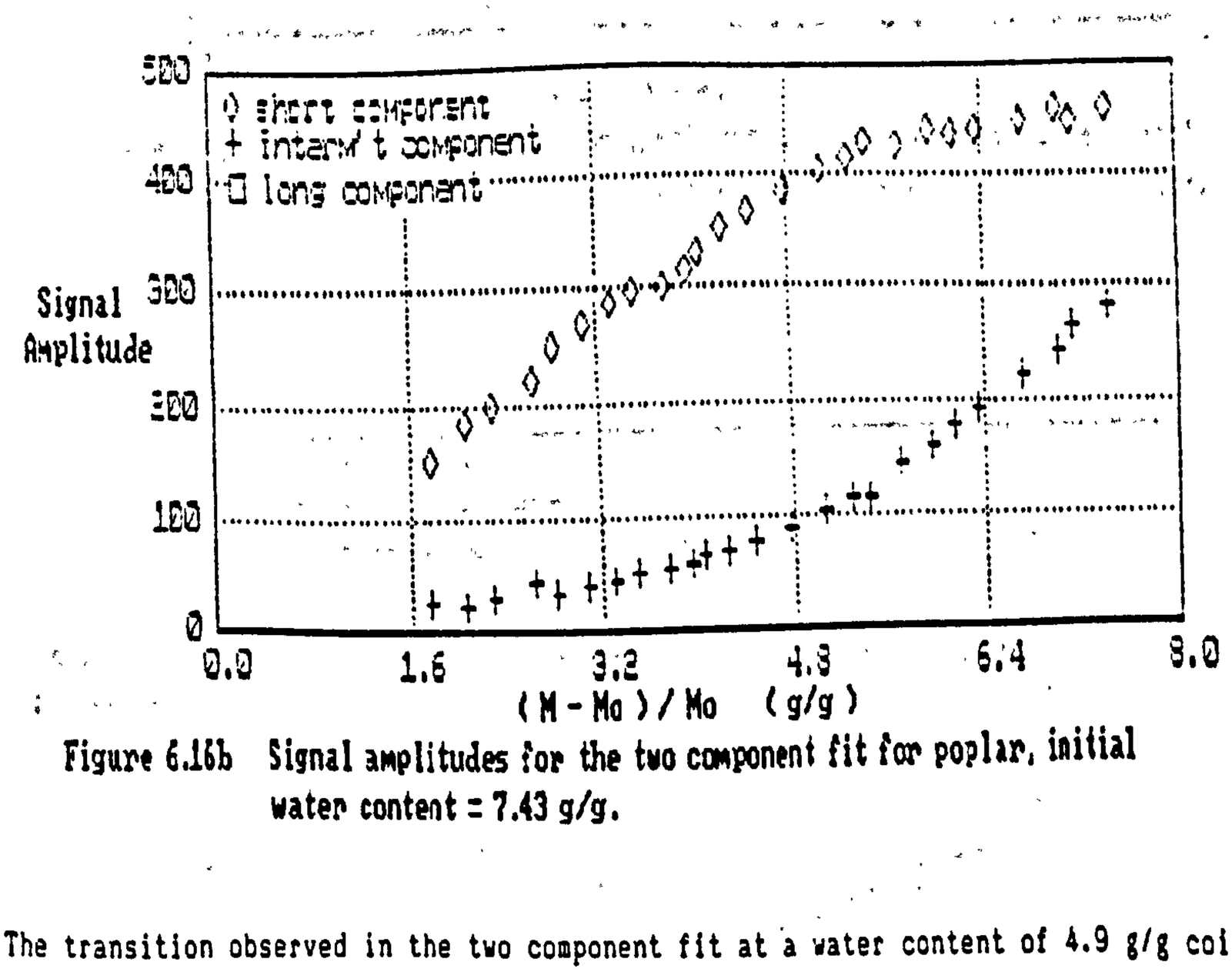

Figure 6.16b Signal amplitudes for the two component fit for poplar, initial water content = 7.43 g/g.

The transition observed in the two component fit at a water content of 4.9 g/g coincides with the point at which the amplitude of the third begins to decrease. It corresponds to the same transition observed at water contents of around 2.6 g/g in timber that has been better preserved.The notions put forward above may be sufficient to account for the behaviour of the

spin-spin relaxation times in water-logged wood for which the degradation is not advanced. The appearance of a third component at higher moisture contents leads to speculation about the validity of this model.

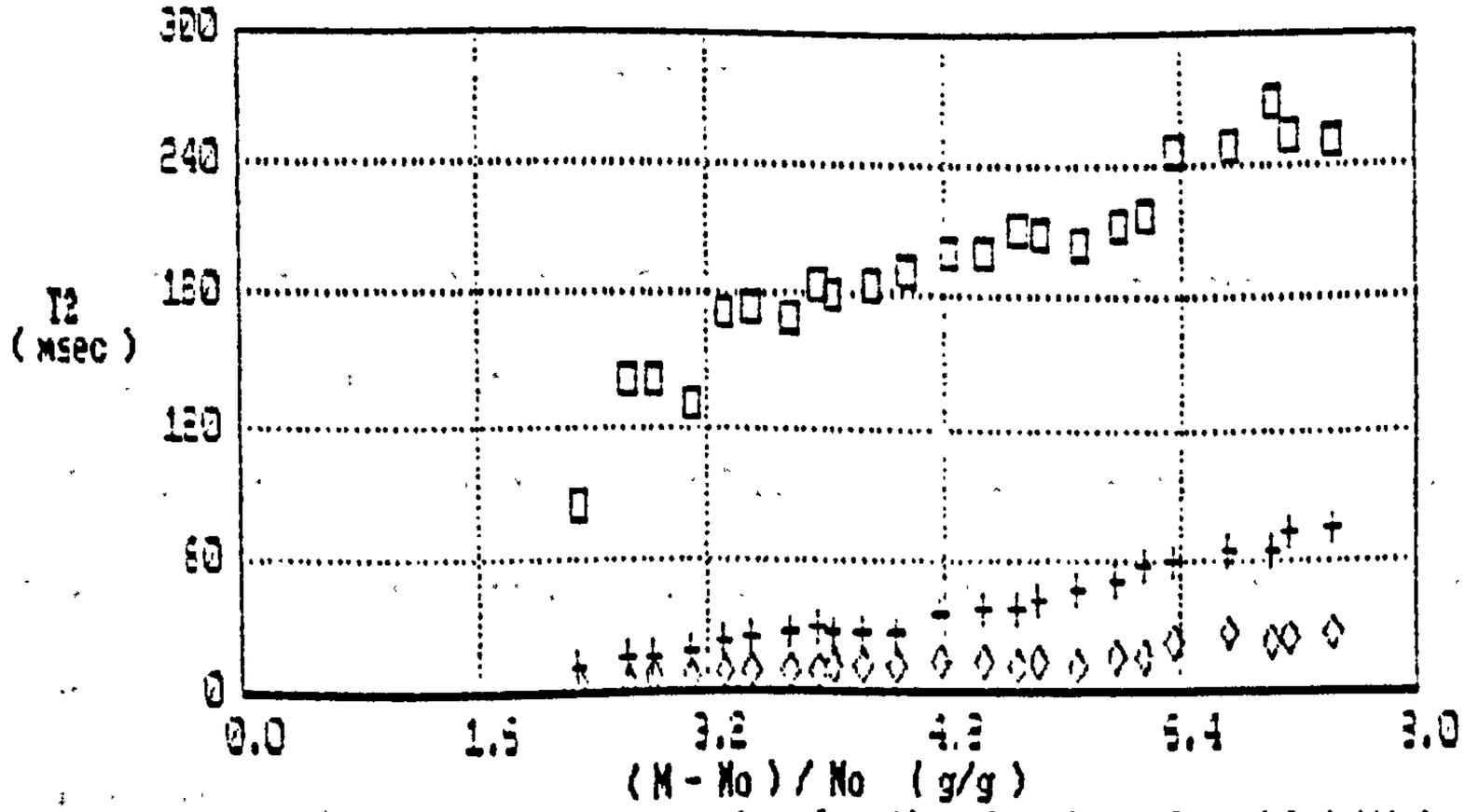

Figure 6.17a Three component spin-spin relaxation times in poplar with initial water content of 7.42 g/g, as a function of weight loss during drying.

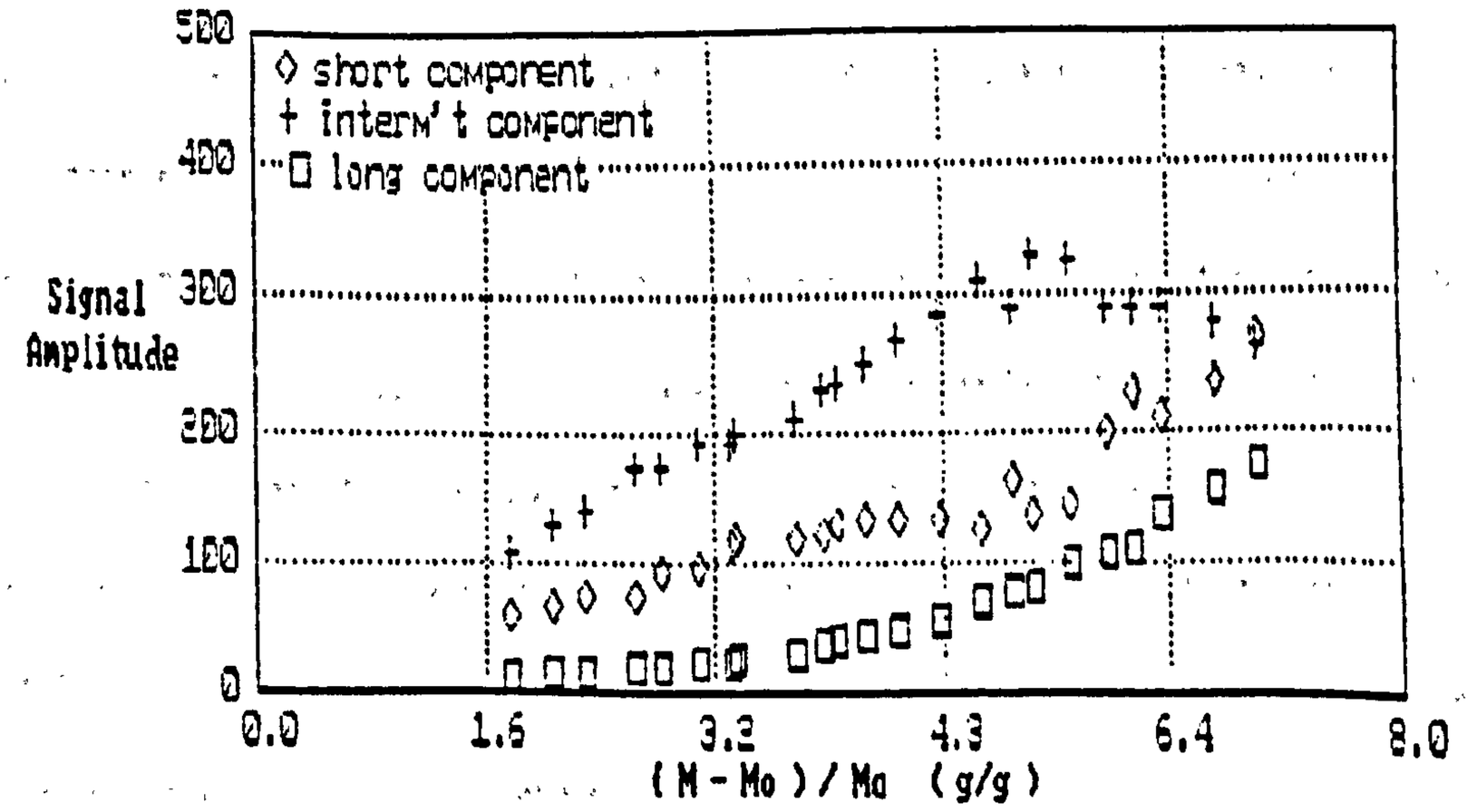

Figure 6.17b Three component signal amplitudes for poplar. Initial water content = 7.43 g/g.

In well preserved timbers the amplitude of the intermediate component remains independent of the total water content of the sample until the data becomes two-component, at which point it accounts for 60% of the total signal amplitude. The amplitude of the short component also accounts for 60% of the total signal amplitude when the data first becomes two component. These points, together with the fact that the value of $T2_{inter}$ is of the same order of magnitude as $T2_{short}$ in the case of two components leads to the postulate that the intermediate fraction corresponds to water within the fibres.

The large and short components can then be assigned to water within the vessels. The value of $T2_{long}$ maintains a constant value of around 220 msecs, which is consistent with the value of $T2_{long}$ observed in the vessels, and $T2_{short}$ has a value that falls from 25msecs to 14msecs, which is not inconsistent with $T2_{short}$. The change from three to two component behaviour may possibly be caused by the fall in the amount of water within the vessels leading to a loss of resolution.

The idea that the water in the vessels becomes two component at higher water constants appears to explain the character of the spin-spin relaxation until one considers the relative amplitudes of the long and short components. According to the arguments presented above, the short component should contribute 6% of the signal or less if it is indeed the bound phase. The actual contribution is nearer 60%, which is where the model becomes tenuous. If one calculates the value of $T2_{long}$ at the point where the two component fit becomes valid using the amplitudes and values of T2 for the vessels as measured from the three component fit, one arrives at a value of 18 milliseconds, which is clearly not consistent. Whether this evidence is sufficient to discount the idea of compartmentation between vessels and fibres in not clear as existence of the third component is itself in doubt.

Results similar to those observed during this work were found in samples of muscle tissues[22]. The data was interpreted in terms of three components of water, and the decay times and their associated amplitudes match those in wood. The cells in muscle are designed, like those in wood, from fibrillar units, and the similar relaxation behaviour may not therefore be unexpected. Differences in the dehydration dynamics are noted however: As the moisture content of the muscles was reduced the amplitude of the long and intermediate decays fell while the amplitude of the short component maintained its initial intensity until the other components had vanished from the samples. The fraction of water with the fastest rate of decay was associated with that which is most closely related to the protein within the muscle, and it was suggested that extracellular water might be the origin of the long T_2 component. Brownstein and Tarr[23] used the relaxation in frog gastronemus muscle as a test case for their work in which the component of relaxation with the longest relaxation time was considered to originate from extracelluiar water,separate to the intracellular component. The relaxation of the intracellular component was evaluated using the diffusion equation, treating the geometry of the cells as having a cylindrical symmetry. The decay of the magnetisation is then given by;

$$M(t) = M(0)_{extracellular} \times \exp(-t/T_{extracellular}) + \sum_{i=0}^{m} Mi(0) \times \exp(-t/Ti_{intracellular}) \qquad 6.4$$

Mi(0) and Ti are found using equations that are similar to equation 6.3. This model successfully predicted the behaviour of the transverse relaxation in the muscle.

In wood the intercellular voids are packed with lignin in the form of the middle lamella. The volume occupied by the middle lamella contributes only a few percent to the total volume of the wood, and it is therefore unlikely to give rise to $T2_{1...}$. The assignment of $T2_{1...}$ to the extracellular component is also negated by studies of the spin-lattice relaxation described below.

Brownstein's approach to the transverse relaxation in fresh wood was to assume that two phases of water resided in the wood[113]. The first is the water of hydration within the wood where diffusion is inhibited. Above the saturation value for the wood a second layer or water exists for which the diffusion is similar to that observed in bulk water. The relaxation of the spins was considered to be due to a combination of diffusion and magnetic sinks on the surface of the wood, with the density m(r,t) of the proton magnetic moment obeying a modified diffusion equation as described in section 4.3.1.

The solution to the equation, subject to the appropriate boundary conditions, yields a sum of exponentials. Brownstein[113] derived a transcendental equation for the nth relaxation time $T_{(n)}$;

$$(b/a-1)\Gamma_n.\tan(\Gamma_{(n)}) = 1 \qquad 6.5$$

where

$$T_{(n)} = a^2/(D_1\Gamma_n^2) \qquad 6.6$$

b represents the amount of water in the second layer, a is the quantity of water in the hydration layer, and D_1 is the diffusion coefficient of the water in this layer.

The overall time scale of the relaxation times, $T_{(n)}$, is determined by the single adjustable parameter a^2/D_1, which does not effect the form in which the $T_{(n)}$ vary with b/a. (See figure 6.18). The theory was successful in predicting the behaviour of spin-spin relaxation times of water in fresh timbers with moisture contents upto 1.4 g/g. By choosing a suitable value of a^2/D_1 for the first mode (n=0), the values of the second mode (n=1) can theoretically be predicted.

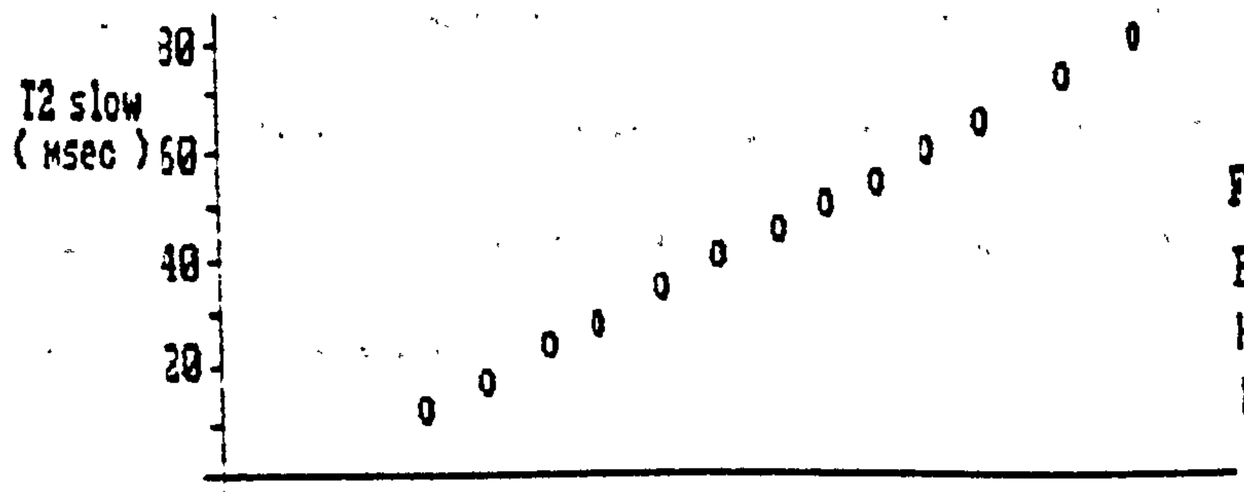

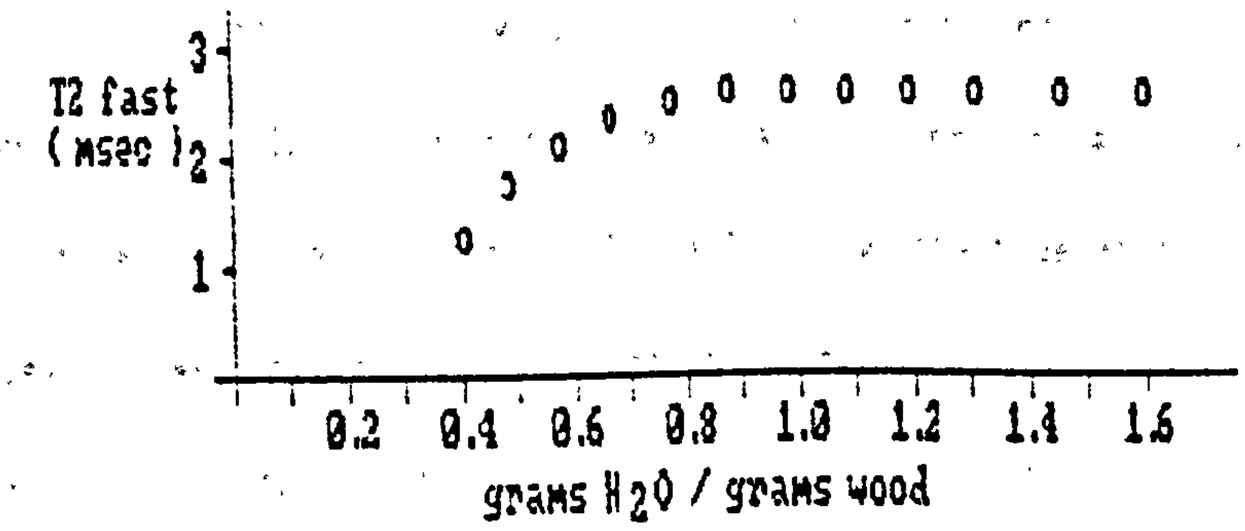

Figure 6.18
Brownstein's analysis of Hahn's T2 data for Northern white-cedar wood.

Sample	(Min-Mo)/Mo	$T1_{slow}$	$T1_{short}$	% $T1_{slow}$
Ash	5.2	436	21	87
Birch	7.5	502	6.5	83
Elm	5.3	257	60	62
Oak	3.3	130	32	62
Pine	6.0	298	145	80
Poplar	4.3	420	85	60

Table 6.3 Variation in T1 for different samples and degrees of degradation.
(Values accurate to ±5% for $T1_{short}$, and ±10% for $T1_{slow}$)

The theory breaks down in the case of water-logged timbers. Equations 6.5 and 6.6 predict that for the first mode $T_{(0)}$ increases linearly with water content, and this may be identified by its dependence on b/a with the shorter of the two relaxation times in the two component fit. In order to fit the curve a value of 3.38 msecs is required for a^2/D_t. The value used by Brownstein[13] in fresh timbers was 25.8 msecs, leading to an upper bound for the thickness a of the hydration layer of 0.09μm. Using a value of 3.38msecs to make the fit for

the short component should produce a value of T_{1s} that is approximately 0.24 milliseconds, not the value of 200 msecs observed. Using this model does not therefore predict the correct values of the decay times in water-logged wood at the water contents studied. It may be possible, however, to attribute the failure of this model to the ad-hoc boundary and initial conditions that were applied.

Spin-lattice decay in water-logged wood is non-exponential above and below the freezing event. Figure 6.19 illustrates the variety of longitudinal relaxation behaviour that can be expected in different samples. Table 6.3 shows the time constants and relative populations used to describe the different decays in the figure. The characterisation of water within wood is difficult using T1 measurements because of the inaccuracies involved, but the following observations can be made;

(a) The decay of the longitudinal component of magnetisation in water-logged wood that has a medium to high degree of degradation can typically be resolved into two components with 60-80% of the signal relaxing with $T1_{long} \approx 200$-330 msecs, and 20-40% of the signal relaxing with $T1_{short} \approx 40$-120 msecs.

(b) Both $T1_{long}$ and $T1_{short}$ are independent of temperature between the range of 275K and 355K.

(c) In heavily degraded timbers the proportion of the signal relaxing at the slower rate increases, and both $T1_{long}$ and $T1_{short}$ attain higher values. The exact values of $T1_{long}$ and $T1_{short}$ and the relative populations are complicated functions of both the species and moisture content of the wood.

(d) As the water content of the wood is reduced, both $T1_{long}$ and $T1_{short}$ fall, and the populations of both components are diminished without preference to either. In woods where the degradation is not advanced $T1_{long}$ can be as low as 14.5 msecs even before the drying process has started.

(e) Below the freezing event both relaxation times fall with temperature.

As indicated in (a), the spin-lattice relaxation times for the two components are slightly greater than the spin-spin times. Rather more surprisingly, the relative populations of the two fractions do not correspond to those seen in T2 measurements, and the majority of water relaxes at a slower rate in contrast to the observations made in transverse relaxation studies. This is an extremely important result. It means that the two values of T1, and the two values of T2 cannot be related to two identifiable populations of water.

The fact that the relaxaton times are inoependent of temperature (See Figure 19a), may be explained using the diffusion model. Assuming that the water molecules are moving with correlation times that are low, T1 should be seen to increase with temperature. However, as the temperature increases, the diffusion rates of the molecules are likely to increase, and the interaction rate between water and macromolecules will increase, lowering the T1 values, and offsetting changes due to temperature.

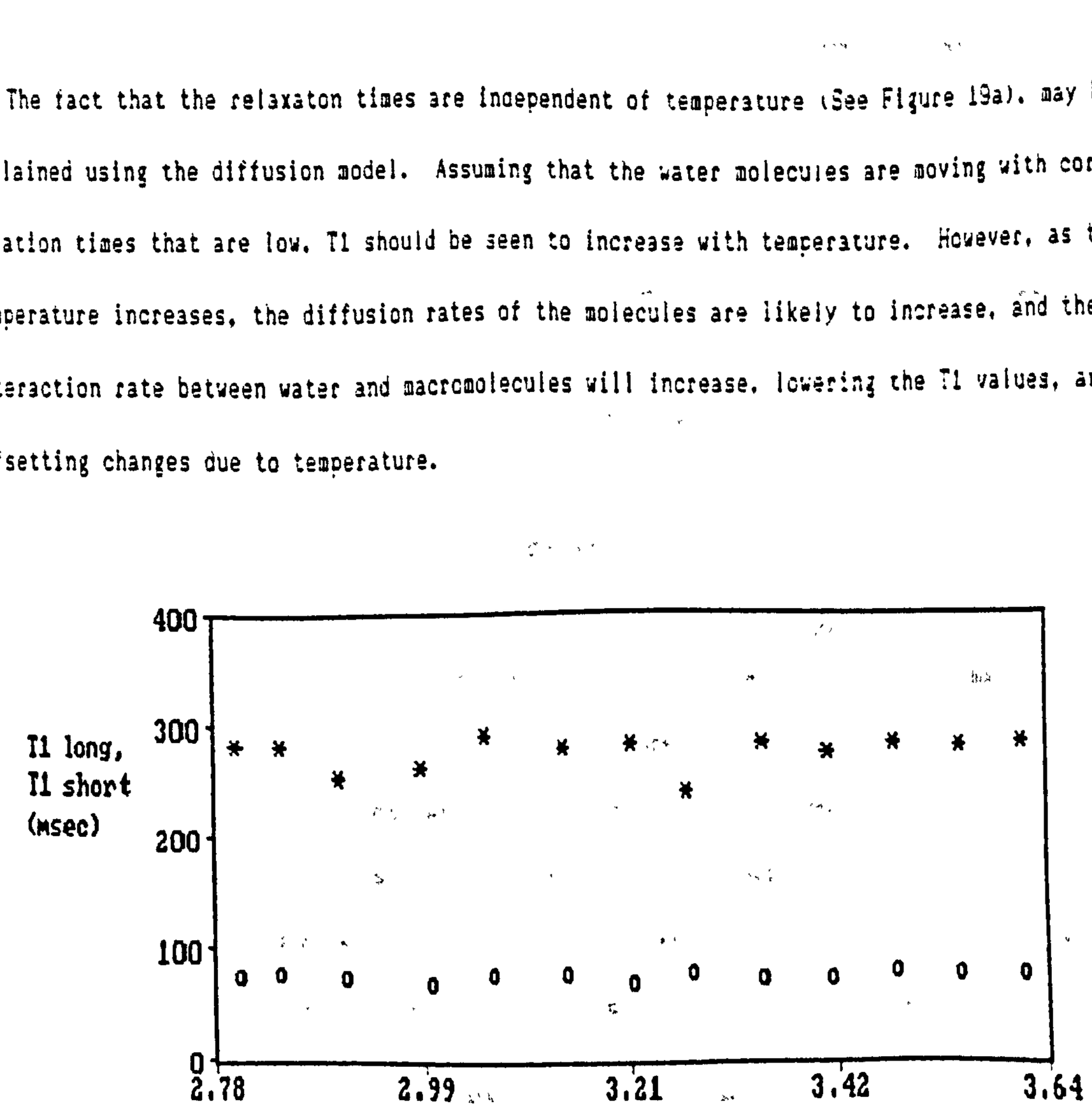

Fig. 6.19a. T1 long (*) and T1 short (o) as a function of temperature for waterlogged poplar above the freezing event.

Spin-Lattice Relaxation in Wood

Figure 6.19 Various Species/Degradation

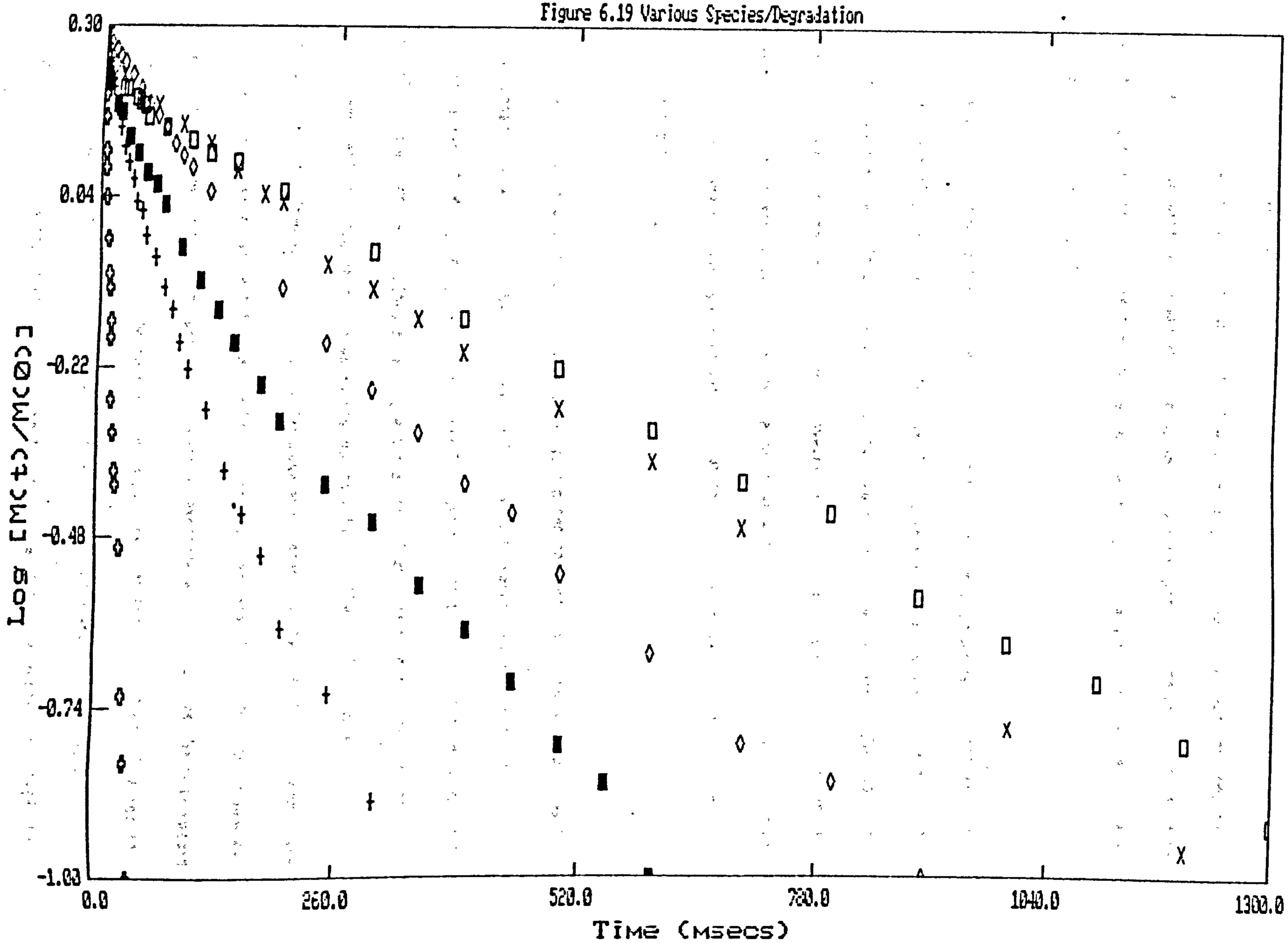

The three component spin-spin decay that is observed in the heavily degraded timbers even at low water contents may be an indication that the two-phase model is incorrect. Three overlapping resonances were observed in the proton spectra of Norway Spruce and Sugar Maple that had been saturated in distilled water[114]. The position of each resonance depended upon the orientation of the wood in the magnetic field, and it was thought that the origin of the different signals was from different morphological regions within the wood. The nature of these regions was not defined.

It seems likely that a three component fit for the data is a better representation than a two component fit, despite the fact that the third component is not always defined. If so then the two-component fit will be a weighted average of the three components. Even assuming that the three-component model is correct, however, it is unlikely that any one fraction represents the non-freezable water alone, but rather that each of the three fractions is a combination of exchanging bound and free water for which the degree of destructuring differs from one population to another.

Evidence that the different types of water within the samples are in exchange with each other comes from a study of the T2 relaxation times as the temperature of the sample is cycled between 275K and 350K. According to the BPP theory of section 3.2.1 for an ensemble of nuclei whose motion is described by a single correlation time, the spin-spin relaxation should monotonicly increase with temperature due to a fall in the static component of the dephasing field. However, the discrete multiphase model predicts that exchange between fractions within a sample can lead to a reduction in the observed relaxation times, and since exchange is a thermally activated process the rate of exchange will increase as the temperature of the sample is raised. Under the appropriate conditions, therefore, it is possible for the effects of exchanging nuclei on T2 to swamp the effects of temperature on the dephasing field, in which case the observed relaxation times will be seen to decrease with rising temperature.

Figure 6.20 shows the effects of temperature on the two-component fit for water in poplar. As the temperature is increased $T2_{short}$ initially increases, in accordance with the BPP prediction. The rate at which $T2_{short}$ rises with temperature steadily declines, until at about 315K a maximum is reached, and the curve takes a downward turn. From 315K to 355K $T2_{short}$ continues to decline, indicating that an exchange between fractions is in effect.

In the case of the slowly relaxing component, the relaxation time decreases with increasing temperature over the entire range studied, and exchange processes dominate the behaviour of $T2_{long}$. As the temperature of the system is increased there is a slight shift in the populations of the two components, with nuclei in the immobile phase moving into the mobile fraction. This behaviour persists to varying degrees in woods at all moisture contents.

As the temperature is cycled the curves for the upward and downward legs follow the same paths. Some evaporation is expected at the higher temperatures which would account for the apparent non-reversibility observed.

An interesting observation was made during experiments in which the temperature behaviour of the two-component transverse relaxation times were studied as a function of the water content of the wood. The sample used had an initial water content of 4.0 g/g. The sample was partially dried to a moisture content of 1.3 g/g, and then rehydrated. Following rehydration the sample was again dried, this time to a water content of approximately 0.9 g/g.

The long component of the transverse relaxation time fell with increasing temperature in the fully saturated timber, and the short component T2 exhibited a maximum at 315K as above. As the water contentwas lowered the form of the $T2_{short}$ curve was preserved, but the magnitude of $T2_{short}$ fell in a way that was consistent with studies made at constant tempera-

Figure 6.20 VARIATION OF SPIN-SPIN RELAXATION WITH TEMPERATURE FOR POPLAR AS A FUNCTION OF WATER CONTENT

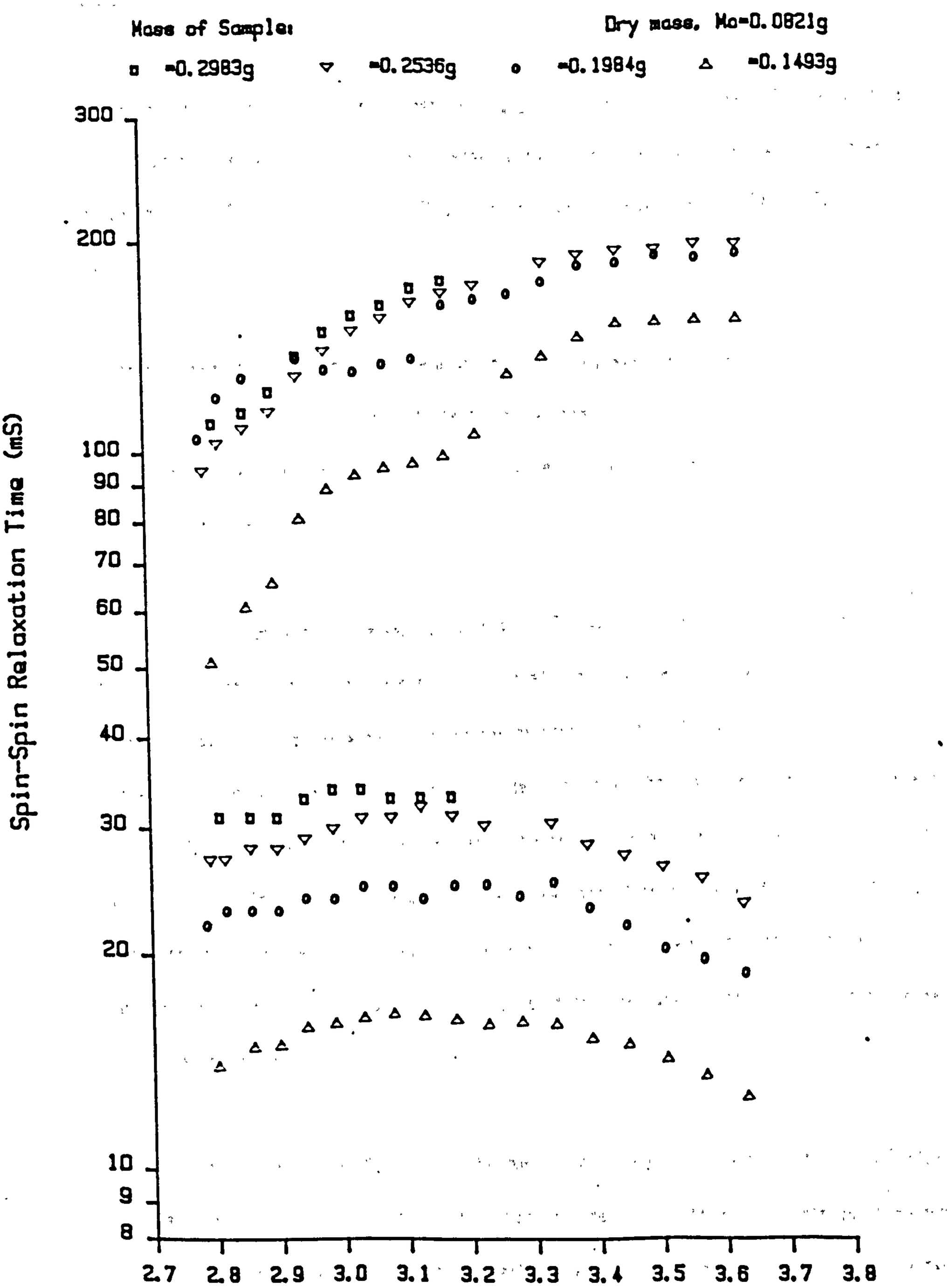

ture. The value and behaviour with temperature of the long component T2 was not initially effected by the loss of water from the wood. Again this was consistent with earlier measurements.

As the water content was further reduced $T2_{long}$ continued to decrease. The value of the long component relaxation time suddenly began to fall, and a saddle point became apparent at approximately 315K. The lowering of $T2_{long}$ in this way is predicted by figures 6.13 and 6.14.

After rehydration the spin-spin relaxation times regained their previous values and characteristics, which indicated that the drying process had not had a significant, long-lasting effect, and that this process is to a large extent reversible provided that the drying is not complete.

As the water content of the sample was reduced $T2_{short}$ fell in the usual way, and $T2_{long}$ exhibited a temperature dependence typical of that for a system in which exchange predominates. However, at a moisture content of about 0.9 g/g the behaviour of $T2_{long}$ with temperature changed dramatically. Instead of decreasing as the temperature of the sample was raised, $T2_{long}$ increased. This suggests that the transition at low moisture contents in the value of $T2_{long}$ is caused by a diminished exchange rate of nuclei between the populations that contribute to the slowly relaxing component. It should be pointed out that this result was not reproducable, but is worthy of note, at it may indicate an end to exchange processes at low water contents.

In light of the earlier discussion one can obviously question the validity of analysing the temperature scanning data using two components instead of three. At higher moisture contents a three-component fit is generally better than a two component fit. Similarly the data

at higher temperatures can be described more effectively using a three component fit, but at temperatures of 310K and below the third component is difficult to resolve, and may indeed no longer be present.

In the cases where three components can be resolved certain trends can be seen:

(a) The rapidly relaxing component has a value $T2_{rapid}$ that is independent of temperature for any given water content. As the water content is reduced $T2_{rapid}$ decreases, typically from 20 msecs to around 9 msecs.

(b) The intermediate component has a $T2_{inter}$ value of about three times $T2_{rapid}$ over the range of temperatures and water contents used. The intermediate relaxation time passes through a maximum at about 315K.

(c) The relaxation time of the slowly relaxing component. $T2_{slow}$ has a range of values between 100 and 300 msecs. $T2_{slow}$ decreases with increasing temperatures.

(d) Water is most readily removed from the third fraction. As the water content of the sample is reduced from saturated values the population of the intermediate phase remains constant until a significant portion of the fast and slow phases have been lost. The intermediate fraction contributes approximately 60% of the total signal, and the slow component about 30%.

(e) As the temperature increases there is a slight increase in the population of the intermediate phase at the expense of both the fast and slow relaxing populations.

Similar results to those described above for the case of poplar were found in other species of wood removed from the Mary Rose such as ash and beech.

It is suggested here that the two or three component fits to the data are no more than convenient representations of a continuous distribution of relaxation times. The magnetisation decay curve is then expressed as;

$$M(t) = M(0)\int_0^\infty P(T_2).\exp(-t/T_2).dT_2 \qquad 6.7$$

for the relaxation in the transverse direction, and a similar expression exists for relaxation in the longitudinal direction. $P(T_1)$ and $P(T_2)$ represent the normalised distributions of relaxation times for T_1 and T_2. These two distributions need not be the same. However, for any particular relaxing spin within the system, $T_1 > T_2$, and the two distributions must be consistent with this fact. In figure 6.21 two hypothetical distributions are shown which might give rise to the two component fit that has been used to characterise the sample. The blocks drawn over the distribution represent the two and three component fits which best describe the distribution when discrete values of T_1 and T_2 are used.

Figure 6.21 Hypothetical distribution of relaxation times in wood leading to observation of two component decays.

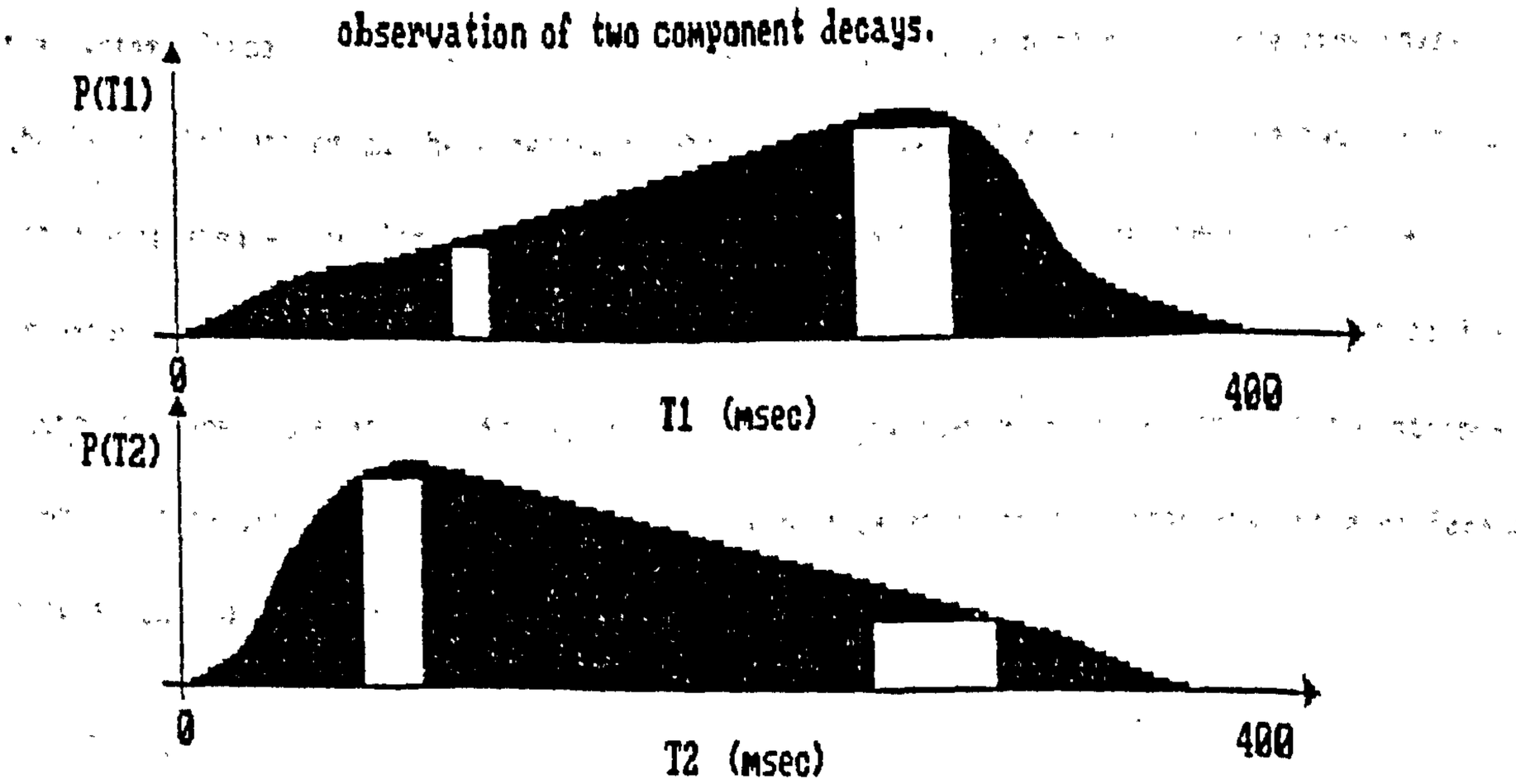

The distribution of T_1 and T_2 values is shown by the Brownstein and Tarr[23] model to be a consequence of the size of pores within the sample. Cohen and Mendelson[15] considered the relaxation of water in porous systems as being a combination of relaxation in the bulk and diffusion processes that carry the spins in the bulk to the surface of the pores in rocks, where they exchange with rapidly relaxing spins of the hydration layer. Within a pore of radius r, a uniform magnetisation is established across the pore in a time,

$$T = (r_2/6D)(S1/V). \qquad 6.8$$

where D is the self diffusion rate, S/V is the surface to volume ratio of the pores, and l is the thickness of the adsorbed layer. Below a certain critical size, which in porous rocks was taken to be $r < r_c = 6mm$, a single average relaxation $T_{...}$ time is observed

$$\text{i.e.} \quad (T_{...})^{-1} = \frac{(1 - S1/V)}{T_{....}} + \frac{(S1/V)}{T_{.....}} \qquad 6.9$$

and $T_{...}$ depends upon the surface to volume ratio of each particular pore.

The shape of the $P(T_1)$ and $P(T_2)$ distributions are determined by the distribution of pore sizes in the sample, and the relaxation times of the bound and free phases of water within the system. Since T1 need not equal T2 for the bound phase, or possibly for the free phase, the two distributions can be expected to differ, thus giving feasibility to the two distributions suggested above. The precise nature of $P(T_1)$ and $P(T_2)$ cannot be specified, but would be expected to vary from sample to sample, and within the same sample under different conditions of temperature and concentration. The possible existence of these continuous distributions as a result of different pore sizes is a more general approach than assigning different populations to specific cell types.

The fact that the T1 values were independent of temperature can be explained by the fact that although normally when one is in the region of motional narrowing the T1 would be expected to increase with temperature, the rate of relaxation is enhanced in porous substances by the increased rate at which diffusion processes feed the spins in the bulk to the region of the hydration layer.

The increase in the amplitude of the slowly relaxing T1 component in degraced samples can be explained in terms of a distribution of T_1 values in terms of an shift in the populations caused by either a more open and porous system, which undeniably exists within water-logged wood, or an increase in T_1 bound, and is most likely to be a combination of the two.

In spherical pores the ratio of S/V = 3/r. Using the data from freezing curve experiment, the bound water within the sample contributes to about 10% of the total. Therefore Sl/V = Sl/r ≈ 0.1. According to Brownstein's calculations[13] the thickness of the hydration layer, l in fresh timbers, is about 0.09μm, leading to an average pore radius r_{av} = 2.7μm, which is a factor of 5 down on the average cell width. If it is assumed that water within exist at all levels within the cell wall, and that all of this water is exchangeable with the water within cell lumens, then l ≈ 3μm, and r_{av} ≈ 90μm. Given that this analysis is based on a spherical pore, whereas in reality the cells in wood are tubular, this value seems a reasonable one for the pore size as seen by an average water molecule diffusing within the system. The T1 and T2 data is therefore consistent with a heavy presence of water residing in the voids within the cell walls that is in exchange with the large quantities of water in the cell lumens. Can the relaxation phenomena therefore reflect the nature of the wood cell wall?

The dehydration of fibrous muscle tissue leads to a denaturation of the protein structure that is reflected in the signal amplitude of the non-freezing water. After rehydration the ampiitude of the non-freezable component was seen to decrease with decreasing temperature, whereas prior to dehydration the amount of mobile water is constant below the freezing event.

In water-logged wood the dehydration-rehydration cycle produces no such effect in spite of the fact that the T2 values of the wood are greater in rehydrated samples than in samples that have never been dried, where the long T_2 is increased from the typical value of 210 msecs. to about 300 msecs. Evidence that some denaturation takes place may come from studies of the non-freezable component:

Below 273K the transverse relaxation of the non-freezing water is two component. 60% of the magnetisation decays with a relaxation time of about 4 msecs at 270K, and 40% with a relaxation time of 0.17 msecs. As the water content of the sample is reduced T2 of the fast relaxing component sucdenly increases to match the relaxation time of the other component. A single decay is therefore observable at moisture contents of less than about 2.5 g/g, which is the transition point at which the transverse decay changes from three to two components at temperatures above the freezing point. This event is indicative of a change in the morphology of the wood. Upon rehydration the fast relaxing component is again in evidence.

The two component nature of the non-freezable phase leads to the assumption that two types of bound water exist within the wood at higher water contents resulting in the appearance of the third relaxation time at ambient temperatures. If so then the two effects could give rise to the disappearance of the phase of bound water as the moisture content is reduced. The water may be lost from the system during drying, or its motional properties may be modified by changes in the structure of the wood leading to a transformation of phase. As the bound water in question has the fastest decay one can relate it to water that is most intimately associated with the constituents of the cell walls, and as such it is unlikely that it will be the easiest to remove.

If the water lost to the system it is probably because the regions within the cells that this water occupies are disturbed by the drying process. it could be for example that this water occupies the fissures between elementary fibrils, and that at higher moisture contents this water imparts a mobility to the fibrils which is lost upon drying due to the formation of hydrogen bonded bridges of water molecules between the fibrils.

A more plausible explanation is perhaps that the rapidly decaying signal originates from an extremely mobile fraction of protons attached to the xylem itself. If this were the case, then the disappearance as the water content is lowered and the structure becomes more and more rigid is predictable. However this is not reflected in the amplitude of the frozen component which would be expected to decrease by about 40% at the transition. The nature of this second component, and its possible connection with the appearance of a third component at high water contents above the freezing point remain undetermined.

From the studies of single and multi-component relaxation data presented above it is concluded that water in the hydration layer dominates the character of the magnetisation decay. Single component data indicates that the fibre saturation point of highly degraded samples is equivalent to the value found in solutions of celluloses, but in less degraded samples this value is increased to about 0.40 g/g, which is the same as is observed in fresh timbers.

The decays in both the transverse and longitudinal directions are non-exponential. They are consistent with theories of molecular exchange between water in a bound phase and water in an unbound phase. Some contribution to the relaxation may also result from chemical exchange between protons in the water and protons attached to the xylem. The bound and unbound phases cannot be resolved, indicating that the exchange between the two fractions is rapid. Direct evidence of exchange processes comes from studies of relaxation behaviour as a function of temperature.

The different components of the magnetisation decay cannot be related to water in different compartments within the system. The two and three component fits are more likely to result from a distribution of pore sizes that in turn lead to a continuous distribution of relaxation times. The bound phase occupies the voids in the wood cell wall caused by the hydrolysis of the xylem, and is far less mobile than the water in the cell lumens. The nature of the distributions for transverse and longitudinal decays have not been established.

Dehydration of the sample is reversible provided that it is not advanced. In cases where the bound water has been left in tact there is evidence of a reversible transition in the morphology of the cell wall material caused by variation of the total water content of the wood. Further investigation is necessary to qualify the origin of this transition.

6.3. NMR studies on Water-logged Wood impregnated with Polyethylene-Glycol Solutions.

The preservation of water-logged wood by impregnation with polyethylene-glycol (PEG) solutions relies on the ability of the polymer to impregnate the system and prevent the cell wall collapse by bulking voids within the structure of the wood. Different degrees of degradation require that different grades of polymer be used in order to infiltrate and support different regions within the wood.

NMR relaxation measurements were carried out on a number of samples of water-logged wood that were impregnated using a variety of water-polymer mixtures to establish whether the water and polymer could be resolved from the transverse decay curves, and if so what deductions could be made about the behaviour of the two molecular species once resident in the wood. Different grades of PEG have been used to determine if possible the different types of

behaviour provoked within the wood by their presence on the molecular dynamics of the water in the system, and to establish if possible, how the dehydration of PEG impregnated samples differs from untreated water-logged wood.

As an aid to the interpretation of results preliminary experiments were carried out on the PEG/water system, to establish typical relaxation rates for polymer and water mixtures. The rates of relaxation for the water and polymer molecules are discussed in terms of the relaxation mechanisms described by Ullman and Liu[1981].

6.3.1. The Polyethylene-glycol/Water System.

Measurements were carried out on samples of PEG to determine the effect on the spin-spin and spin-lattice relaxation times of varying molecular weight, concentration and temperature. As expected the decay of the magnetisation in both the transverse and the longitudinal directions is multi-exponential. Two time constants are required to describe the shape of the curve: one of which may be associated with the relaxation of protons in the water, and one the relaxing protons in molecules of PEG.

The temperature dependence of the spin-lattice and spin-spin relaxation times for both the fast and slowly relaxing components in 50% solutions are illustrated in figures 6.22a-f. In general, the more mobile a population of protons is the longer the relaxation time becomes provided that the correlation times are in the region of motional narrowing, i.e. $\tau_c < \omega_o^{-1}$, when many of the local fields experienced by static or slow moving molecules are averaged to zero in fast moving populations. Thus the long relaxation times have been assigned to the water protons and the short relaxation time to the less mobile PEG protons. This is supported

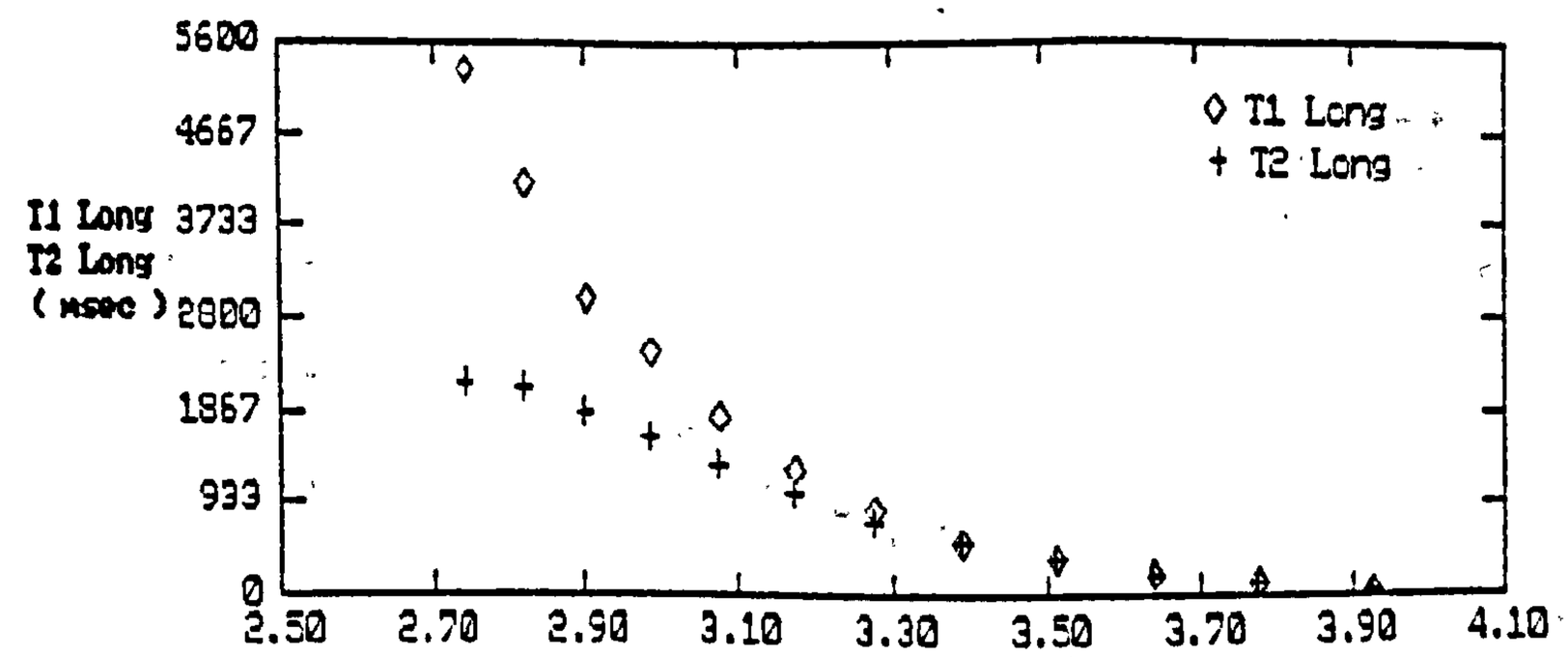

Figure 6.22a Spin-spin against Spin-lattice relaxation times as a function of temperature in 50 % solution of PEG 1540.

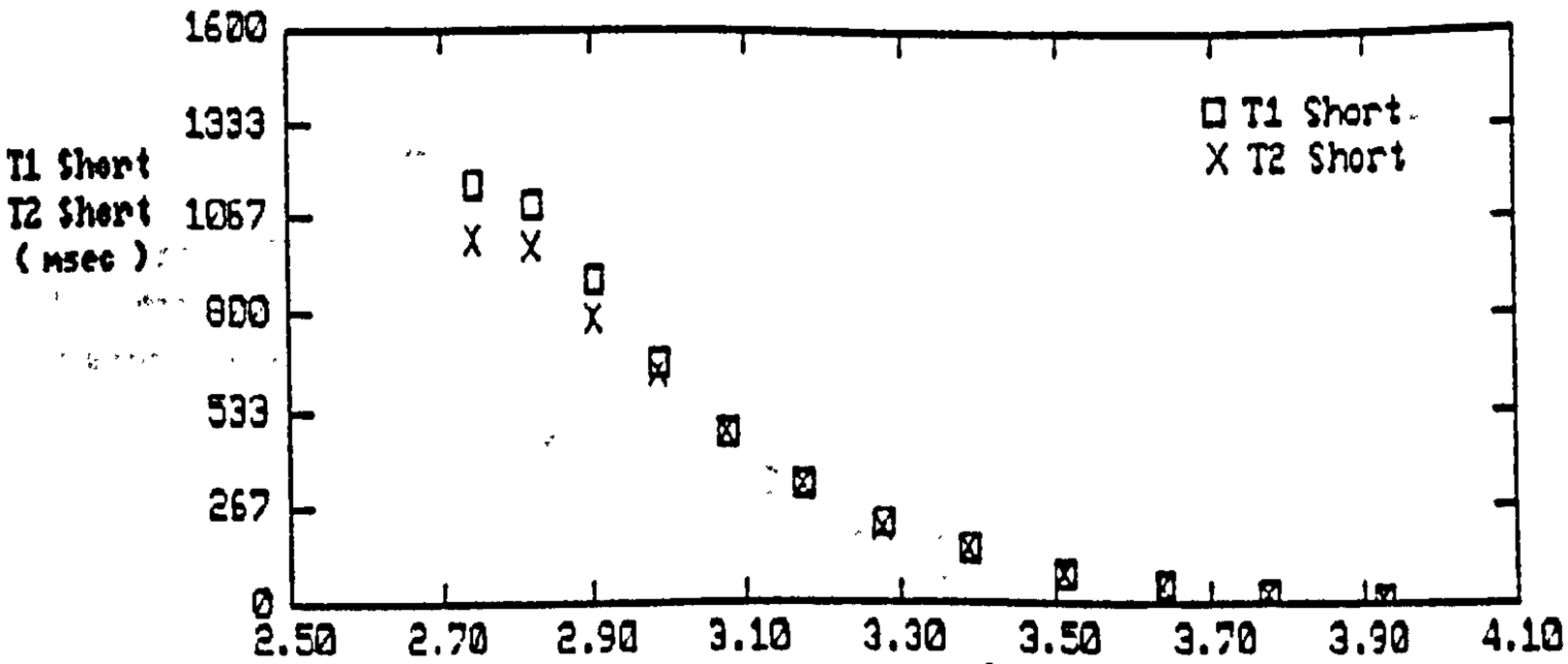

Figure 6.22b Spin-spin against spin-lattice relaxation times as a function of temperature in 50 % solution of PEG 1540.

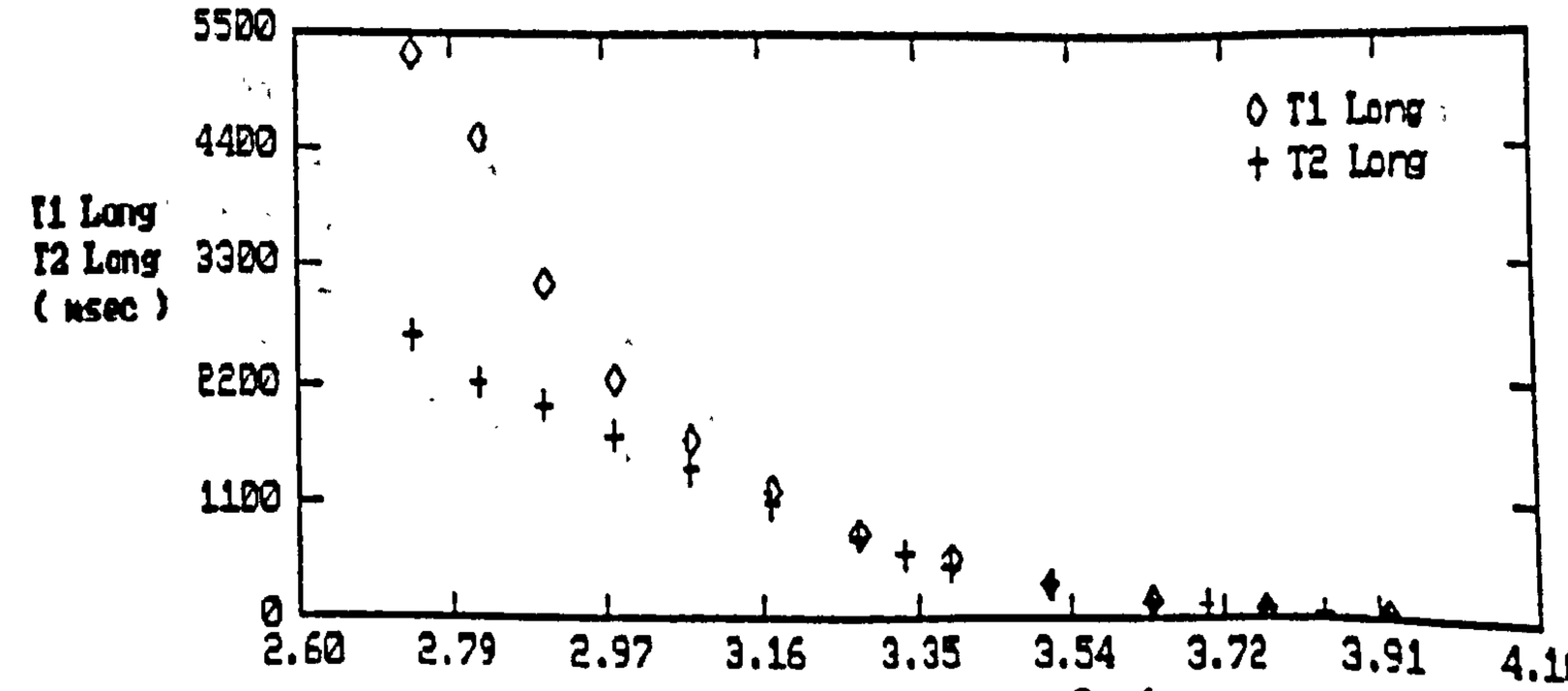

Figure 6.22c Spin-spin against Spin-lattice relaxation times as a function of temperature in 30 % solution of PEG 4000.

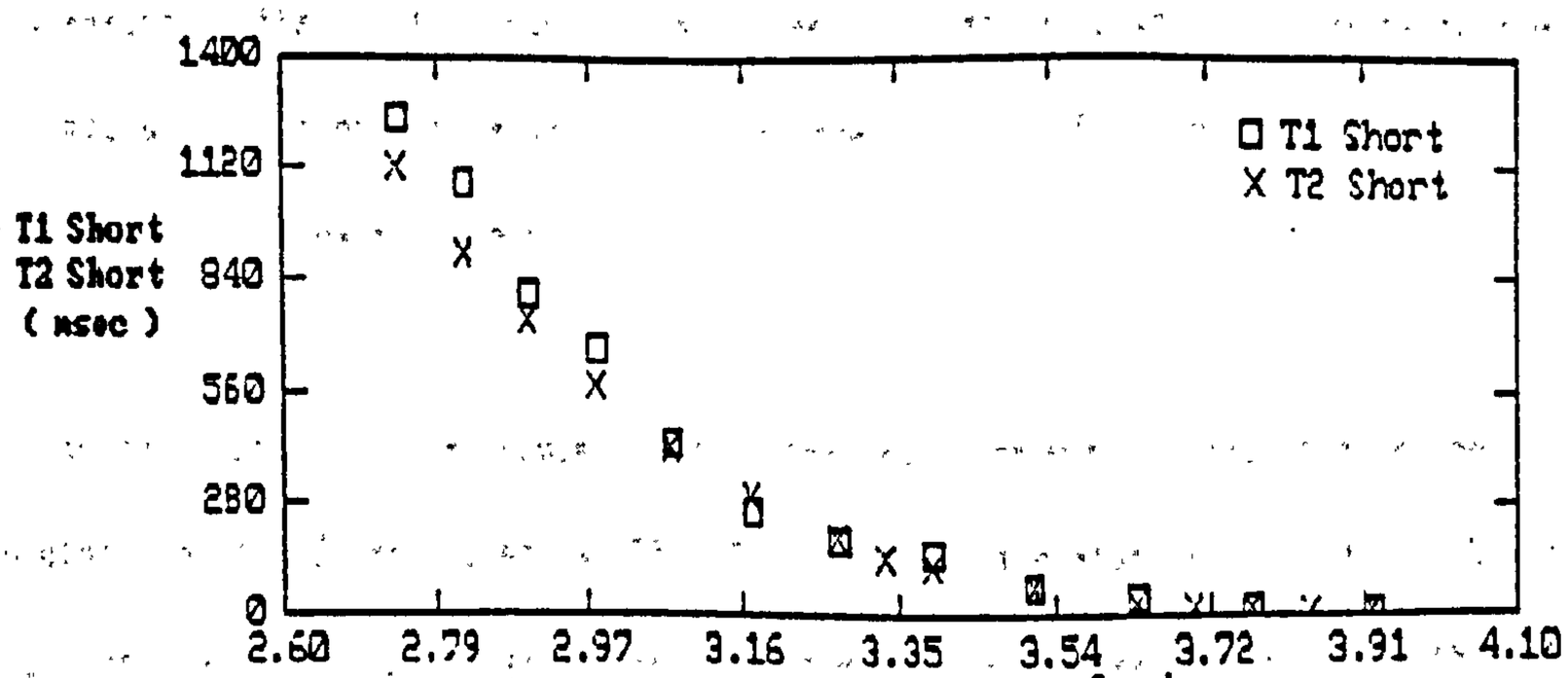

Figure 6.22d Spin-spin against spin-lattice relaxation times as a function of temperature in 50 % solution of PEG 4000.

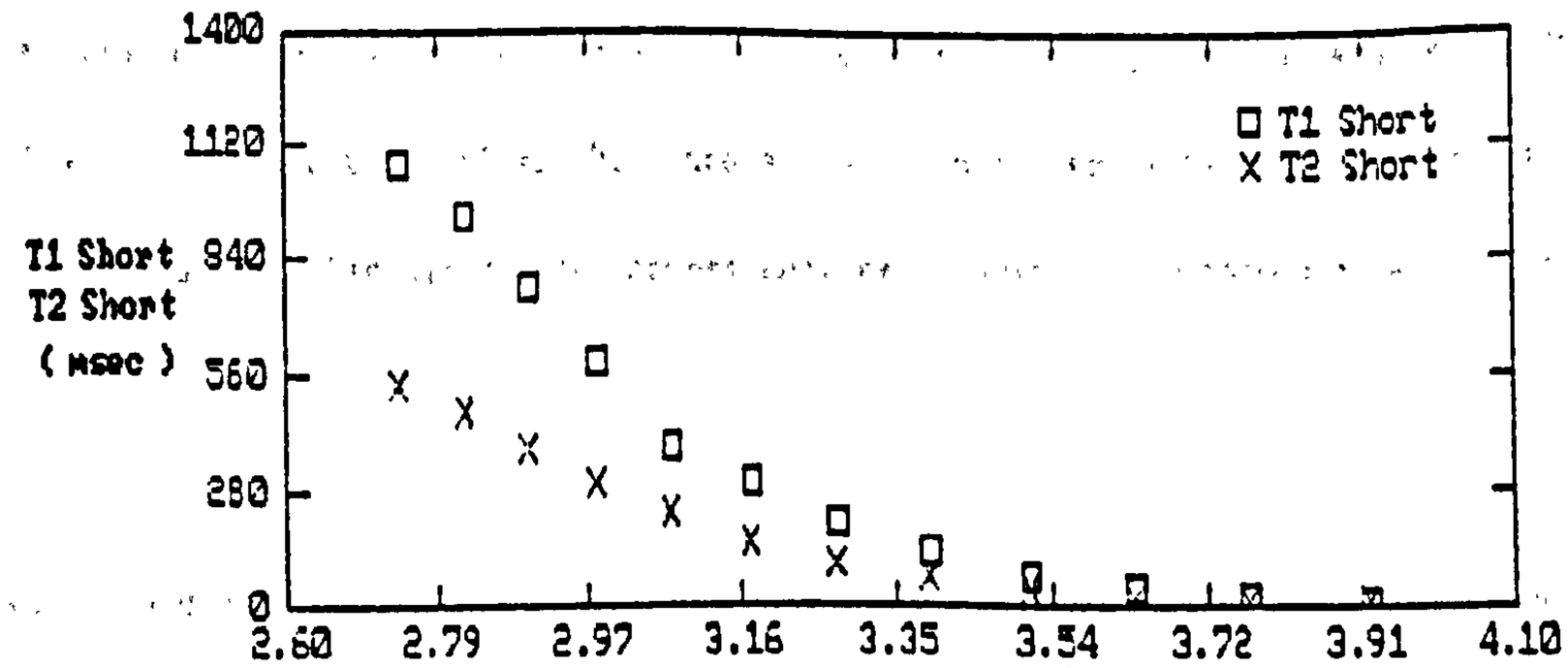

Figure 6.22e Spin-spin against Spin-lattice relaxation times as a function of temperature in 50 % solution of PEG 20,000.

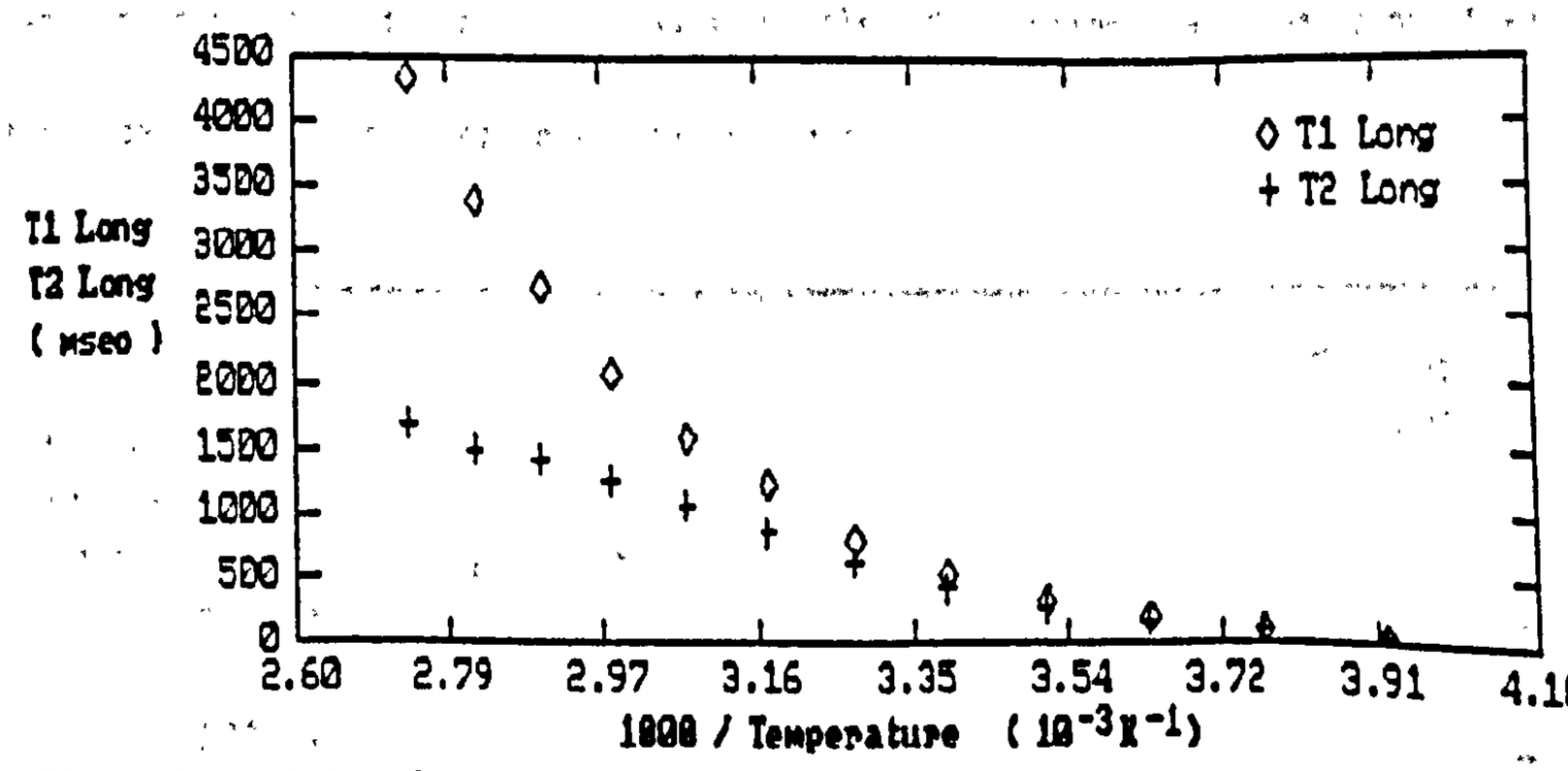

Figure 6.22f Spin-spin against spin-lattice relaxation times as a function of temperature in 50 % solution of PEG 20,000.

by the measurement of the relative amplitudes of the two components which are close to the calculated values. The temperature was varied between 270K and 360K, and the results are characterised by the following points;

(i) Using solutions of low molecular weights the short component attributed to the protons in the PEG molecules has T1 = T2 over the temperature range studied. Using PEGs of high molecular weight T2 is less than T1, suggesting possibly that the molecular motion of the larger PEG molecules is restricted and that viscosity effects play a role in the determination of the relaxation times.

(ii) The long component which is attributed to the protons in the water molecules has T1 = T2 at low temperatures but as the temperature is increased T1 becomes progressively longer than T2. This difference becomes more pronounced as the molecular weight is increased.

Figures 6.23a-d show the relaxation data for the 25% solutions of PEG with two different molecular weights. As with the 50% solutions the low molecular weight solutions have T1 = T2 for the short relaxing components, and T1 greater than T2 for higher molecular weights. The water relaxation shows similar trends as those for the 50% solutions, but the point at which T1 deviates from T2 occurs at much lower temperatures.

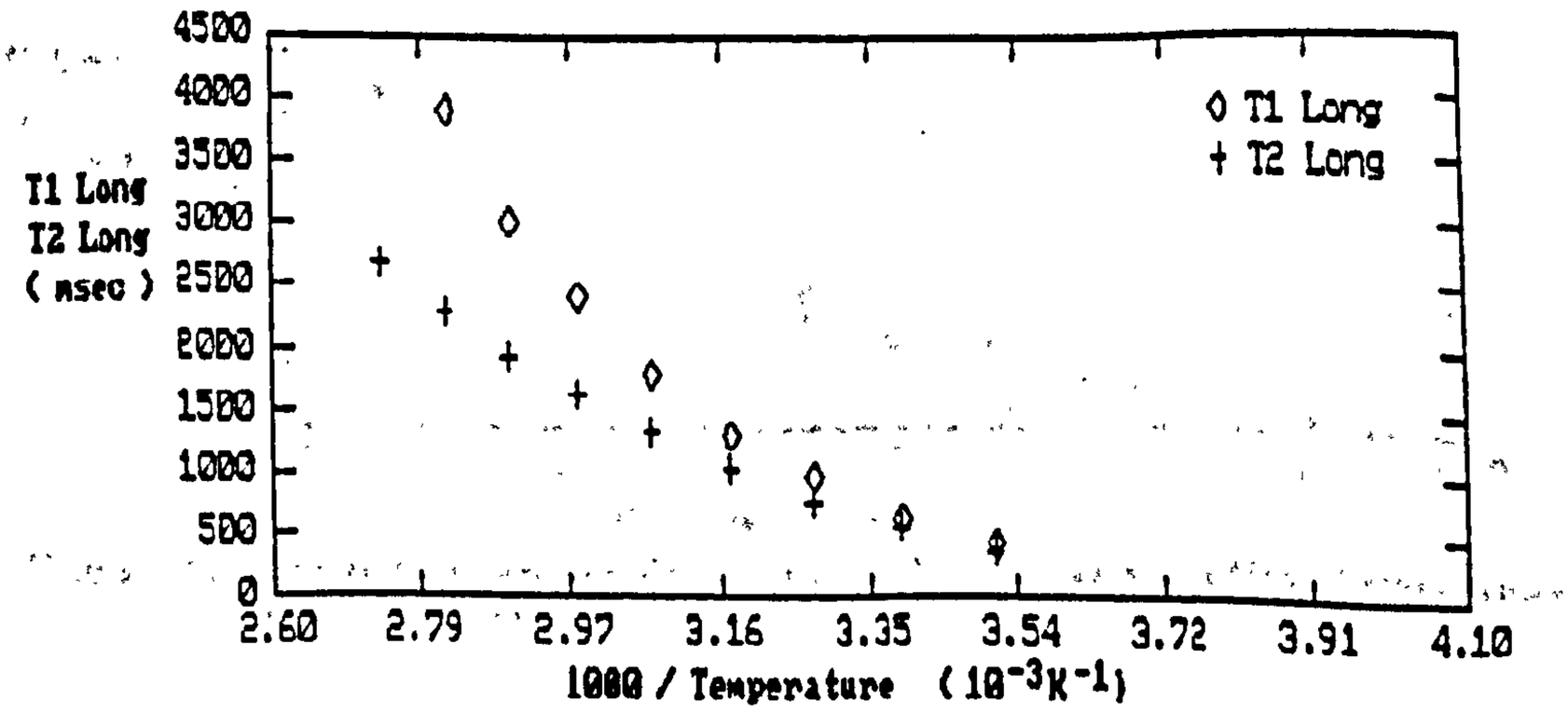

Figure 6.23a Spin-spin against Spin-lattice relaxation times as a function of temperature in 25 % solution of PEG 20,000.

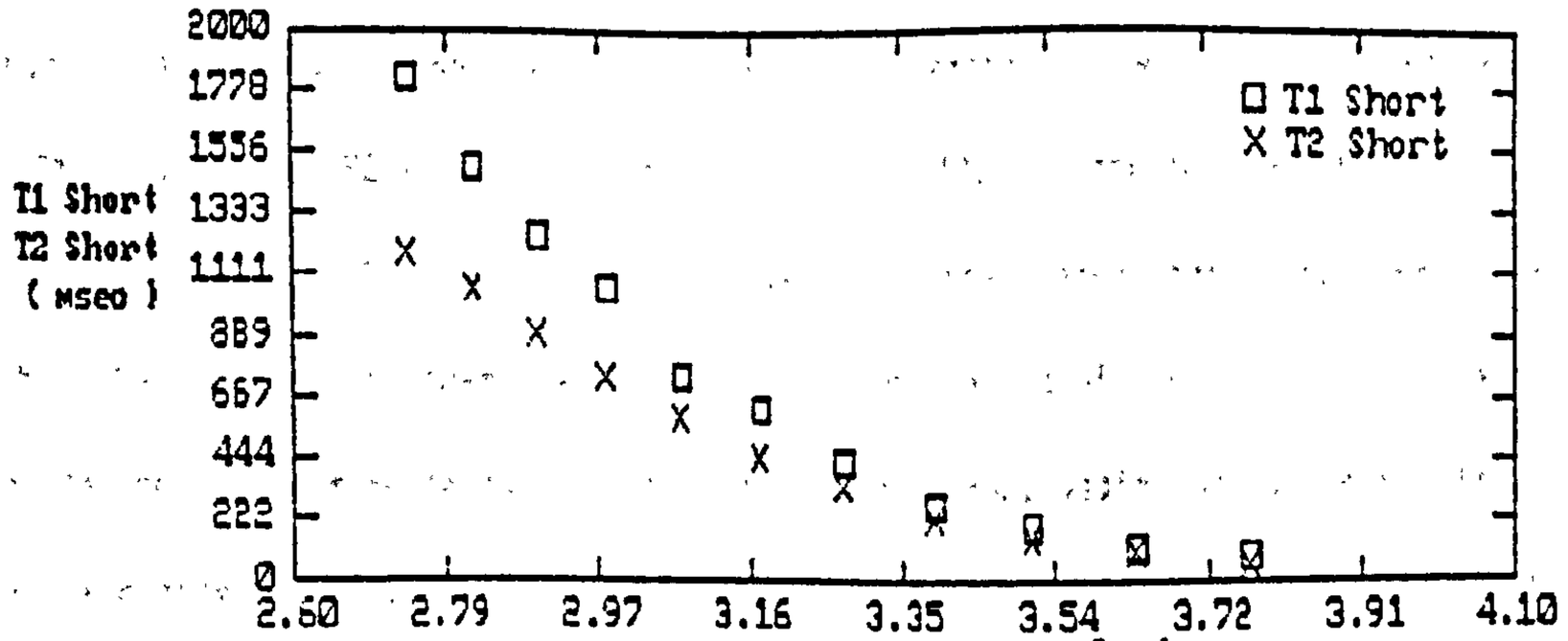

Figure 6.23b Spin-spin against Spin-lattice relaxation times as a function of temperature in 25 % solution of PEG 20,000.

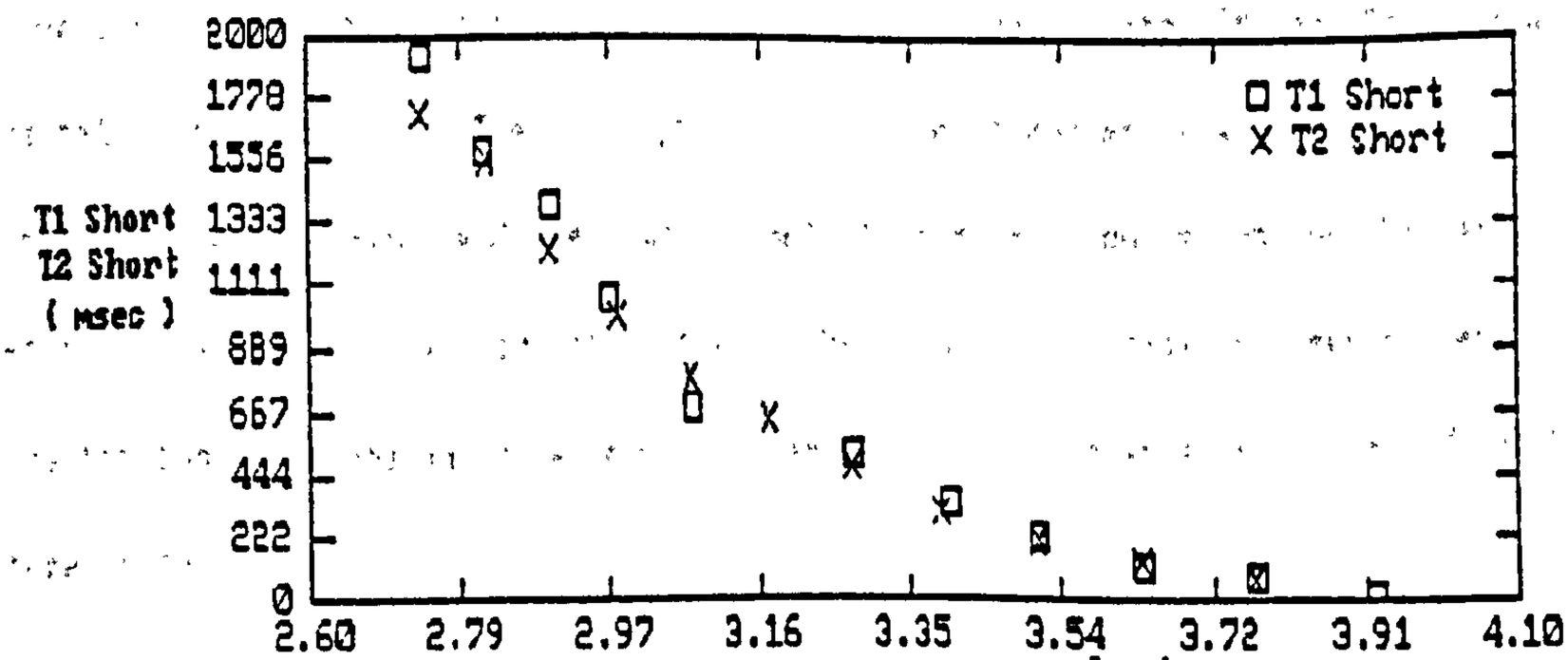

Figure 6.23c Spin-spin against spin-lattice relaxaton times as a function of temperature in 25 % solution of PEG 1000.

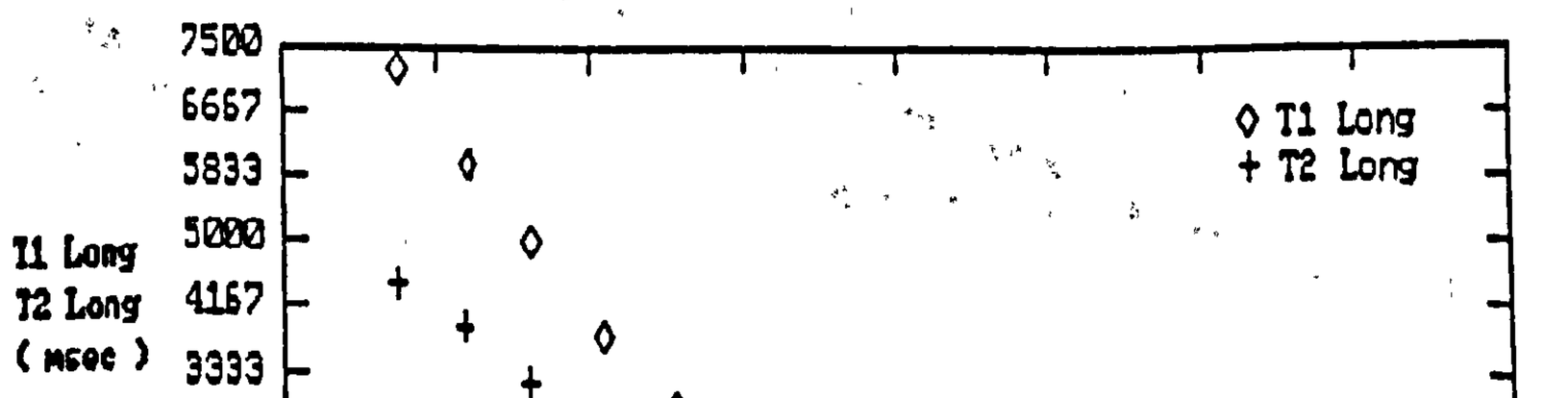

Figure 6.23d Spin-spin against Spin-lattice relaxation times as a function of temperature in 25 % solution of PEG 1000.

The graph in figure 6.24 compares the longitudinal relaxation times of PEG in 25% solution and 50% solutions of PEGs of different molecular weights. It can be seen that the solutions containing only 25% PEG have relaxation times which are longer than those containing 50% PEG, but these times are independent of the molecular weight of the PEG used. The concentration dependence is more pronounced at lower temperatures, again indicating the influence of viscosity effects. The transverse relaxation times of the PEG protons in solution are illustrated in figure 6.25. Again there is a concentration dependence which is stronger at low temperatures, but the relaxation times are also influenced by the molecular weight of the polymer used. The relaxation times of the protons in water for the 25% and 50% solutions are illustrated in figure 6.26. The spin-lattice relaxation times are again independent of the PEG molecular weight used, and are lower in solutions of high concentration. The effects of concentration are greater at low temperatures. The spin-spin relaxation times decrease in high concentration solutions and show some dependence on molecular weights of the PEG as the temperature is raised.

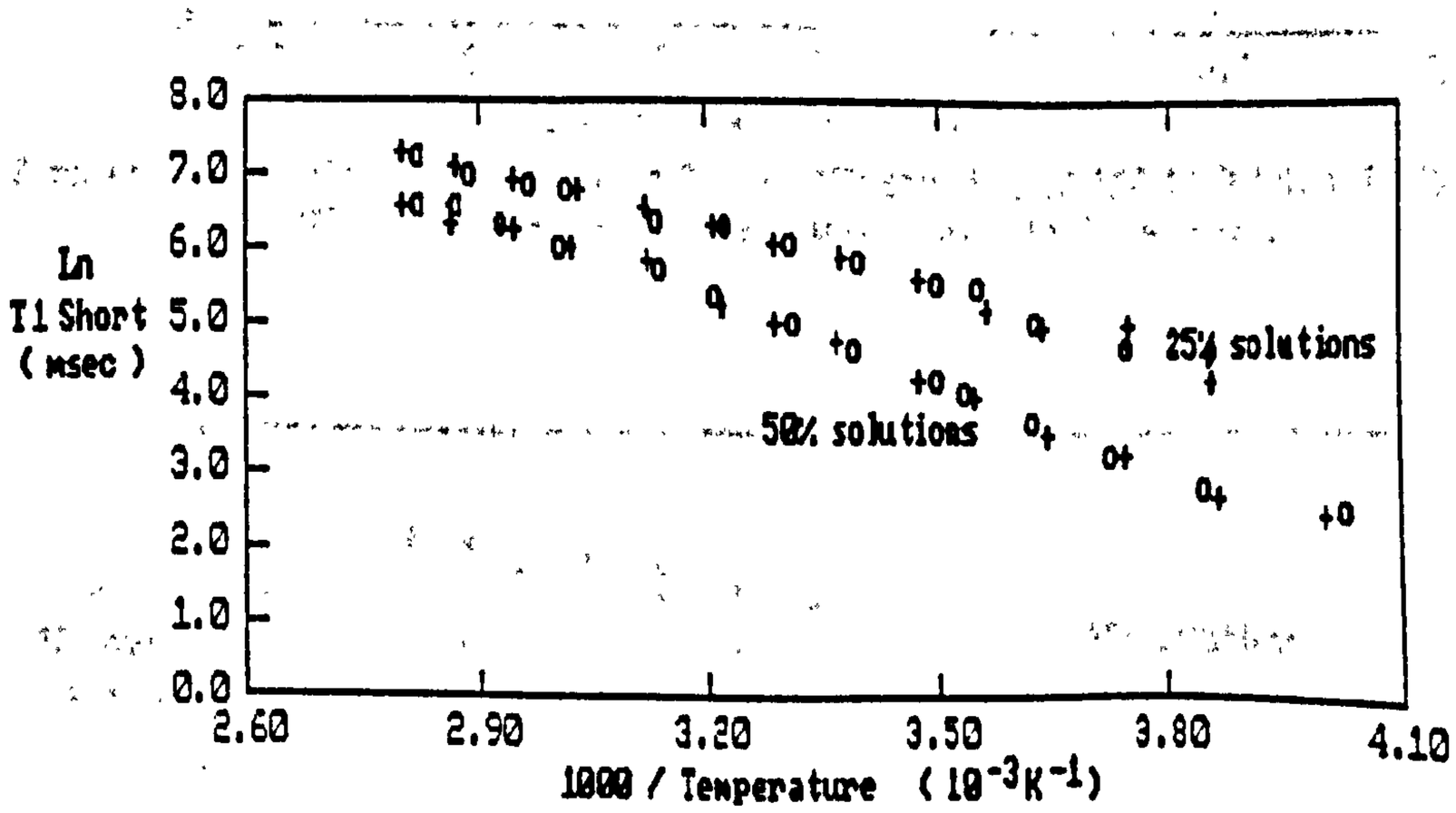

Figure 24. Spin-spin relaxation of 25% and 50% solutions of PEG 1000 (o), and PEG 20000(+), as a function of inverse temperature. Short (PEG) component.

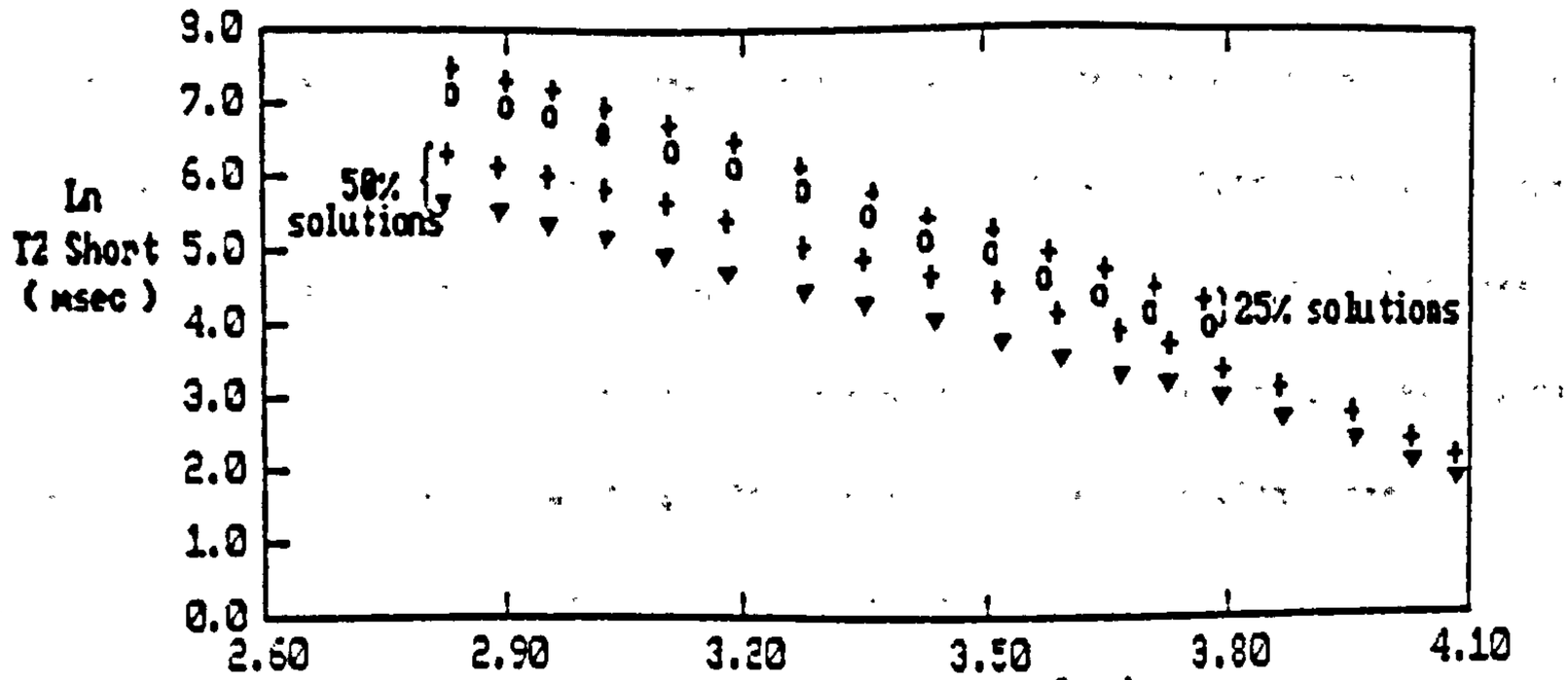

Figure 25. Spin-spin relaxation of 25% and 50% solutions of PEG 1000 (+), 4000 (o), and 20,000 (v), as a function of inverse temperature. Short (PEG) component

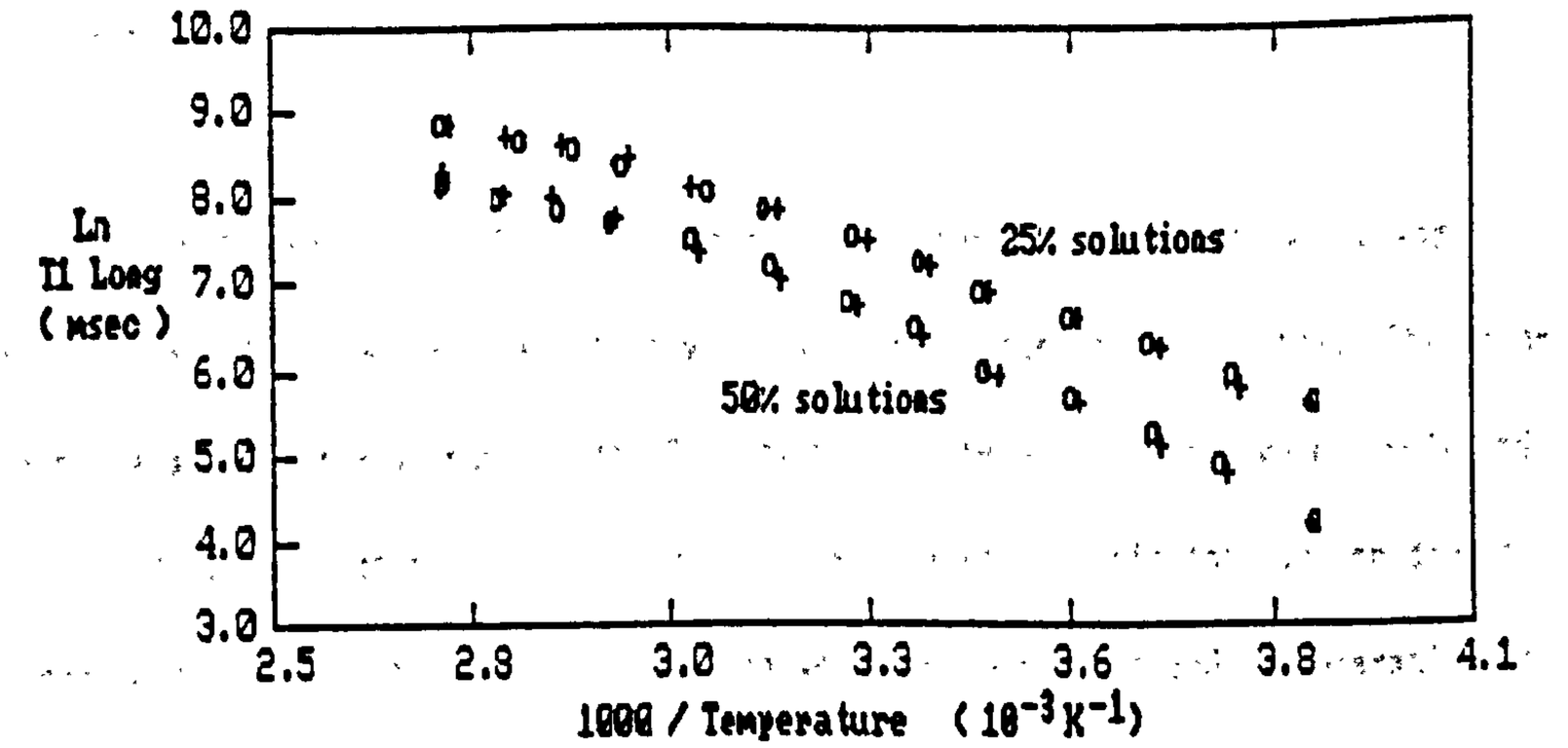

Figure 6.26a Spin-lattice relaxation in 25% and 50% solutions of PEG 1000 (o), and PEG 20,000 (+) as a function of temperature. Long (H_2O) component.

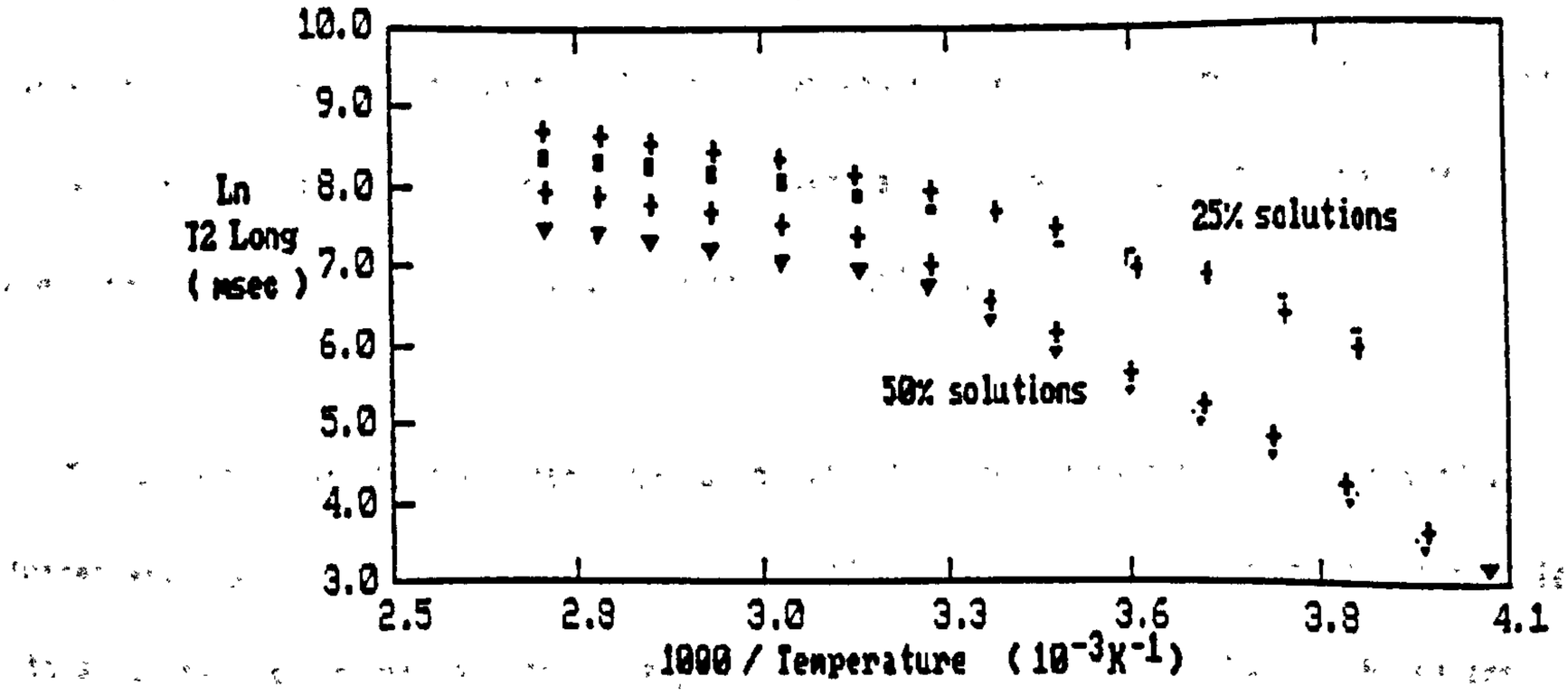

Figure 6.26b Spin-spin relaxation in 25% and 50% solutins of PEG 1000 (+), 4000 (•), and 20,000 (v) as a function of temperature. Long (H_2O) component.

Finally, the graphs in figure 6.27 show the effect of varying the concentration of PEG in solutions at a temperature of 300K. Both T1 and T2 of PEG decrease with increasing concentration, and within experimental error the influence of the molecular weight on the PEG relaxation times is slight. As the concentration is reduced the spin-lattice relaxation time begins to exceed the spin-spin relaxation time. T1 and T2 of the solute decrease with increasing concentration and are independent of the molecular weight of the PEG.

The spin-lattice relaxation times were dependent upon the resonant frequency used. As the frequency increased T1 became longer. This behaviour suggests the presence of a distribution of correlation times describing the motion of protons along the polymer chain.

Measurements of T1 and T2 for PEGs in dilute aqueous solutions were made by Liu and Ullman[116]. The results above are consistent with their measurements and findings. The principle mode of relaxation for protons in the PEG chains is a result of the dipole-dipole and spin rotation interaction between hydrogen nuclei. The strength of this interaction depends upon the inverse sixth power of of the distance between the spin pairs and so relaxation in the polymer is dominated by interactions between near neighbours. Liu and Ullman considered that the effects of the hydrogen nuclei other than those attached to the same monomeric unit could be neglected. The effect of the solvent on the relaxation times was determined experimentally by Heatley and Walton[117] using deuterated samples. They concluded that proton relaxation times are effected very little by deuteration of either solvent or polymer, and are therefore determined by intra-molecular interactions.

The structure of these monomeric units is determined by the repulsive and attractive forces associated with the molecular steriochemistry and is similar in the melt and soluble state to that in the crystalline state proposed by Tadokoro et al[118]. The C-H bonds are

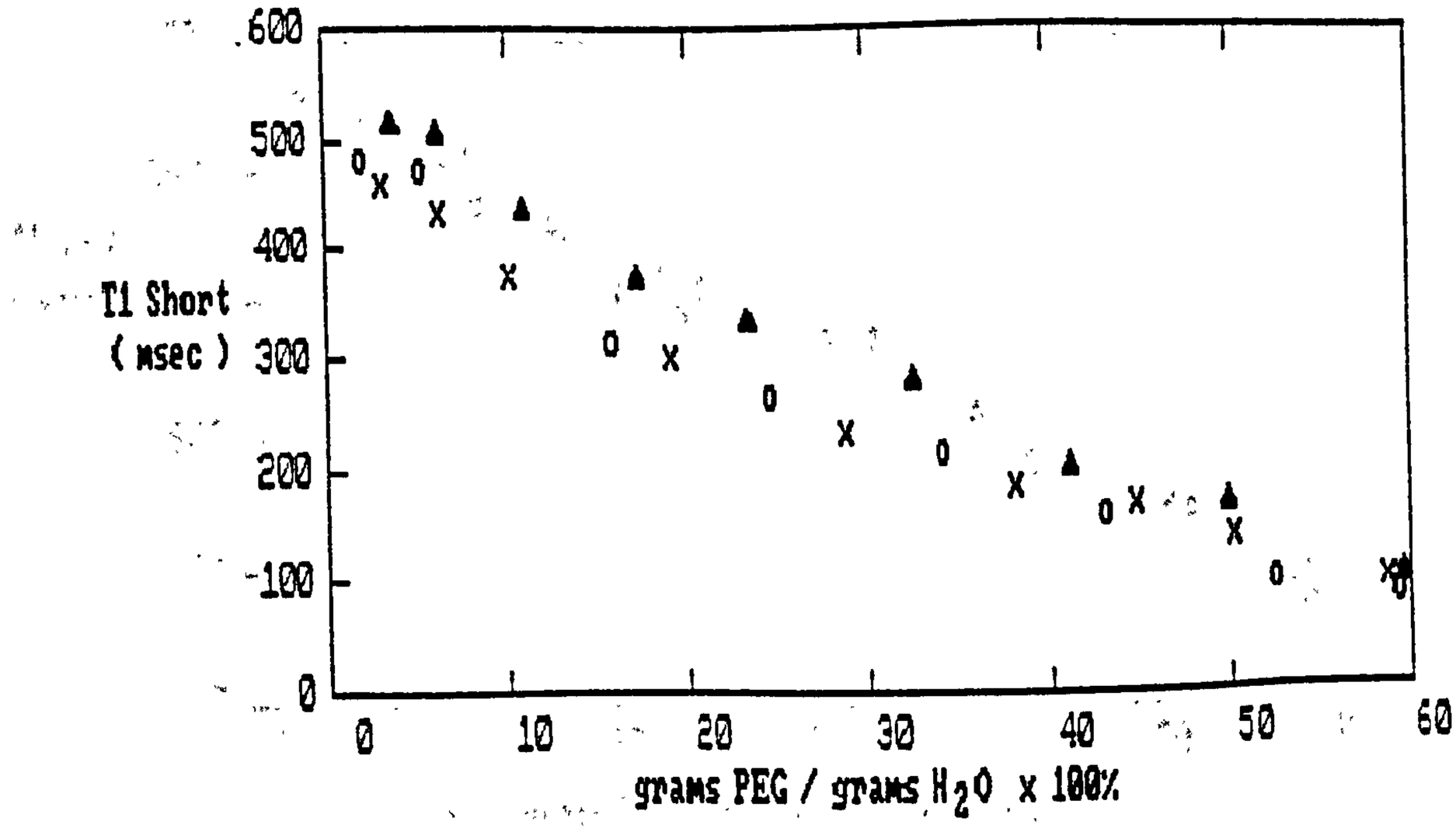

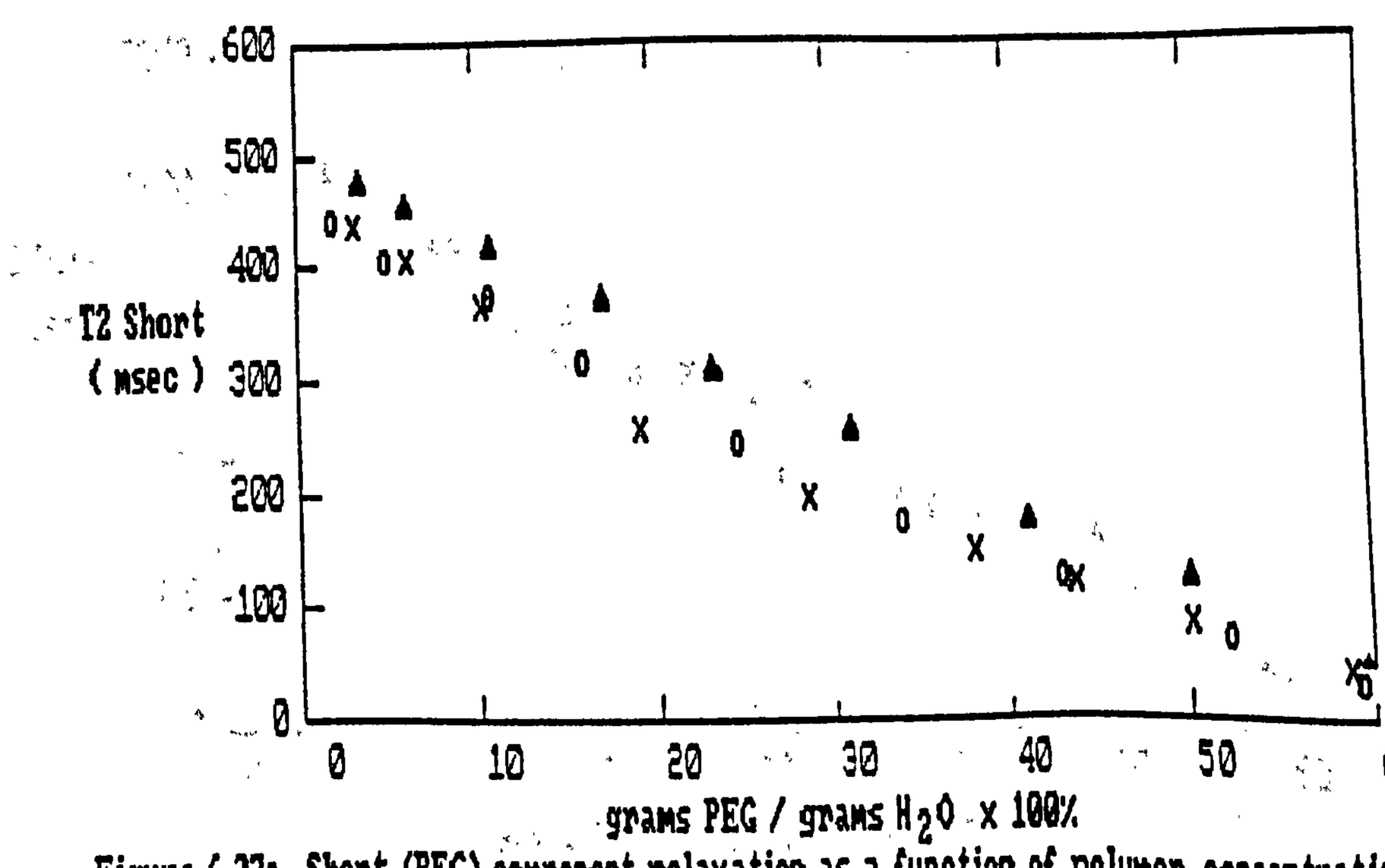

Figure 6.27a Short (PEG) component relaxation as a function of polymer concentration in solutions of PEG 1000 (▲), 4000 (o) and 20,000 (x).

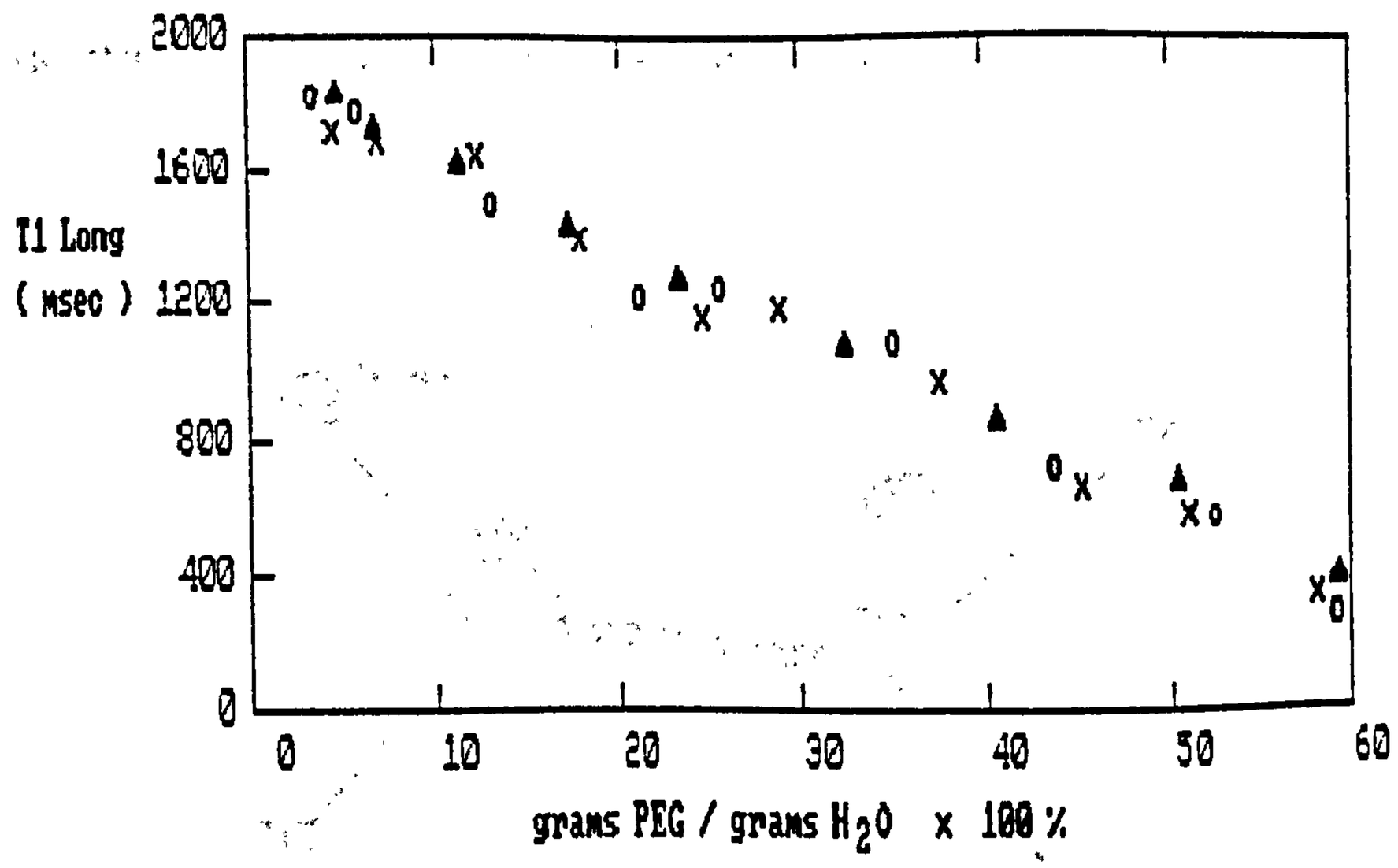

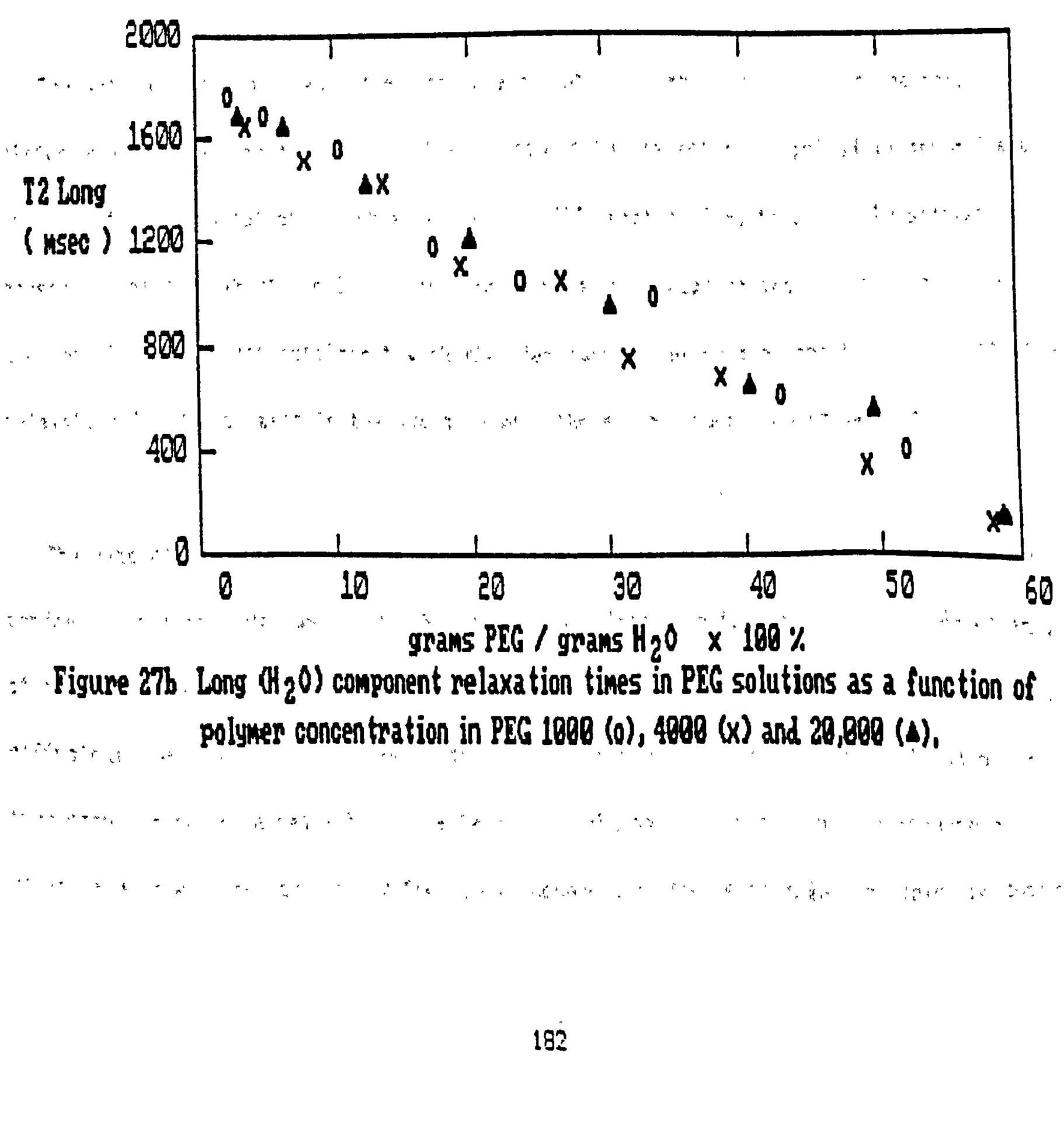

Figure 27b. Long (H_2O) component relaxation times in PEG solutions as a function of polymer concentration in PEG 1000 (o), 4000 (x) and 20,000 (▲).

tetrahedral and approximately 1.10 Angstroms in length. Each monomeric unit can adopt one of three conformations; trans, gauche, and gauche', which describe the position of the two oxygen atoms in the O-C-C-O unit. These are illustrated below;

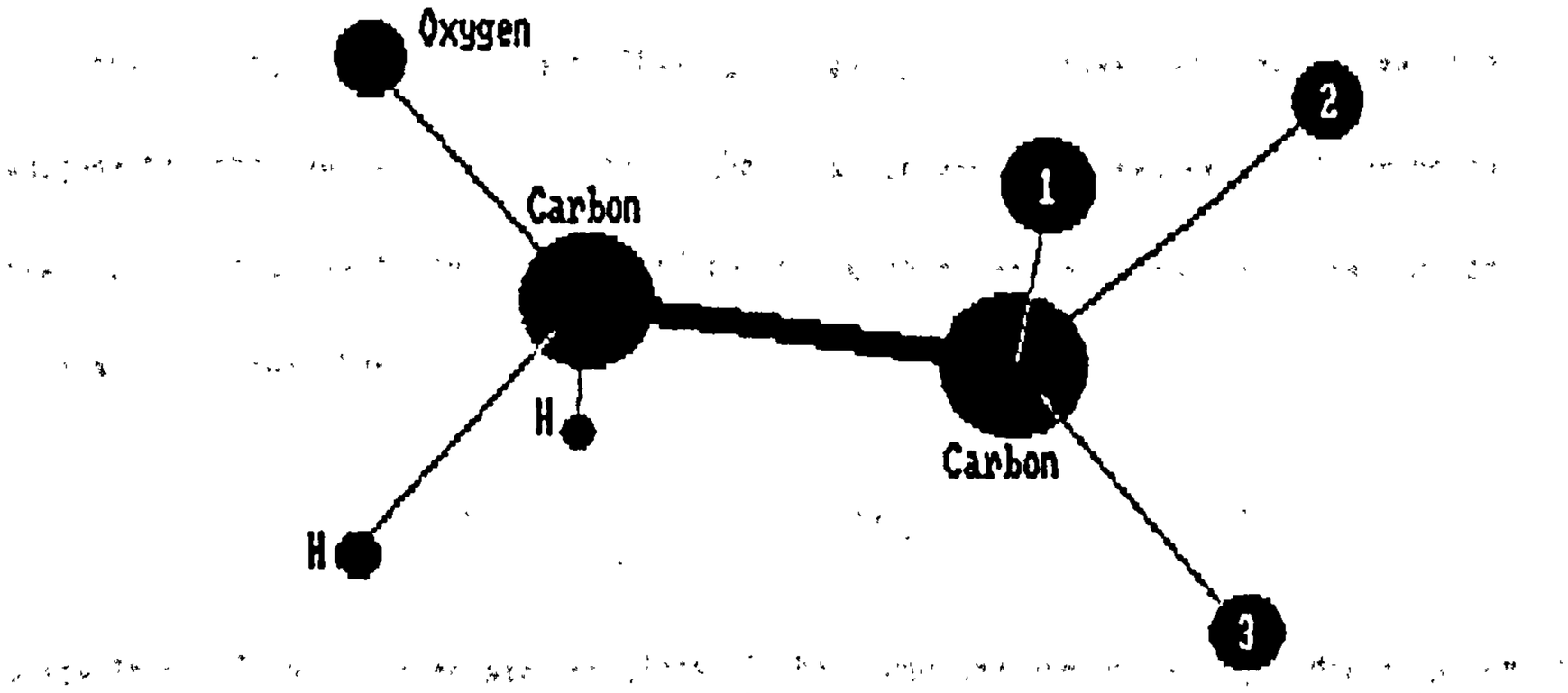

Figure 6.28 Relative positions of oxygen atoms in O-C-C-O bond in gauche (1), gauche' (2), and trans (3) conformations.

The motion of the hydrogen atoms can take one of two forms. The first is the rotational diffusion of the entire monomeric unit with respect to the external applied magnetic field. The second involves rotameric jumps between the different conformations of the monomer unit caused by rotation about the C-C bonds. The results of relaxation measurements performed by Liu and Ullman[116] were consistent with the idea that the principle contribution to the spin relaxation in the polymers is the jumps between the gauche-gauche' conformations.

The rate at which the structure of monomeric units transform is considered to be independent of the molecular weight of the polymer, and independent, albeit to a lesser extent, of the concentration of the solution, as the effects are not long range. On the other hand, diffusional rotation of the monomeric segments depends heavily on the amount of chain entanglement which increases with both molecular weight and concentration. The spin-spin relaxation is effected by the low frequency component of the local magnetic field and depends

to a greater degree on the diffusional rotation of the monomers than the spin-lattice relaxation time. This leads to the increased rate of transverse relaxation at higher molecular weights and concentrations.

The relaxation times of the water in PEG/water systems are depressed from those observed in distilled water. At low temperatures they are independent of molecular weight but vary with the concentration of polymer. They can be explained in terms of a two phase model whereby the observed relaxation time is the usual weighted average of bound and unbound phases. If h represents the fraction of polymer within the solution, and K is the co-ordination number then;

$$\frac{1}{T} = \frac{Kh}{Tb} + \frac{(1-Kh)}{Tu} \qquad 6.10$$

where Tb and Tu are the relaxation times of the bound and unbound phases. Manipulation of this equation leads to[116]

$$\frac{1}{Tb_i} = C_i + \frac{M_i}{K} \qquad 6.11$$

Where the subscript i = 1or2, and relates to the spin-lattice and spin-spin relaxation. Using the data of figure 6.27, M_1 = 3.57, C_1 = 0.305, M_2 = 3.25, and C_2 = 0.463. There is evidence from a number of sources that two water molecules associate with each monomeric unit in the polymer. In the measurements made in this work it would appear that equation 6.11 is no longer valid for polymer concentrations greater than 1 g/ml. This corresponds to a monomer to water molecule ratio of about 1:2. Setting K = 2 therefore, Tb_1 = 478 msecs, Tb_2 = 478 msecs. This rather surprising result indicates that $T1_b$ = $T2_b$ for the bound phase using polymer concentrations of less than 1g/ml.

The weakness of this approach is that the constants C_i equate to Tu_i; the relaxation times of the unbound phase. This leads to values of Tu_1 = 3.28 secs and Tu_2 = 2.16 secs, which are equivelent within experimental error to the relaxation times of distilled water at

the same temperature. Moreover, one would have expected to see a difference in the two relaxation times of the water in the bound phase because of a decrease in the mobility of the bound phase, and because of an increase in spin diffusion between the polymer and water molecules. The fact that this change is not observed may be a reflection of the mobility of the polymer itself, or it may indicate the weakness of the polymer-water interaction.

The deviation of T2 from T1 for water at higher temperatures remains unexplained. Raising the temperature is expected to enhance the mobility of the water and polymer molecules, thereby increasing the liquid nature of the solutions. This should lead to similar T1 and T2 values. Although the exchange of nuclei between the polymer and water molecules may lead to the low T2 values it does not explain the fact that the separation of T1 and T2 takes place at lower temperatures in lower concentrations. It is thought that the difference in T1 and T2 of the water content is the result of oxygen contamination of the samples, which were not vacuum sealed after preparation.

6.3.2 A Pulsed NMR Study of Water-logged Wood Impregnated with Polyethylene-Glycol Solutions.

The spin lattice relaxation times observed in degraded and water-logged wood indicate that a large proportion of water resides within a bound layer of water that most probably occupies voids created in the cell walls of the wood. A combination of diffusion and exchange processes give rise to relaxation times in these samples that are determined by the distribution of cell and pore sizes within the sample, with larger pores giving rise to longer relaxation times. The uptake of large PEG molecules impregnating this system may preferentially occupy the large pores, or they may get trapped within the smaller voids in the wood, thereby filling these gaps and displacing the water which would otherwise occupy them. These effects could be expected to change the relaxation behaviour of water within the wood by dis-

turbing the initial distribution of water at different sites within the samples, and by the direct influence on the dynamic properties of water molecules by the macromolecules. T_2 behaviour in samples of water-logged wood have therefore been monitored as a function of the uptake of PEG, to establish whether they reflect the modified dynamic behaviour of the water in the wood, or the redistribution of polymer within the sample.

Several sections of water-logged poplar were cut from a block of moderately well preserved wood (initial water content 5.7 g/g) and soaked in solutions of polyethylene-glycol having a variety of molecular weights and concentrations. The effects on the spin-spin magnetisation characteristics of the initial uptake of PEG 3400 was monitored over a period of twenty days using solutions with concentrations between 5 and 50%. In freshly cut samples the transverse decay was at least two component, with 70% of the signal relaxing with a characteristic time of 49.8 msecs, and the remainder with a time of 170 ± 20 msecs.

The transverse decay of the poplar saturated in 5%-20% solution was resolved into two components. The relative populations of the fast and slow relaxing component were constant over the twenty day period, whilst the relaxation time of the slowly relaxing component increased to a value of 240 ± 18 msecs, T2 of the fast relaxing component stayed relatively constant at 51 ± 4 msecs.

One would not expect a polymer of this size to have penetrated the cell walls. The polymer initially permeates the most accessible regions of the wood which are the vessels, the cell lumen and middle lamella. One can therefore conclude that if the two component fit is correct at least a proportion of the nuclei contributing to the slowly relaxing component reside in one or more of these accessible regions. The slight increase in the spin-spin relaxation time of the slowly relaxing component may be explained if one assumes that the relaxation rate of this component is greater than that observed for protons in distilled water because of its interactions with water bound to the wood. These interactions reduce the

average Brownian mobility of the unbound water molecules and the relaxation rates may be further enhanced by paramagnetic centres present in the cell walls of the wood. The PEG molecules within the samples would be expected to reside close to the cell walls occupying hydrogen bonding sites in preference to the water molecules so blocking these exchange interactions, and leading to a greater value of T2.

The constant value of approximately 50 msecs for $T_{2_{max}}$ may indicate that there are regions within the wood that have not been penetrated by the polymer. Molecules of PEG 3400 are relatively large, and to test whether any areas of the wood where large bodies of water could accumulate were inaccessible to the polymer, freezing curves were produced for the impregnated samples. In normal PEG/water solutions the water freezing point is depressed by the PEG molecules. Typically the water turns to ice at temperatures of between 235 to 245K in concentrated PEG solutions. As the concentration of the solution is lowered the freezing event becomes smeared over a wider temperature range so that there is a steady decline in the signal amplitude with temperature.

Two samples of poplar were soaked for eighteen months in 40% PEG with degrees of polymerisation of 1500 and 4000. In both cases the signal amplitudes show no sign of attenuation even at temperatures as low as 230K. This suggests that the molecules of PEG have permeated all regions occupied by water that is freezable in normal water-logged wood, even using the relatively large PEG 4000 molecules. However it does not exclude the possibility that regions exist that are inaccessible to PEG where non-freezable water exists.

In samples that were soaked in solutions of 50% PEG 3400 the transverse relaxation times are reduced to 26 msecs for $T2_{max}$ and 147 msecs for $T2_{min}$. This increased rate of relaxation is consistent with the T2 of water in the PEG-water system at higher concentrations, where the greater viscosity of the solution results in lower T2's. That the PEG effects both

fast and slow components again suggests that if the multi-component nature of the system is a consequence of compartmentation within the sample then each compartment is impregnated by the large PEG molecules to some degree.

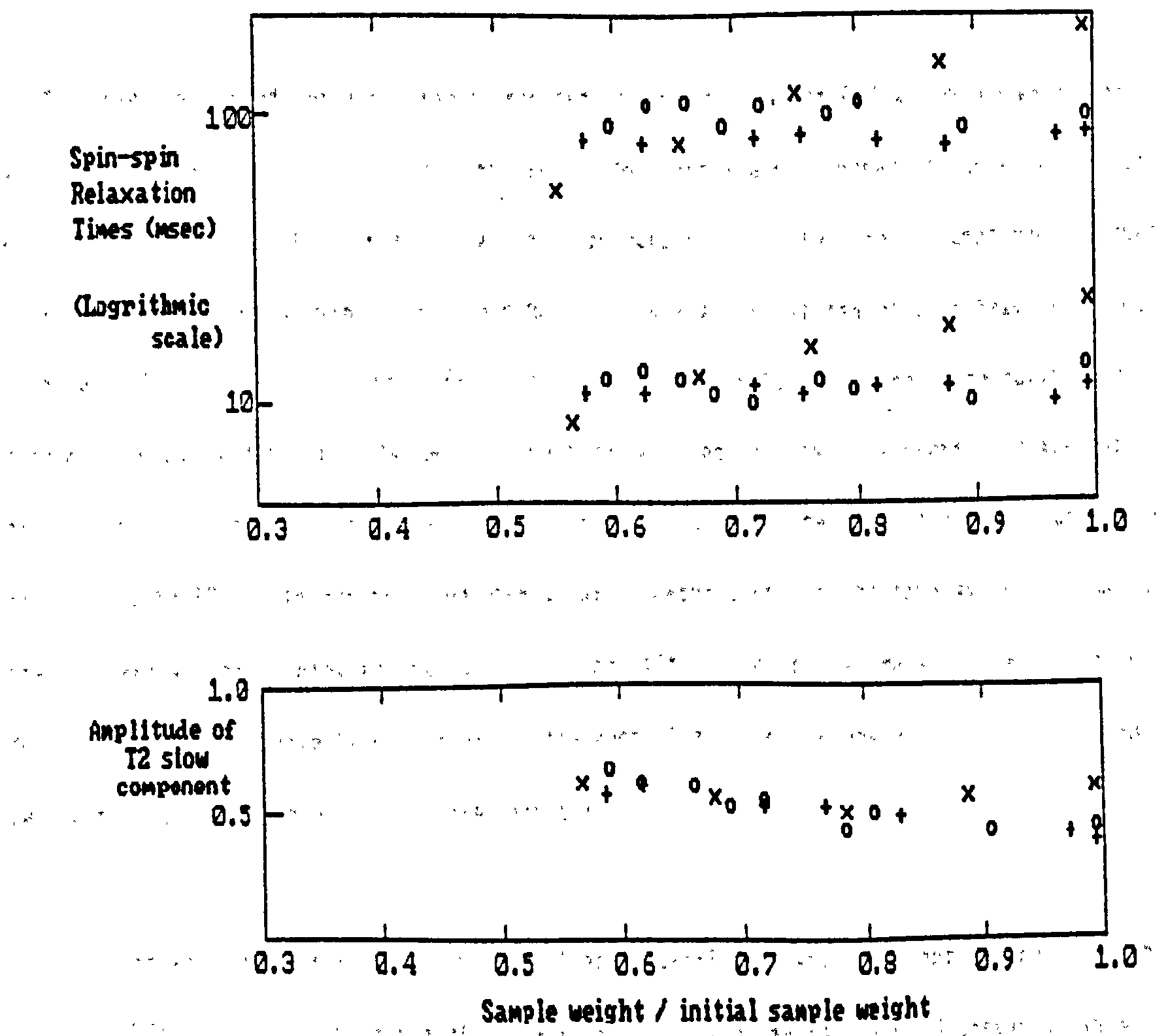

Figure 6.29 Two component spin-spin relaxation in water-logged poplar as a function of weight loss during drying. Poplar was pre-treated with PEG 300 (o), PEG 400 (+), and PEG 3400 (x).

The signal arising from the protons attached to the PEG molecules cannot be distinguished from the decay. At low water contents the bonding of large PEG molecules to the cell walls broadens the NMR signal beyond detection. The result of resolving the decays above into three components suggests that there is a shift in the relative populations of each component as impregnation takes place, with an increase in the quantity of tightly bound protons at the expense of the number in the populations of the intermediate and mobile phases. Given that

the prime mechanism for relaxation is a result the diffusion of molecules to the region of the 'bound' water layer or to paramagnetic centres on the xylem surfaces, this suggests that there is a shift in the distribution of diffusion lengths which water molecules must cover before interacting with spins of a shorter T2, to lower values.

The preservation of certain timbers requires the use of smaller PEG molecules which can penetrate the wood cell wall and support heavily degraded skeletal areas of the xylem. PEGs with degrees of polymerisation of 300 and 400 are commonly used in such circumstances. Figure 6.29 contrasts the spin-spin relaxation behaviour observed in samples of wood heavily impregnated with PEGs that vary in molecular weight from 300 to 3400. Following impregnation the samples were allowed to dry. The decays have been resolved into two components and are shown as a function of weight/initial weight of the sample. It should be noted that the samples impregnated with PEG could not be dried even at oven temperatures to the same extent as the untreated sample. This indicates that between 20 and 40% of the initial mass of the sample is due to the PEGs that have been absorbed by the wood. The following observations can be made regarding the behaviour of T2 in these samples;

(i) The spin-spin relaxation times for fresh water-logged wood and samples treated with PEGs for which the degree of polymerisation is greater than 1000 decrease as water is removed from the wood.

(ii) For samples treated with PEGs that have degrees of polymerisation less than 1000 the T2 values are independent of the water content of the sample.

(iii) In untreated samples, and in samples treated using PEG with DPs greater than 1000, the bulk of the signal relaxes with the slow relaxation, while in impregnated timbers where the size of the PEG molecules used is less than 1000, this fraction is reduced to between 40 and 50% of the total.

PEGs with degrees of polymerisation less than 1000 are liquid in the bulk at room temperature, which may account for the different relaxation characteristics of the transverse magnetisation. If the PEGs remain in a viscous liquid state within the wood then one might not expect to see any change in the relaxation times until the amount of liquid within the sample is very much reduced. The increased viscosity of the fluid would reduce the number of interactions between the molecules within the solution and the wood cell walls, thus maintaining the values of T2 at some intrinsic level. Using PEGs of higher grade, the removal of the water may lead to the precipitation of large PEG molecules which could enhance the rate of decay of the remaining fluids via spin diffusion and chemical exchange.

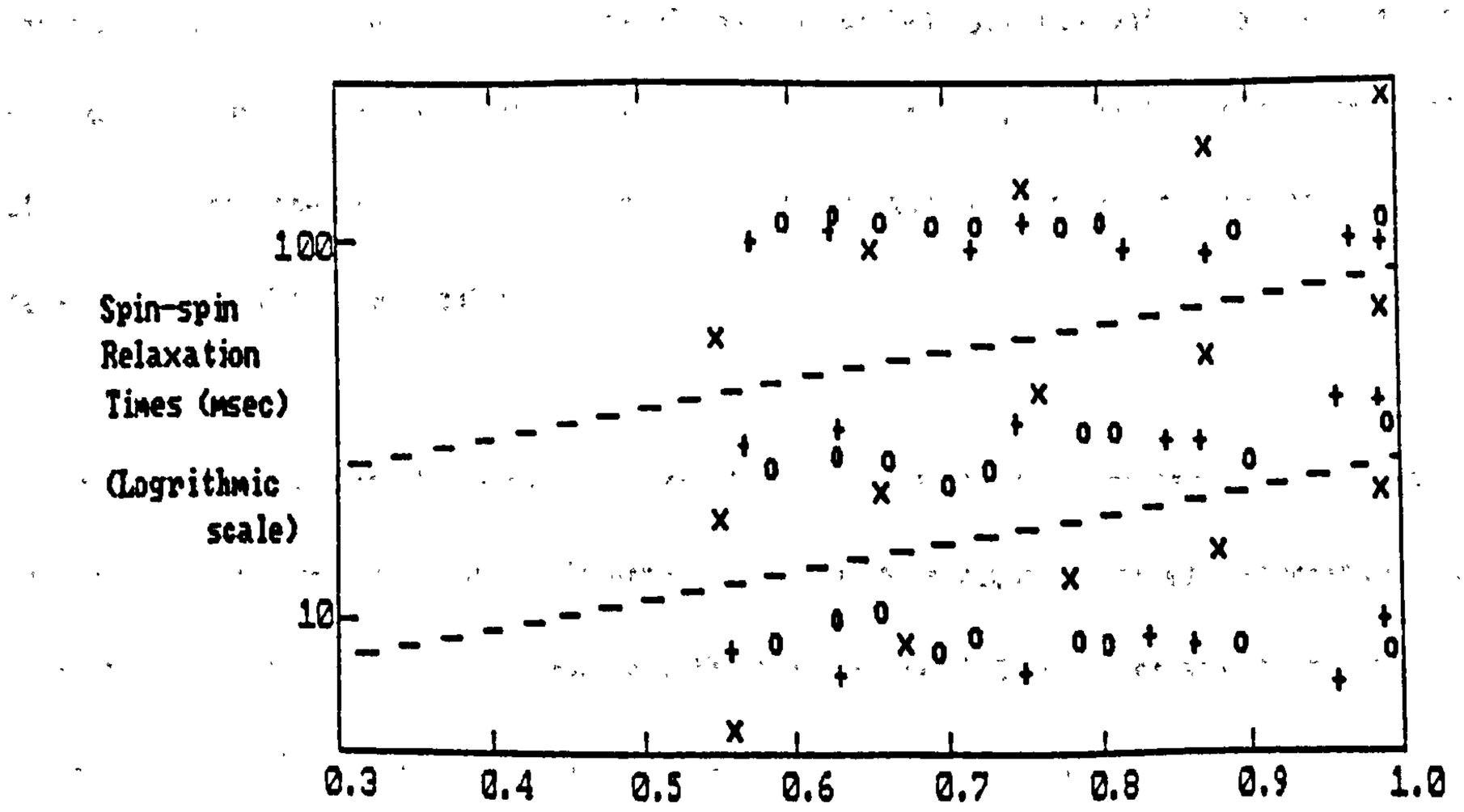

Figure 6.30 Three component spin-spin relaxation in water-logged poplar as a function of weight loss during drying. Poplar was pre-treated with PEG 300 (o), PEG 400 (+), and PEG 3400 (x).

It is possible that the different components of the relaxation curve relate to similar spin species in the sample that may be physically partitioned, attached to different molecular species, or attached to similar molecular species with different modes of motion.

It may also be that the decay curve represents a complicated aggregate of all these effects, which to a good approximation happens to be describable using a double exponential function. A three component fit represents the data equally well and the results are shown in figure 6.30. Meaningful conclusions are difficult to draw from these multi-exponential representations if an aggregate is indeed what is being seen. It seams reasonable to associate the mobility of protons within the samples to the value of T2. At higher water contents there is a small fraction of very mobile protons evident in samples of untreated woods, and woods treated with 'solid-like' polymers. This is almost certainly water molecules that during the length of the T2 experiment do not interact strongly with higher molecules. In samples treated with liquid-like polymers this non-interacting fraction of water is no longer apparent. This may be due to the fluidity of the smaller PEG molecules which, because they are more mobile, can escape the close attentions of the cell matrix, and better occupy the voids within the wood, thus mixing with the water in the wood and increasing the interaction rate between water and macromolecules.

At low water contents the amount of free water in all samples is reduced. In the samples treated with 'solid-like' PEGs the interactions are more frequent and of such strength as to cause the fall in T2. In samples treated with 'liquid-like' PEGs the increase in the frequency and strength of the interactions is offset by the mobility of the macromolecules which can impart mobility to the remaining water and sustain the relatively long T2.

The temperature dependence of water in untreated water-logged wood indicates that exchange mechanisms play a significant role in the determination of relaxation characteristics. Figure 6.31 shows the temperature dependence of the two component fit for T2 in samples of PEG impregnated timbers. One sample was impregnated using a 40% solution of PEG 3400, and the other using 100% PEG 600. Both curves follow the same pattern i.e. the spin-spin relaxation times for both components decrease with inverse temperature in accordance with BPP theory. A decisive and very important result is that the exchange processes that were evident in non-

treated samples are no longer dominant in the T2 temperature dependence, indicating that whilst the motional properties giving rise to relaxation in these samples on a local level are not substantially effected, the exchange effects may be suppressed by a fall in the translational freedom of the water molecules.

At around 273K there is a change in the rate at which T2 falls off with inverse temperature. Although there is no evidence from freezing curve experiments of a change in state at the freezing point of water it appears that the shift towards the rigid lattice condition is accelerated below 273K.

It is perhaps not surprising that the study of NMR relaxation times in impregnated water-logged wood does not reveal more information regarding the interactions between PEG, xylem and water; the PEG-water and wood-water systems are individually very complicated. Combining the two leads to a highly involved arrangement, in which the ensemble of spins undergo a wide range of activities that lead to distributions of correlation times that cannot be easily characterised. What is clear is that the presence of the large PEG molecules has a profound effect on the dynamics of water in the samples, most notably stemming the rate of exchange between different types of water in the wood. The sites occupied by the different molecular weights cannot be specified using the NMR data presented above, only the more general comment that the molecules initially occupy sites within the largest pores in the sample can be made for the case of large PEG molecules. Using sufficiently high concentrations at least some PEG, regardless of molecular size, appears to occupy sites previously occupied by free water, so that the amount of non-interacting water within the samples disappears.

Figure 6.31
VARIATION OF SPIN-SPIN RELAXATION WITH TEMPERATURE
FOR POLPAR IMPREGNATED WITH 40% PEG 3400 SOLUTION▼
&100% PEG 600▫

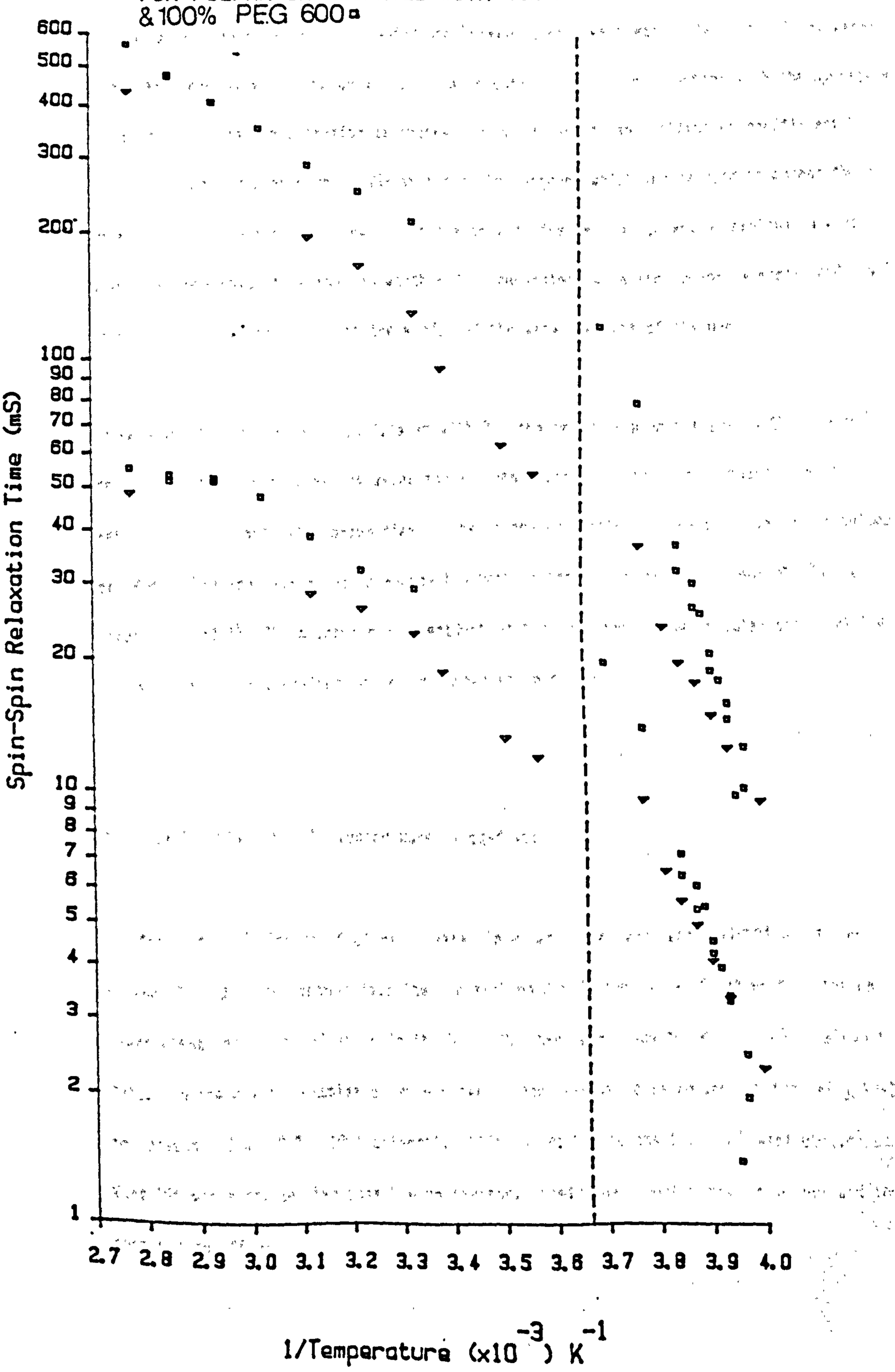

6.4 A Study of Self-diffusion for Water in Untreated and Treated Water-logged Woods Using NMR Field Gradient Techniques.

The relaxation data in both treated and untreated samples suggest that the bulk of water within the wood behaves like pure liquid water until it comes into contact with the hydration layer following random diffusion processes. The value of the self diffusion coefficient D, can be monitored directly using NMR spin-echo techniques, which may be used to assess the nature of this diffusion. Measurements of the self diffusion coefficient of protons in wood have been undertaken to establish whether D is consistent with the two-phase model, and how D is effected by the structure of the wood, and the water content of the wood.

In samples of water-logged wood treated with PEG the relaxation data suggests that there is greater interaction between the water and macromolecular species. This should also be reflected in the diffusion properties of the molecules within the wood; an even distribution of PEGs within the sample should reduce the mean proton diffusion coefficient D'. On the other hand, if the PEG molecules are resident on the surfaces of the cellular structure then D' should be largely unaffected by the impregnation of PEG.

6.4.1 Self Diffusion in Untreated Water-logged Wood.

The self diffusion coefficient of water in water-logged wood was measured using the pulsed field gradient method described in section 3.5.3. The value of the self diffusion coefficient for distilled water in the bulk, D_o, has been found to be 2.5×10^{-5} $cm^2 sec^{-1}$ at 23°C. In freshly cut samples of water-logged wood this value is reduced by typically 10-20% to between 2.0 and 2.3×10^{-5} $cm^2 sec^{-1}$. Effects leading to the fall in D were considered by Wang[124] who suggested two possible mechanisms, namely the direct hydration effect and the obstruction effect.

The direct hydration effect leads to lower values of D because water in the bound phase has a reduced translational velocity. Two phases that are in rapid exchange give rise to an observed value of D that is the weighted average of both. In the case of water that is bound and free this can be expressed as

$$D_{obs} = P_b.D_b + P_f.D_f \qquad 6.12$$

where D_b and D_f are the self diffusion coefficients of water in the bound and free states, and P_b and P_f represent the probabilities of molecules being in the hydration layer or otherwise. If the water molecules are tightly bound then D_b will be several orders of magnitude less than D_f, and the first term on the right hand side of equation 6.12 may be dropped to give;

$$D_{obs} = P_f.D_f = D_f - \frac{[H2O]b}{[H2O]t}.D_f \qquad 6.13$$

where [H2O]b is the population of the bound water phase, and [H2O]t is the total population of water in the wood.

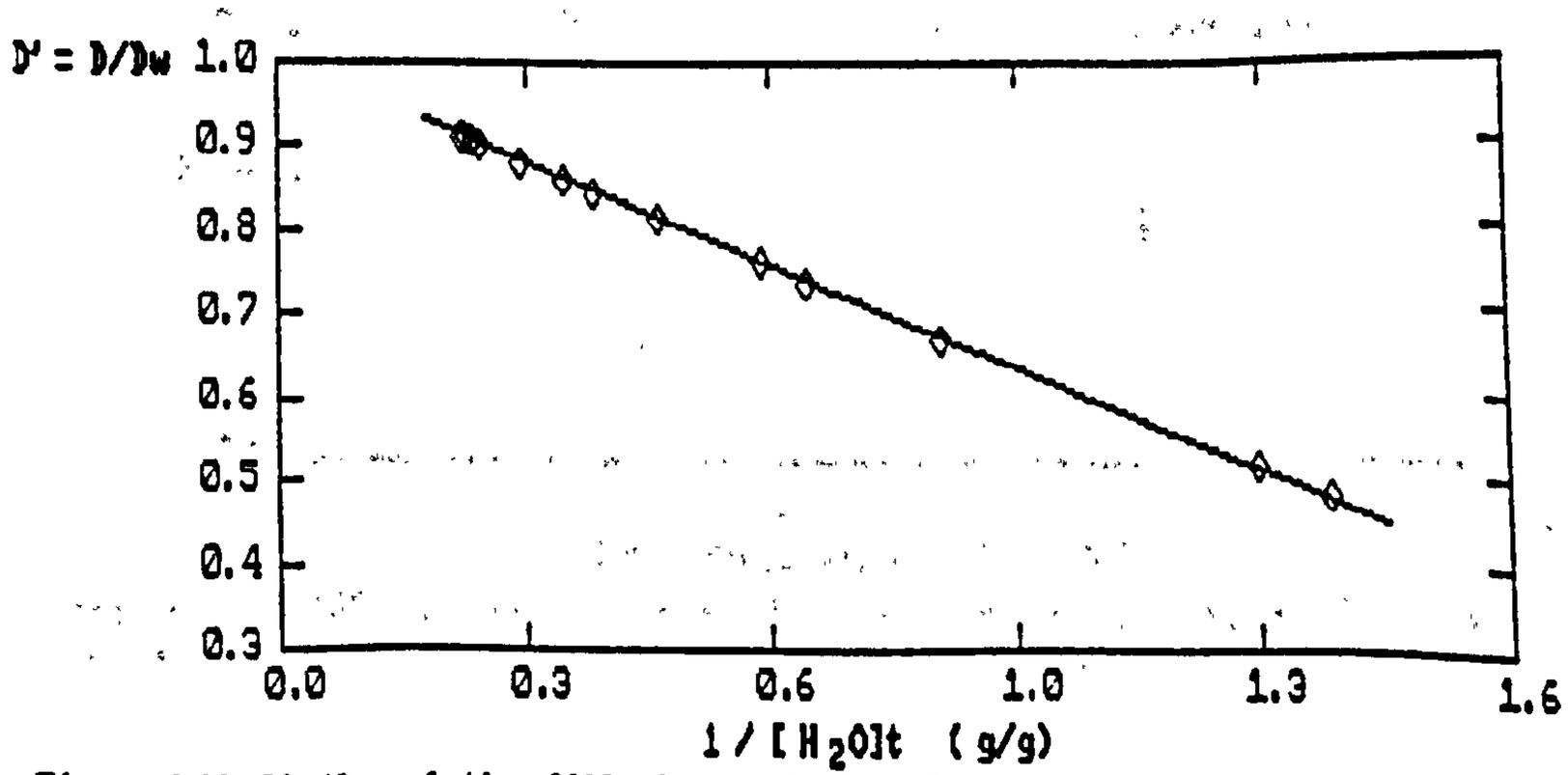

Figure 6.32 D', the relative diffusion coefficient for water in water-logged poplar as a function of $1/[H_2O]t$, for the longitudinal direction.

Figure 6.32 shows the behaviour of $D' = D_{obs}/D_o$ as a function of $[H2O]t^{-1}$ for a sample of poplar that is oriented within the probe so that the longitudinal direction of the wood is aligned with the field gradient. Below water concentrations of 1g/g the NMR signal becomes too weak to measure D' reliably. If equation 6.13 is correct then as the sample is dried the value of D' should fall linearly with the inverse water content of the sample, intersecting the Y axis at $D' = D_f/D_o$, and the gradient should equal $[H2O]b.D_f$. The solid line in the figure, calculated using $D_f = D_o$ and $[H2O]b = 0.38$ g/g, is a good representation of the data within experimental error. The significance of this result is that water external to the hydration layer diffuses at a rate equal to water in the bulk, and that the hydration layer consists of 0.38g of bound water per gram of wood, which is in good agreement with other work. D_f has been shown to equal D_o by MacGregor et al[119], who measured the diffusion rate of water that was extracted directly from the sample. At the same time the above result indicates that the diffusion rate of water molecules in the bound phase is orders of magnitude lower than from water in the bulk, and the amount of water within the bound phase remains relatively constant during drying, in agreement with freezing curve experiments.

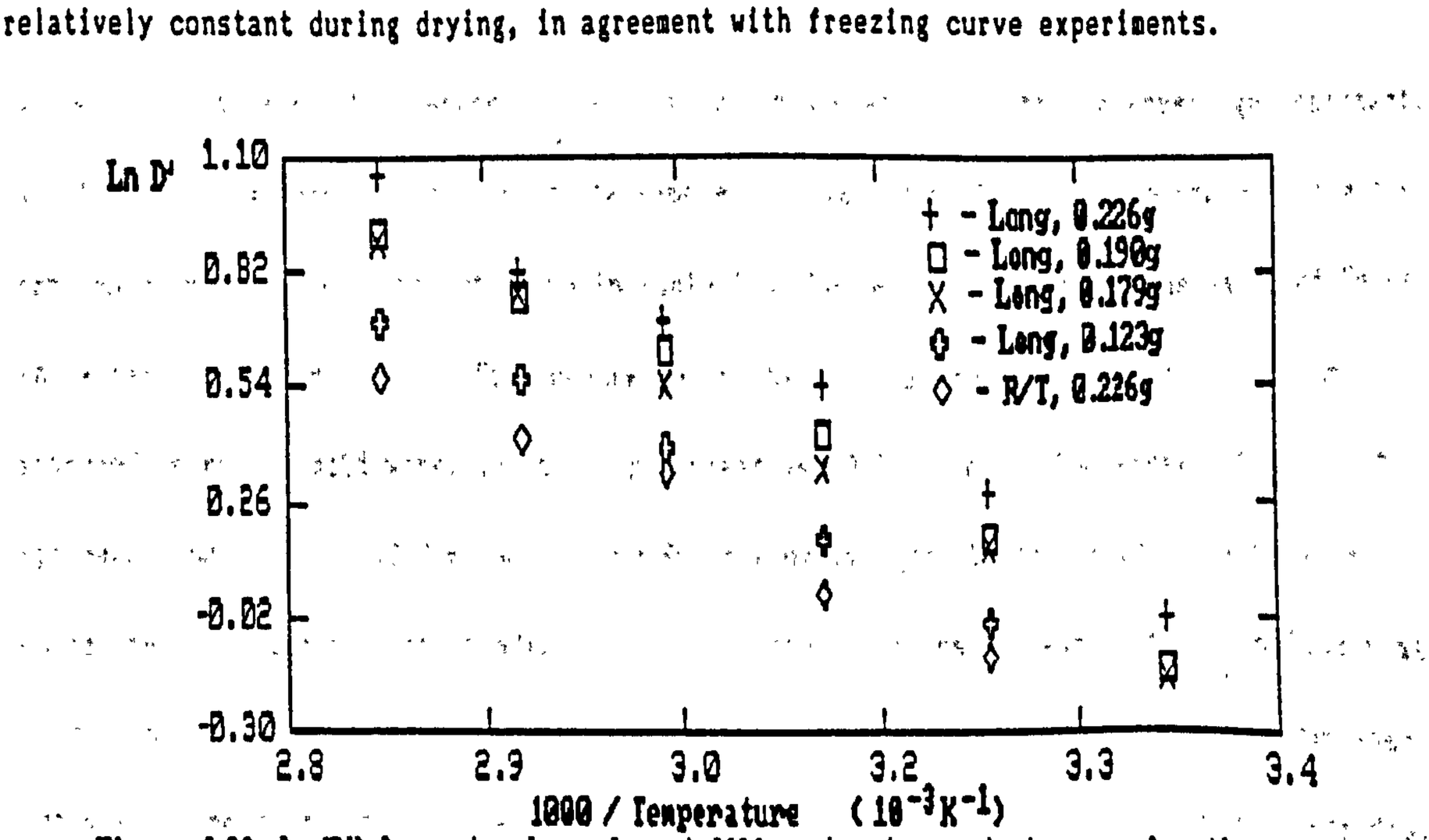

Figure 6.33 ln (D') for water in poplar at different water contents, as a function of inverse temperature. Also shown is the value in the radial/tangential direction.

Equation 6.12 above is valid only if there is a rapid exchange of water molecules between the bound and mobile phases. As the total water content of the system falls the reduced diffusion rate is caused by an increase in the amount of time that an average water molecule spends within the hydration layer, which in turn can be interpreted as an increase in the strength of the interaction between an average water molecule and the cell wall material. If there is an increase in the strength of the interaction then as diffusion is a thermally activated process one might expect it to be reflected in the activation energy of diffusion. In ice the activation energy is close to 52 KJ mol^{-1}. Figure 6.33 shows the semi-log plots of D' against inverse temperature for wood aligned longitudinally with the field gradient at a series of different water contents.

Assuming that

$$D' = D'o \times \exp(-Ea/RT) \qquad 6.14$$

where Ea is the activation energy for the diffusion process, R is the universal gas constant, and T is the absolute temperature of the sample, the values of Ea have been deduced from the gradients in the figure and are shown in table 6.4. There is no change in the value of Ea as the water content is lowered. Furthermore Ea in the wood is equal to the activation energy measured in pure liquid water which is approximately 19.7 KJ mol^{-1}. The energy of a single hydrogen bond is about 10.0 KJ mol^{-1}, and Ea is roughly equal to the amount of energy required to break two hydrogen bonds. This rather perplexing result leads one to conclude that D' can only be reduced by the hydration effect if water in the hydration layer has the same activation energy as that of the mobile phase, or that the water in the hydration layer does not diffuse a measurable distance on the time scale of this experiment. This would appear unlikely and one is tempted to consider other possible mechanisms leading to reduced values of D'.

Sample	Orientation	Weight (g)	Activation energy (KJ mol^{-1})
1	Longitudinal	0.226	18.02
2	Longitudinal	0.190	18.22
3	Longitudinal	0.179	18.54
4	Longitudinal	0.123	18.56
5	Radial/Tang'	0.226	16.13

Table 6.4 Activation energies for diffusion in poplar.

The obstructive effect leads to an apparent fall in D' because the translational motion of water molecules is hindered by the presence of boundaries and macromolecules. In such cases there need not be a change in the intrinsic diffusion rate of the water which must travel longer path lengths in order to traverse the same distances in any specified direction. The time scale of the experiments in this work could be varied between 30 and 170 msecs. During this time the range of distances travelled by a water molecule with a rate of self diffusion equal to that of free, unbounded water, would be between 12 and 30 microns. The long axes of longitudinally oriented cells are large in comparison, and the water molecules in the lumen of these cells would not exhibit bounded diffusion in this direction. A significant amount of water resides in the medullary rays, however, which could could lead to partially restricted diffusion along the longitudinal axis. The resulting value of D' may then be the weighted average of one fraction which is bounded and one that is unbounded.

Robertson[20] has quantified the value of D' for the one dimensional case where a population of resonant nuclei are bounded by parallel, impermeable borders and has found that it is sensitive to the time over which the system is observed t'.

$$D'(t') = \frac{Dobs(t')}{Din} = \frac{96}{\pi^2}.t'^{-\frac{1}{2}} \sum_{n=0}^{\infty} \frac{1}{(2n+1)^4} \times$$

$$\left[t' - \frac{3 - 4\exp\{-\tfrac{1}{2}(2n+1)^2\pi^2 t'\} + \exp\{-(2n+1)^2\pi^2 t'\}}{(2n+1)^2\pi^2} \right] \qquad 6.15$$

where t' is the observation time t, measured in units of "diffusion time", t_d. i.e. $t' = t/t_d$, where $t_d = a^2/Din$. Din represents the intrinsic relaxation rate of the water in the system, i.e. the self diffusion rate in unbounded samples, and a represents the separation of the boundaries. Dobs is the measured diffusion rate. For water in wood, Din is taken as being equal to the diffusion rate of pure water Dw. The form of equation 6.15 is illustrated in figure 6.34.

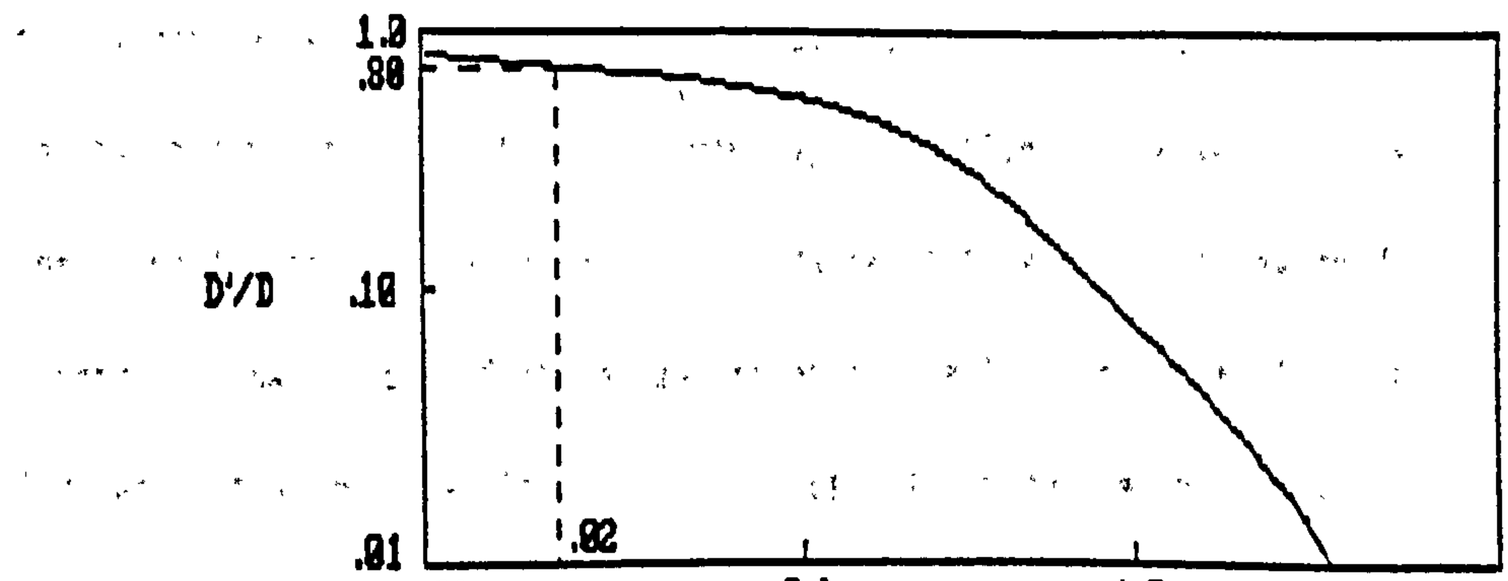

Figure 6.34 Solution of Robertson's[20] one-dimensional compartment model.

Figure 6.35 shows the specific self-diffusion coefficient D', for water diffusing in the longitudinal direction in water-logged wood as a function of Delta, which represents the time scale on which diffusion is measured. The range of Delta is limited by experimental and systematic considerations, but D' is independent of Delta over the range studied, having a constant value of approximately 0.8. From figure 6.34, this corresponds to a value of t' of around 0.02. Using the maximum value of t = 171 msecs, this requires a maximum boundary separation of approximately 140μm in order to adequately account for the data. Since the length of the cells is more usually orders of 10^2 greater than this one can conclude that D' is not determined by the compartmentation of the total water population.

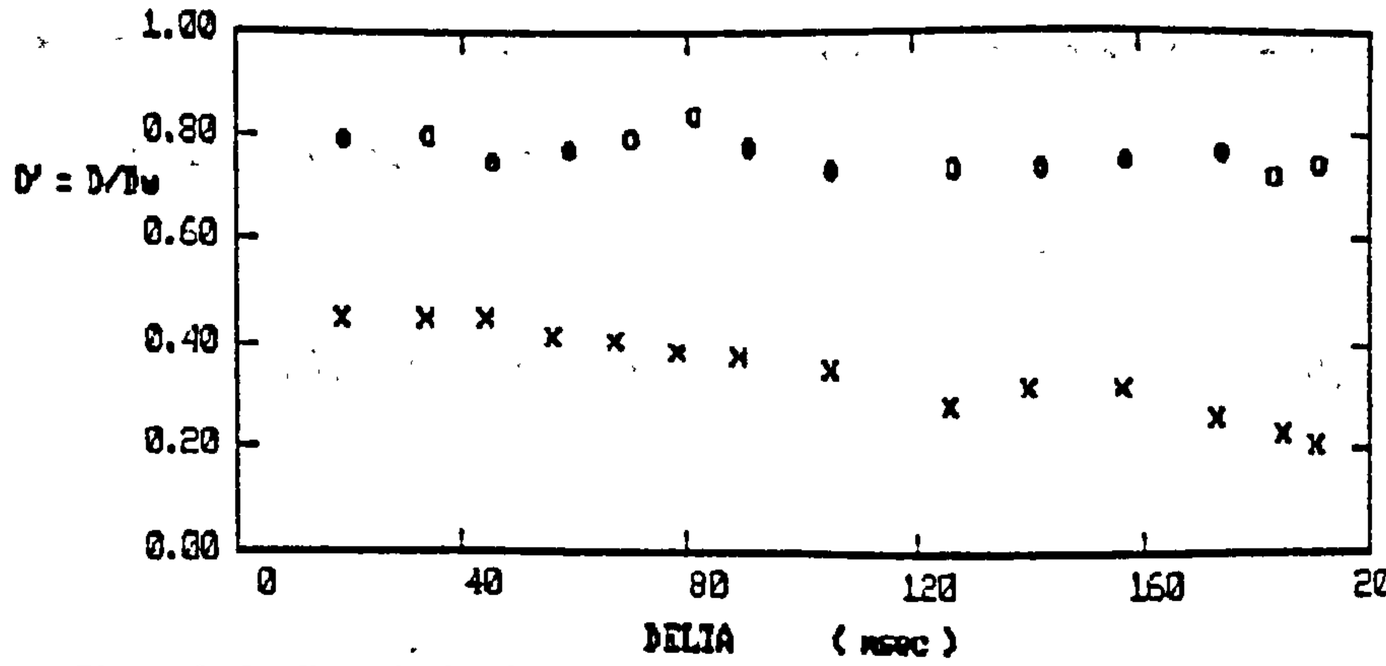

Figure 6.35 The relative diffusion coefficient D', as a function of experimental time scale, for poplar in logitudinal (o), and R/T (x) directions.

The above argument does not exclude the possibility that the water is bounded by permeable membranes which could result in a lower average diffusion rate. If the depression of D' in the longitudinal direction is caused by a fraction of the water being bounded, then an upper value for the separation of the boundaries can be put at a few hundred microns, which is beyond the lower limit of the diameters of the cells in the medullary rays. It has been estimated that as much as 50% of the walls of cell lumen are marked with pits and spiral thickenings. In popular the diameter of these pits are between 8 and 13μm, and MacGregor et al[114] have suggested that the depression of D' for water travelling parallel to the longitudinal axis in poplar may be caused by a proportion of the water being bounded within these pits. The results of this study are not consistent with this view though, as it is estimated that the amount of water held within these pits is unlikely to account for more than 4% of the total water population. As pointed out by MacGregor et al[111], a contribution from water held in the medullary rays will increase the amount of bounded water, provided that the diameter of the cells within the rays is less than 1-10μm for these samples. MacGregor et al[111] could account well for their data by assuming that the distance between boundaries is around 5-15μm, and the fraction of bounded water was consistent with the fractional volume of transverse elements within the woods. Chang et al[21], on the other hand, claimed that the effects

of compartmentation could account for no more than 10% of the attenuation in D' observed in their studies on muscle tissues. They pointed out that in the limiting case when $t >> (2/\pi^2)t_e$, equation 6.15 reduces to the form

$$Dobs' \approx (a^2/10D_{int}t^2) \qquad 6.16$$

i.e. the observed diffusion rate becomes inversely proportional to the intrinsic diffusion rate. If the fraction of bounded water leading to the fall in Dobs' that is seen in wood cannot be monitored by varying Delta, then it is a safe assumption that equation 6.16 holds for that fraction. As the temperature of the system is varied, an increase in D_{int} should be matched by a decrease in D'obs, and vice-versa. No such effect was observed in muscle fibres, for which the ratio of $Dobs'/D_{int}$ maintained a constant value. Similarly no such effects were observed during this work, which suggests therefore that compartmentation cannot be wholly responsible for the reduced value of Dobs.

The diffusion of water in wood is anisotropic. The value of D' in an arbitrary direction perpendicular to the long axis of the cells ,$D'_{\perp/\tau}$, is illustrated in figure 6.35 and is lower than D' in the longitudinal direction. In figure 6.35 $D'_{\perp/\tau}$ is plotted as a function of Delta. As the value of Delta is increased the value of $D'_{\perp/\tau}$ is steadily attenuated, from a value of about 0.38 at t = 45 msecs, to 0.24 at t = 171 msecs. Utilising figure 6.34, this indicates the presence of water that is bounded by barriers having a characteristic separation of a between 26 and 33 microns. The diameter of fibres in popular range from 23 to 26 microns, and 20-30% of the total water within the sample may be expected to reside within the lumens of fibres. One may therefore suggest that the effects observed in figure 6.35 result from the restricted diffusion in the transverse direction of water molecules within this population.

Experiments were carried out to test for anisotropic effects in the radial and tangential directions. Whilst the identification of the longitudinal axis of wood is trivial, the radial and tangential directions are not so easily distinguished, especially in small samples. Small samples were therefore placed with the longitudinal axis perpendicular to the direction of the field gradient and the samples could be rotated about the longitudinal axis, so that $D'_{R//T}$ could be observed as a function of the angle between the radial axis and the field gradient. The results are illustrated in figure 6.36, which shows the value of $D'_{R//T}$ as a function of sample orientation for a series of water contents.

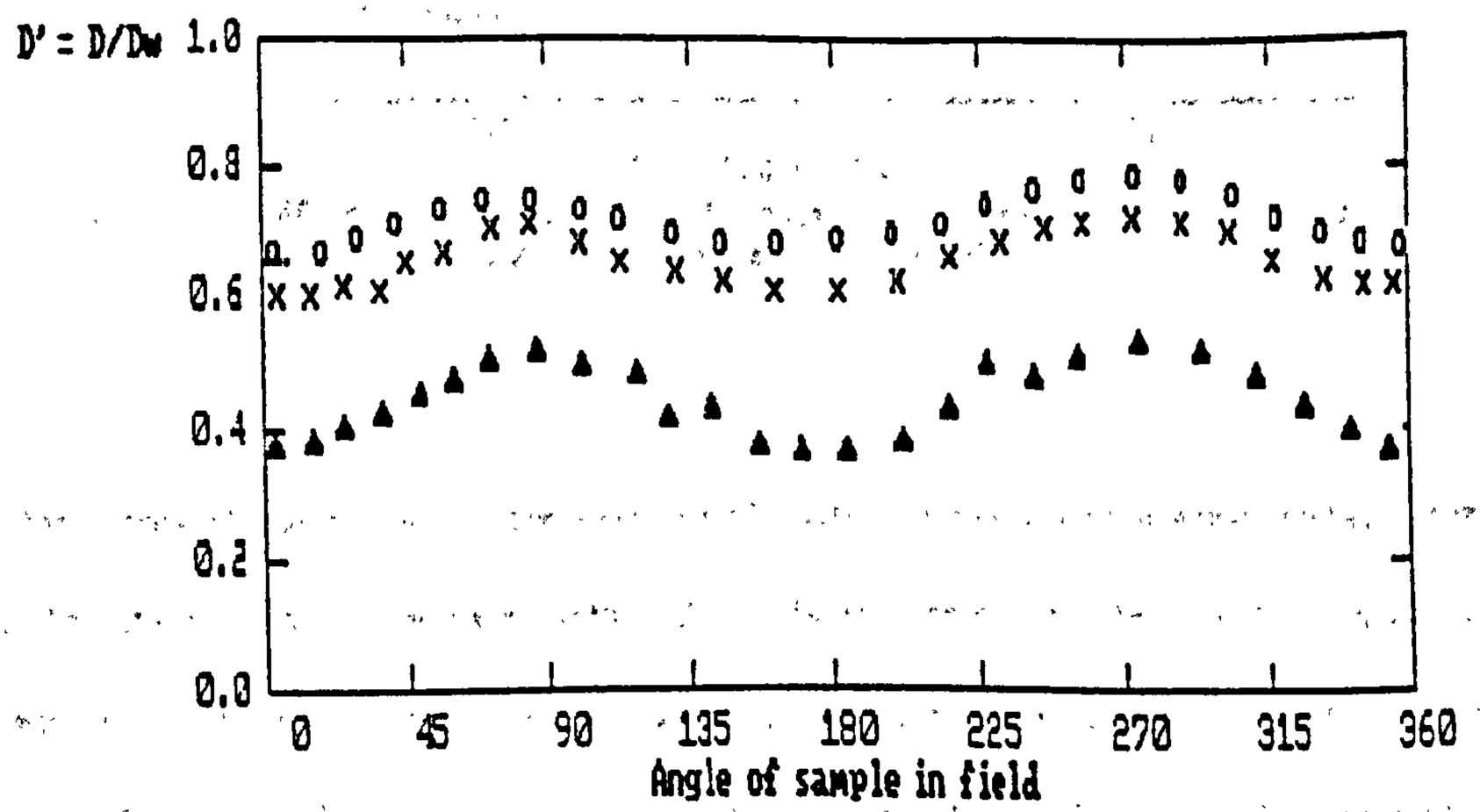

Figure 6.36 Anisotropy of diffusion coefficient in waterlogged poplar. D' is shown as a function of the angle of sample in field for samples weighing 0.106g (o), 0.061g (x) and 0.039g (▲).

The value of $D'_{R//T}$ is cyclic, and one can conclude that self-diffusion in the radial direction precedes at a different rate to diffusion in the tangential direction. The peaks in $D'_{R//T}$ are associated with the alignment of the radial axis of the sample with the field gradient and value of $D'_{R//T}$ is taken to represent D'_R, the self-diffusion coefficient of water in the radial direction. D'_T, the value for the self diffusion coefficient in the tangential direction, is equated to the value of $D'_{R//T}$ at the troughs. As the water content of

the sample is reduced both D'_{ℓ} and D'_{T} decrease, and the difference in D'_{ℓ} and D'_{T} is increased. The effects become more pronounced as the water content is lowered. The behaviour of D' in the longitudinal, radial and tangential directions are contrasted in figure 6.37.

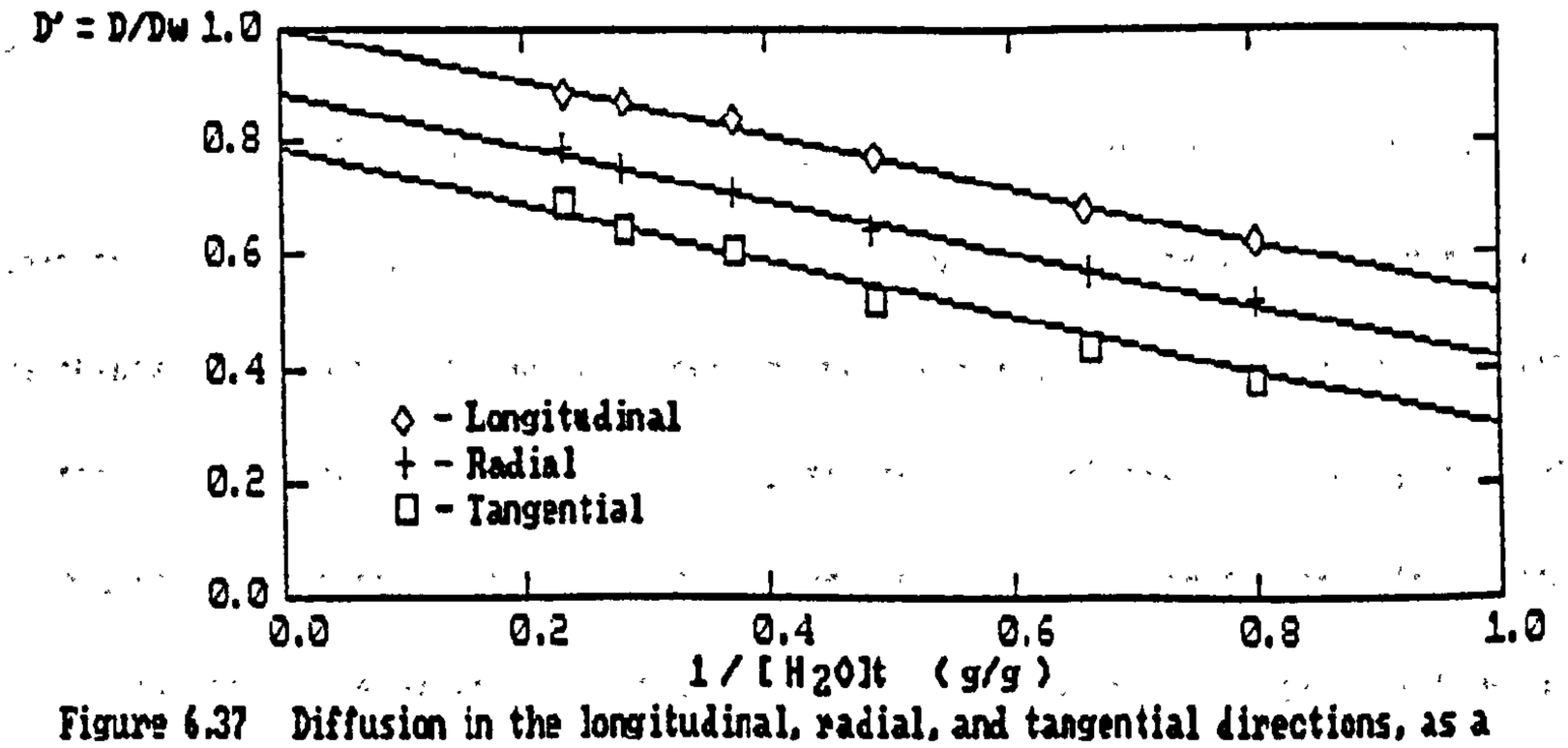

Figure 6.37 Diffusion in the longitudinal, radial, and tangential directions, as a a function of 1 / total water content of sample.

The slopes of the graphs are the same for all water contents within experimental error, and the rate at which D' decreases with $[H2O]t^{-1}$ is independent of the direction in which it is measured, but the intercept, which from equation 6.13 represents the self diffusion coefficient of the free phase, is reduced in the radial direction, and again in the tangential direction. This implies that D_f is lower for these orientations, but also via equation 6.13 that $[H2O]b$, the quantity of water in the hydration layer, also has an orientational dependence. Although it is possible that diffusion takes place within the hydration layer, giving rise to an apparent change in the amount of hydration water from a diffusional view point. This result, together with the fact that the activation energy of self diffusion is independent of the water content throws doubt on the notion that the hydration effect is responsible for the low value of D'in the radial and tangential directions.

The anisotropic nature of the diffusive tensor reflects the structural composition of wood. The resistance to diffusion is least in the direction in which the majority of cells are aligned, i.e. the longitudinal direction. A large number of cells orient radially and this leads to the intermediate rate of diffusion observed for this direction, whereas there are no major cellular components that traverse the wood in the tangential direction giving rise to the lowest D' value. In view of this one favours the obstruction effect as an explanation of the fall in D'. The fall in D' with reduced water content is then explained as a consequence of shrinkage in the wood upon drying. As the water leaves the wood the gradual collapse of the larger voids leads to a greater proportion of the water being in a confined environment, and therefore to a fall in the observed diffusion coefficient. The shrinkage is itself anisotropic, being greatest in the tangential and radial directions, and one might therefore expect to see a difference in the rate at which D' falls with [H2O]t for the longitudinal, radial and tangential directions. The fact that it does not may be because water within a pore that has collapsed falls into a restricted state and does not contribute to the NMR signal.

The results described above are somewhat inconclusive. In particular the narrow range of delta permissible does not allow for distinct characterisation of the boundaries to diffusion in the direction of the three different axes in the wood, leaving a question mark over the probable cause of reduced diffusion in the longitudinal direction in fully water-logged timbers, and in all three directions as the water content is reduced. It seems likely that the hydration effect plays a significant role on the determination of D' in these cases, however the hydration effect does not explain the anisotropic nature of the diffusion coefficient. On the other hand the obstruction effect seems to play an important role in reducing D' in the radial and tangential direction, but does not adequately describe the behaviour of D' with water content. The cause of the fall in D' in wood is most probably therefore a combination of both effects.

6.4.2. Diffusion in Treated Water-logged Woods.

The relaxation experiments described earlier indicate that in untreated samples there is a considerable number of protons in different regions of the cells of the wood that undergo either chemical or molecular exchange. It was suggested that these exchange processes are attenuated by the presence of large PEG molecules, which should be reflected by a depression in the self-diffusion coefficient of protons within the sample.

The self-diffusion coefficients of hydrogen nuclei in water-logged woods that have been immersed for some time in solutions of polyethylene-glycols are reduced by an order of between 10 and 100 compared to untreated samples. As a preliminary experiment three samples of poplar were soaked in solutions of 100% PEG 300, 100% PEG 400, and 50% PEG 3500. After six hours the weight of all three samples had increased by 2-3%, implying that some at least some PEG had entered the samples in each case. Prior to soaking, the self diffusion coefficients for the water in the wood were typically around 2.0 x $10^{-5}cm^2sec^{-1}$. After the period of six hours there was a dramatic reduction in the value of D in each sample.

Sample Sol'n	D' before soaking	D' after soaking
PEG 300	0.82	0.084 ± .012
PEG 400	0.79	0.067 ± .018
PEG 3500	0.78	0.06 ± .05

The Values of D' were measured several times each, and the large error in the value of D' for the sample soaked in 50% PEG 3500 reflects the poor quality of the data. The measurements were taken at a temperature of 297K.

The low values of D' match values obtained in studies of PEG/D_2O mixtures. D' for PEG 300 molecules in D_2O are shown in figure 6.38 for a range of temperatures and concentrations. To attain a value of D' = 0.084 at a temperature of 297K requires the concentration of polymer to be greater than 60% by weight, and the small increase in sample weight indicates that the concentration of PEG within the wood is far less than this value.

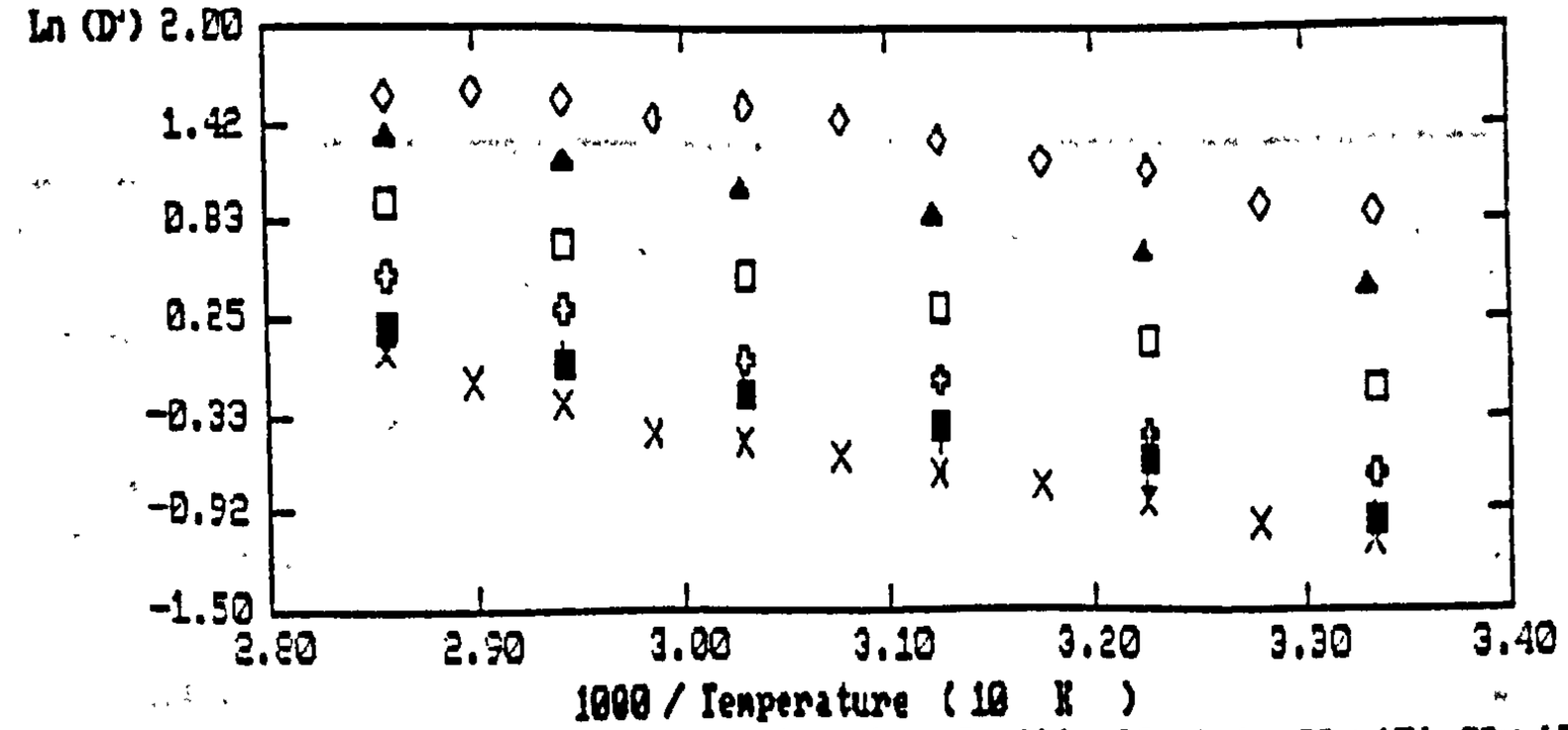

Figure 6.38 Ln (D') against inverse temperature for 10% (◇), 30% (▲), 50% (□), 70% (◊) 80% (■), 90% (X) solutions of PEG 300.

In samples that have been well saturated in PEG 300 and PEG 400 solutions there is a reduction in the orientational dependence of the diffusion coefficient, and a steady reduction in the activation energy for diffusion as to 3.8Kcal/mol on the sample soaked in PEG 300, and to 3.1Kcal/mol in the sample soaked in PEG 400 solution. These values are lower than the value observed in pure liquid water (4.7Kcal/mol). X-ray diffraction has shown that for water in the bulk there is short range order between the molecules caused by weak hydrogen bonds. This structure is rapidly forming and reforming as the molecules tumble, but in solutions of PEG it would seem that this short range structure is disrupted by the presence of the macromolecules, and the inter-molecular interactions are weakened. The activation energies were measured for different concentrations of polymer solution, and the results are shown in figure 6.39. As polymer is added to D_2O there is an initial fall in the activation energy. This initial decrease is caused by the destructuring effect described above, and is

matched by a slight increase in the diffusion rates observed in the system. With the further addition of polymer the activation energy begins to rise to the value observed in distilled water, and the diffusion of the polymers is slowed down. (see figure 6.39). If the lowering of the activation energy of diffusion for water in water-logged wood by the addition of PEG is caused by the destructuring effect, then the amount of PEG within the wood must be such that within the samples the concentration of the PEG/water solutions is less than about 15%.

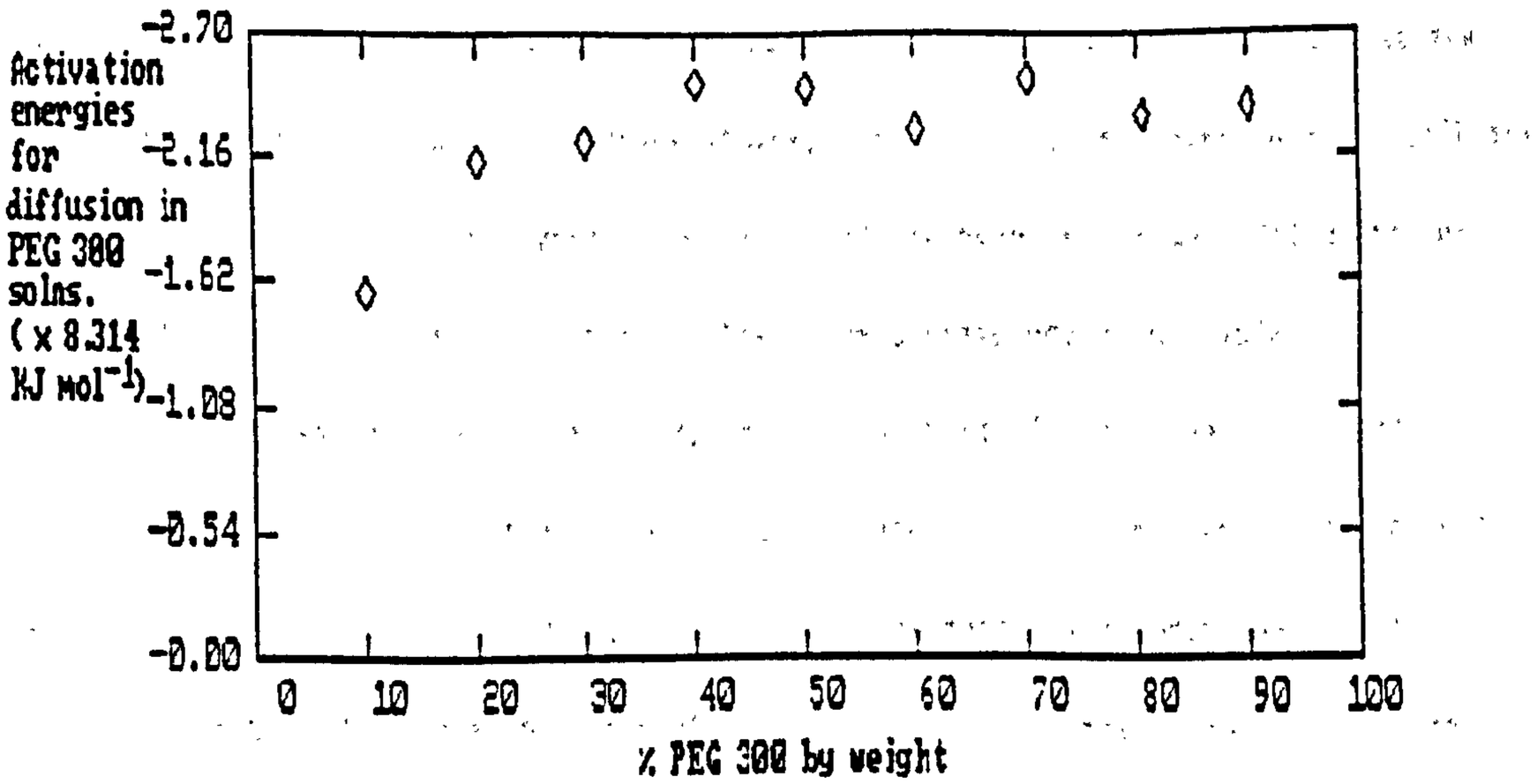

Figure 6.39 Activation energies in solutions of PEG 300 / D_2O.

The obstruction effect described in section 6.4.1 can take one of two forms. First there is the case where membranes within the system can confine molecules to regions of the wood, and this is believed to be a contributing factor to the depressed value of D'. There is also the case where the translational motion of water molecules is impeded by the presence of macromolecules. This kind of obstruction would be isotropic in a locally homogeneous solution. Assuming that the concentration of polymer within the wood is low, then to depress D' to such a great extent would require that the motion of the polymers is very greatly reduced, perhaps even halted by their proximity to the cell walls of the wood. This need not impede the rotational diffusion of water molecules, and the effect on the relaxation times of the water in treated samples would by negligible. The reduced translational motion of the water molecules

would however effect the rate of chemical exchange between protons in the different regions of the wood, which the leads to the modification of the temperature dependence of the spin-spin relaxation times of water in treated samples.

6.5 Conclusions.

In water-logged wood there exists at least two populations of water molecules that are distinguished by the fact that at low temperatures, i.e. below the freezing point of ordinary water, one phase retains a high degree of mobility and its hydrogen atoms still contribute to the proton NMR signal. It is believed that this phase corresponds to a population of molecules that interact strongly with the matter in the walls of the xylem cells, and is equivalent to the water of hydration found in fresh timbers at relative humidities below the fibre saturation point. Freezing curves indicate that the quantity of bound water within the wood is approximately 0.38 grams per gram of solid material. In fresh timbers the fibre saturation point for many timbers occurs at around 0.38 grams of water per gram of solid. The relaxation times of water molecules within this phase are much longer than for equivalent water molecules in fresh timbers, and indicates that the degree of degradation as well as the neighbouring water in the rest of the system reduce the average strength of the interaction between the xylem and water molecules. This interacting water is called 'bound' or 'non-freezable' water, and is commonly found in many hydrated systems.

The remaining water molecules within the system are relatively free from interactions with the molecules of the cell walls and undergo the usual change of phase from liquid to solid as the temperature is lowered. As the wood is dried this phase is removed almost exclusively from the sample, and only when all of this 'unbound' or 'freezable' fraction has been removed does the bound water begin its evacuation. As long as the quantity of bound

water has not been depleted during the drying process the sample of wood may be rehydrated to its original form. The unbound fraction is considered to have motional properties that are similar to pure water in the bulk.

The two populations of water within water-logged wood constantly exchange molecules, and deuteration studies indicate that the structure of degraded and water-logged wood is very open and accessible. There are no regions of the wood where the bound fraction cannot mix and exchange molecules with the unbound population. In addition to exchange of water molecules between the two phases the protons attached to molecules of the xylem itself may undergo chemical exchange with protons of water molecules. The exchange of protons from one environment to another is clearly demonstrated by the temperature dependence of the transverse relaxation times, which seem to indicate that there is a distribution of exchange rates.

Values of single component relaxation times for water in water-logged wood are less than for fresh water but greater than for new timbers. The times of both T1 and T2 in degraded samples both show a proportionality to the amount of water within the wood provided that none of the bound water has been removed. This fact is consistent with a two-phase model, but indicate that the amount of water held in the 'bound' phase is less than that found from freezing curve experiments, having a value of about 0.14 grams of bound water per gram of solid. In relatively well preserved timbers such as some of the heartwoods found on the Mary Rose, however, the two component model can only explain the behaviour of single component T1 and T2 values by assuming that the values of T1 and T2 for the bound water fraction are themselves functions of the water content of the wood and this leads to the postulation that there exists two kinds of bound water; a 'primary' and a 'secondary'. Evidence of the existence of secondary bound water also comes from the multi-exponential nature of the non-freezable component. Secondary bound water exists at water contents over 0.14g/g, and the quantity of secondary bound water that the system can sustain reaches a saturation value at water contents of about 0.4 g/g. It would appear then that with freezing curve analysis one

observes both the primary and secondary bound water, whereas for single component relaxation measurements only the primary bound water has a sufficiently high relaxation rate to be distinguished from the freezable fraction.

The value of 0.14 g/g of primary bound water within the system is consistent with measurements of the amount of bound water found in samples of hydrated cellulose from a variety of sources. Below water contents of 0.14 g/g there is evidence of the formation of bridge-like structures between adjacent molecules of xylem build from hydrogen-bonded water molecules.

Examination of the magnetisation decay curves for spin-lattice and spin-spin experiments shows clearly their non-exponential behaviour, and at least two time constants are required to explain the data. In dehydration experiments the two-component spin-spin behaviour indicates two transition points that occur at water contents of about 2.7 g/g and between 0.4 and 0.8 g/g. The relative populations of the two components vary, and the ease with which the different components can be removed from the wood also changes, which prompt changes in the behaviour of the spin-spin relaxation times of the two components. The relative populations of the two components are such that the molecules contributing to the signal of each component cannot be identified as the molecules within the bound and unbound layers. Rather each component would appear to consist of a blend of both bound and free water in different proportions.

The nature of the NMR relaxation in water-logged wood is not unique, similar results have been observed in other fibrous materials such as meat tissue. In the past the multi-component decays have been analysed in terms of different populations of water that are compartmentalised in some way within the samples. An attempt to explain the two component nature of the transverse NMR behaviour in terms of the physical nature of the wood was made by assuming that populations of water in the fibres and vessels of the wood behave differently

and consist of different proportions of bound and free water. The model is successful until one considers the transverse NMR behaviour in more degraded samples where a third component can be resolved. Furthermore studies of the longitudinal NMR decay for these samples suggest the invalidation of this model.

It seems more likely that in samples of water-logged wood there is a continuous distribution of relaxation times brought about by a distribution in pore sizes and relaxation times for water in both bound and free phases, as well as in the self diffusion rates of water within the sample, and by the different proportions of bound water held within each pore. The distribution and magnitude of the observed relaxation times are thought to be established via the mechanisms described by Brownstein and Tarr[23], and expanded upon by workers studying the NMR characteristics of porous systems such as rocks. In this sense the two component and three component fits to the data that are presented in this work are merely approximations which describe the envelope of the distribution function.

Straight forward measurements of T1 and T2 on polymer impregnated samples of water-logged wood do not provide any information about the amount of polymer that has made its way into the wood. The proton NMR signal of PEG molecules in solution can be resolved into a component originating from the macromolecules and a component originating from the water. The relaxation of polymer protons is governed by conformational changes along the chain of the molecule. The relaxation mechanism of the water in PEG solutions is complicated by the formation of hydration layers along the polymer chain. At high concentrations of polymer, viscosity effects come into play to restrict the motion of both polymer and water molecules. When wood is immersed in a PEG solution the contribution to the signal due to protons in the PEG molecules is no longer resolvable. Instead this signal becomes 'absorbed' into the distribution of relaxation times observed in untreated timbers.

The impregnation of PEG into water-logged wood does not restrict the rotational motion of the water molecules in the wood, and the relaxation rates and multi-component nature of the relaxation of the wood-water-PEG composite do not differ significantly from those of samples that have not been impregnated by the larger molecules. The presence of PEG within the system, however, has a profound effect on the translational freedom of the water molecules. This is reflected in the reduced value for the self diffusion coefficient of the water in the wood, the temperature dependence of the transverse relaxation rates which no longer exhibits exchange effects, and the relationship between the spin-spin relaxation times and the water content of impregnated samples.

The different grades of PEG, upto molecular weights of 4000, all penetrate the water-logged areas of wood where free water exists to the same degree, though prolonged soaking is required when the degree of polymerisation of the PEG is increased. Whether or not the lighter grades penetrate the infra structure of the cell walls better than heavier grades hasn't been established through this work. The NMR properties of impregnated woods does suggest that the lighter grades allow a greater degree of motional freedom for the water molecules. This degree of mobility is maintained even at lower water contents, whereas using high grades of PEG the mobility of the water molecules is greatest at high water contents.

At low water contents the water mobility is restricted, probably as a result of the precipitation of the polymer onto the xylem cell walls and the strong interaction of the water and solid-like PEG molecules.

The self diffusion coefficient of water in water-logged woods are depressed from the values observed in pure distilled water. This depression could be the result of either an obstruction mechanism, whereby the effective path-lengths for diffusion are increased by obstacles in the way, or it result from hydration effects whereby the protons held within the

hydration layer lead to a reduced average rate of diffusion. The anisotropic nature of the diffusion coefficient, and its water-content dependence lead to the conclusion that in reality the lower rate of self diffusion is probably a combination of both these effects.

The rate of translational diffusion in PEG impregnated water-logged woods is reduced by a factor of 10. There is a reduction in the anisotropy of D', and the activation energy for diffusion is lowered in impregnated samples, leading one to suggest that the obstruction effect is the primary cause of the fall in D'.

In the introductory section of this chapter five questions were posed which set out the aims of this work. The first four have been answered to a certain degree in this chapter, and it remains to say something regarding the application of NMR in assessing the treatment parameters required for the preservation of water-logged timbers.

Simple, straight forward NMR measurements that can be made without first making a considerable initial capital outlay are the water contents of woods, the spin-lattice relaxation times, and the spin-spin relaxation times. Of these only the first gives any detailed, and unambiguous information about the state of the wood in its initial saturated form, and even this measurement is less straight forward than it at first appears. Each time the water content of a sample is measured using NMR, for example, certain parameters have to be established such as the relaxation rate of the signal originating from the solid content, which must be known in order to be able to compensate for the dead time of the spectrometers receiver mechanism. Given that water contents can be measured with far more accuracy and certainty using the relatively cheap oven-dry process, the use of NMR seems an unnecessary overkill.

The relaxation of PEG molecules within wood cannot be resolved from the rest of the signal. The fact that the proton NMR signal stemming from the molecules of PEG is effectively invisible once the PEG has impregnated the system means that assessing the degree of impregnation via single T1 and T2 measurements is not possible. Nor can T1 and T2 be realistically used to establish degrees of degradation in water-logged wood since the values of these entities are determined by extremely complicated processes which appear to vary from one specimen to another.

Making detailed NMR studies on samples of water-logged wood requires a hefty capital investment which cannot be justified in terms of the information that one is likely to ascertain from such investigations. The results of the temperature and water content studies performed in this work, whilst useful in determining the nature of the system, cannot unfortunately, be readily applied to the preservation procedure.

References:

1. Franks F. "Water - A comprehensive treatise." Pub. Plenum Press, New York. (1972)
2. Skaar C. "Water in Wood" Syracuse University Press. Syracuse. (1972)
3. Derbyshire W. "Water - A comprehensive treatise." Vol 7. Plenum Press, New York. (1980)
4. Stamm A.J. "Wood and Cellulose Science." Ronald Press, New York. (1964)
5. Carles J.E., Scallan A.M. J. App. Polym. Sci. Vol 17, pp1855-1865. (1973)
6. Ogiwara Y., Kubota H. J. App. Polym. Sci. Vol 13, p1689. (1969)
7. Boesen C.E. Cell. Chem. Tech. Vol 4, p149. (1970)
8. Neal J.L., Goring D.A.I. J. Polym Sci. C. Vol 28, p103. (1969)
9. Child T.F. Polymer. Vol 13, p259. (1972)

10. Hsi E., Hossfield R., Bryant R.G. J. Coll. Interface Sci. Vol 62(3), p389. (1977)

11. Froix M.F., Nelson R. Macromolecules. Vol 8, p726. (1975)

12. Panshin A.J., de Zeeuw C. "Textbook of Wood Technology." McGraw-Hill, New York. (1980)

13. Brownstein K.R. J. Magn. Resonance. Vol 40, pp505-510. (1980)

14. Vriesenga J.R., Chandrasekaran S., Luner P. J. App. Polym. Sci. : App. Polymer Symposium 37. pp911-921. (1983)

15. Cohen M.H. Mendelson K.S. J. App. Phys. Vol 53(2), p1127. (1982)

16. Lui K.J., Ullman R. J. Chem. Phys. Vol 48(3), p1158. (1968)

17. Heatley F., Walton I. Polymer. Vol 17, p1019. (1976)

18. Tadakoro S., Murahashi S. Makromol. Chem. Vol 74, p109. (1964)

19. MacGregor R.P., Peemoeller H., Schneider M.H., Sharp A.R. J. App. Polym. Sci. : App. Polymer Symposium 37. pp901-909. (1983)

20. Robertson B. Phys. Rev. Vol 151, p273. (1966)

21. Chang D.C., Rorschach H.E., Nichols B.L., Hazlewood C.F. Annala NY Acadamy 39, p432. (1971)

22. Belton P.S., Jackson R.R., Packer K.J. Biochim. Biophys. Acta. Vol 354, p305. (1974)

23. Brownstein K.R., Tarr C.E. "Importance of classical diffusion in NMR studies of water in biological cells." Phys. Rev. A. Vol 19(6), p2446. (1979)

24. Wang J.H. J. Am. Chem. Soc. Vol 76, p4755. (1954)